MCAT Institute
Progress Report
93-19





# DEVELOPMENT OF A QUIET SUPERSONIC WIND TUNNEL WITH A CRYOGENIC ADAPTIVE NOZZLE

Stephen W. D. Wolf



October 1993

NCC2-604

**MCAT Institute**
**3933 Blue Gum Drive**
**San Jose, CA 95127**

CONTENTS

# DEVELOPMENT OF A QUIET SUPERSONIC WIND TUNNEL WITH A CRYOGENIC ADAPTIVE NOZZLE
# ANNUAL PROGRESS REPORT March 1992 - April 1993

**Stephen W. D. Wolf**

## Introduction:

The main objective of this work is to develop an interim *Quiet* (low-disturbance) supersonic wind tunnel for the NASA-Ames Fluid Mechanics Laboratory (FML). The main emphasis is to bring on-line a full-scale Mach 1.6 tunnel as rapidly as possible to impact the NASA High Speed Research Program (HSRP). The development of a cryogenic adaptive nozzle and other sophisticated features of the tunnel will now happen later, after the full scale wind tunnel is in operation. The work under this contract for the period of this report can be summarized as follows:

1) Provide aerodynamic design requirements for the NASA-Ames Fluid Mechanics Laboratory (FML) Laminar Flow Supersonic Wind Tunnel (LFSWT) as shown in the artist impression on Figure 1.

2) Research design parameters for a unique Mach 1.6 drive system for the LFSWT using an 1/8th-scale Proof-of-Concept (PoC) supersonic wind tunnel.

3) Carry out boundary layer transition studies in PoC to aid the design of critical components of the LFSWT.

4) Appraise the *State of the Art* in quiet supersonic wind tunnel design.

5) Help develop a supersonic research capability within the FML particularly in the areas of high speed transition measurements and schlieren techniques.

The body of this annual report summarizes the work of the Principal Investigator and is presented under logical headings. The order is not significant.

## Drive System Research:

The PoC supersonic wind tunnel has continued to be a valuable workhorse during the period of this report. A schematic and photograph of the PoC supersonic wind tunnel are shown on Figures 2a and 2b. Work with PoC has concentrated on Phase 1 and 2 (Investigation of drive system and instrumentation development) of the PoC experimental program outlined in the first progress report of this contract.[1] The PoC Mach 2.5 drive system[2,3,4] has been modified to operate at Mach 1.6. This reduction of Mach number has resulted from a need to match the initial LFSWT test envelope to actual F-16XL flight test conditions.

A new Mach 1.6 nozzle was installed in PoC during April 1992, and the first runs occurred at the beginning of May 1992. Using the Mach 2.5 two-stage injector system, the PoC operated successfully over a stagnation pressure (Po) range from 5.18 psia to 11.99 psia. The Mach 1.6 test section had the same cross-section as before (1 x 2 inches). However, the test section/supersonic diffuser was made longer than for the Mach 2.5 case, to be compatible with existing hardware. The supersonic diffuser is 6.8 inches long, with the floor and ceiling diverging at $0.25^{o}$ between parallel sidewalls (for boundary layer allowance).

As part of our LFSWT cost saving effort, we examined the need for secondary injectors in the LFSWT Mach 1.6 drive system. Since the normal start compression ratio for Mach 1.6 flows is 1.12:1 compared to 2:1 for Mach 2.5 flows, running a tunnel at Mach 1.6 should be easier than before. However, use of the existing FML compressor requires that the LFSWT must be capable of operating with compression ratios less than unity to achieve the desired test envelope. A series of PoC tests were performed with different secondary injector mass flows and corresponding changes to the exit pressure (Pe). These tests were based on previous compressor studies[5] which showed that Pe will rise with increasing mass flow in the operating band of the LFSWT.

The results of the PoC Mach 1.6 drive system tests are summarized on Figure 3, which shows experimental data plotted against minimum Po and Pe. This data summary clearly shows the need for secondary injectors, if we are to achieve the desired minimum Po. The influence of the secondary injector mass flow on minimum Po is significant compared to the influence of Pe. Consequently, the mass flow of the LFSWT secondary injectors needs to be maintained at high levels similar to the 110 lbs/sec for the Mach 2.5 drive system, assuming the compressor inlet pressure (Pi) is fixed.

The expected increase of Pe to about 8.8 psia, due to using high mass flow secondary injectors, may stop the primary injectors from starting. However, PoC testing shows that the exit Mach number of the primary injectors can be successfully lowered from 2.1 to 1.97, which reduces the starting pressures required. The exit Mach number of the secondary injectors remained unchanged at 2.0 which requires an achievable overpressure of 1.39 (Pe=10.57 psia).

It should also be noted that the purpose-built LFSWT drive system will be more aerodynamically efficient than the evolved PoC design. In particular, the diffuser is much improved. Furthermore, the FML compressor run point will be related to Pe rather than Pi, allowing the possibility of lowering the Pe for a given mass flow.[5] Both these factors will enhance the LFSWT drive system beyond our PoC experience.

The design requirements for the LFSWT are based on our PoC studies. The primary injectors are built so that mass flow and Mach number can be adjusted independently. The range of mass flow is 62 to 124 lbs/sec and the Mach number range is 1.8 to 2.2. These ranges are intended to allow tunnel operation with a variety of drive system configurations depending on test Mach number and compressor power available. The secondary injectors have fixed nozzle blocks designed for Mach 2.0 exit velocity with a combined mass flow of 110 lbs/sec.

During the period December 1992 to February 1993, the effect of model blockage on the PoC drive system was investigated. Potential models were simulated by a 0.1 inch diameter pitot tube positioned on the floor of the test section or on the test section centerline. Effective blockage was varied up to 10% by traversing the probe across the 2 inch width of the tunnel as shown on Figure 4.

Static pressures measured on the PoC sidewall with no probe installed are shown on Figure 5. These pressure distributions illustrate how the test section flow shocks down in the supersonic diffuser at different Po. As expected, the shocks move upstream with decreasing Po. However, over the Po range down to about 5 psia, the test section is free of shocks. A decrease of test section pressure coefficient (Cp) in the flow direction is attributed to inadequate wall divergence to allow for the boundary layer growth along the test section walls.

Static pressures measured with the probe installed are shown on Figure 6. These pressure distributions illustrate the dramatic effect of introducing the probe across the tunnel width, at the higher and lower ends of the Po range. The test section flow is started ahead of the model for all probe configurations. Furthermore, the effect of this model blockage was maximized by placing the probe near the entrance of the test section. The shock train generated by the probe was reflected at least four times within the long PoC test section/supersonic diffuser. We expect the number of shock train reflections to reduce to about two in the LFSWT test section.

Consequently, we can expect the total pressure of the LFSWT test section flow exiting into the mixing region to be higher than that achieved in the PoC. This increase of total pressure will provide the LFSWT drive system with extra power to overcome unexpected pressure losses elsewhere in the tunnel.

Quiet Flow Research:

**Settling Chamber**

In the previous annual report[3] a modular settling chamber was installed in the PoC to provide a low-disturbance free stream (See Figure 7). The change of Mach number from 2.5 to 1.6 produces an increase in tunnel mass flow by a factor of 2.1 for a given Po. This change arises from the growth of the throat area of the nozzle to achieve the desired area ratio for Mach 1.6 flow. The test section size was not changed.

Flow disturbance measurements were made in the plane of the PoC settling chamber exit on the tunnel centerline (X=-6) using a total pressure probe fitted with a 0.093 inch diameter pressure transducer (See Figure 4). The ratio of the total pressure rms (Prms) to stagnation pressure (Po) is below 0.14% over the entire Po range (for the frequency range 30Hz to 50KHz). The spectra of this pressure data shows broadband frequency response. These data indicate that the settling chamber is low disturbance. As expected, the pressure ratio increases with Po as the settling chamber mass flow rises (See Figure 8). Further reduction in the turbulence pressure ratio was realized by fitting two extra screens upstream of the honeycomb in the settling chamber. (One screen was 20-mesh and the other closest to the honeycomb was 42-mesh.) This settling chamber configuration was tested to confirm design refinements for the LFSWT.

The design of the LFSWT settling chamber has evolved from the PoC studies, and the integration of pressure reduction elements (see Figure 9). The goal is pressure disturbances less than 0.2% at the settling chamber exit with flows up to 21 lbs/sec. The LFSWT design incorporates pressure reduction elements (i.e., filters) to reduce inlet piping disturbances being fed into the settling chamber. These elements also allow a smaller inlet pipe to be used for low Po operation, by raising the inlet pipe pressure and preventing choking. This feature provides cost savings and a more practical solution to the inlet piping/tunnel interface for low Po operation.

**Laminar Flow on Tunnel Walls**

The new fixed block Mach 1.6 nozzle fitted to the PoC was designed using the Riise methodology, which was applied to the PoC Mach 2.5 nozzle. The fifth-order polynomial contraction and Riise nozzle contour are tabulated in Table 1. Since the test section geometry was unchanged, the nozzle throat height and nozzle length both changed, as well as the nozzle contour. The throat height grew from 0.378 inch to 0.8 inch, which reduced the vertical inlet/nozzle contraction ratio from 13:1 to 6:1. The horizontal inlet/nozzle contraction ratio remained unchanged at 2.46:1. The PoC nozzle length shrunk from 5.114 inches to 3.468 inches.

Vibration measurements were made close to the PoC Mach 1.6 nozzle using a capacitive-type accelerometer. At Po = 5 psia, the acceleration was 0.045g over the frequency range 14-1000Hz. At Po = 9 psia, the acceleration was 0.041g. In the PoC, there was no means of isolating the nozzle test section from the injector drive system. The effect of nozzle/test section vibration on laminar flow is currently unknown and will be studied in the LFSWT, which incorporates vibration isolation for the settling chamber, nozzle and test section.

Temperature of the PoC flow is controlled passively. The thermal mass of the PoC nozzle and test section is large relative to the flow surfaces. Hence, wall temperature stability is

achieved within a few minutes of starting a run and is relatively insensitive to changes in Po (mass flow). The wall temperature is generally $20^0$ F below ambient, and is similar to the inlet stagnation temperature. Repeatability of laminar flow measurements is monitored at the end of each run to check for temperature drift. No effects of temperature drift have been observed in the measurements discussed here.

Laminar flow studies started in the PoC at Mach 2.5 have now been extended to Mach 1.6. Again, theses studies have involved the use of different types of instrumentation to confirm the state of the test section boundary layers. In addition to using hot-wire, hot-film and Preston tube instrumentation, we successfully applied two schlieren techniques to the visualization of low-pressure, supersonic boundary layers.

Mach 1.6 hot-wire measurements were made on the floor centerline of the PoC test section, using a constant-temperature anemometer. The streamwise location in the test section matched the convenient location for the Mach 2.5 measurements relative to the nozzle throat (X=6.83). The hot-wire was 5 micron in diameter and made of Tungsten. The height of the hot-wire above the floor was fixed at 0.069 inch. The hot-wire signal rms over the frequency range 30Hz to 50kHZ is shown on Figure 10, plotted against Po. At a Po of about 7.3 psia, there is a decisive change in the slope of the data from numerous tests. This repeatable change in slope is a clear indication that transition has occurred. The comparison with the Mach 2.5 data shows that transition occurs at a lower Po at Mach 1.6, which may indicate a sidewall influence on the floor boundary layer. The transition Reynolds numbers (related to distance from the nozzle throat) is approximately 1.3 million at Mach 1.6, which is less than the 1.4 million Reynolds number at Mach 2.5. Hot-wire data with settling chamber disturbances introduced by a probe illustrate the sensitivity of the boundary layer to free stream disturbances.

Measurements were made with a 0.015 inch OD Preston tube in the same streamwise location as the hot-wire (X=6.83) at repeat test conditions, as shown on Figure 11. Again, there is a slope change in the data which is indicative of transition at a Po of about 7 psia. Notice that the probe Cp for laminar flow is less at Mach 2.5 than at Mach 1.6 as expected. The size of the Preston Tube was reduced to take account of the thinner boundary layer thicknesses at Mach 1.6. On Figure 12, data from a larger 0.029 inch OD Preston tube are shown at different X locations to confirm this situation. Only one of these 0.029 inch probe OD data sets indicates transition downstream of the test section (at X=8.38), because the boundary layer is thicker at this streamwise location.

Flow visualization of the supersonic boundary layer on the floor of the PoC was achieved by using a novel focusing schlieren technique with our original polycarbonate windows. Unfortunately, the reduction in light intensity due to these windows made boundary layer density gradients indistinct and glass inserts were fitted to improve the visualization. The new windows allowed our focusing schlieren system (shown on Figure 13) to capture images of the boundary layer at different Po. The depth of focus of the system was of the order 0.25 inch. In Figure 14, we compare pictures of the boundary layer on the tunnel centerline, at two values of Po, after image processing (subtraction of a reference wind-off image and contrast enhancement). Clearly, the boundary layer at Po = 11 psia is thicker than at Po = 6.8 psia, contrary to Reynolds number effects. Furthermore, some turbulent bursting is present in the boundary layer at Po = 6.8 psia (indicative of the transition process) which appears to stop when Po is approximately 7.2 psia. This observation of transition, of course, compares very well with our other instrumentation. Furthermore, over the Po range from 7.2 to 11 psia no change in the boundary layer was observed, so the bursting phenomena is distinct from any other aerodynamic effects.

Real-time visualization of the floor boundary layer was also obtained using conventional Toepler schlieren. We made a high speed cine-film (400 fps) of the boundary layer over the complete Po range, which clearly showed the same turbulent bursting occurring around Po = 7 psia. This further collaborated our previous findings, despite the fact that this schlieren technique integrates the boundary layer density gradients across the entire width of the tunnel.

Due to size constraints, it was impractical to traverse any probes streamwise through the PoC test section/nozzle. However, a hot-film array was bonded to the tunnel ceiling so that the movement of transition with Po could be observed. Care was taken to mount the array so that the flow over the array would not encounter any surface irregularities, such as the leading edge of the substrate. The array consisted of 20 hot-films attached to a Kapton substrate (see Figure 15a). A special PoC window was made which allowed one edge of the substrate to protrude through the window carrying the hot-film signal leads. The window sealed around the substrate to prevent flow into the tunnel. The substrate was 0.002 inch thick and the hot-film and leads were less than 0.001 inch thick. The hot-film array was bonded to the ceiling of the PoC nozzle and test section, as shown in Figure 15b, and extended upstream to the entrance of the contraction. The hot-film sensors were positioned in the plane of the tunnel centerline at 0.5 inch intervals.

The hot-film signals were monitored one at a time, because only a single specialist constant-current circuit was available. The hot-films were operated at a current of 125 milliamps, which corresponds to a 1.3 overheat condition. The hot-films could not be operated in a wind off condition without risk of sensor burnout. The hot-film results are summarized on Figure 16 for different Po. There is a peak in signal rms for each Po which is due to transition on the PoC ceiling. These peaks move upstream with increasing Po, in the same manner as the transition front was observed to move using schlieren visualization. At the location of other test section flow measurements (X=6.83) transition is shown to occur at a Po of about 6 psia, which is significantly lower value than found in the floor measurements. Unfortunately, bubbling of the hot-film array was observed during these hot-film tests, which curtailed further useful measurements, and may indeed have contaminated all the hot-film data. However, these tests did confirm that there is a transition front moving the length of the test section walls. No transition was detected in the nozzle during these tests.

In conclusion, four transition locating techniques have been used in the PoC. Three of these techniques are in rough agreement. Clearly, laminar flow was being maintained through the nozzle and part of the test section on the centerline, satisfying one of the requirements of quiet flow. The actual cause of transition in PoC is not clear. In fact, transition was not predicted in any part of the PoC test section by CFD analysis. We are sure that more knowledge will be gained from studying the larger LFSWT. It may then be possible to delay the onset of transition until higher Reynolds numbers, above 2 million per foot, as achieved on flat plates.

Test Section Flow Quality:

Test Section flow disturbance measurements were made in the plane of the PoC nozzle exit (X=3.47) on the tunnel centerline (See Figure 4). The same total pressure probe fitted in the settling chamber was used, with a 0.093 inch diameter pressure transducer. The ratio of the total pressure rms (Prms) to stagnation pressure (Po) is below 0.09% over the entire Po range (for the frequency range 30Hz to 50KHz). The dynamic pressure data has broadband frequency response. These data indicate that the test section flow is low disturbance at the entrance over the Po operating range. As found in the settling chamber measurements, the pressure ratio (turbulence) increases linearly with Po (See Figure 17). The two data sets are from different tunnel runs separated only by time. As expected, repeatability at low Po is difficult to achieve because the signal to noise ratio is very large.

A limited off-centerline survey of the flow at the test section entrance (X=3.47) is shown in Figure 18. These data indicate that the turbulence at this streamwise location has a three-dimensional distribution, which is not symmetrical about the tunnel centerline. For the data taken +0.9 inches from the tunnel centerline, the pitot probe is within 0.05 inch of the sidewall and is partially immersed in the sidewall boundary layer. Unfortunately, there is no

corresponding turbulence survey of the settling chamber flow to determine if the settling chamber is the cause of this disturbance three dimensionality observed in the test section. Since disturbances from the tunnel walls will propergate downstream along Mach lines, the maximum streamwise displacement of wall/corner disturbance and centerline measurement is 1.396 inches at Mach 1.6. (Lower Mach numbers in the nozzle will reduce this displacement). So, if wall/corner disturbances were the cause, the origin of the disturbance must be downstream of the nozzle throat. Therefore, the disturbances cannot be directly linked to the upstream edges of the nozzle windows, which are located in the contraction.

Off-centerline surveys of the floor and ceiling boundary layers were made in the PoC test section using a 0.015 inch OD Preston tube. Measurements were made at three streamwise locations on the floor (X=4.52, 6.83, and 8.38) and one streamwise location on the ceiling (X=6.83). The floor Preston tube data are shown on Figures 19a, 19b and 19c over the Po range. At X=4.52, the boundary layer appears two-dimensional out to between +0.5 and +0.75 inches from the centerline. At X=6.83, the boundary layer has some symmetry about the plane of the tunnel centerline, but two-dimensionality is within $\pm 0.25$ inch of the centerline. At X=8.38, the two-dimensionality of the boundary layer extends out to between +0.25 and +0.5 inch from the centerline. Interestingly, the flow should be shocking down at this downstream location, when Po is less than 6 psia (See Figure 5), but this is not shown in the pressures. Data near the sidewall/floor corner shows that the probe Cp asymptotes to about 0.5 for Po greater than 6 psia. The sidewall induced boundary layer flows described by King[6] may be responsible for this behavior, and more studies are planned in the larger LFSWT to improve our understanding.

The off-centerline boundary layer survey on the PoC ceiling at streamwise location X=6.83 is shown on Figure 20. As measured on the floor (See Figure 19b), the boundary layer exhibits some symmetry about the plane of the tunnel centerline with limited two-dimensionality on the tunnel centerline. There are differences between the floor and the ceiling surveys at the same streamwise location. The cause of these differences is not known, but the removal and replacing of the PoC windows to change the location of the probe may have been a factor.

There are several conclusions to be drawn from these measurements. Firstly, two-dimensional quiet flow is restricted in the PoC. Secondly, no propagation of disturbances can be inferred from the data. Finally, more research is required to realize the clearly defined quiet test core envisaged in quiet wind tunnels, as shown on Figure 21.

LFSWT Support:

As project engineer for the LFSWT, the Principal Investigator has defined the aerodynamic lines of the new LFSWT, which have been published in a Requirements Document (See Appendix A). Detailed design of the LFSWT was started by NASA engineers in January 1992 and was finally completed in February 1993. During this period, constant supervision of the design was required due to inadequate design management. The only changes to the design during this period were the installation and size of the secondary injectors based on PoC research. Weekly progress meetings were essential to co-ordinate activities.

Fabrication of the LFSWT started in September 1992 and has involved overseeing the machining of the nozzle in Tennessee. The tunnel installation was on schedule at the end of this contract period. The time spent by the Principal Investigator and others in checking the LFSWT drawings and ensuring accuracy has saved an enormous amount of time in the machine shop. Furthermore, the machine shop has now adopted a improved scheme for tracking the progress of a project based on our requirements for meeting schedules and budgets.

I participated in several meetings with the NASA Ames Director of Aerophysics, Dr. Ron Bailey through the year. In these meetings, I was responsible for presenting an update of

PoC/LFSWT technical issues. The continued financial support of Aerophysics Directorate relies on the success of these meetings.

The main features of the LFSWT will be laminar flow on the nozzle and test section walls at low supersonic Mach numbers, a low-disturbance settling chamber (See Figure 9), all-round optical access to the test section, nozzle/test section vibration isolation, and a two-stage ambient injector drive system. The design philosophy includes important features for research flexibility which simplify configuration changes and improve access to the nozzle and test section. The fixed nozzle block is designed according to the methodology of Riise. This design makes the nozzle long relative to the exit height (23.376 inches in length) with minimized curvature (minimum radius of curvature is order 56 inches) which is known to promote natural laminar flow. The contraction shape is a fifth order polynomial to eliminate flow separations and is 48 inches long in the vertical plane and 20 inches long in the horizontal plane. The nozzle/contraction is designed as one component so there are no steps or gaps on the floor and ceiling of the nozzle. The steps and gaps between the nozzle and the test section are being held to 0.001 inch or less. Surface finish of the nozzle will be to a 10L standard. We consider these requirements are essential to maintaining natural laminar flow through the LFSWT test section, even at low Reynolds numbers.

Instrumentation Development:

During this contract period, instrument development work has concentrated on Schlieren flow visualization. The results of which have been previously described (See Figure 14).

We now have a mark III version of our *Focusing Schlieren* system (shown on Figure 13) which is based on a design by Weinstein of NASA Langley.[7] We have improved the optical components and the mounting hardware, so that the system is more permanent and repeatable. In addition, glass window inserts were fitted in the PoC to reduce out-of-focus images and increase illumination intensity. This change and increased separation between optical components made the schlieren system sensitive enough to visualize supersonic boundary layers with small density gradients at low stagnation pressures. Nevertheless, the boundary layer image captured on a single frame is difficult to see and requires image processing to improve image contrast. High speed video (200 fps) has proved to be successful and gives a clear view of transition bursting.

The small size of PoC has been a limiting factor during this development work. It is hoped that the LFSWT will open up new opportunities for flow visualization with extensive nozzle/test section optical access.

State-of-the-Art Appraisal:

The ongoing library search continues in the following topics: supersonic wind tunnel and nozzle design; surface temperature effects on transition; effects of surface shape and roughness on transition; supersonic mixing layers; supersonic diffusers; transition detection instrumentation. This task is simplified by use of STAR and NOVA combined with a PC computer database, created by the Principal Investigator. This database provides immediate access and sorting of all citations for extraction of information and cataloging. Currently, the database contains 842 citations. The most informative citations concerned turbulence measurements in quiet tunnels, as we start to build a consensus on how to quantify the term quiet.

An important aspect of appraising the *State-of-the-Art* is meeting other scientists at conferences. During the period of this report, I participated in the AIAA 7th Aerospace

Ground Testing Conference held in Nashville, Tennessee during July 1992, the International Conference on Methods of Aerophysical Research in Novosibirsk, Russia during August/September 1992, the European Forum on Wind Tunnels and Wind Tunnel Test Techniques held at Southampton, England during September 1992, and the Symposium on Aerodynamics and Aeroacoustics held in Tucson, Arizona during February/March 1993. In addition, I visited NASA Langley to discuss quiet wind tunnel testing and instrumentation development with our East coast counterparts. I was fortunate to meet with many scientists from the Commonwealth of States (formally the USSR) and Europe. From discussions with these scientists, I was able to learn that there are some partially quiet supersonic tunnels in their respective countries. The only existing quiet supersonic tunnels, as we define them, are operating in the USA (NASA-Langley) and France (ONERA) at Mach numbers of 3 and above. Consequently, the LFSWT will provide NASA with a unique testing capability during 1993.

Publication and Presentations

During this contract period, I presented four papers which are attached as Appendices B-E. The first paper was an invited paper which I presented to the AIAA 7th Aerospace Ground Testing Conference held in Nashville, Tennessee during July 1992. This AIAA paper no. 92-3909 is entitled **DEVELOPMENT OF THE NASA-AMES LOW DISTURBANCE SUPERSONIC WIND TUNNEL FOR TRANSITION RESEARCH UP TO MACH 2.5.** The abstract is as follows:

> A unique, low-disturbance supersonic wind tunnel is being developed at NASA-Ames to support supersonic laminar flow control research at cruise Mach numbers of the High Speed Civil Transport (HSCT). The distinctive aerodynamic features of this new quiet tunnel will be a low-disturbance settling chamber, laminar boundary layers on the nozzle walls and steady supersonic diffuser flow. Furthermore, this new wind tunnel will operate continuously at uniquely low compression ratios (less than unity). This feature allows an existing non-specialist compressor to be used as a major part of the drive system. In this paper, we highlight activities associated with drive system development, the establishment of natural laminar flow on the test section walls, and instrumentation development for transition detection. Experimental results from an 1/8th-scale model of the supersonic wind tunnel are presented and discussed in association with theoretical predictions. Plans are progressing to build the full-scale wind tunnel by the end of 1993.

At the International Conference on Methods of Aerophysical Research in Novosibirsk, Russia during August/September 1992, I presented a paper entitled **Design Features of a Low-Disturbance Supersonic Wind Tunnel for Transition Research at Low Supersonic Mach Numbers.** The abstract is as follows:

> Low-disturbance (or "quiet") supersonic wind tunnels are now considered essential for high speed transition research, many years after the fact. This paper will describe progress in the development of a new-generation low-disturbance wind tunnel, which can operate continuously up to Mach 2.5, at low unit Reynolds numbers (Re). These test conditions match the anticipated High Speed Civil Transport (HSCT) cruise conditions and also the flight conditions of the NASA F-16XL research aircraft used in the High Speed Research Program (HSRP). The tunnel, called the Laminar Flow Supersonic Wind Tunnel

(LFSWT), is scheduled to be on-line before the end of 1993 at NASA-Ames Fluid Mechanics Laboratory (FML).

At the European Forum on Wind Tunnels and Wind Tunnel Test Techniques held at Southampton, England during September 1992, I presented an extended version of the above paper entitled **Design Features of a Low-Disturbance Supersonic Wind Tunnel for Transition Research at Low Supersonic Mach Numbers.** The abstract is as follows:

> A unique, low-disturbance supersonic wind tunnel is being developed at NASA-Ames to support supersonic laminar flow control research at cruise Mach numbers of the High Speed Civil Transport (HSCT). The distinctive design features of this new quiet tunnel are a low-disturbance settling chamber, laminar boundary layers along the nozzle/test section walls, and steady supersonic diffuser flow. This paper discusses these important aspects of our quiet tunnel design and the studies necessary to support this design. Experimental results from an 1/8th-scale pilot supersonic wind tunnel are presented and discussed in association with theoretical predictions. Natural laminar flow on the test section walls is demonstrated and both settling chamber and supersonic diffuser performance is examined. The full-scale wind tunnel should be commissioned by the end of 1993.

Finally, I presented an invited paper entitled **Adaptive Wall Technology for Minimizing Wind Tunnel Boundary Interferences - Where Are We Now?** at the Symposium on Aerodynamics and Aeroacoustics held in Tucson, Arizona during February 28/March 2, 1993 to commemorate Professor Bill Sear's 80th birthday. The abstract is as follows:

> The status of adaptive wall technology to improve wind tunnel simulations for 2- and 3-D testing is reviewed. This technology relies on the test section flow boundaries being adjustable, using a tunnel/computer system to control the boundary shapes without knowledge of the model under test. This paper briefly overviews the benefits and shortcomings of adaptive wall testing techniques. A historical perspective highlights the disjointed development of these testing techniques from 1938 to present. Currently operational transonic Adaptive Wall Test Sections (AWTSs) are detailed, showing a preference for the simplest AWTS design with two solid flexible walls. Research highlights show that quick wall adjustment procedures are available and AWTSs, with impervious or ventilated walls, can be used through the transonic range up to Mach 1.2. The requirements for production testing in AWTSs are discussed, and conclusions drawn as to the current status of adaptive wall technology. In 2-D testing, adaptive wall technology is mature enough for general use, even in cryogenic wind tunnels. In 3-D testing, this technology is not been pursued aggressively, because of the inertia against change in testing techniques, and preconceptions about the difficulties of using AWTSs.

Summary of Progress

1) The LFSWT project is in the fabrication stage and the wind tunnel should be running at Mach 1.6 in June 1993.

2) We have documented natural laminar flow on the PoC test section walls up to a unit

Reynolds number of about 2 million per foot at Mach 1.6, using a variety of measurement techniques.

3) The PoC settling chamber is low-disturbance with turbulence less than 0.2%.

4) The PoC test section flow is quiet (turbulence less than 0.1%) on the nozzle exit centerline.

5) Off-centerline PoC measurements show three-dimensionality in the test section flow which will require further investigation in the LFSWT.

6) An efficient tunnel drive system has been developed for Mach 1.6 operation of the LFSWT, using two stages of ambient injectors.

7) An array of instrumentation for transition detection is available for use in the LFSWT when the new tunnel comes on-line.

8) Focusing schlieren has been used successful to observe the transition phenomena in a supersonic boundary layer.

References:


1. Wolf, S.W.D.: **Development of a Quiet Supersonic Wind Tunnel with a Cryogenic Adaptive Nozzle - Annual Progress Report, May 1990 - April 1991.** NASA CR-186769, February 1991, 106 pp. N91-23195.

2. Wolf, S.W.D.; Laub, J.A.; and King, L.S.: **An Efficient Supersonic Wind Tunnel Drive System for Mach 2.5 Flows.** AIAA Paper 91-3260. In: Proceedings of the AIAA 9th Applied Aerodynamics Conference, Baltimore, Maryland, September 23-25, 1991, vol.1, pp. 461-471. A91-53769.

3. Wolf S.W.D.: **Development of a Quiet Supersonic Wind Tunnel with a Cryogenic Adaptive Nozzle - Annual Progress Report, March 1991 - April 1992.** NASA CR-188055, May 1992, 68 pp. N92-27976.

4. Wolf, S.W.D.; Laub, J.A.; King, L.S.; and Reda, D.C.: **Development of the NASA-Ames Low-Disturbance Supersonic Wind Tunnel for Transition Research up to Mach 2.5.** AIAA Paper 92-3909. Presented at the AIAA 17th Aerospace Ground Testing Conference, Nashville, Tennessee, July 6-8, 1992, 10 pp. A93-24488.

5. Laub, J.A.; and Wolf, S.W.D.: **The FML Compressor as a Drive System for the LFSWT: A Narrative.** In: Wolf, S.W.D. : Development of a Quiet Supersonic Wind Tunnel with a Cryogenic Adaptive Nozzle - Annual Progress Report, March 1991 - April 1992, NASA CR-188055, May 1992, 10 pp. N92-27978.

6. King, L.S.; and Demetriades, A.: **Comparison of Predictions with Measurements for a Quiet Supersonic Tunnel.** AIAA Paper 93-0344. Presented at the AIAA 31st Aerospace Sciences Meeting, Reno, Nevada, January 11-14, 1993, 11 pp.

7. Weinstein, L.M.: **Large-Field High-Brightness Focusing Schlieren Systems.** *AIAA Journal*, vol. 31, no. 7, July 1993, pp. 1250-1255.

# Table 1 - PoC Mach 1.6 Nozzle and Contraction Coordinates

| X | Y | X | Y | X | Y |
|---|---|---|---|---|---|
| -6.000 | 2.453 | -2.000 | 0.831 | 2.204 | 0.499 |
| -5.900 | 2.452 | -1.900 | 0.781 | 2.290 | 0.501 |
| -5.800 | 2.452 | -1.800 | 0.735 | 2.406 | 0.504 |
| -5.700 | 2.450 | -1.700 | 0.691 | 2.493 | 0.506 |
| -5.600 | 2.447 | -1.600 | 0.650 | 2.610 | 0.508 |
| -5.500 | 2.442 | -1.500 | 0.612 | 2.698 | 0.510 |
| -5.400 | 2.435 | -1.400 | 0.578 | 2.816 | 0.511 |
| -5.300 | 2.425 | -1.300 | 0.547 | 2.904 | 0.512 |
| -5.200 | 2.413 | -1.200 | 0.519 | 2.993 | 0.513 |
| -5.100 | 2.398 | -1.100 | 0.494 | 3.111 | 0.513 |
| -5.000 | 2.380 | -1.000 | 0.473 | 3.200 | 0.514 |
| -4.900 | 2.358 | -0.900 | 0.455 | 3.319 | 0.514 |
| -4.800 | 2.334 | -0.800 | 0.439 | 3.408 | 0.514 |
| -4.700 | 2.306 | -0.700 | 0.427 | 3.468 | 0.515 |
| -4.600 | 2.274 | -0.600 | 0.417 | | |
| -4.500 | 2.240 | -0.500 | 0.410 | | |
| -4.400 | 2.202 | -0.400 | 0.405 | | |
| -4.300 | 2.162 | -0.300 | 0.402 | | |
| -4.200 | 2.118 | -0.200 | 0.401 | | |
| -4.100 | 2.071 | -0.100 | 0.400 | | |
| -4.000 | 2.022 | 0.000 | 0.400 | | |
| -3.900 | 1.970 | 0.120 | 0.403 | | |
| -3.800 | 1.916 | 0.241 | 0.405 | | |
| -3.700 | 1.859 | 0.361 | 0.409 | | |
| -3.600 | 1.801 | 0.481 | 0.413 | | |
| -3.500 | 1.741 | 0.602 | 0.418 | | |
| -3.400 | 1.680 | 0.722 | 0.424 | | |
| -3.300 | 1.617 | 0.843 | 0.430 | | |
| -3.200 | 1.554 | 0.963 | 0.437 | | |
| -3.100 | 1.490 | 1.083 | 0.444 | | |
| -3.000 | 1.426 | 1.204 | 0.450 | | |
| -2.900 | 1.362 | 1.308 | 0.456 | | |
| -2.800 | 1.298 | 1.395 | 0.461 | | |
| -2.700 | 1.235 | 1.508 | 0.468 | | |
| -2.600 | 1.173 | 1.602 | 0.473 | | |
| -2.500 | 1.111 | 1.699 | 0.478 | | |
| -2.400 | 1.051 | 1.800 | 0.483 | | |
| -2.300 | 0.993 | 1.903 | 0.487 | | |
| -2.200 | 0.937 | 2.010 | 0.492 | | |
| -2.100 | 0.883 | 2.092 | 0.495 | | |

X - Streamwise station relative to throat (inches)
Y - Displacement of wall from the tunnel centerline (inches)

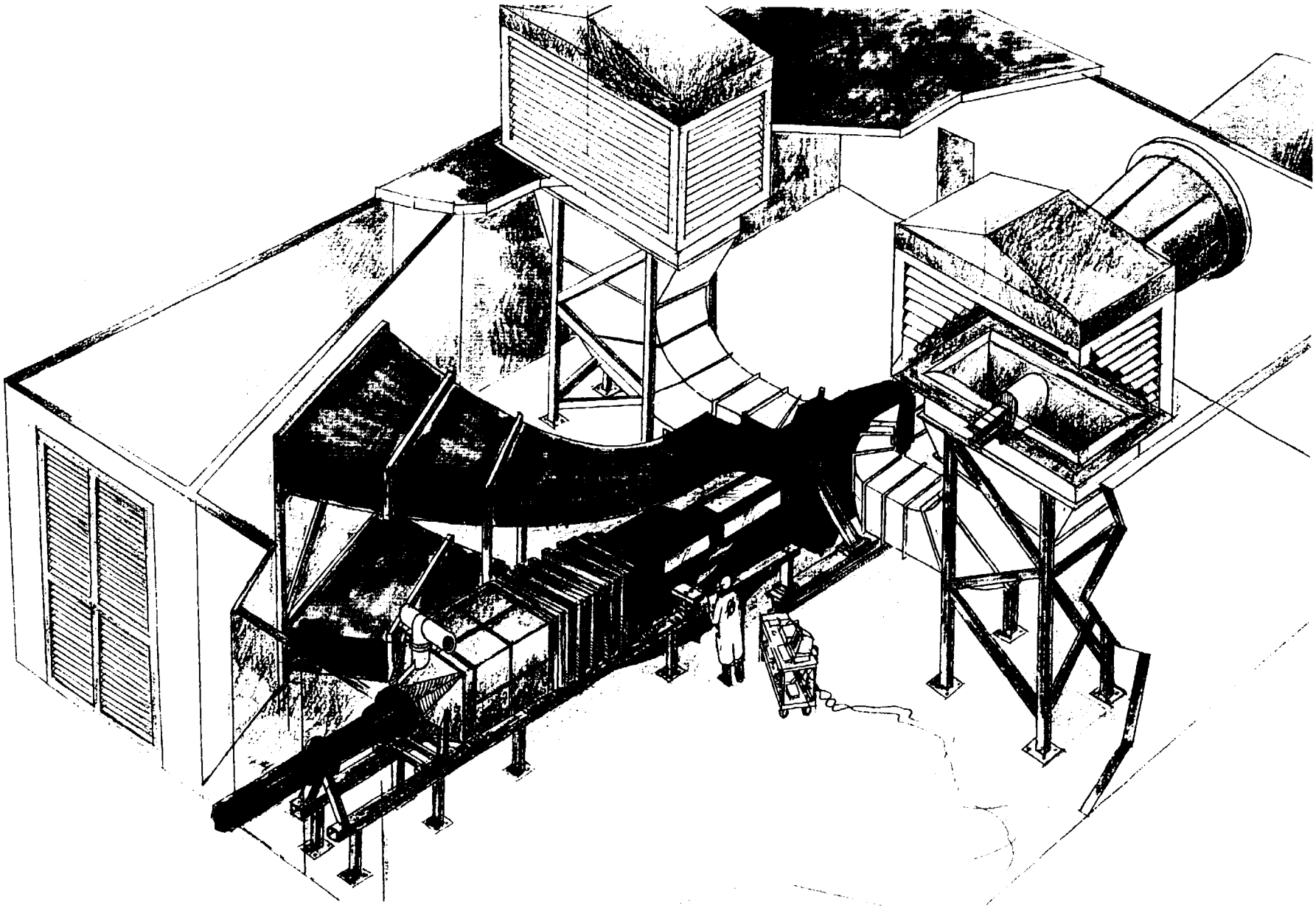

Fig. 1 - Layout of the Laminar Flow Supersonic Wind Tunnel

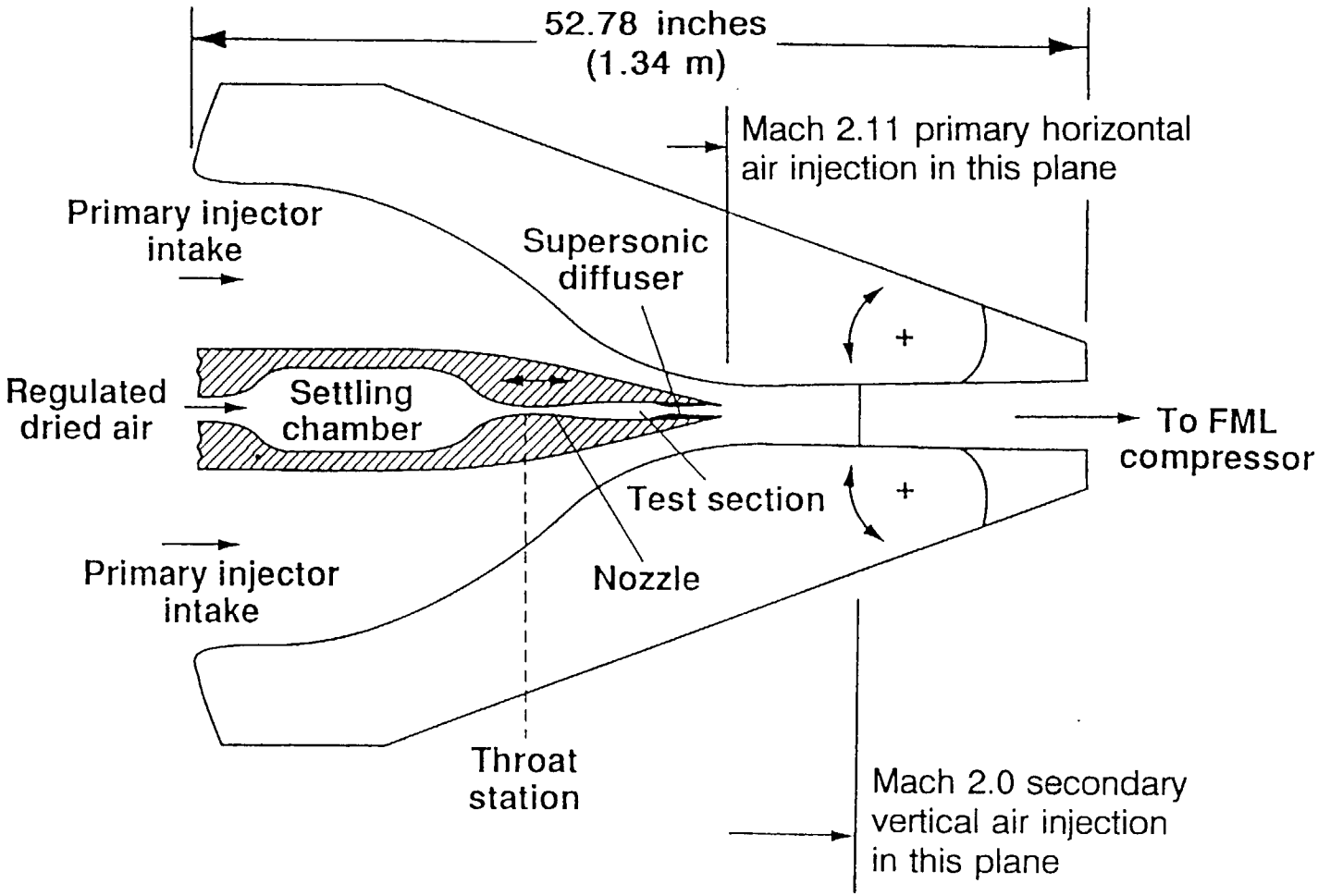


Fig. 2a - Schematic of the Proof-of-Concept Supersonic Wind Tunnel

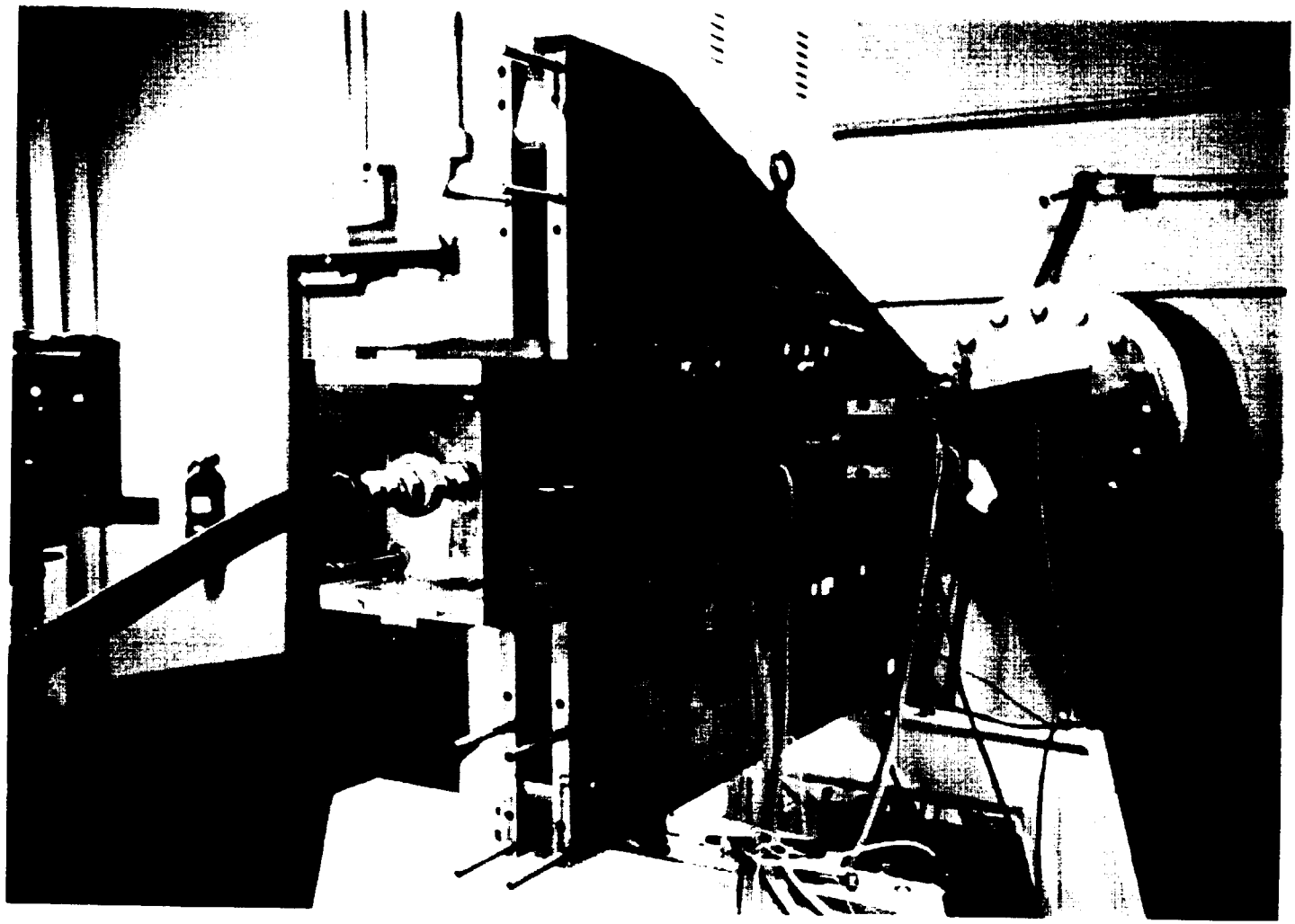

Fig. 2b - PoC supersonic wind tunnel in operation with hot-film array

# PoC Secondary Injector Data Summary

Mach 1.6 Operation

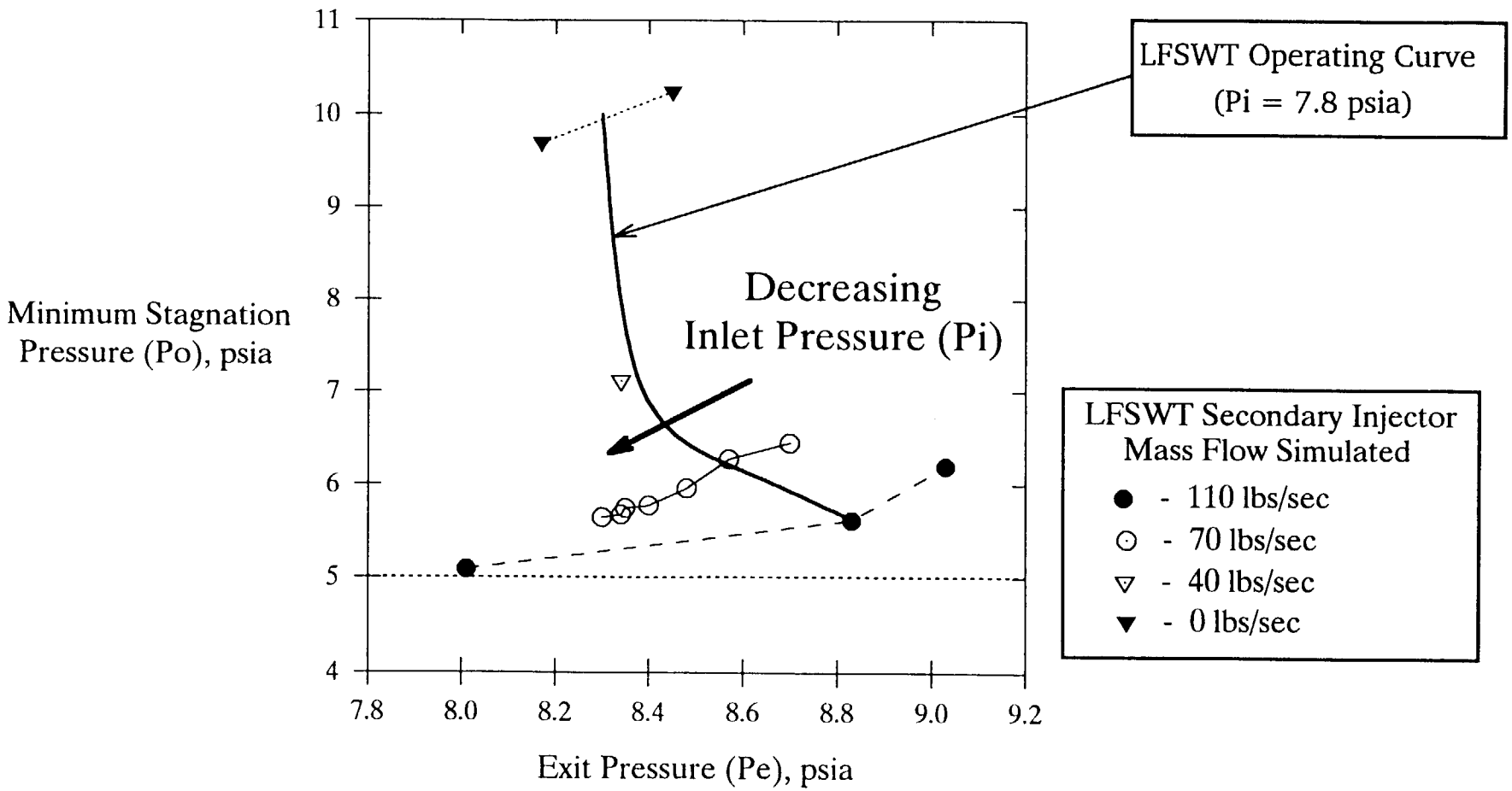


Fig. 3 - Influence of secondary injector mass flow on minimum Po


Fig. 4 - Traversable pitot probe located at the PoC nozzle exit

# PoC Test Section Pressure Data at Mach 1.6

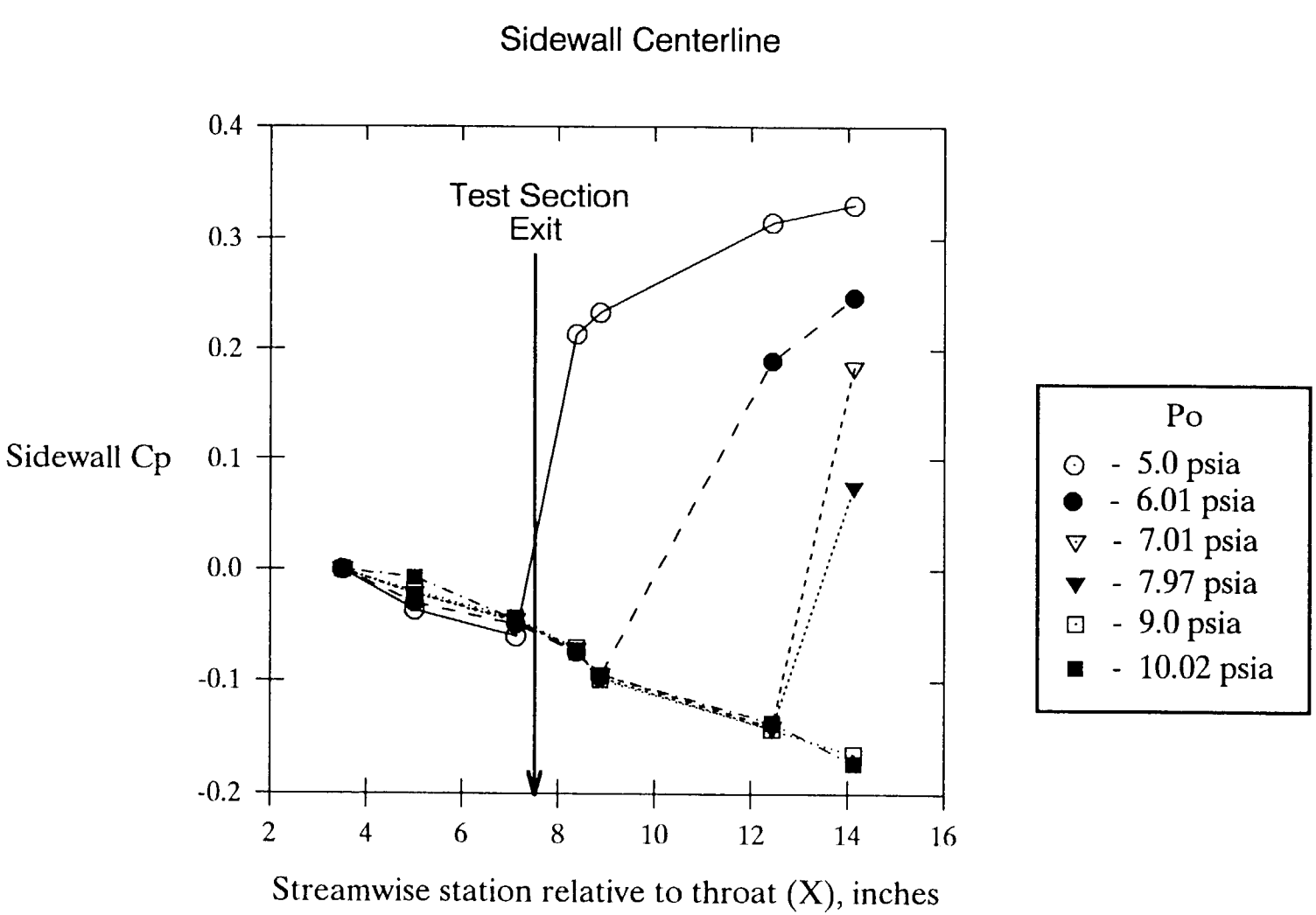


Fig. 5 - Effect of stagnation pressure on PoC pressures

# PoC Test Section Pressure Data at Mach 1.6

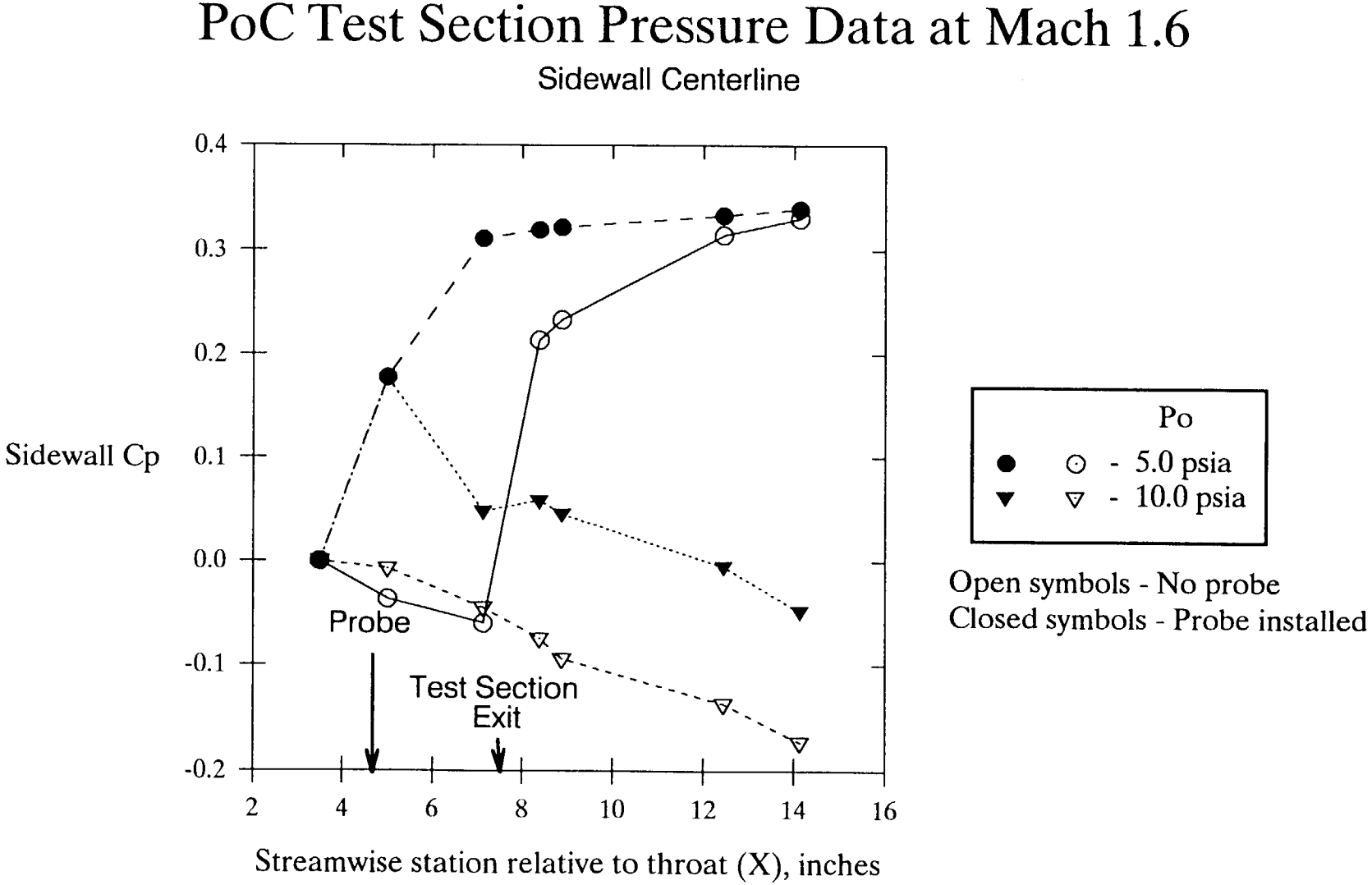


Fig. 6 - Influence of 10% blockage probe on PoC pressures

# PoC Settling Chamber & Nozzle Assembly

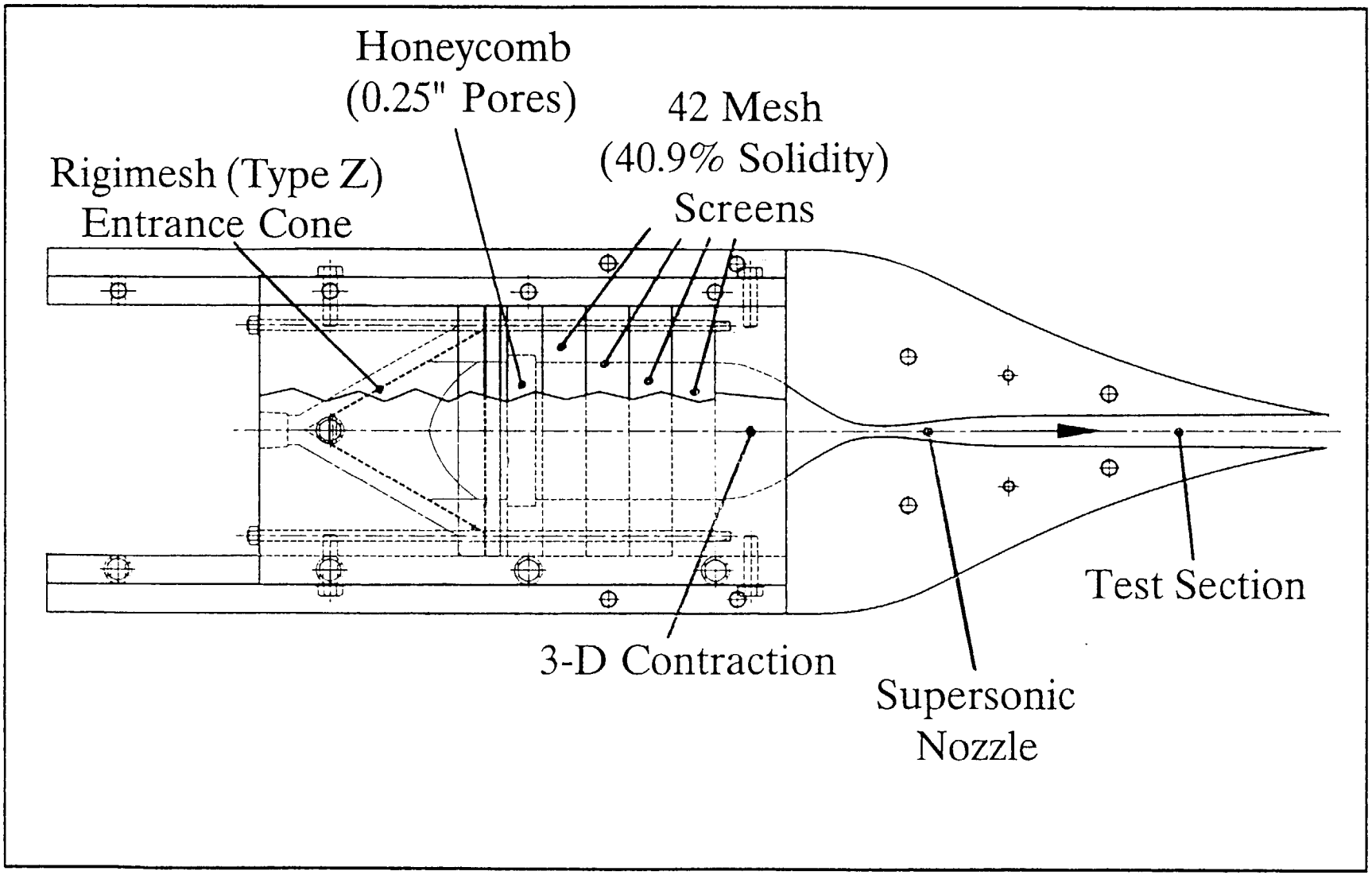


Fig. 7 - Schematic of the PoC low-disturbance settling chamber

# PoC Settling Chamber Pitot Data

Contraction Entrance Centerline (X=-6); 0.1 inch Probe dia.; Mach 1.6 Operation

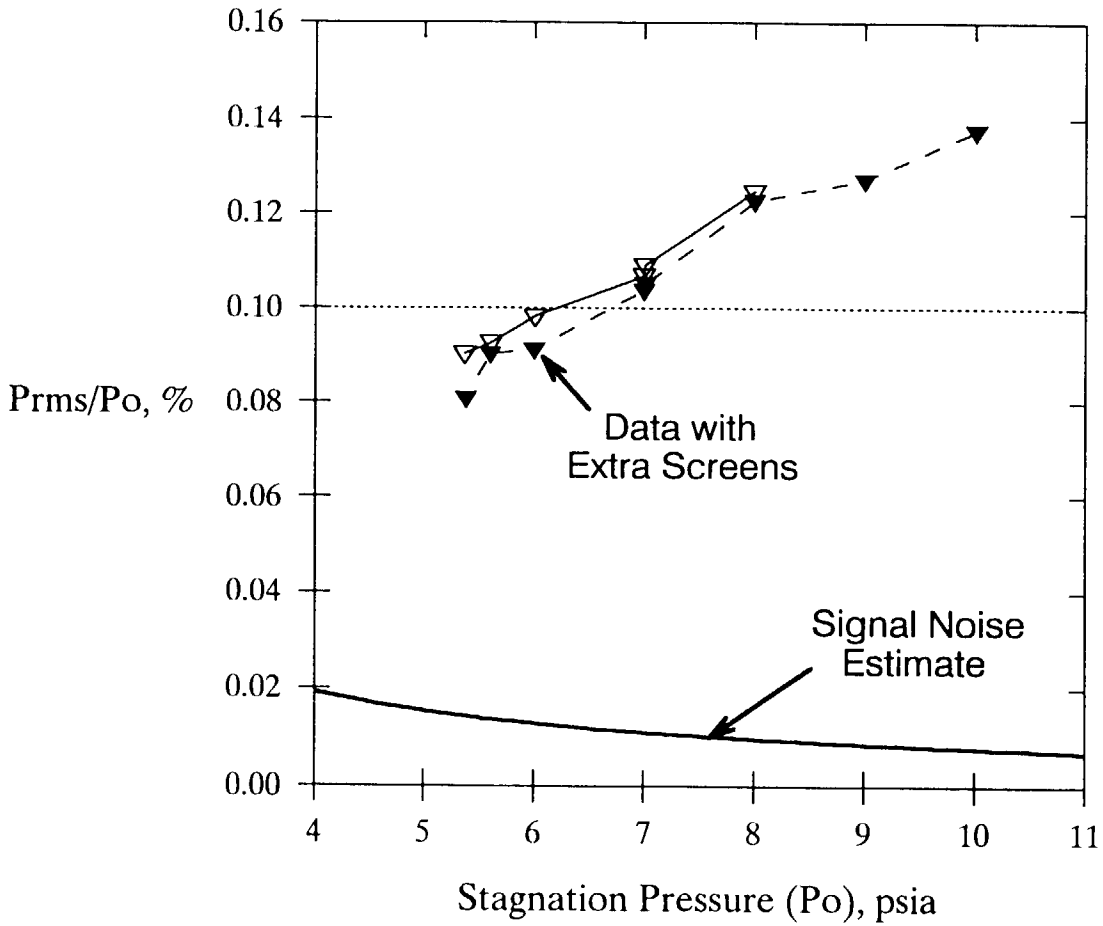


Fig. 8 - Turbulence measurements in the PoC settling chamber

# NASA-Ames LFSWT-I Settling Chamber and Nozzle

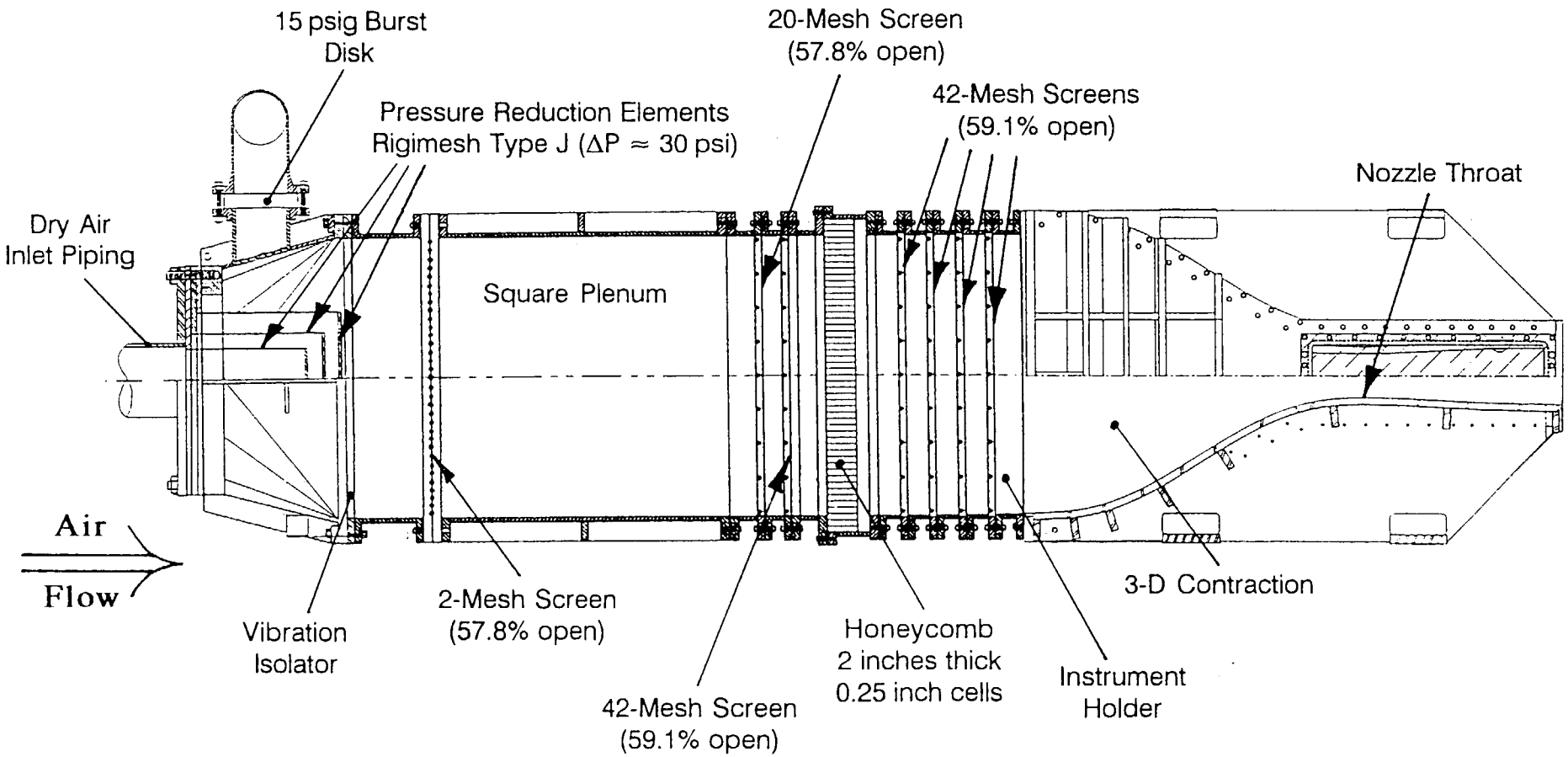


Fig. 9 - Schematic of the LFSWT low-disturbance settling chamber

# PoC Test Section Hot-Wire Data at Mach 1.6

0.069 inch Above Test Section Floor; 3.36 inches From Nozzle Exit (X=6.83); 5 micron Tungsten Wire

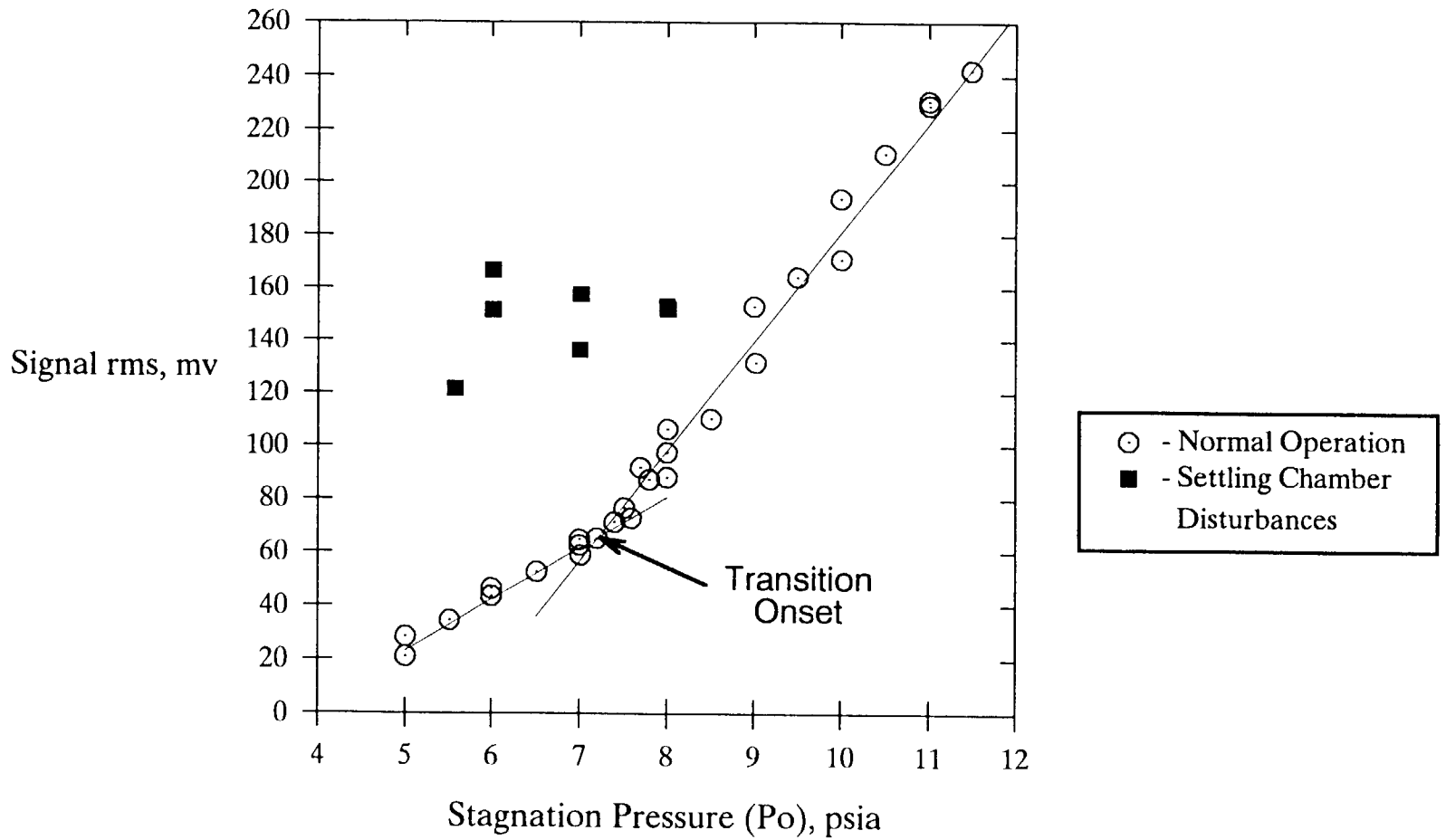


Fig. 10 - Summary of hot-wire data from the PoC test section

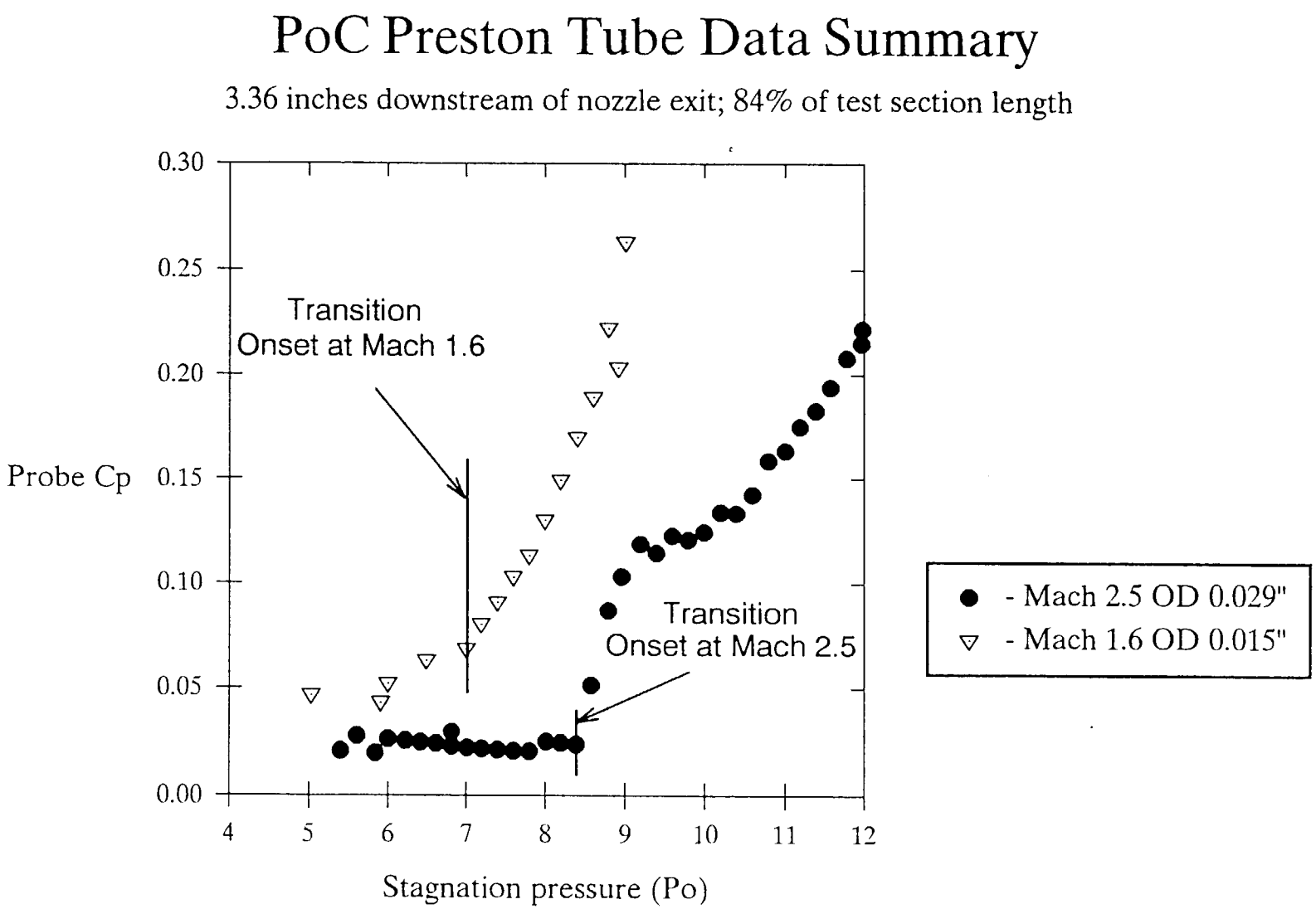


Fig. 11 - Comparison of PoC Preston tube data at Mach 1.6 and 2.5

# PoC Test Section Preston Tube Data at Mach 1.6

0.029 inch OD Probe Unless Otherwise Stated; Located on Centerline of Floor or Sidewall

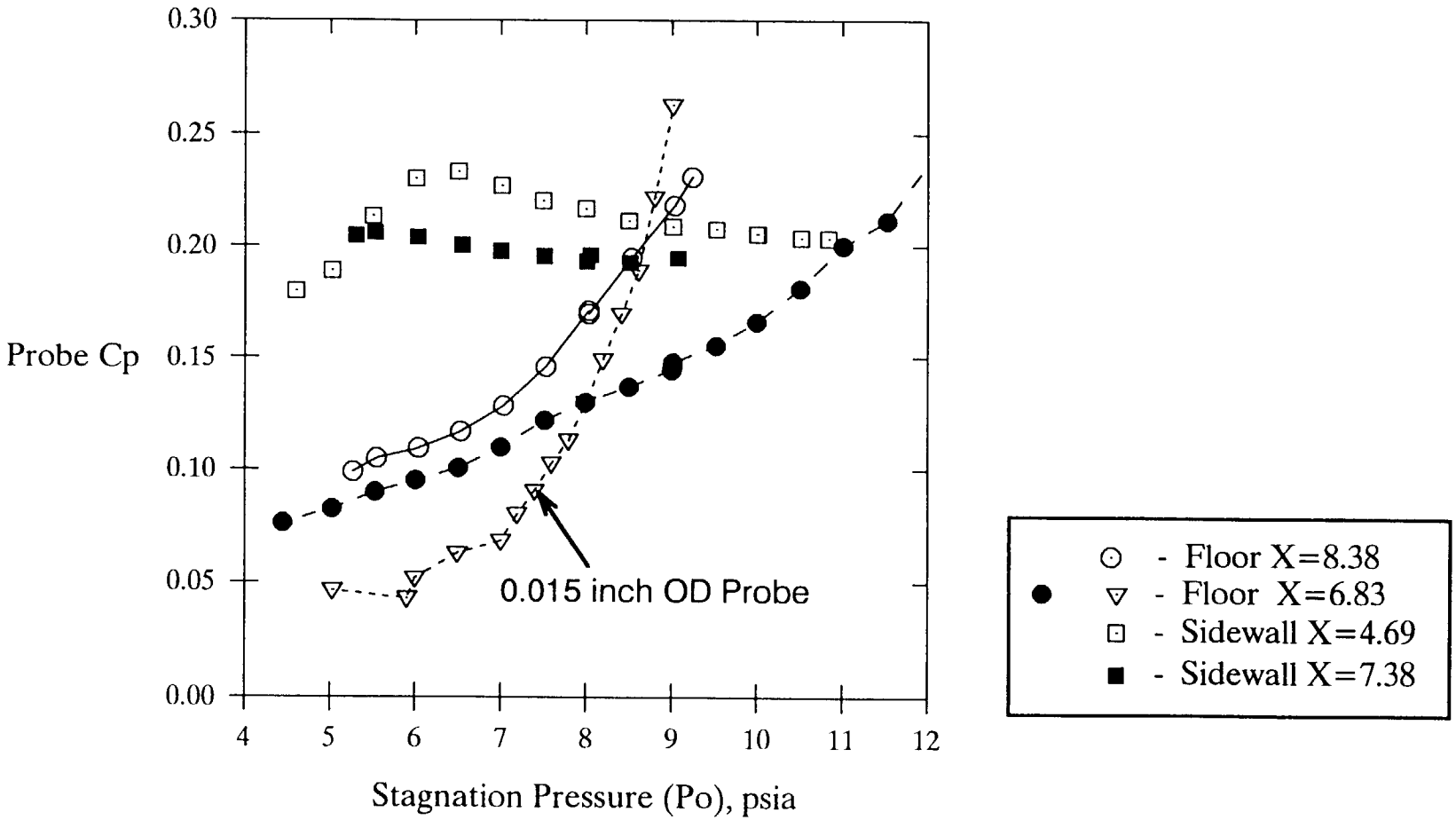


Fig. 12 - Comparison of Preston tube data from the PoC test section

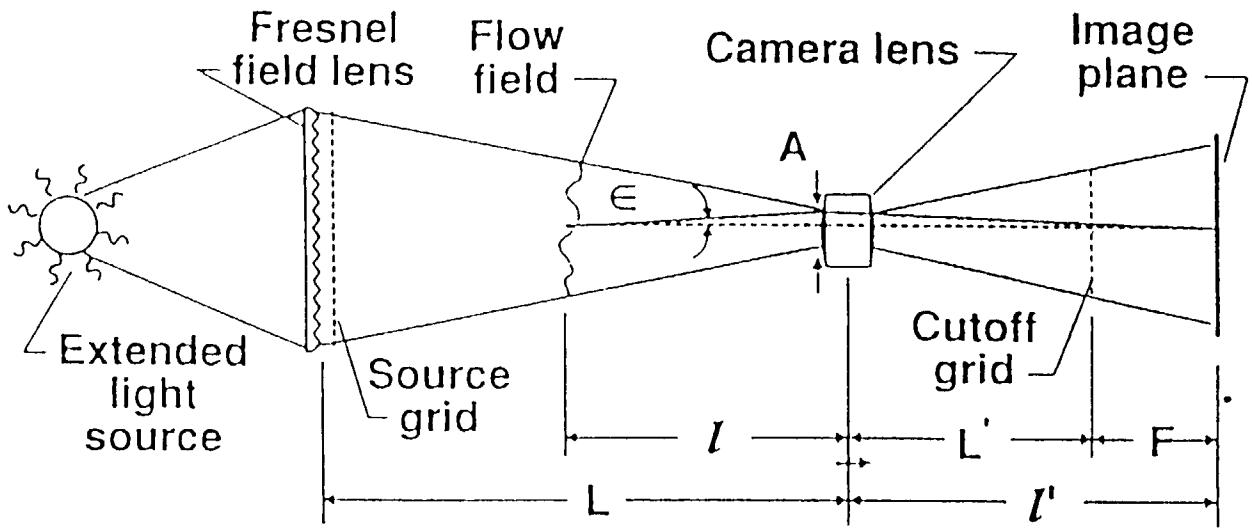


A = 5 inches; Focal Length = 16 inches
L = 96 inches; /'= 24 inches

Fig. 13 - Layout of the focusing schlieren systerm used with the PoC

# PoC Focusing Schlieren Visualization

Test Section Floor (X=6.83); Focus Plane on Centerline; Mach 1.6 Operation

Po = 6.8 psia Transitional Boundary Layer

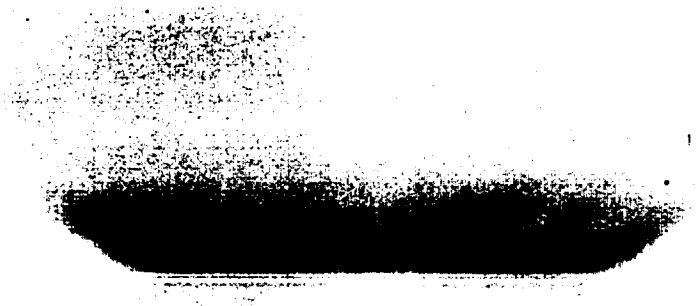

Po = 11 psia Turbulent Boundary Layer

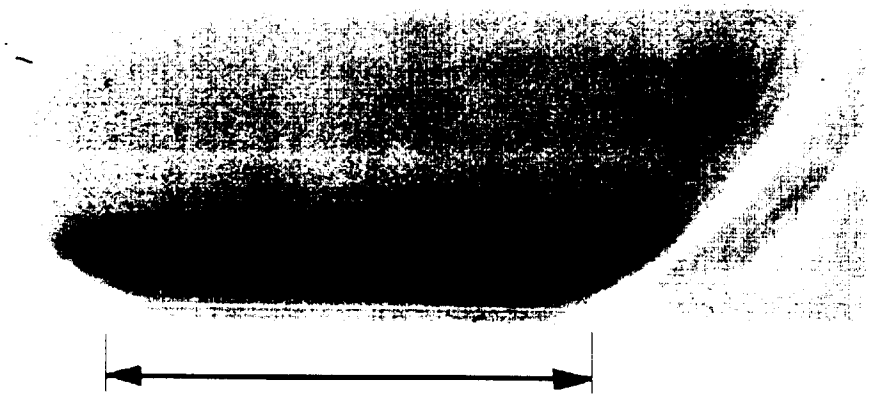


Fig. 14 - Visualization of PoC boundary layers on the test section floor

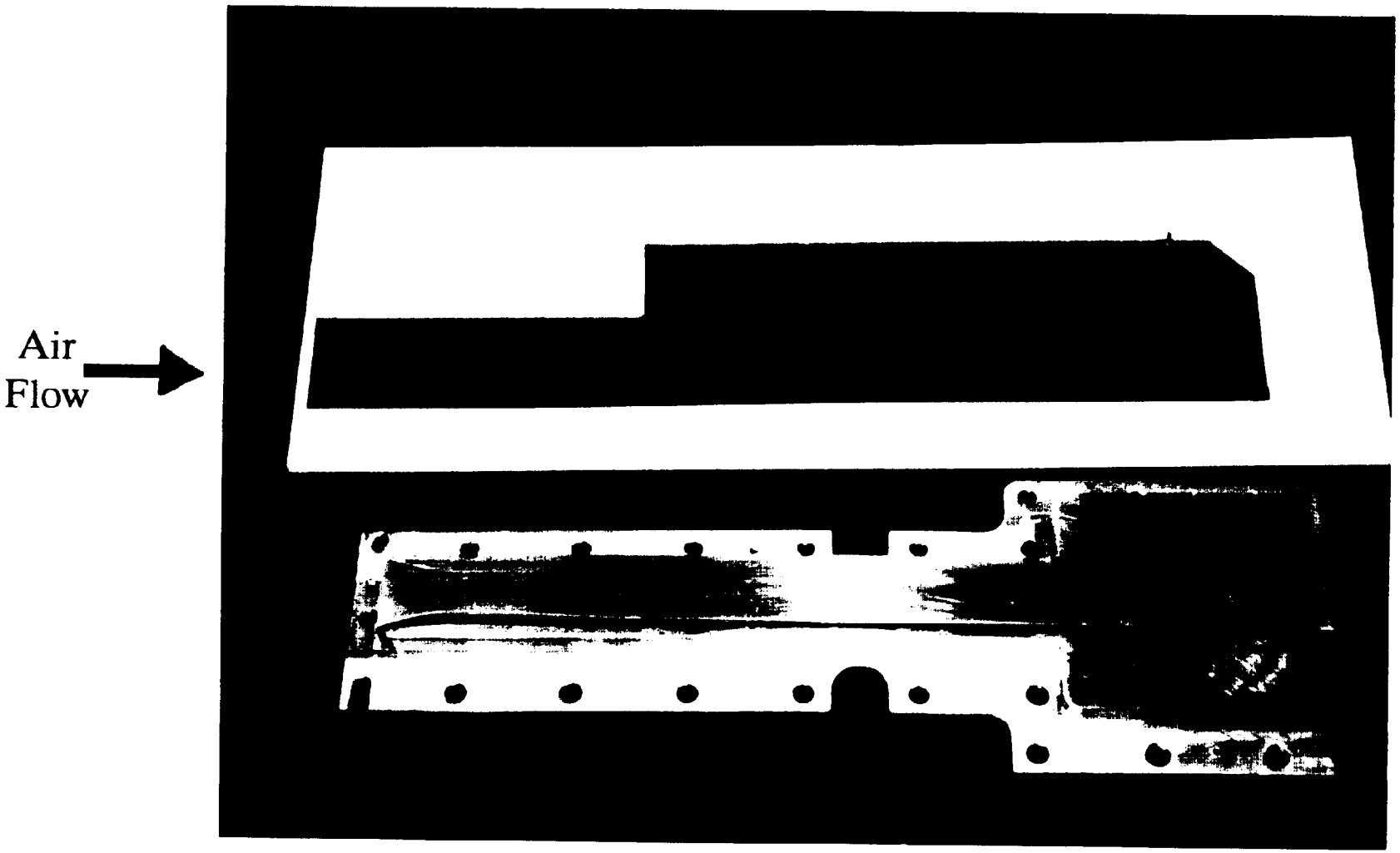


Fig. 15a - Hot-film array and special split PoC window blank before installation

PoC Hot-Film Array Setup
February 1993

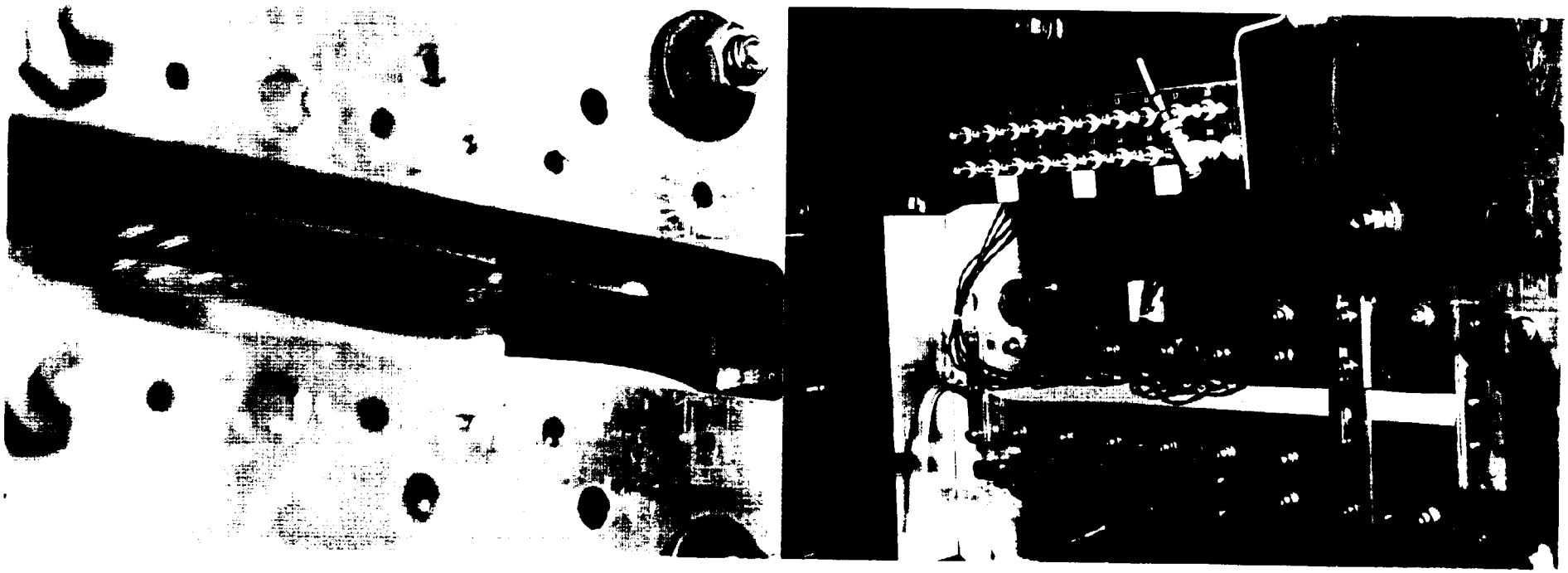

Hot-Film Array Bonded to the PoC Nozzle/Test Section Top Wall

Electrical Connections to the Hot-Films Through the Two-Piece Window Blank

COLOR PHOTOGRAPH

Fig. 15b - Hot-film array setup in the PoC supersonic wind tunnel

# PoC Hot-Film Array Data at Mach 1.6

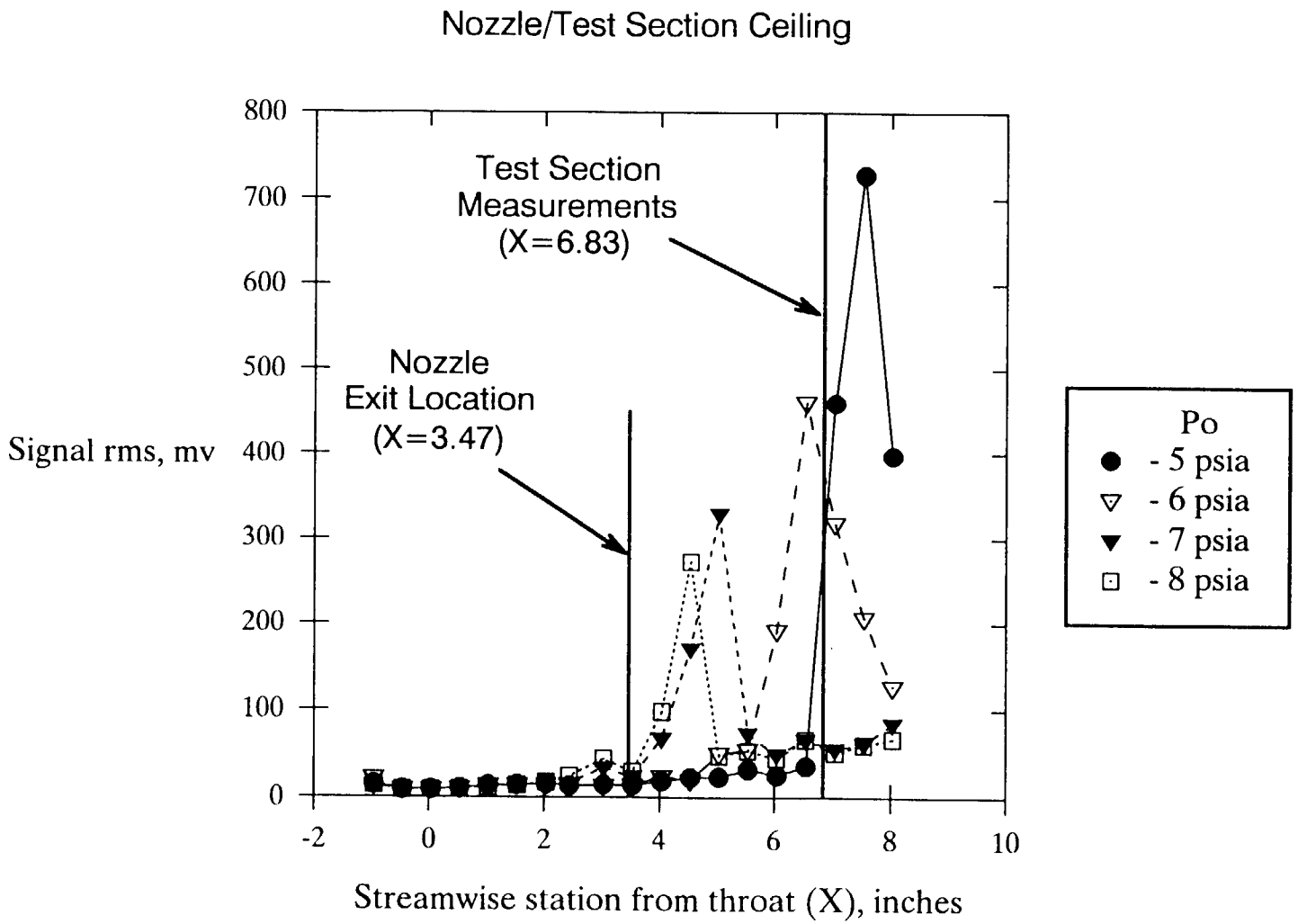


Fig. 16 - Hot-film data from the PoC nozzle and test section ceiling

# PoC Test Section Pitot Data

Nozzle Exit Centerline (X=3.47); 0.1 inch Probe dia.; Mach 1.6 Operation

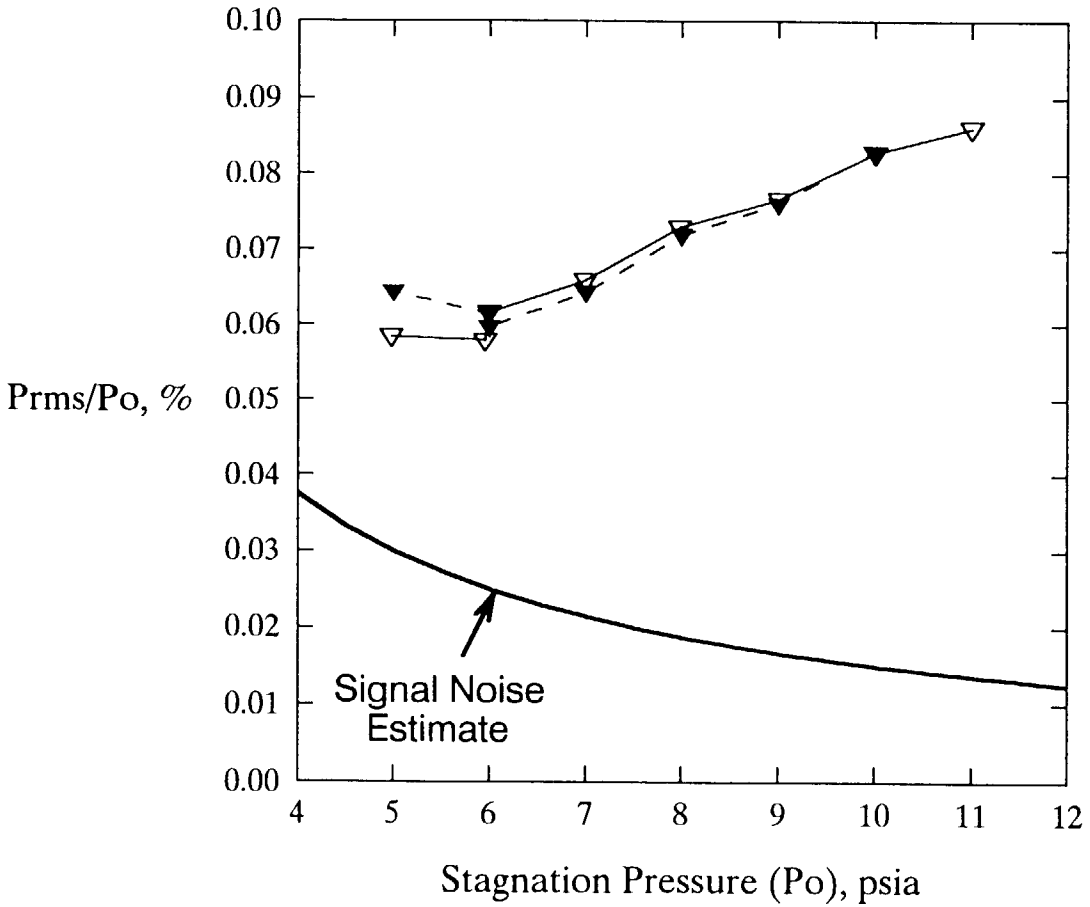


Fig. 17 - Turbulence measurements in the PoC test section

# PoC Test Section Pitot Data

Nozzle Exit Plane (X= 3.47); 0.5 inch Above Floor; 0.1 inch Probe dia.; Mach 1.6 Operation

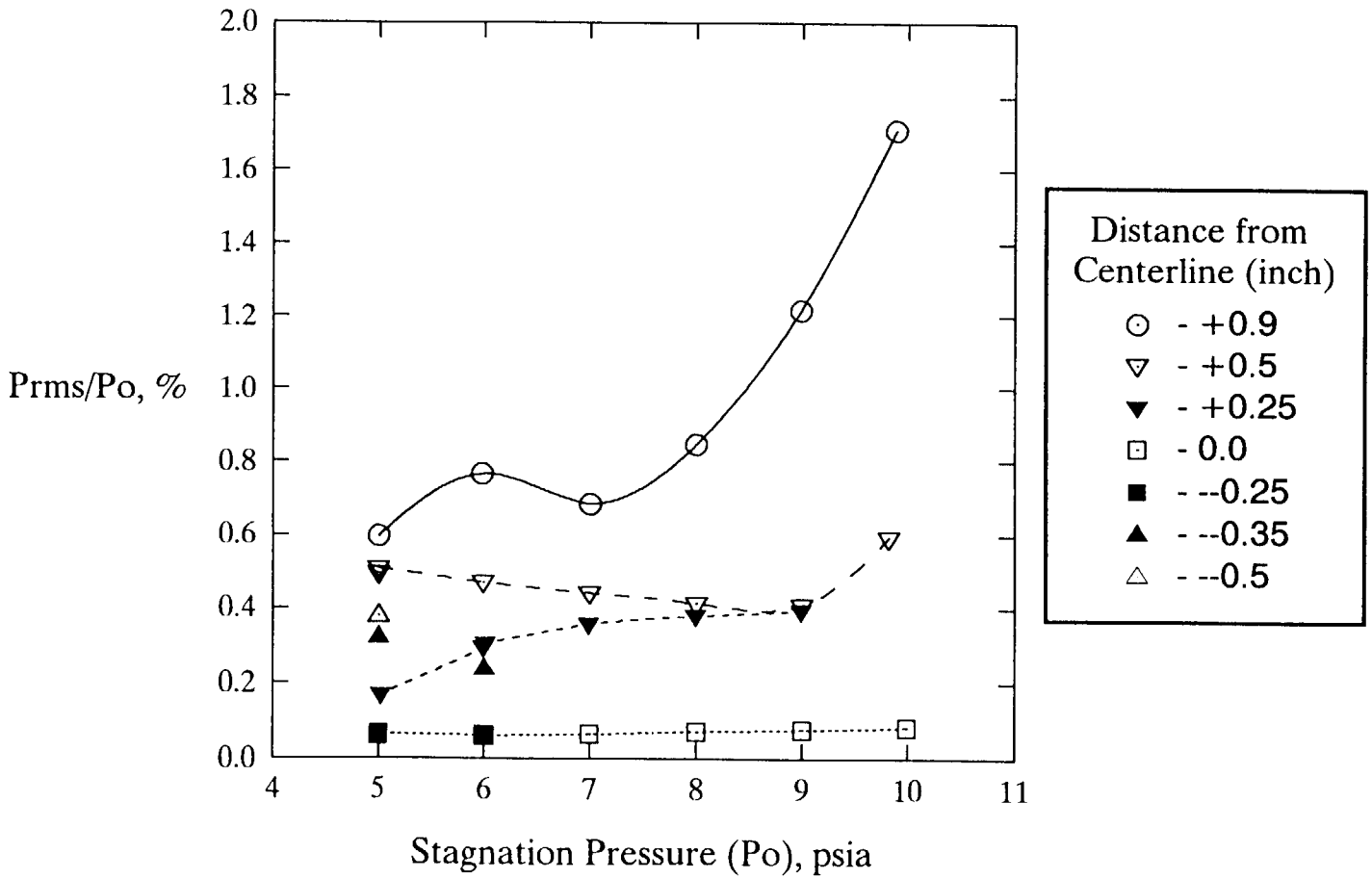


Fig. 18 - Turbulence measurements at the PoC nozzle exit

# PoC Preston Tube Data

Floor Mounted 0.015" OD Probe; 1.05 inch From Nozzle Exit (X=4.52); Mach 1.6 Operation

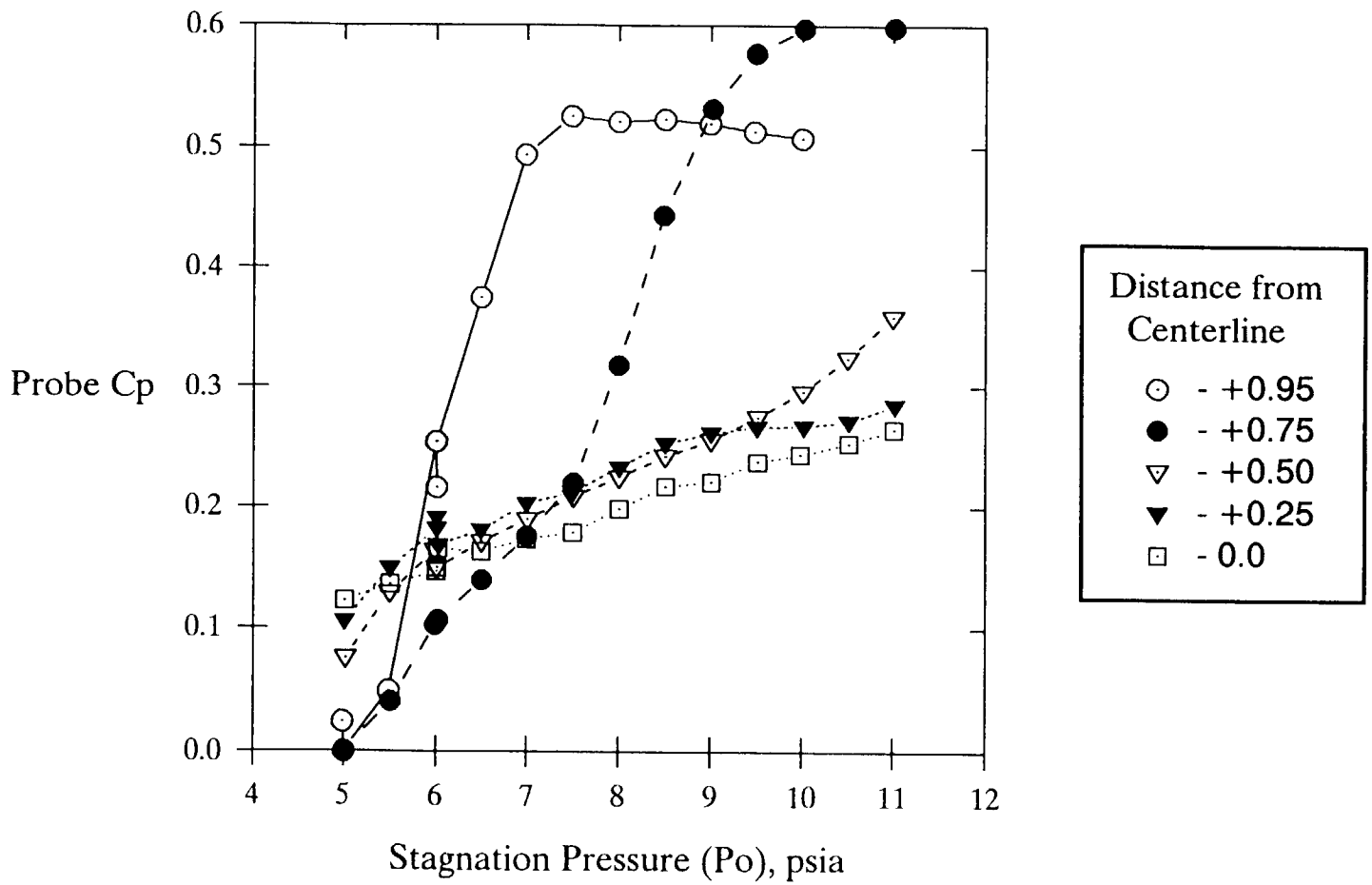


Fig. 19a - Preston tube data on the PoC floor at X = 4.52 inches

# PoC Preston Tube Data

Floor Mounted 0.015" OD Probe; 3.36 inches From Nozzle Exit (X=6.83); Mach 1.6 Operation

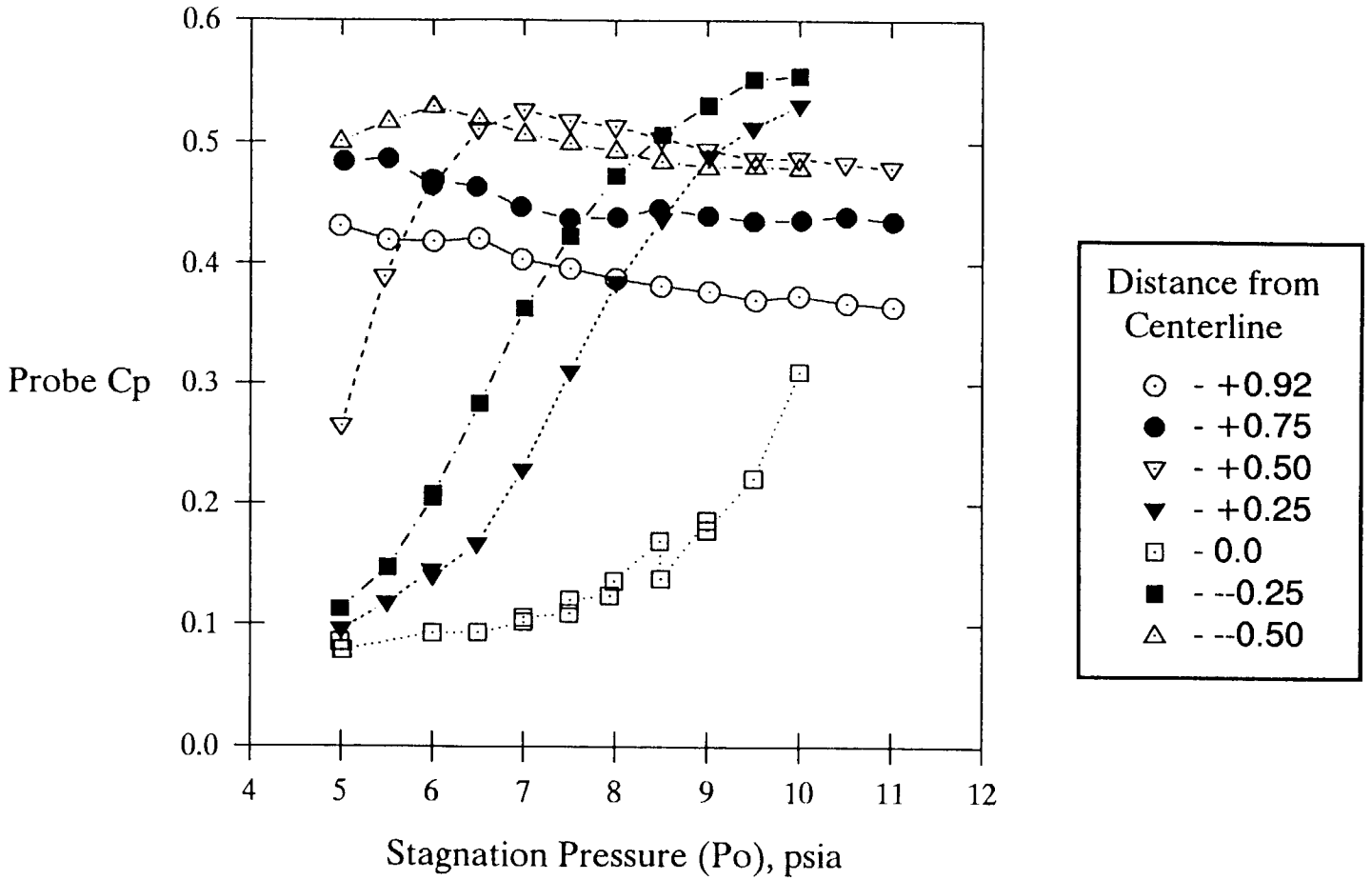


Fig. 19b - Preston tube data on the PoC floor at X = 6.83 inches

# PoC Preston Tube Data

Floor Mounted 0.015" OD Probe; 4.91 inches From Nozzle Exit (X=8.38); Mach 1.6 Operation

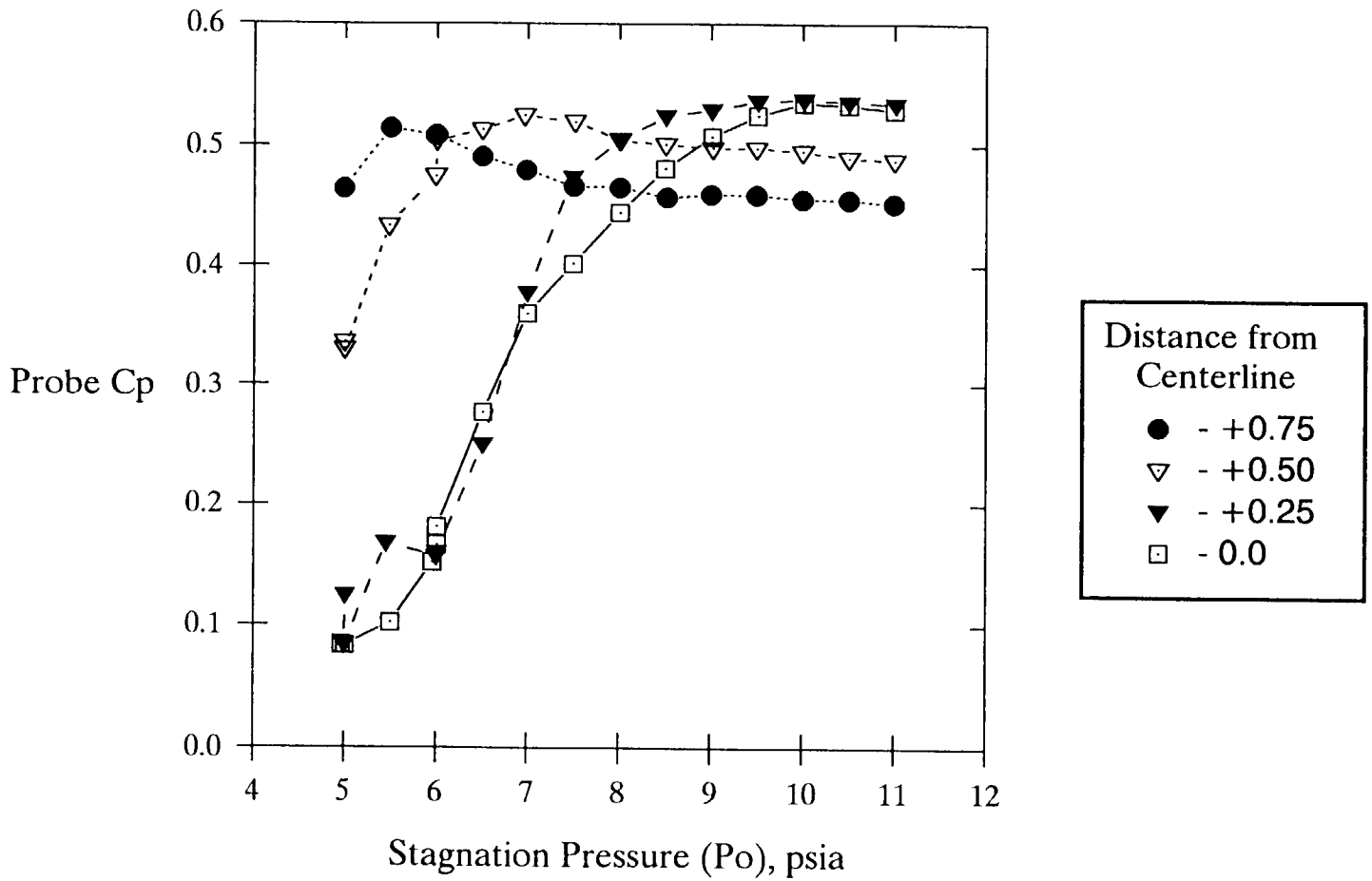


Fig. 19c - Preston tube data on the PoC floor at X = 8.38 inches

# PoC Preston Tube Data

Ceiling Mounted 0.015" OD Probe; 3.36 inches From Nozzle Exit (X=6.83); Mach 1.6 Operation

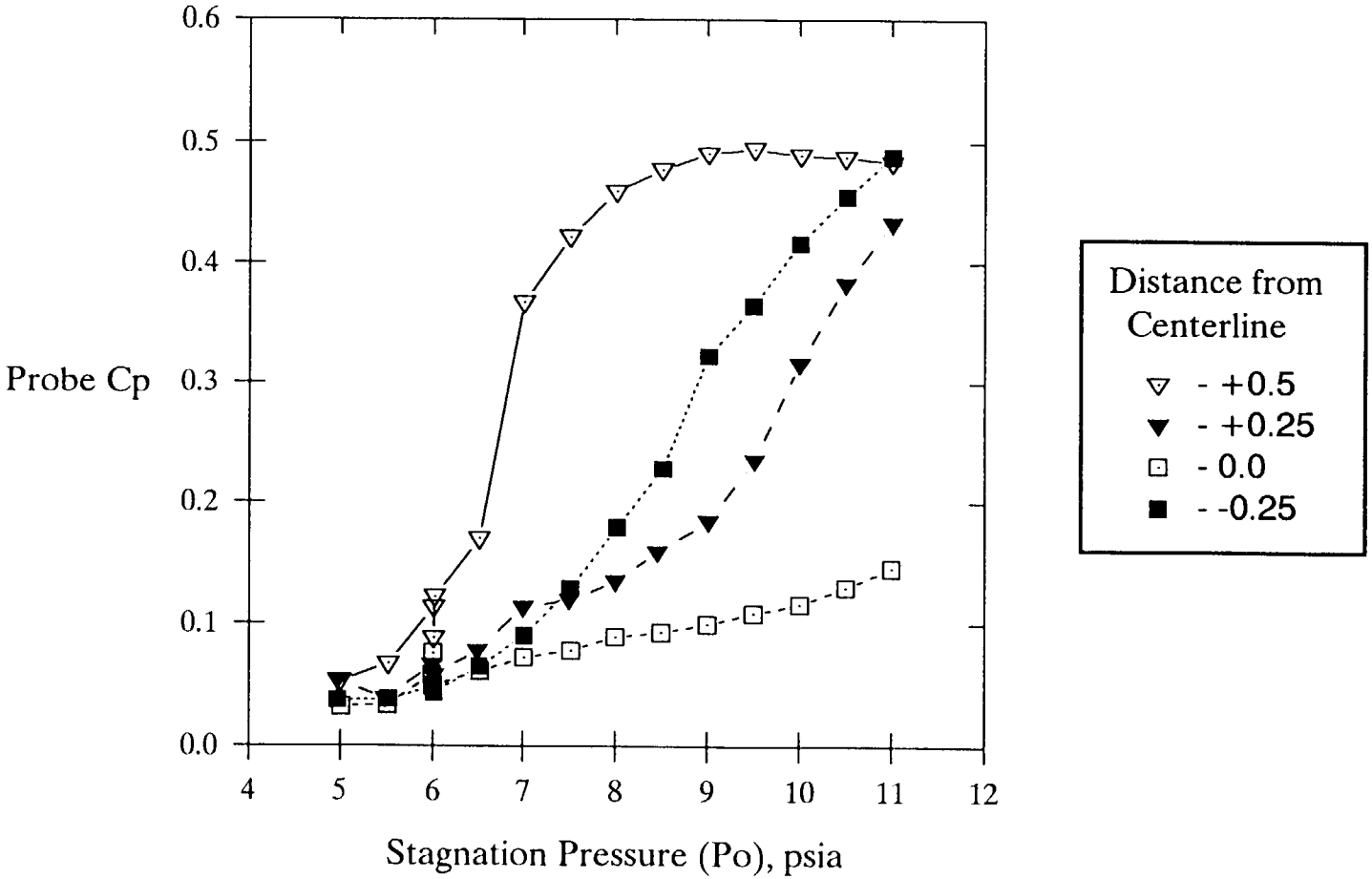


Fig. 20 - Preston tube data on the PoC ceiling at X = 6.83 inches

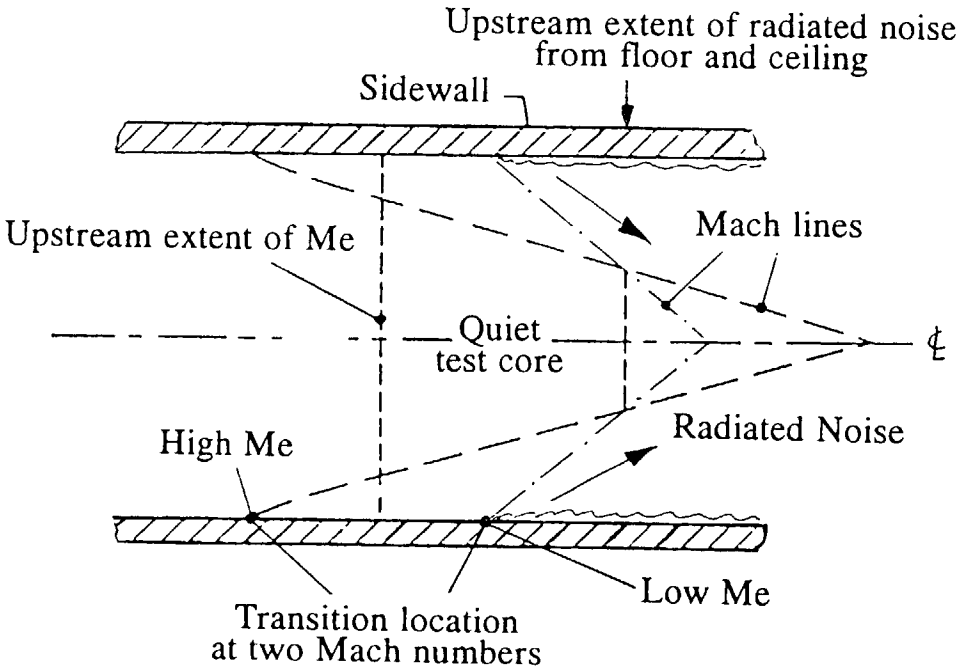


Fig. 21 - Potential boundaries of a quiet test core at two Mach numbers

# APPENDIX A

# Requirements Document

for the

# Laminar Flow Supersonic Wind Tunnel

in the

# Fluid Mechanics Laboratory

# NASA, Ames Research Center

# Moffett Field, California

April 15, 1992

by: Jim Laub
Stephen Wolf
Lyn King
Dan Reda

## Table of Contents

## Purpose and Scope

The purpose of this Requirements Document is to serve as a guide for Code E to design and fabricate the Laminar Flow Supersonic Wind Tunnel (LFSWT). The LFSWT will operate continuously at Mach 1.6 over a stagnation (Po) pressure range from 5 to 20 psia. This document will be reviewed periodically and will be revised as the need arises and is agreed upon by the design engineering project manager and the research team project manager. The scope of this document establishes the parameter guidelines from which this facility is to be designed. Specifically, this guide provides:

1. Divides the wind tunnel components into logical work packages
2. A description of each design package
3. Describes areas of concern
4. Identifies the person (s) responsible for designing each component and the RFR interface
5. Specifies the estimated design schedule for each component
6. Specifies the estimated design cost plus a 20% Code E contingency
7. Specifies the parameters and tolerances required for a successful design

It should be noted that all schedule and cost estimates have been generated through Code EEF supplied data and are based on the best information available at the time. These estimate are subject to change as more current information becomes available. Further, all of the design parameters have been supplied by the LFSWT project team. These parameters will become more refined as research continues but will remain basically unchanged.

This Requirements Document, dated April 1992, contains the official design requirements for a Mach 1.6 LFSWT in the FML.

## 3.0 Black Box

3.1 Description

The Black Box is the first pressure reducer and flow conditioner located upstream of the Settling Chamber. This component will attach to the settling chamber through an adaptor and is proposed to contain a number of porous cylindrical pressure reducing components. These components, coupled with a possible honeycomb flow straightener is expected to enhance the flow conditioning requirements placed upon the Settling Chamber.

3.2 Area of Concern:

Being designed as the first pressure reducer, it is important that the Black Box drops the inlet conditioned air pressure and velocity from a pressure of ~40 psia to the required pressure equal to the desired stagnation pressure (Po) set point plus the pressure drop across the Setting Chamber flow conditioning components. The integrity of the Black Box must be capable of continuous operation at up to 21 lbs/sec flow rates while reducing pressure without collapsing or rupturing internal flow conditioning components.

3.3 Task Assignment: Gary French

Customer Interface: Steve Wolf/Jim Laub

3.4 Design Schedule: 2/92 through 4/92

- Engineering: 100 hrs.
- Drafting: 120 hrs.
- Estimated Design Cost $9,240

3.5 Design Parameters: To be determined by design engineer.

- When operating at sub atm pressures, the Black Box cannot leak.
- Length: 25"
- Overpressure relief device may be required. The relief device must be capable of pressure cycling on the order of 5 to 60 psia.
- Operating range, 5 to 60 psia and air flows up to 21 lbs/sec.
- Modular design for maintenance purposes
- Vibration isolation between settling chamber and the Black Box
- Minimum inlet pressure is 20 psia at 5.66 lbs/sec. flow.

## 4.0 Settling Chamber

4.1 Description:

The Settling Chamber (SC) is the primary flow conditioning component. The flow enters the SC from the Black Box and exits at the desired Po. The air will flow through a; Rigimesh (Type Z) flow spreading cone, Rigimesh (Type Z) sheet, honeycomb, and four screens. The SC must be of modular design such that screens can be added or removed as dictated by pressure drop requirements, flow quality at a given Po and maintenance.

4.2 Areas of Concern:

1. Maximum length
2. Cone integrity and flow requirements (max flow=21 lbs/sec)
3. Flexibility for component array changes as needed
4. Number of components necessary to provide low-disturbance free stream at the contraction entrance
5. Ease of maintenance

4.3 Task Assignment: Gary French

Customer Interface: Steve Wolf/Jim Laub

4.4 Design Schedule: 2/92 through 7/92

- Engineering: 200 hrs.
- Drafting: 300 hrs.
- Estimated Design Cost $21,000

4.5 Design Parameters:

- Maximum length = 164.69"
- Minimum length = 92.69"
- SC C/L height = 72" above floor
- Mating surface between SC and entrance to contraction must be flush to ± 0.001"
- Cone housing length = 56.69"
- Honeycomb length = 12" ±0.015" having no seams
- Total length of screen holders = 96" max.
  24" min.
- The screen holding area length of the SC must be adjustable to 96"
- Honeycomb core size = 0.25"
- Screen = 42 mesh, 40.9% solidity. Min. screen separation = 1"

## 5.0 Nozzle/Contraction

5.1 Description:

The nozzle/contraction consists of a three-dimensional contraction, a two dimensional throat and the supersonic nozzle. The nozzle/contraction accelerates the low disturbance SC flow to Mach 1.6 at the nozzle exit. At this time, one nozzle (M=1.6) is required. However, this nozzle must be designed in such a manner as to allow for easy and quick interchange with future nozzles. The support structure should be designed to accommodate the possibility of a future flexible plate nozzle with upper and lower wall accessibility. The air flow should see no joints on the upper or lower walls of the nozzle/contraction. Optical access is required through both side walls using Zelux-W polymer material for the windows. Instrumentation and probe access is required on the sidewalls.

5.2 Areas of Concern:

1. Surface finish requirements
2. Shape conformity
3. Joint with test section
4. Ease of nozzle change
5. Leakage around window

5.3 Task Assignment:
Dan Kalcic

Customer Interface:
Steve Wolf
Lyn King/Jim Laub

5.4 Design Schedule: 2/15 through 5/15

- Engineering: 212 hrs
- Drafting: 120 hrs.
- Estimated Design Cost $13,944

5.5 Design Parameters:

- Inlet size: 39.24" ±0.015" square
- Overall contraction length to nozzle throat: 48.0" ±0.015"
- Nozzle width: 16" ±0.005" continuous
- Nozzle length (M=1.6)= 27.376" ±0.005"
- Nozzle exit height: 8" ±0.005" continuous and parallel Spanwise

- Contraction and nozzle finish = 10L ± 0/4
- Steps and Gaps should not exceed ±0.001"
- Nozzle shape and contraction contour for M=1.6 supplied to Code E separately
- Zelux-W polymer windows extending from US of the throat through the test section and overlapping the nozzle walls
- All walls and windows must seal leak tight
- The 5 th order Polynomial formula for the contraction sidewall, floor and ceiling follows:

All dimensions are in inches

Sidewalls

° $Y= -69.72 (X/L)^5 + 174.3 (X/L)^4 -116.2 (X/L)^3 + 19.62$
where L = 20" = Length of contraction and X = 0 to 20"

Floor & Ceiling

° $Y= -98.7882 (X/L')^5 + 246.9705 (X/L')^4 - 164.647 (X/L')^3 +19.62$
where L'= 48" and X = 0 to 48"

## 6.0 Test Section

6.1 Description

The LFSWT will require two test sections (TS) for the M=1.6 case. One TS will be used for calibration purposes and will be instrumented accordingly. The second will accommodate a model and be appropriately instrumented. Both TS's will require flow visualization from all sides. The calibration TS will require an adjustable supersonic diffuser and an instrumentation probe capable of traversing into the nozzle for boundary layer as well as free stream measurements. The test, TS will require a model support system.

6.2 Areas of Concern:

- TS vibration isolation from the supersonic diffuser and primary injectors
- Flow visualization of all walls
- Model support
- Will tunnel start with a swept wing mounted in the TS?
- Traversing probe capable of entering the nozzle throat area
- Easy access and removal/replacement

6.3 Task Assignment:

Dan Kalcic

Customer Interface:

Dan Reda/Lyn King

Steve Wolf/Jim Laub

6.4 Design Schedule and Man hrs. 2/92 through 4/92

- Engineering: 164 hrs.
- Drafting: 120 hrs.
- Estimated Design Cost $11,928

6.5 Design Parameters:

- Inlet size = 8" high x 16" wide
- TS length = 32"
- TS wall divergence = 0.25° Top & Bottom
- TS C/L height = 72" above floor
- Exit size = 8.638" high x 16" wide
- TS roughness = L10 ±0/4
- Steps and Gaps should not exceed ±0.001"
- All walls must seal leak tight
- Zelux-W polymer windows are required on all four walls.

## 7.0 Supersonic Diffuser

7.1 Description:

The two-dimensional supersonic diffuser (SSD) is the area in which the supersonic flow from the TS is slowed and press. recovery begins. The SSD shall be of modular design such that it can be removed or attached to the TS without affecting the operation of the primary injectors. It will be necessary to design the SSD for adjustable height due to model blockage in the TS. The SSD will have to be at its greatest area ratio with respect to the TS during the wind tunnel start and then decrease to compensate for model blockage. Optical access will be required of the SSD using the same Zelux-W polymer windows aforementioned.

7.2 Areas of Concern:

1. Leaks
2. Speed and freedom of movement
3. Adjustment and calibration procedures

7.3 Design Task Assignment:
Brooke Smith/Gary French

Customer Interface:
Steve Wolf/Lyn King
Jim Laub

7.4 Design Schedule: 2/92 though 4/92

- Engineering: 240 hrs.
- Drafting: 160 hrs.
- Estimated Design Cost $16,800

7.5 Design Parameters:

- SSD length = 41"
- Minimum throat height = 6.056" ±0.005 and walls must be parallel spanwise
- Maximum ramp height = 1.112" ±0.005
- Floor and ceiling wall divergence = 0.25°
- Raising and lowering of the SSD during operation is necessary. A ±0.005" tolerance is required on final position
- Ramp length = 8"
- Variable exit cross-section = 6.344"-8.638" high; 16" wide
- The SSD must be leak tight.
- Vibration isolation from the TS is required
- Modular design to accommodate ease of removal/replacement
- Zelux-W polymer windows in the sidewalls.

## 8.0 Primary Injector

8.1 Description:

The drive system consists of the primary and secondary stages of ambient injection and a supersonic diffuser. It is imperative that structural vibrations due to the drive system be isolated from other components of the wind tunnel. It is also required that total access to the TS not be compromised by the primary injectors.

The primary injectors must have an adjustable throat to optimize fine tuning of both mass flow and Mach#. In the M=1.6 case, only the primary injectors are needed. Consequently, a higher mass flow and lower M# is required, not so in the M=2.5 case. The primary injectors must therefore be designed to accommodate a range of M=1.8 and 2.2 and a total mass flow of 62-124 lbs/sec flow.

8.2 Areas of Concern:

1. What is the baseline operating condition of the primary injectors at M=1.6?
2. Adjustment procedure and calibration
3. Ability to repeat Mach #/mass flow
3. Vibration is of major concern
   - The primary injectors must be isolated from TS.
   - Primary injector flow is unstable so structural vibration is expected to be high.

8.3 Task Assignment: Brooke Smith/Gary French

Customer Interface: Steve Wolf/Jim Laub

8.4 Design Schedule: 3/92 through 7/92

- Engineering hrs.: 240
- Drafting hrs.: 240
- Estimated Design Cost: $20,160

8.5 Design Parameters:

- Variable Throat Area range= 90-180 sq. in.
- Variable Exit Area range= 169-338 sq. in.
- Mach# Range= 1.8-2.2
- Variable Exit Cross Section= 16" wide X 10.56"- 21.12" high
- Throat Length to Exit= 32"
- Injection angle (relative to WT C/L)= 10°
- Total mass flow range= 62-124 lbs/sec.

- Instrumentation; two static pressure taps on C/L of each injector one inch apart. The first tap should be located two inches US of the exit and the second, one inch US of the exit.
- Tolerance= 0.015"
- Zero leak rate DS of throat
- Throat requires a 32 finish
- Access is required to the injector throat and exit area for on-site calibration
- An injector measurement system is required for movement of injector components to pre-determined positions. Position repeatability is essential.

## 9.0 Mixing Region

9.1 Description:

The Mixing Region (MR) is a rectangular shaped flow duct in which pressure recovery and free stream jets from the dual primary injectors and test section join.

9.2 Areas of Concern:

- Leaks

9.3 Task Assignment: 2/92 through 3/92

- Brooke Smith/Gary French
- Customer Interface: Steve Wolf/Jim Laub

9.4 Design Schedule and Man/hrs.

- Engineering: 25 hrs.
- Drafting: 30 hrs.
- Estimated Design Cost: $2,310

9.5 Design Parameters:

- MR length = 51.68"
- Exit cross section = 41.246" high X 29.742" wide
- Provide 3 pressure taps on the C/L of a side wall and on the exit plane of the SSD and both primary injectors.
- The MR must be leak tight.

## 10.0 Secondary Injectors

10.1 Description:

The secondary injectors are designed to assist the primary injectors pull the free stream flow through the TS at Mach numbers up to 2.5 and at lower Po's, down to 5.0 psia. Without the secondary injectors, the Mach number and mass flow of the primary injectors fail to meet the Po=5 criteria at Mach numbers $\geq$ 2.0. It should be noted that design of the secondary injectors is important for future Mach number requirements of the LFSWT. However, fabrication will not be performed as previously scheduled. The secondary injectors will not be required for the M=1.6 case.

10.2 Areas of Concern:

- Flexible design to meet future research requirements
- FML roof loading requirements based on injector inlet weight

10.3 Task Assignment:
Brooke Smith/Gary French

- Customer Interface:
Steve Wolf/Jim Laub

10.4 Design Schedule and Man/hrs: 3/92 through 7/92

- Engineering hrs.: 120
- Drafting hrs.: 120
- Estimated Design Cost: $10,080

10.5 Design Parameters

- Throat area (mass flow: 34.65 lbs/sec) 106 sq. in. ±0.005"
- Exit area (Mach =1.6) 152.53 sq.in ±0.015
- Exit Cross Section = 41.246" high X 3.698" wide
- Throat to exit length = 20"
- Throat to exit finish should be 32
- Injection angle (relative to C/L) = 10°
- Total mass flow = 69.3 lbs/sec
- Length of sidewall flare section = 12"
- Provide 3 pressure taps on each injector C/L, one inch apart working US from the exit plane.
- Secondary Injector attachment points must be sealed leak tight and must be faired smooth at the exit area.

## 11.0 Subsonic Diffuser

11.1 Description:

The subsonic diffuser (SsD) is the last component of the wind tunnel before flow enters the manifold. The function of the subsonic diffuser is to decelerate the injector and test section flows to subsonic speeds before reaching the isolation valve separating the wind tunnel from the manifold. The diffuser will change in geometry from rectangular to round and will pierce the test cell east wall. The flow entering the SsD is inherently unstable and will generate substantial loads.

11.2 Area of Concern:

- Vibration loads

11.3 Task Assignment:
Robert Press

- Customer Interface:
Steve Wolf/Jim Laub

11.4 Design Schedule and Man/hrs: 3/92 through 4/92

- Engineering hrs.: 50
- Drafting hrs.: 60
- Estimated Design Cost: $4,620

11.5 Design Parameters:

- Inlet cross-section = 41.246" high X 36.758" wide
- Outlet cross-section = 60" diameter with flange bolt pattern to match 60" isolation valve bolt pattern.
- Length with 7°total angle = 190"
- Inlet C/L height = 72" above floor
- Exit C/L height = 83" above test cell ground level
- C/L inclination = 3.3°
- Design for high vibration loads and acoustic fatigue
- The SsD must be isolated from US components.

## 12.0 Controls

12.1 Description:

The control system for Test Cell #1 is unique in the FML. It will provide safe control and operation of the HPA as well as provide accurate control of test parameters for the LFSWT. The Genius based system will allow remote opening and closing of the 60" wind tunnel/manifold isolation valve and remote "E" stop of compressor. The control system will not replace the current blue wall mounted control box but will complement it though an umbilical cord that will extend from the bottom of the blue box to a researcher selected remote site. The control system is based on the FML Genius system and is complemented by Intouch man/ system interface software running on a 486/33 mHz PC.

12.2 Areas of Concern:

- HPA system control, safe and orderly start and shutdown
- Fail safe operation of the HPA system
- 60" isolation valve control and fail safe mode
- Stability of settling chamber Po and To set points

12.3 Task Assignment: David Wong

- Customer Interface: Dave Yaste/Steve Wolf/Jim Laub

12.4 Design schedule and Man/hrs.: 1/92 through 3/92

- Engineering hrs.: 200
- Estimated Design Cost: $8,400

12.5 Design Parameters

- Two second air tight closure of 60" isolation valve
- Control of settling chamber set point pressure (psia) to the second decimal place
- "E" stop of HPA system, closure of 60" isolation valve
- Closure of 60" isolation valve, orderly shutdown of HPA system

## 13.0 General

13.1 Description:

The general package of this requirements document pertains to the following:

- Maximum lengths of the wind tunnel
- Support structure, inside and outside of TC #1
- Building Mods

13.2 Area of Concern:

- Ease of WT individual component removal and reinstallation
- Research flexibility compromise
- Roof loading of the secondary injector intakes
- Bending moment and seismic loading of wind tunnel/manifold and support structure

13.3 Task Assignment: Ray Shuler/Robert Press

- Customer Interface: Jim Laub /Steve Wolf

13.4 Design Schedule and Man/hrs.: 4/92 through 7/92

- Engineering hrs: 100
- Drafting hrs: 200
- Estimated Design Cost: $12,600

13.5 Design Parameters:

- Test Cell length: 38'
- Distance between test cell east wall and 60" valve flange =107"
- Maximum length of LFSWT in High Bay= 42.74"
- Maximum total length of LFSWT= 49.312'

## 14.0 Project Management

14.1 Project Manager: Jim Laub
- ° Project Engineer: Steve Wolf
- ° Project Coordinator: Amy Lacer
- ° Project Consultants: Lyn King (CFD), Dan Reda (Transition) and Dave Yaste (Controls and Facility Mods)

14.2 Project Manager Code E Design:
- Owen Greulich: 234 hrs. : Estimated Cost: $9,828
- Bob Meneely (Consultant): 390 hrs.: Estimated Cost: $16,380

**14.3 Total hrs.: 3,745**
- **° EMY: 1.99**

- **Total Estimated Design Cost:**
  - **° $157,290**

## 15.0 Summary

This document has been written to satisfy the need for guidelines to design and fabricate a LFSWT-I. It should be noted that all parameters of design are to be held to the specific tolerance quoted (± 0.015") unless otherwise specified.

This Design Requirements Document contains the following:

- Specific guidelines & numeric parameters for design
- The name(s) of the individuals assigned to a specific design task. It also names the customer (RFR) interface
- An estimated start/design task completion date
- An EMY and design cost estimate

It is recognized that both Code EEF and Code RFR have the right to amend any part or parts of this design package document upon agreement of/by both parties for the success of the project.

# APPENDIX B

# DEVELOPMENT OF THE NASA-AMES LOW-DISTURBANCE SUPERSONIC WIND TUNNEL FOR TRANSITION RESEARCH UP TO MACH 2.5

Stephen W.D. Wolf*, James A. Laub**, Lyndell S. King***, and Daniel C. Reda+
Fluid Mechanics Laboratory
Fluid Dynamics Research Branch
NASA Ames Research Center
Moffett Field, California 94035-1000

## Abstract

A unique, low-disturbance supersonic wind tunnel is being developed at NASA-Ames to support supersonic laminar flow control research at cruise Mach numbers of the High Speed Civil Transport (HSCT). The distinctive aerodynamic features of this new quiet tunnel will be a low-disturbance settling chamber, laminar boundary layers on the nozzle walls and steady supersonic diffuser flow. Furthermore, this new wind tunnel will operate continuously at uniquely low compression ratios (less than unity). This feature allows an existing non-specialist compressor to be used as a major part of the drive system. In this paper, we highlight activities associated with drive system development, the establishment of natural laminar flow on the test section walls, and instrumentation development for transition detection. Experimental results from an 1/8th-scale model of the supersonic wind tunnel are presented and discussed in association with theoretical predictions. Plans are progressing to build the full-scale wind tunnel by the end of 1993.

## Symbols

| | |
|---|---|
| Cp | Pressure coefficient ($\gamma PMe^2/2$) |
| Me | Free stream Mach number |
| P | Local static pressure |
| Po | Tunnel stagnation pressure |
| $P_E$ | Exit (manifold) total pressure |
| Prms | Pressure measurement rms |
| Re | Unit Reynolds number per foot |
| To | Tunnel stagnation temperature |
| u | Local velocity in boundary layer |
| Ue | Free stream velocity |
| X | Streamwise position relative to Mach 2.5 nozzle throat station (positive downstream) |
| $\gamma$ | Ratio of specific heats |

## 1. Introduction

Aerodynamicists now consider the use of a low-disturbance or "quiet" wind tunnel as an essential part of meaningful boundary layer transition research at supersonic speeds. This realization is based on many years of experience with old "noisy" supersonic wind tunnels, and a growing respect for the pioneering research of Laufer[1,2] at the Jet Propulsion Laboratory (JPL) from the mid-1950s to the early-1960s, and the work of Pate and Schueler[3] in the late-1960s. This situation has provided the impetus for the development of a new, unique, continuously-operating Laminar Flow Supersonic Wind Tunnel (LFSWT) in the Fluid Mechanics Laboratory (FML) at NASA-Ames. This LFSWT concept is based on the now decommissioned (but soon to be rebuilt) JPL 20-inch supersonic wind tunnel, which is the first documented quiet supersonic wind tunnel.[4] The proposed test envelope for the LFSWT was chosen to cover a significant portion of the HSCT operating envelope with a Re range of 1 to 3 million per foot and a Mach number range from 1.6 to 2.5. Also, the LFSWT test envelope will cover the test conditions flown by NASA F-16XL aircraft in support of Supersonic Laminar Flow Control (SLFC) studies, as shown in Figure 1.

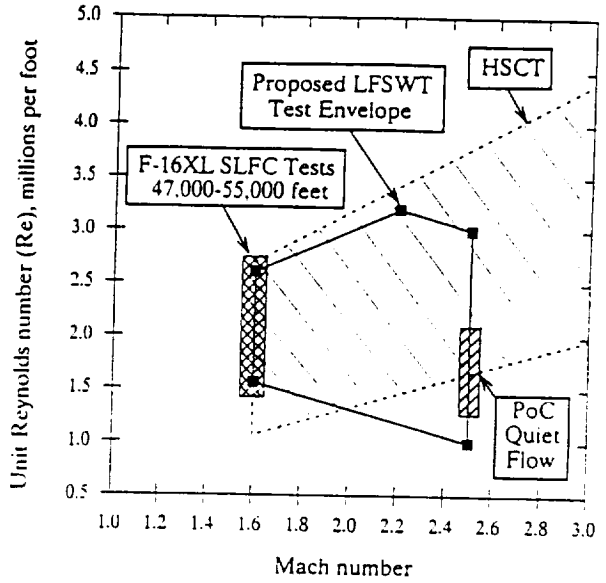


*Fig. 1 - Proposed LFSWT test envelope compared with the flight envelopes of the HSCT at cruise and the F-16XL SLFC flight tests.*

The LFSWT is currently being designed as a research tunnel with an 8 inch (20.32 cm) high, 16 inch (40.64 cm) wide and 32 inch (81.28 cm) long test section, sized to operate at mass flows up to 21 lbs/sec (9.5 kg/sec). The use of existing support equipment (the FML indraft compressor and the NASA-Ames 3000 psi (207 bar) dry air supply) will significantly reduce the project costs, and will allow the LFSWT to be brought on-line more rapidly to impact the critical technology development phase of the HSCT before 1997.

The decision to use the FML non-specialist indraft compressor to power the LFSWT created several technical concerns. The FML compressor has a measured capacity of 228,000 icfm (about 143 lbs/sec - 65 kg/sec with a minimum $P_E$ of 8 psia - 0.55 bar) and a pressure ratio of 1.8:1. Consequently, to achieve the low end of the Re range, the LFSWT must operate with a Po which is less than the minimum $P_E$. This means that the LFSWT compression ratios will be uniquely less than unity ($Po/P_E$ down to 0.625:1 with Re = 1 million per foot at Po = 5 psia - 0.34 bar). So, the utilization of the FML compressor precludes the use of a conventional drive system to achieve the desired Re range. Consequently, a novel drive system was developed using an 1/8th-scale model of the LFSWT, which we call the Proof-of-Concept (PoC) supersonic wind tunnel. The initial PoC drive system is described in detail by Wolf et al[5] and requires less than half of the normal run compression ratio. The drive system works by using compressor mass flow capability (which greatly exceeds the mass flow necessary for the test section flow alone) to drive two stages of ambient injectors, which pull the flow through the test section at low Po. Two stages of injectors became necessary so that the primary injectors could operate at a higher Mach number, which then lowered the exit pressure of the test section flow and allowed the PoC to operate at a lower Po.

* Research Scientist, MCAT Institute. Senior Member AIAA.
** Facility Operations Manager, Fluid Dynamics Research Branch.
*** Research Scientist, Fluid Dynamics Research Branch. Member AIAA.
+ Senior Research Scientist, Fluid Dynamics Research Branch. Assoc. Fellow AIAA.

This paper contains a brief description of PoC and its recent modifications for drive system tuning and quiet flow studies to aid the LFSWT design process. We describe the ongoing combination of theoretical and experimental research efforts to ensure there is quiet flow in the LFSWT. While we use the PoC for laminar flow studies, we are also developing and gaining experience with the latest instrumentation for transition research. This experience will aid our development of quiet nozzles, improve flight test measurements, and also give FML the tools required for future transition research when the LFSWT comes on-line. This activity is discussed with particular reference to hot-wires, hot-film gages, focusing schlieren, and liquid crystal coatings. We intend that this paper should help others engaged in supersonic transition research by outlining the important aspects of developing a *State-of-the-Art* supersonic transition research facility.

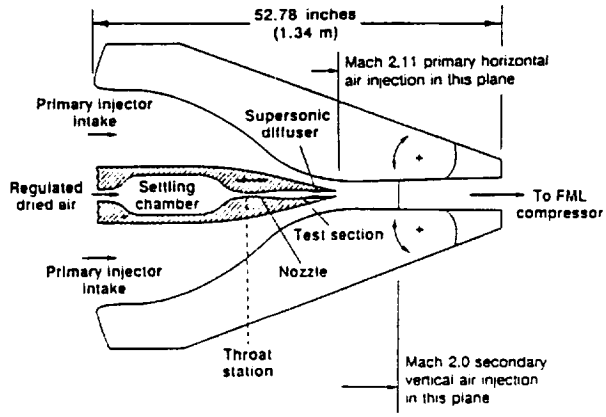


*Fig. 2 - A schematic layout of the PoC supersonic wind tunnel.*

## 2. Tunnel Hardware Development

The aerodynamic lines of the LFSWT are being studied with the aid of the PoC. A schematic of the PoC layout is shown in Figure 2 to illustrate the novel dual-stage injector drive system. It should be noted that the two stages of injectors are orientated at right angles to one another, from practical considerations. The PoC test section is 1 inch (2.54 cm) high and 2 inches (5.08 cm) wide. The only nozzle tested so far is a two-dimensional, fixed-block, Mach 2.5 type, designed according to the methodology of Riise[6] used at JPL. The nozzle design is considered long, with the surface curvature minimized. The nozzle has a throat to exit length of 5.114 inches (13 cm), with a throat height of 0.38 inch (9.65 mm). The nozzle and test section are made from 6061-T6 aluminum. The flow surfaces along the nozzle are hand finished to about a 2L standard (roughness height 2 microinches - 0.05 micron). We consider the laminar flow requirements for the nozzle surface finish at low Re to be less stringent than those required for the Mach 3.5 Langley Pilot Quiet Tunnel.[7] A two-dimensional nozzle was chosen to minimize focusing of disturbances, due to shape imperfections, on the tunnel centerline, and also to allow complete optical access to the nozzle and throat for transition studies associated with wind tunnel development. The three-dimensional PoC contraction is 6 inches (15.24 cm) long on the floor and ceiling and 2.5 inches (6.35 cm) long on the sidewalls. The sidewall contractions are shorter to make the sidewalls parallel upstream of the nozzle throat for optical access.

The test section is fed with regulated, dried air which has a dew point of about -50°F (227 K) from the existing NASA-Ames 3000 psi (207 bar) supply. Of course, the dried air is essential to eliminate any condensation effects in the test section, as found in the experimental results discussed later. The PoC dual-stage injectors draw in ambient air from the surrounding room. The exit Mach number of the primary injectors is 2.11, while the secondary injectors operate at Mach 2. The air mass flow ratio between injectors and test section rises to a massive 27:1 at the minimum Po of 5.4 psia (0.37 bar).

The secondary injectors were originally positioned for convenience 31.24 inches (0.79 m) downstream of the primary injectors. To shorten the overall drive system, the secondary injectors were redesigned to allow the separation between injector stages to be reduced to a minimum of 6.46 inches (16.41 cm). The new secondary injectors are shown with minimum stage separation in Figure 3. In addition, a family of secondary injector nozzle blocks was made to study the reduction of injector mass flow from the reported 1.648 lbs/sec to 1.099 lbs/sec (0.747 kg/sec to 0.498 kg/sec respectively), with the exit Mach number fixed at Mach 2, based on previous PoC experience.[5]

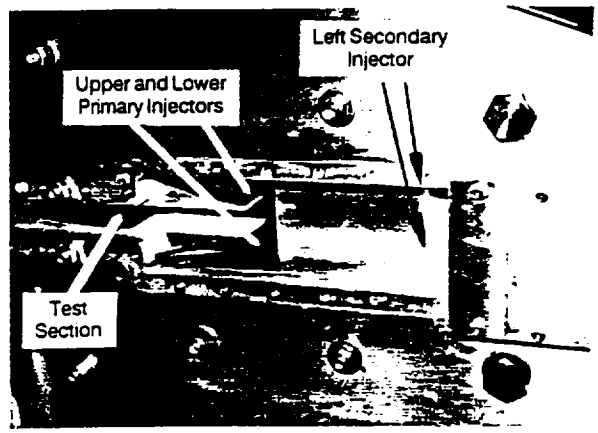


*Fig. 3 - The relative position of the primary and secondary stages of ambient injectors in the PoC, with the right-hand secondary injector and window removed.*

The PoC was initially fitted with an open two-dimensional settling chamber. This simple settling chamber was only adequate for drive system studies. We have now installed a larger three-dimensional settling chamber equipped with multiple flow straighteners and conditioners and a contraction ratio of 12:1 (based on test section area) for low-disturbance operation. A schematic of the settling chamber is shown in Figure 4, highlighting its modular design, which allows component holder interchangeability. The flow velocity in the settling chamber is 20 fps (6.1 m/sec) with Po = 15 psia

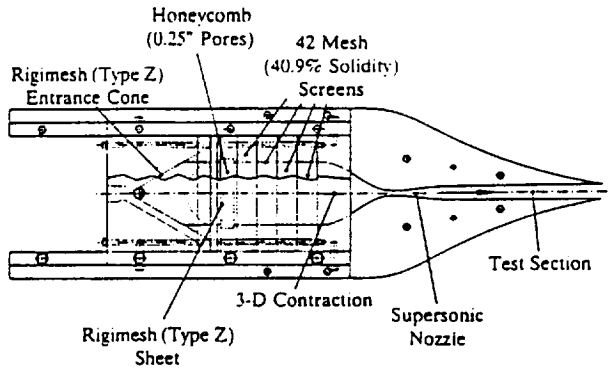


*Fig. 4 - Schematic of the new PoC settling chamber.*

(1.02 bar) and To = 50°F (283 K). Figure 5a shows the new PoC settling chamber in situ. The settling chamber design is based on knowledge of the literature, in particular the work of Beckwith.[8] The versatile design can accommodate boundary layer suction upstream of the contraction, should this prove necessary.

The associated three-dimensional contraction was made integral with a new Mach 2.5 nozzle (the same shape as the original nozzle[5]) and a new longer test section/supersonic diffuser (see Figure 5b). This design removes all hardware joints on the nozzle floor and ceiling upstream of the test section. The shape of the contraction was calculated using a fifth-order polynomial, with zero surface slope and curvature at the upstream and downstream ends. The new test section is 4 inches (10.16 cm) long (compared to the original length of 0.665 inch - 1.69 cm) with slightly diverging floor and ceiling. The supersonic diffuser[5] is unchanged except the ramp height was increased by 0.019 inch (0.48 mm) to maintain a throat height of 0.76 inch (1.93 cm).

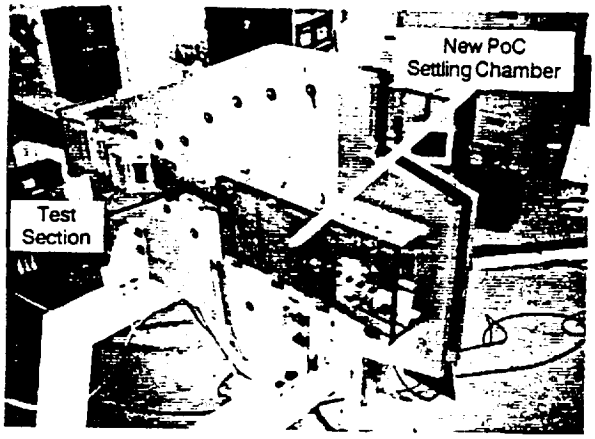


*Fig. 5a - The new PoC settling chamber in situ.*

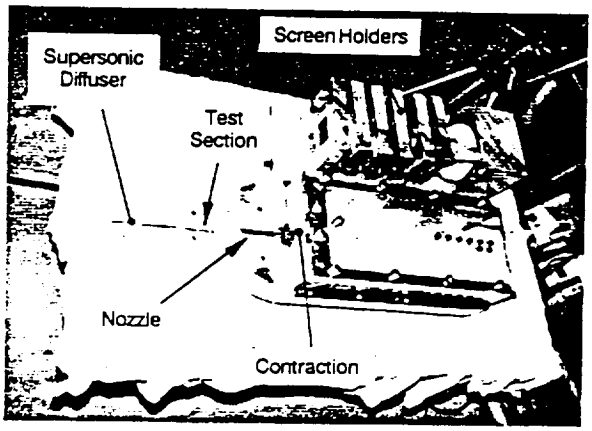


*Fig. 5b - A display of new PoC settling chamber components.*

We use a porous material in the settling chamber to provide both isolation from upstream air supply noise and turbulence, and a means to spread the inlet pipe flow into the settling chamber with minimum disturbances. To this end, we utilize both a cone and flat sheet of Rigimesh type-Z material, which is 0.009 inch (0.23 mm) thick and has a pore size of approximately 39 microinches (1 micron). The pressure load on the $60^{0}$ cone is supported by a perforated sheet on the downstream side of the cone. This perforated sheet is sufficiently open to minimize flow blockage. The flat sheet is supported by a 1 inch (2.54 cm) thick honeycomb sheet with a 0.125 inch (3.17mm) cell size.

The honeycomb sheet is followed by 4 screens each made from 42-mesh stainless steel cloth with 40.9% solidity. The screen separation is equivalent to 63 mesh lengths, which is more than the 50 mesh lengths required for small structure turbulence decay according to Groth and Johansson.[9]

As part of the continuing improvement of tunnel controls, a new Po control system was installed along with the connection to the 3000 psia (207 bar) dry air supply. The Po control system is based on a Fisher DPR-900 integral controller which monitors Po and drives the PoC air regulator. The system allows Po to be set rapidly and held within an accuracy of 0.05 psia (0.0034 bar).

The instrumentation used in the PoC includes pressure taps for steady-state measurements, and hot-wires (single 4 and 5 micron Tungsten wire types), Kulite (XCS-093) pressure transducers, and TSI (Model 1237) platinum hot-film gages for dynamic measurements. The static pressures are measured using a scanivalve system connected to a standard PC A/D converter card. The hot-wires are powered by FML's own constant-temperature bridge circuit with the output signal fed to a Tektronix 2642A Fourier Analyzer system, as are all the dynamic measurements. The Kulites are powered by high frequency response signal conditioners (Dynamic 8000s with a 3dB dropoff at 500KHz). The hot-film gage is powered by a constant-current bridge devised by Demetriades at Montana State University. The Tektronix 2642A Fourier Analyzer system can sample an input signal at up to 512KHz with 16-bit resolution, and provide 4096-point real-time FFTs, data capture and display. All data is then collected on to a PC computer for data archiving, post processing and data presentation.

Dynamic measurements can be made in either the test section or in the settling chamber. In the test section, the hot-wire is buried in the supersonic diffuser molding to minimize blockage, as shown in Figure 6. The hot-wire probe protrudes 0.625 inch (15.9 mm) upstream into the test section, at an X location of 8.375 inches (21.27 cm), and sits about 0.069 inch (1.75 mm) above the test section floor. A Preston tube with a 0.029 inch (0.73 mm) outside diameter was fitted in place of the test section hot-wire for some tests. The hot-film gage was flush mounted in the left sidewall, on the test section centerline, at an X location of 6.69 inches (16.99 cm).

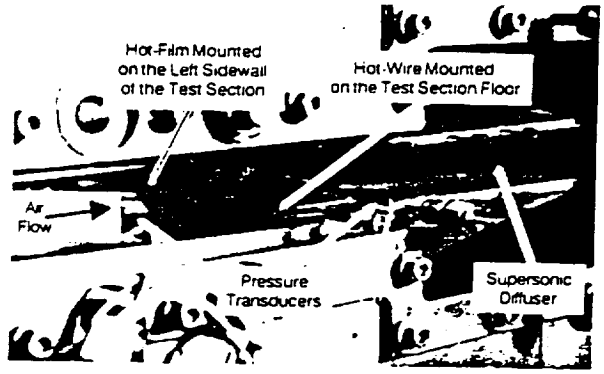


*Fig. 6 - Hot-wire and hot-film instrumentation mounted in the PoC test section.*

In the settling chamber, a special instrumentation holder block allows two probes to be mounted side-by-side and inserted in any holder location. Three interchangeable traversable probes are available: pitot pressure probe fitted with a Kulite; a temperature probe fitted with a type-T thermocouple; and a hot-wire probe fitted with a 4 micron Tungsten wire. These probes can be used for detailed mapping of the flow field at any location in the settling chamber.

The PoC polycarbonate Lexan-type windows have been used with a focusing schlieren system[10] to observe wave patterns in the supersonic diffuser and mixing region. Alternatively, one window can be replaced by an aluminum blank for use of shear-stress-sensitive liquid crystal coatings (discussed later).

## 3. Numerical Research

In attaining a quiet environment necessary for transition studies in a supersonic wind tunnel, there are two main sources of disturbances which need to be carefully addressed and minimized to the extent possible. One is free stream turbulence arising from the settling chamber and upstream piping. Another significant source is the sound field radiated by turbulent tunnel-wall boundary layers. Pate and Schueler[3] and others have shown the adverse effect of radiated noise on transition Reynolds numbers at supersonic speeds. For the LFSWT, it is therefore desirable that the boundary layers remain laminar within the nozzle and test section as far as possible. Malik[11] and others have shown that compressible stability theory with the $e^N$ method predicts boundary layer transition onset arising from Tollmein-Schlichting (TS) waves and Görtler vortices. For sufficiently small free stream turbulence levels in the tunnel, the value of N may approach 10, which is the value associated with high altitude flight in the quiescent atmosphere. Stability calculations within the present context may then serve two purposes: (1) as a predictive tool in designing the nozzle and test section; and (2) as a diagnostic tool in analyzing the experimental results.

The flow through a two-dimensional nozzle, test section, and supersonic diffuser is analyzed computationally with three different codes in order to predict both the mean flow and boundary layer stability and transition. A Navier-Stokes (NS) code, previously described by Wolf et al[5], is used to predict the mean flow quantities in the tunnel. For purposes of analyzing the stability characteristics of the wall boundary layers, the mean flow is assumed laminar in the nozzle and test section, but with turbulent boundary layers in the supersonic diffuser. A boundary layer code by Harris and Blanchard[12] is next employed to provide detailed boundary layer quantities and derivatives for use by the stability code of Malik,[11] since the resolution requirements to accurately obtain first and second derivatives in the boundary layer are not easily met with a NS code. The Malik code uses linear spatial stability theory to analyze the stability of two-dimensional and axisymmetric, compressible wall-bounded flows. Wall curvature is accounted for, so the analysis considers both TS waves (1st, 2nd, etc. modes) and Görtler vortices. Transition onset is predicted with the $e^N$ method.

The PoC/LFSWT nozzle in the present study was intentionally made long so that instabilities arising from curvature effects would not cause transition. This decision was supported by the study of Wolf.[13] Calculations indicate that this approach was successful, in that the maximum N factor due to Görtler vortices thus far computed is less than 4. No significant TS instabilities at the PoC operating conditions have yet been found numerically.

## 4. Experimental Program

LFSWT drive system tuning has now continued beyond the initial drive system design studies, which successfully demonstrated that Mach 2.5 flow could be achieved over the desired Re range.[5] This additional tuning became necessary to address concerns over the drive system length and the ability of the FML compressor to provide sufficient mass flow. The PoC was used to carry out the necessary drive system tuning. For this purpose, the PoC was modified to allow the separation between the two injector stages to be varied and the mass flow of the secondary injectors to be reduced. Both these parameters were previously fixed on the PoC.[5]

Following the drive system tuning, the experimental program has focused on studying quiet flow in the PoC. Preliminary flow measurements were made in the settling chamber and the extent of natural laminar flow that exists along the PoC test section walls has been documented at Mach 2.5. Of course, the existence of laminar flow on the nozzle walls is a critical element of a quiet supersonic wind tunnel. Our intent with the LFSWT is to go beyond this requirement and obtain laminar flow throughout the test section. This situation will eliminate the existence of a test rhombus bounding the quiet flow, which will allow testing anywhere in the test section. This means that the model will not have to be positioned in a variable test rhombus, which greatly simplifies the method of model support.

Initially, we are concerned with obtaining natural laminar flow on the nozzle and test section walls using passive laminar flow control. These passive means are a low-disturbance free stream, a low curvature, long nozzle and a smooth wall finish. The documentation of natural laminar flow, using the solid block Mach 2.5 nozzle, is the first stage of an ongoing verification of the LFSWT test envelope.

For the quiet flow studies, the PoC was fitted with a new low-disturbance settling chamber/nozzle/test section, instrumentation for dynamic measurements, and a closed-loop control system for setting and maintaining Po. Dynamic flow measurements in the test section and settling chamber were then made to document the flow quality in PoC over the entire Re range. To assist with verification of our instrumentation, the settling chamber was degraded and the associated effects on laminar flow in the PoC test section were documented and are discussed later.

## 5. Instrumentation Development

### 5.1 Hot-Wire

The use of hot-wires is well documented but still requires considerable operator interpretation, particularly at supersonic speeds.[14] We use a 5 micron Tungsten wire built at NASA-Ames in our supersonic testing. This wire type is durable and has a typical calibrated response rate of 15KHz, using a square wave with the wind off. During tunnel operation, the probe is in the outer portions of the floor boundary layer and can only be calibrated when laminar flow is present. However, the response calibration does not change from wind off to wind on in this situation. Nevertheless, we are currently unable to calibrate the output of the hot-wire to aerodynamic parameters, so our data are only qualitative at present.

As PoC testing has progressed, we have gained experience with the use of hot-wire instrumentation. The new FML constant-temperature anemometer has worked flawlessly and provides a high level of adjustability. Wind-off signal noise is extremely low. By experience, we have found that the signal rms can be best recorded as an average of 20 samples taken without interruption. Our waveform analyzer requires less than a second to perform this average of 20 4096-point FFTs under PC software control. The signal spectrum is then available for storage and printing.

### 5.2 Hot-Film

Hot-films are well know detectors of shear stress. We employed a commercially available hot-film gage mounted on a cylindrical glass substrate. The heat-sink effect associated with this configuration (run as a constant temperature sensor) was found to be very large. This finding necessitated the building of a specialist constant-current circuit to drive the sensor and maintain a low output signal DC voltage for ease of measurement.

Concern over the repeatability of the hot-film data from the PoC led to an independent transition-detection calibration of the hot-film in another quiet supersonic wind tunnel at Mach 3. This calibration was undertaken by the Montana State University and involved the hot-film being exposed to laminar, transitional and turbulent boundary layers. However,

this calibration only allows us to qualitatively assess the hot-film data from the PoC.

### 5.3 Focusing Schlieren System

Based on the pioneering work of Weinstein[10] at NASA-Langley, a focusing schlieren system has been developed for use with the PoC. The main features of this system are:

1) The windows do not have to be made of schlieren-quality glass, any transparent material is good and in this application polycarbonate windows are used.

2) Thin slices of the flow can be observed with similar resolution to conventional schlieren systems.

3) Mirrors are not required.

4) Simple setup allows view changes at will.

5) A point light source is not required.

These features have proven to be very important to this project and have allowed flow visualization to occur in a timely manner and to change rapidly with research needs.

The concept was developed back in the late 1940s and provides a very versatile system ideal for research. The PoC system has been used to observe the drive system performance in the supersonic diffuser[5] and in the mixing region. We are currently attempting to use this schlieren system to observe boundary layers and to detect transition to turbulence. For this purpose, the focusing schlieren system is being enhanced with the addition of a high intensity spark illumination and cylindrical lenses for boundary layer magnification.

### 5.4 Liquid Crystal Coatings

The liquid crystal coating technique is a method for visualization of surface shear stress patterns in both steady and transient flows, as reported by Smith[15] and Reda.[16] In the present application, one of the PoC windows was replaced by an aluminum (black) insert and the flow surface was coated with a shear-stress-sensitive/temperature-insensitive liquid crystal film. The coated areas (in the supersonic diffuser and mixing region) were obliquely illuminated by white light through the opposite window. Then the color-change response of the liquid crystal film to surface shear stress events was photographed on video and movie film. Framing rates from 30 to 1000 images/sec were utilized.

We have tested the frequency response of the newly-formulated liquid crystal compound (Hallcrest BCN/192) by using the PoC startup and off-design operation to create highly transient flows. During these tests, all boundary layers on the nozzle and sidewall surfaces were turbulent because the low-disturbance settling chamber had not yet been installed. These observations showed the liquid crystal coating response time to be less than, or equal to, the time between sequential images taken at 1000/sec (i.e., one millisecond).

## 6. Experimental Results

### 6.1 Drive System Tuning

Since the last report on the PoC drive system[5], measurements in the primary injector exits show that the actual Mach number of the primary injectors is 2.11. This is significantly less than the previously estimated Mach 2.4 and shows that the influence of the second stage of injectors is much smaller than previously thought. Nevertheless, the PoC drive system continues to operate over the desired Po range with a $P_E$ of 8 psia (0.55 bar).

The movement of the secondary injectors upstream towards the primary injectors had no noticeable effect on the performance of the PoC. The reduced separation distance of 6.46 inches (16.41 cm) was sufficiently long to allow 2 wave reflections in each of the primary injector flows, above and below the test section flow, as shown in Figure 7. The comparison of static pressures (shown in Figure 8) indicates that the test section flow was not affected by the secondary injector movement. This shortening of the PoC drive system will result in a 198 inch (5.03 m) reduction in the length of the LFSWT. Unfortunately, both sets of PoC data indicate that the test section Mach number was reduced below 2.5.

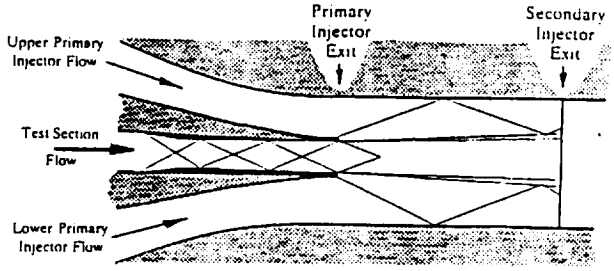


*Fig. 7 - Schematic of the shock patterns in the mixing region between the PoC injector stages.*

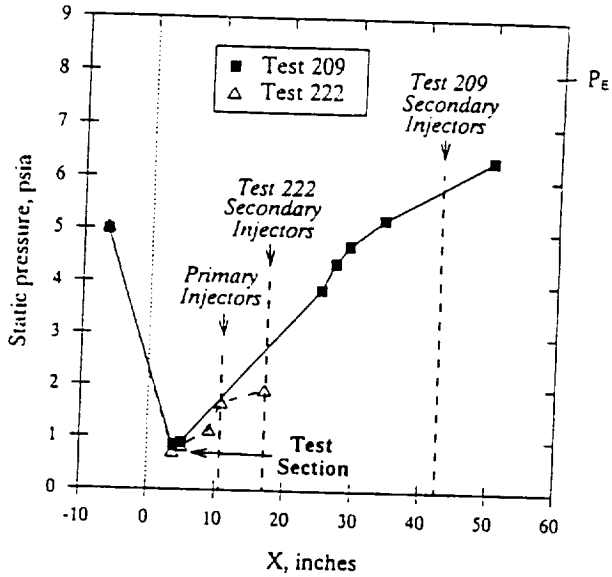


*Fig. 8 - Comparison of PoC pressures with different secondary injector locations, at a minimum Po of 5 psia (0.34 bar).*

This loss of desired test Mach number was traced to the degradation of our temporary air drier prior to these tests. The resulting condensation effects in the nozzle (which were not visible to the operators) actually caused the test Mach number to go down. Once the PoC was connected to the NASA-Ames 3000 psi (207 bar) dry air supply, good air quality was restored and the test Mach number returned to 2.5. Furthermore, we now use a hydrometer to continuously monitor the dew point of the inlet air to check for sufficient dryness, which we define as a dew point of less than -15° F (247 K).

The drive system tuning continued with a study of the effects of reducing the mass flow of the secondary injectors. This was an attempt to lower the overall mass flow requirement of the LFSWT drive system. We reduced the PoC

secondary injector mass flows in stages (by 11%, 22% and 33%) and found that the minimum Po for Mach 2.5 operation had risen for each reduction in mass flow. Adjustment of the primary injectors failed to produce any significant improvement in the minimum Po. This effort confirmed that the LFSWT drive system for Mach 2.5 operation requires up to 184 lbs/sec mass flow at a maximum Po of 15 psia (1.02 bar), if the Po range from 5 to 15 psia (0.34 to 1.02 bar) is to be preserved with $P_E$ = 8 psia (0.54 bar).

## 6.2 Quiet Flow Studies

### 6.2.1 Settling Chamber

The new PoC low-disturbance settling chamber (previously described) has been operated over a Po range from 5 to 15 psia (0.34 to 1.02 bar). This Po range corresponds to a mass flow range of 0.097 lbs/sec (0.044 kg/sec) to 0.358 lbs/sec (0.162 kg/sec) for To = 50°F (283 K). The static pressure distributions across the components of the settling chamber are shown in Figure 9 for different Po. It can be seen that the maximum pressure drop of about 2.5 psia (0.17 bar) occurs across the flat sheet of Rigimesh. The Rigimesh cone supports minimal pressure load, which simplifies the necessary support structure for the full-scale LFSWT cone.

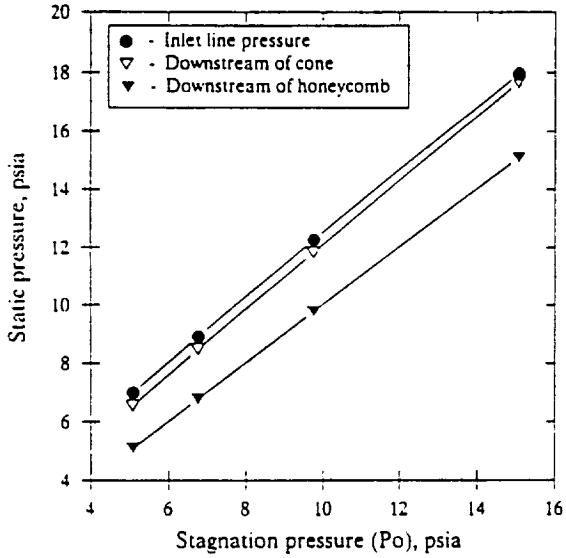


*Fig. 9 - Pressure distributions through the PoC settling chamber.*

Preliminary flow disturbance measurements were made in the plane of the settling chamber exit (at a single location on the tunnel centerline) using a Kulite total pressure probe and a 4 micron Tungsten hot-wire. The Kulite data are shown in Figure 10 over the Po range for two settling chamber configurations, with and without the honeycomb and Rigimesh sheet installed. The ratio of the Prms with Po shows a significant rise with the honeycomb and Rigimesh sheet removed. This pressure ratio drops with increasing Po. With all the settling chamber components in place, the pressure fluctuations are of the order 0.1%. The sharp increase in pressure ratio at low Po has been traced to tunnel leaks which caused unstarting of the nozzle flow.

The hot-wire data from the settling chamber are shown in Figure 11. Again, about a fourfold increase of signal rms is associated with the removal of the honeycomb and Rigimesh sheet. The signal levels, with all the settling chamber components in place, are reasonably low compared to the 0.7 mV wind off noise level. However, in the absence of a hot-wire calibration of volts-vs-velocity, these data can only be discussed qualitatively.

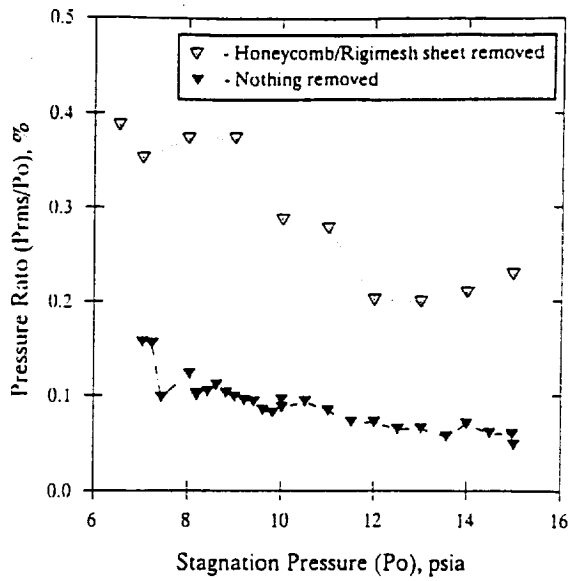


*Fig. 10 - Summary of Kulite pressure data from the PoC settling chamber.*

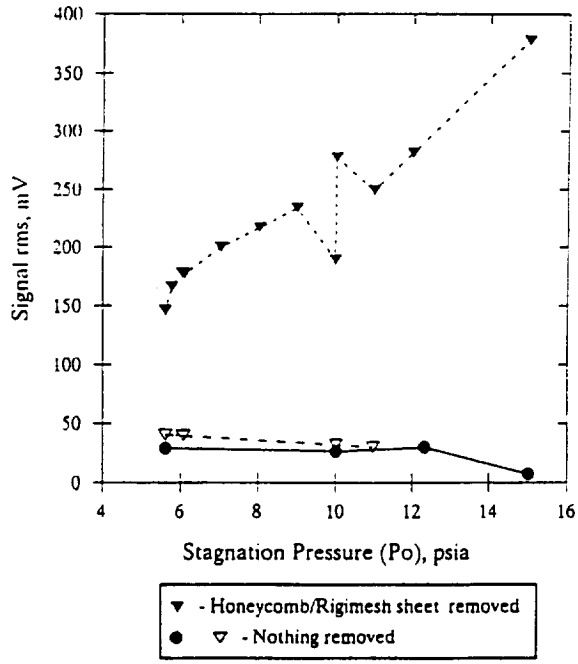


*Fig. 11 - Summary of the uncalibrated hot-wire data from the PoC settling chamber.*

### 6.2.2 Laminar Flow

Our laminar flow studies involve the use of different types of instrumentation to confirm the state of the test section boundary layer. The detection of boundary layer transition tends to be qualitative and our goal was to find at least 2 measurement techniques which agreed about the location of transition.

We found that the hot-wire measurements made above the PoC test section floor, in the outer portions of the boundary layer (see Figure 12), show a sharp rise in signal rms when Po is about 9 psia (0.61 bar). The hot-wire signals for Po = 8.02 psia (0.54 bar) and 9 psia (0.61 bar) are shown in Figure 13a. The difference in the signals is indicative of

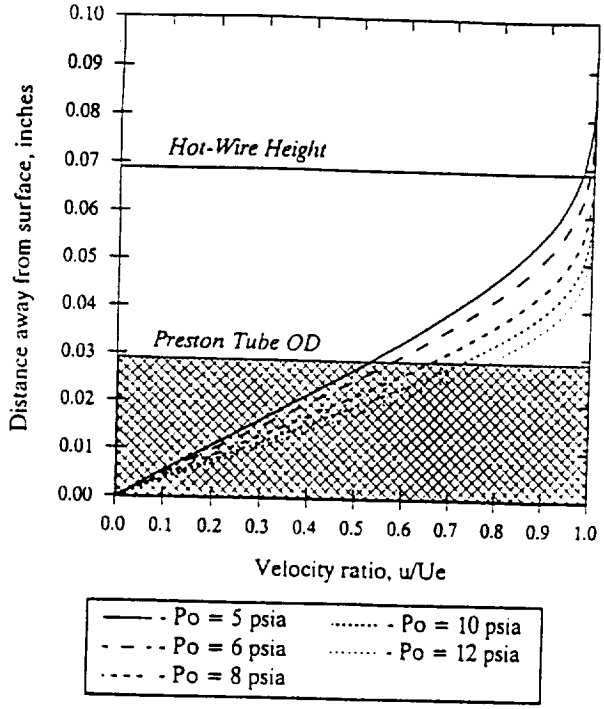


*Fig. 12 - Calculated laminar boundary layer profiles in the PoC test section (X = 8.375 inches - 21.27 cm).*

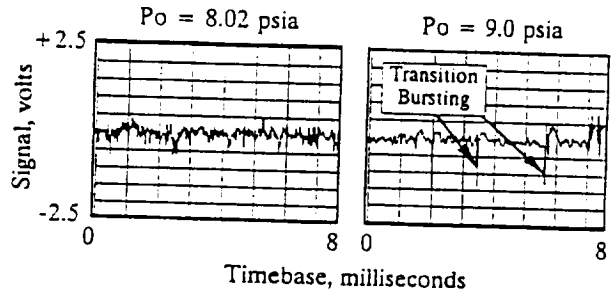


*Fig. 13a - Comparison of hot-wire signals from the PoC test section at different Po, near transition onset.*

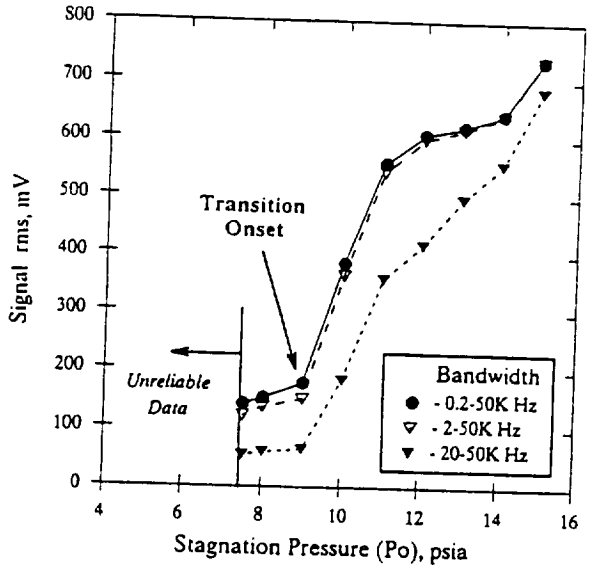


*Fig. 13b - Summary of hot-wire data from the PoC test section at Mach 2.5 (X = 8.375 inches - 21.27 cm).*

transition bursting. The signal spectrums are broadband with no discrete frequencies.

The associated rise in signal rms is independent of the signal bandwidth, as shown in Figure 13b. In fact, the hot-wire signals follow a pattern over the Po range which is associated with a familiar non-bypass transition process[17], where the transition bursting reaches a maximum frequency. Unfortunately, the uncalibrated hot-wire data can only be used qualitatively. The hot-wire data at lower Po in this test series were unreliable due to intermittent tunnel leaks, but low signal rms was observed down to a Po of 5.4 psia (0.37 bar).

To check the reliability of the hot-wire data from the PoC test section, the honeycomb and Rigimesh sheet were removed from the settling chamber. The uncalibrated hot-wire data taken with and without the honeycomb and Rigimesh sheet installed, are shown in Figure 14. Clearly, the increase of free stream turbulence (previously documented) had the effect of initiating transition onset, at the same location, at a lower Po of about 6 psia (0.41 bar) and hence a lower Re. Note, in this data set that a low signal rms was achieved down to a Po of 6 psia (0.41 bar) before tunnel leaks occurred.

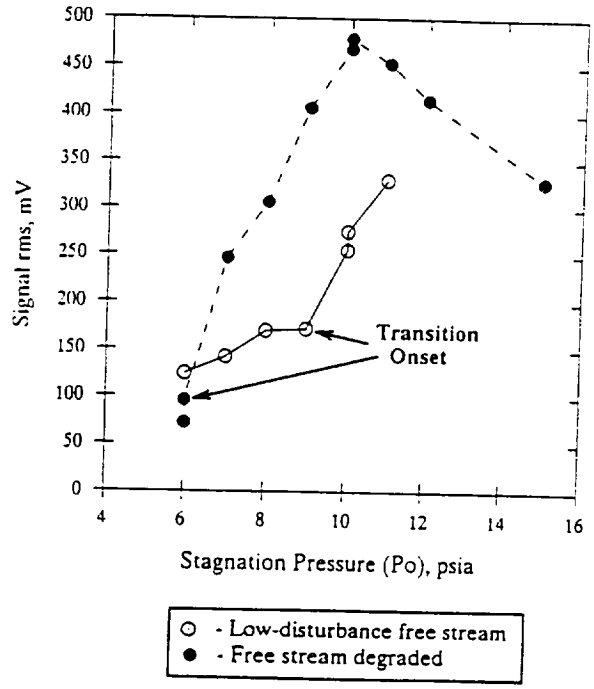


*Fig. 14 - Effect of different free stream disturbance levels on hot-wire data from the PoC test section at Mach 2.5.*

In another series of tests, the hot-wire was replaced by a Preston tube. This tube was sized to fit in the lower half of the floor boundary layer (See Figure 12). The data from the Preston tube are shown in Figure 15, over an extended Po range from 5.4 psia (0.37 bar) to 20 psia (1.36 bar). This Po range corresponds to an Re range from 1.25 to 4.64 million per foot. It is clear that there is a significant rise in the probe Cp at a Po of about 8.5 psia (0.58 bar). This rise is associated with transition onset where the boundary layer profile starts changing from a laminar type to a turbulent type.[18] The probe Cp reaches a plateau at about 16 psia (1.09 bar).

The sidewall boundary layers were studied with a flush-surface-mounted hot-film. The hot-film data are shown in Figure 16 over an extended Po range up to 20 psia (1.37 bar). The calibration of the hot-film is only qualitative[19] as indicated on Figure 16. Nevertheless, the hot-film data show that the boundary layer on the sidewall remained laminar over

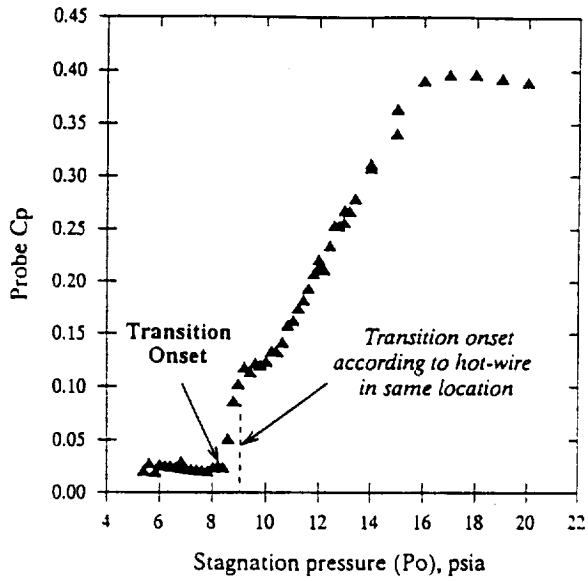


*Fig. 15 - Summary of Preston tube data from the PoC test section at Mach 2.5 (X = 8.375 inches - 21.27 cm).*

the entire Re range, at an X location of 6.69 inches (17 cm), with no tunnel leaks. The hot-film signal rms is seen to jump to expected levels for turbulent flow only when tunnel leaks caused the nozzle flow to unstart. This flow break down caused transition bypass to occur on the sidewall, as shown in Figure 16, where hot-film data with and without tunnel leaks are compared. In addition, the same leaks cause transition bypass to occur on the test section floor and ceiling, as measured by the hot-wire probe in the test section.

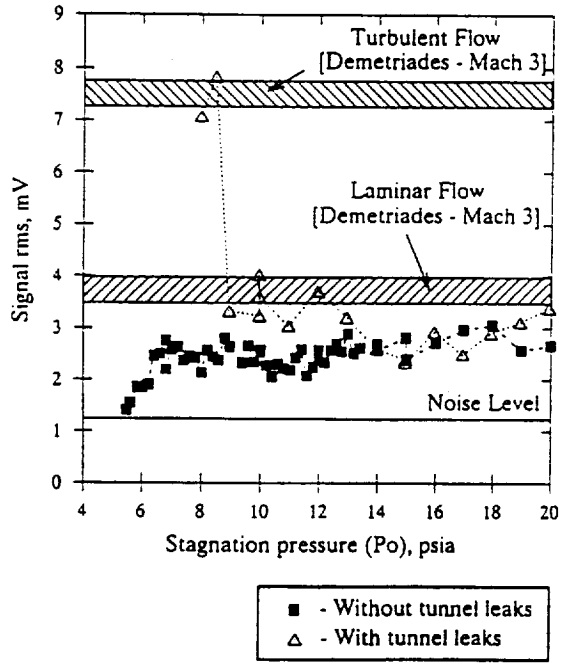


*Fig. 16 - Summary of hot-film data from the PoC test section sidewall at Mach 2.5 (X = 6.69 inches - 17 cm).*

During these laminar flow studies there was some concern about the drift in temperature of the inlet air and the PoC nozzle/test section structure. The air supply to the PoC is not heated and the inlet air temperature is always lower than ambient due to the expansion across a single air regulator. We monitor the inlet air temperature on a regular basis to check for repeatability of test conditions. The thermal mass of the PoC is large compared to the heat transfer associated with the nozzle/test section flow. We have observed the PoC structure reaching near temperature equilibrium within about the first 5 minutes of running. This temperature equilibrium is affected only slightly by changes of inlet air mass flow, despite noticeable changes in the inlet air temperature. To assess the long term effects of temperature drift, we operated the PoC for 2 1/2 hours continuously and monitored our hot-wire and hot-film instrumentation. No significant changes in the test section flow were observed during this test.

## 7. Discussion of Results

The latest LFSWT drive system tuning has defined both the maximum mass flow required and the dual injector separation for Mach 2.5 operation. These parameters are 184 lbs/sec (83.46 kg/sec) for the mass flow and 51.68 inches (1.31 m) for the injector separation. Unfortunately, recent investigations of the FML compressor have revealed that a $P_E$ of 8 psia (0.34 bar) cannot be maintained at the high mass flows now required for Mach 2.5 operation. In fact, $P_E$ rises to 8.8 psia (0.6 bar) at high mass flows precluding PoC operation below a Po of 15 psia (1.02 bar). A decision has therefore been made to concentrate the initial LFSWT operating envelope on a lower Mach number. We have chosen Mach 1.6 in order to support F-16XL SLFC flight testing.

Preliminary measurements in the PoC settling chamber show that the free stream flow entering the nozzle/contraction is low-disturbance, according to Beckwith et al.[20] Of course, the flow entering the LFSWT settling chamber will have to pass through a different array of valves and pressure reducers at 64 times larger mass flows. However, we know that the noise and turbulence entering the LFSWT settling chamber will be less than that of a blowdown wind tunnel.[7] Nevertheless, the modular design of the PoC settling chamber is the best currently available for the LFSWT and the design will proceed accordingly.

In fact, the settling chamber effectiveness has been verified by the existence of laminar flow in the PoC test section. Two transition measurements (hot-wire and Preston tube) agree that transition occurs 84% along the test section floor at a Po of about 8.5 psia (0.58 bar) which corresponds to a Re of about 2 million per foot. Furthermore, when the settling chamber effectiveness is reduced by removing the honeycomb and Rigimesh sheet, transition occurs at a lower Po. This result is actually a repeat of Laufer's work[2] at JPL, which highlighted the strong effect of free stream turbulence on transition, particularly at Mach numbers less than 2.5. This result is also further proof that the complete settling chamber is producing low-disturbance flow to sustain laminar flow to a higher Re.

The steadiness of the supersonic diffuser flow has also been verified by the existence of laminar flow in the test section. The new PoC test section is 3.335 inches (8.47 cm) longer than before, so the PoC can better simulate the LFSWT test section flow. This improvement, combined with dynamic instrumentation has allowed us to document the extent of steady flow at the inlet of the supersonic diffuser, as part of our laminar flow studies. The minimum Po at which Mach 2.5 could be maintained steadily was 5.4 psia (0.37 bar) without tunnel leaks. Below this Po, the average test section Mach number dropped and the hot-wire probe in the test section experienced significant velocity fluctuations. This onset of unstart has previously been observed (with the aid of our focusing schlieren system) as the entire supersonic diffuser flow becoming oscillatory and highly unstable. It is clear that once the inlet flow to the supersonic diffuser becomes oscillatory that laminar flow is lost.

The absence of transition on the PoC sidewall was expected, because of the short run lengths coupled with favourable pressure gradients and the absence of curvature. Consequently, the extent of quiet flow in the PoC is determined by the transition location on the floor and ceiling of the test section. In the LFSWT, transition may occur first on the sidewalls (as occurs in the Mach 3.5 Langley Pilot Quiet Tunnel[7]) and this is one of the reasons for making the test section cross-section rectangular. By placing the sidewalls further from the tunnel centerline than the floor and ceiling, we can potentially maintain a quiet test core to higher Re. Also, the rectangular shape of the test section and supersonic diffuser means the primary injectors need only be mounted on the long floor and ceiling of the test section/supersonic diffuser, leaving the test section sidewalls clear of ducting.

Obviously, the tunnel leaks in the PoC (referred to earlier) have severely hampered research at low Po. The problem is peculiar to the small-scale of the PoC and has been traced to internal leak paths around the PoC windows. This is a legacy of using the PoC for much longer than originally planned. A solution to the problem has now been found by potting the windows in a silicone-based sealer instead of vacuum grease.

The existence of laminar flow in a small wind tunnel like PoC (with short flow lengths) does not guarantee long lengths of laminar flow in a larger wind tunnel like the LFSWT. Preliminary CFD analyses predicted that transition would not occur along the PoC Mach 2.5 nozzle or test section. Unfortunately, this prediction has been disproved by the PoC experiments. Nevertheless, this information should help improve future transition predictions for the PoC and hence for the LFSWT. Presently, we can confirm that laminar flow can exist at a location 84% along the PoC test section floor from Po = 5.4 psia (0.37 bar) to Po = 8.5 psia (0.59 bar), which corresponds to an Re range of 1.25 to 1.97 million per foot with a To of about 50°F (283 K), as shown in Figure 1.

## 8. Future Plans

Based on the inability of the FML compressor alone to drive the LFSWT at Mach 2.5, the validation of the LFSWT test envelope will continue by operating PoC at Mach 1.6 in the near future. We hope to study and document quiet flow and LFSWT drive system parameters for Mach 1.6 before the end of June 1992, to impact the LFSWT design process. At the same time, further flow measurements will be made in the settling chamber with different configurations.

Instrumentation development will continue using commercially available hot-film arrays, which span the entire length of one wall of the contraction/nozzle/test section. This measurement technique should allow documentation of where transition occurs at a given Re. In addition, work with the focusing schlieren and liquid crystal coatings will continue to document PoC transition. New hot-wire mounts will hopefully allow hot-wire calibration in the free stream, so we can relate the hot-wire data to flow velocity. Also, the X location of the test section hot-wire probe will be varied to study the PoC flow at different streamwise locations.

Quiet wind tunnel development work will continue with CFD analyses directed at active control of supersonic transition using nozzle wall heating and cooling together with nozzle contour and length changes. This effort will support the eventual expansion of the actual LFSWT test envelope for quiet flow to the proposed envelope shown in Figure 1.

## 9. Conclusions

1) Preliminary flow studies in the new PoC settling chamber indicate that the free stream is low-disturbance.

2) Natural laminar flow has been documented along at least 84% of the PoC test section at Re from 1.25 to 1.97 million per foot.

3) A linear stability analysis ($e^N$ method) is now available at NASA-Ames to assist our nozzle design studies and quiet wind tunnel development.

4) The uniquely efficient Mach 2.5 PoC drive system has been successfully shortened by 24.78 inches (62.94 cm), which is equivalent to reducing the length of the LFSWT by 16.5 feet (5.03 m).

5) The maximum mass flow required for the LFSWT Mach 2.5 drive system is 184 lbs/sec (83.46 kg/sec) with a $P_E$ of 8 psia (0.54 bar) , which exceeds the capabilities of the FML compressor alone.

6) Design of the LFSWT is now proceeding with an emphasis on Mach 1.6 operation.

## References


1. Laufer, J.: **Factors Affecting Transition Reynolds Numbers on Models in Supersonic Wind Tunnels.** Journal of Aeronautical Sciences, vol. 21, no. 7, July 1954, pp. 497-498.

2. Laufer, J.: **Aerodynamic Noise in Supersonic Wind Tunnels.** Journal of the Aerospace Sciences, vol. 28, no. 9, September 1961, pp. 685-692.

3. Pate, S.R.; and Schueler, C.J.: **Radiated Aerodynamic Noise Effects on Boundary-layer Transition in Supersonic and Hypersonic Wind Tunnels.** AIAA Journal, vol. 7, no. 3, March 1969, pp. 450-457.

4. Kendall, J.M.: **Supersonic Boundary Layer Transition Studies.** JPL Space Programs Summary 37-62, vol. 3, April 1970, pp. 43-47.

5. Wolf, S.W.D.; Laub, J.A.; and King, L.S.: **An Efficient Supersonic Wind Tunnel Drive System for Mach 2.5 Flows.** AIAA Paper 91-3260. In: Proceedings of AIAA 9th Applied Aerodynamics Conference, vol. 1, September 1991, pp. 461-471.

6. Riise, H.N.: **Flexible-Plate Nozzle Design for Two-Dimensional Supersonic Wind Tunnels.** JPL Report no. 20-74, June 1954.

7. Beckwith, I.E.; Chen, F.-J.; Wilkinson, S.P.; Malik, M.R.; and Tuttle, D.G.: **Design and Operational Features of Low-Disturbance Wind Tunnels at NASA Langley for Mach Numbers from 3.5 to 18.** AIAA Paper 90-1391. Presented at the AIAA 16th Aerodynamic Ground Testing Conference, June 1990.

8. Beckwith, I.E.: **Comments on Settling Chamber Design for Quiet, Blowdown Wind Tunnels.** NASA TM-81948, March 1981.

9. Groth, J.; and Johansson, A.V.: **Turbulence Reduction by Screens.** Journal of Fluid Mechanics, vol. 197, 1988, pp. 139-155.

10. Weinstein, L.M.: **An Improved Large Field Focusing Schlieren System.** AIAA Paper 91-0567, January 1991.

11. Malik, M.R.: **$e^{N(eN)}$: A New Spatial Stability Analysis Program for Transition Prediction Using the $e^N$ Method.** High Technology Corporation, Report No. HTC-8902, March 1989.

# APPENDIX C

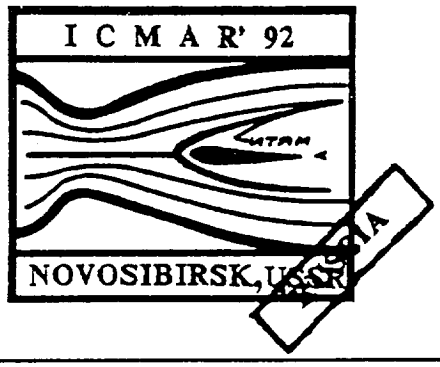


# DESIGN FEATURES OF A LOW-DISTURBANCE SUPERSONIC WIND TUNNEL FOR TRANSITION RESEARCH AT LOW SUPERSONIC MACH NUMBERS

**Stephen W.D. Wolf, James A. Laub, Lyndell S. King and Daniel C. Reda**

Fluid Dynamics Research Branch
Fluid Mechanics Laboratory
NASA Ames Research Center
Moffett Field, CA 94035-1000, USA

Preprint of paper for the
**International Conference on Methods of Aerophysical Research**

August 31- September 4, 1992
Novosibirsk, Russia

# DESIGN FEATURES OF A LOW-DISTURBANCE SUPERSONIC WIND TUNNEL FOR TRANSITION RESEARCH AT LOW SUPERSONIC MACH NUMBERS

Stephen W.D. Wolf*, James A. Laub**, Lyndell S. King***, and Daniel C. Reda+
Fluid Mechanics Laboratory
NASA Ames Research Center
Moffett Field, California 94035-1000, USA

## Introduction

Low-disturbance or "quiet" wind tunnels are now an essential and indispensable part of meaningful boundary layer transition research at supersonic speeds. This realization is based on many years of experience with old "noisy" supersonic wind tunnels, and a growing respect for the pioneering research of Laufer[1] at the Jet Propulsion Laboratory (JPL) from the mid-1950s to the early-1960s, supported by the work of Pate and Schueler[2] in the late-1960s. In addition, this realization has received recent emphasis due to an appreciation of the risk associated with inadequate flight test measurements "validating" CFD transition predictions. Of course, the wind tunnel can provide controlled test environments and is much better suited to the job of validating CFD predictions. It is the combination of wind tunnel, CFD and flight test that provides the best hope of solving one of the last great mysteries of aerodynamics, namely transition to turbulence. Based on this premise, NASA-Ames has embarked on the development of a unique Laminar Flow Supersonic Wind Tunnel (LFSWT) in the Fluid Mechanics Laboratory (FML) at NASA-Ames to fill the void.

The concept behind the LFSWT design is based on the now decommissioned (but soon to be rebuilt) JPL 20-inch supersonic wind tunnel, which just happened to be the first documented quiet supersonic wind tunnel because of its high-quality origins.[1] From the outset, the LFSWT has been designed as a quiet research tunnel which is capable of continuous operation. The proposed test envelope of the LFSWT was chosen to cover a significant portion of the potential HSCT operating envelope, with a Re range of 1 to 3 million per foot and a Mach number (Me) range from 1.6 to 2.5. In addition, this LFSWT test envelope will cover the test conditions flown by NASA's F-16XL aircraft in support of Supersonic Laminar Flow Control (SLFC) studies, as shown in Figure 1. The maximum test section size was fixed by the desire to utilize an existing dry air source with an open-circuit tunnel design.

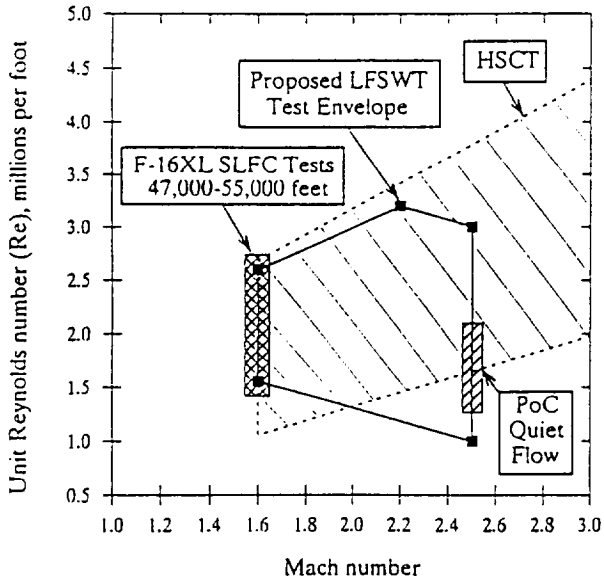


*Fig. 1 - Proposed LFSWT test envelope for quiet operation.*

What actually defines a quiet supersonic wind tunnel? A turbulence level of 0.05% in the test core is considered to be quiet enough. This low level of turbulence is achieved with a combination of a low-disturbance free stream (core flow), laminar flow along the nozzle/test section walls, steady diffuser flow and minimal mechanical vibration of nozzle/test section.

The LFSWT is currently being designed with an 8 inch (20.32 cm) high, 16 inch (40.64 cm) wide and 32 inch (81.28 cm) long test section, sized to operate at mass flows up to 21 lbs/sec (9.52 kg/sec). The use of existing support equipment (the FML indraft compressor and the 3000 psi (207 bar) dry air supply) will reduce costs and bring the LFSWT on-line more rapidly. The LFSWT is expected to impact the critical technology development phase of the HSCT before 1997.

* Research Scientist, MCAT Institute. Senior Member AIAA. AMRAeS.
** Facility Operations Manager, Fluid Dynamics Research Branch.
*** Research Scientist, Fluid Dynamics Research Branch. Member AIAA.
+ Senior Research Scientist, Fluid Dynamics Research Branch. Assoc. Fellow AIAA.

The decision to use the FML non-specialist indraft compressor to power the LFSWT created several technical concerns. To achieve the low end of the Re range, the LFSWT must operate with a Po which is less than the minimum $P_E$. This means that the LFSWT compression ratios will be uniquely less than unity ($P_o/P_E$ down to 0.625:1 with Re = 1 million per foot at stagnation pressure (Po) = 5 psia - 0.34 bar). So, the utilization of the FML compressor precludes the use of a conventional drive system. Consequently, a novel drive system was developed using an 1/8th-scale model of the LFSWT, which we call the Proof-of-Concept (PoC) supersonic wind tunnel.

A detailed description of this drive system is beyond the scope of this paper and has already been covered by Wolf et al.[3] The drive system requires less than half of the normal run compression ratio to both start and run. The drive system works by utilizing the huge compressor mass flow capability (which greatly exceeds the mass flow necessary for the test section flow alone) to drive one or two stages of ambient injectors. It is these injectors which pull the flow through the test section at low Po. Two stages of injectors became necessary for Mach 2.5 operation to allow the primary injectors to operate at a higher exit Mach number. This in turn lowered the exit pressure of the test section flow and allowed the PoC to operate at compression ratios less than unity. The LFSWT drive system for Mach 2.5 operation will require up to 184 lbs/sec (83.4 kg/sec) mass flow at a maximum Po of 15 psia (1.02 bar), if the Po range from 5 to 15 psia (0.34 to 1.02 bar) is to be preserved with $P_E$ = 8 psia (0.54 bar).

It is expected that the LFSWT, when commissioned, will be the only quiet tunnel to operate at low-supersonic Mach numbers. Researchers at NASA Langley have chosen to devote over 10 years of quiet wind tunnel work at Mach 3.5 and above, and appear wary of the problems of building a low-supersonic quiet tunnel.[4] This is a surprising situation considering the research interest in transition at low-supersonic Mach numbers. The concerns at Langley stem from the need to maintain laminar boundary layers further downstream from the nozzle throat. This need arises because the Mach lines, along which acoustic disturbances radiate from turbulent boundary layers, are much more normal to the flow at low-supersonic speeds. Consequently, longer runs of laminar flow are required to provide the same length of quiet test core at low-supersonic Mach numbers (as shown in Figure 2).

We do not have similar concerns at NASA-Ames for three reasons. At low-supersonic Mach numbers, both the length and curvature of the supersonic nozzle is less and therefore deters the development of Tollmein-Schlichting (TS) waves and Görtler vortices (known transition promoting disturbances). Furthermore, the unit Reynolds numbers (Re) necessary to match flight values are low, generally less than 3 million per foot (as shown in Figure 1). Operating the tunnel at low Re, helps promote natural laminar flow on all the tunnel walls, and also relaxes the requirement for a highly polished surface finish on the walls of the nozzle throat. Finally, it is reported[1] that the free stream disturbances have a dominant effect on the transition process at Mach numbers below 2.5. Hence, we can reasonably expect the importance of a quiet nozzle to be less than that of the settling chamber at low-supersonic Mach numbers. Fortunately, the settling chamber of a supersonic tunnel can be treated in a similar fashion to that of a large low-disturbance subsonic tunnels about which much is already known. It is for these reasons, that we consider the design of a low-supersonic quiet wind tunnel to be less complex than that of any existing high Reynolds number high-supersonic/hypersonic quiet tunnel.

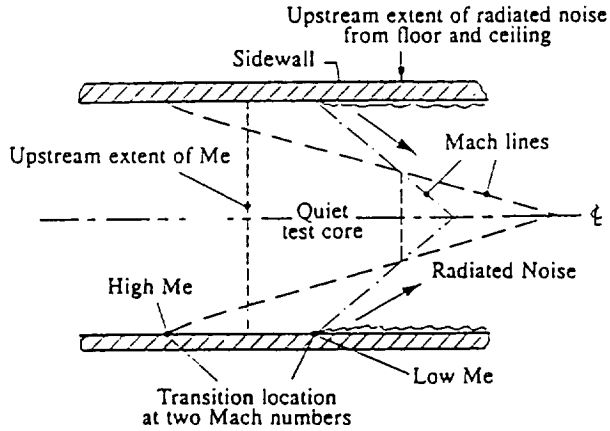


*Fig. 2 - Different lengths of laminar flow are required to maintain the same size quiet test core at two Mach numbers.*

We have embarked on a combination of theoretical and experimental research efforts at NASA-Ames, to ensure that the LFSWT will provide the necessary quiet test core. While we are using the PoC for design studies, we are also developing and gaining experience with the

latest instrumentation for transition research, in particular hot-films, focusing schlieren and liquid crystals. This experience will aid our development of quiet nozzles, improve flight test measurements, and also give FML the tools required for future transition research, when the LFSWT comes on-line.

## Quiet Flow Studies

### Settling Chamber

Preliminary flow disturbance measurements were made in the plane of the settling chamber exit (at a single location on the tunnel centerline) using a Kulite total pressure probe and a 4 micron Tungsten hot-wire. The velocity in the settling chamber is 20 fps (6.1 m/sec) for Mach 2.5 operation. The Kulite data are shown in Figure 3 over the Po range for two settling chamber configurations[3] (complete and without the honeycomb and sintered mesh - Rigimesh sheet installed). The pressure disturbances (the ratio of the total pressure rms (Prms) to Po) show a significant rise of 0.2-0.3% with settling chamber components removed. The pressure disturbances drop with increasing Po and hence mass flow. With all the settling chamber components in place, the pressure fluctuations are of the order 0.1%. The sharp increase in disturbances at low Po has been traced to tunnel leaks.

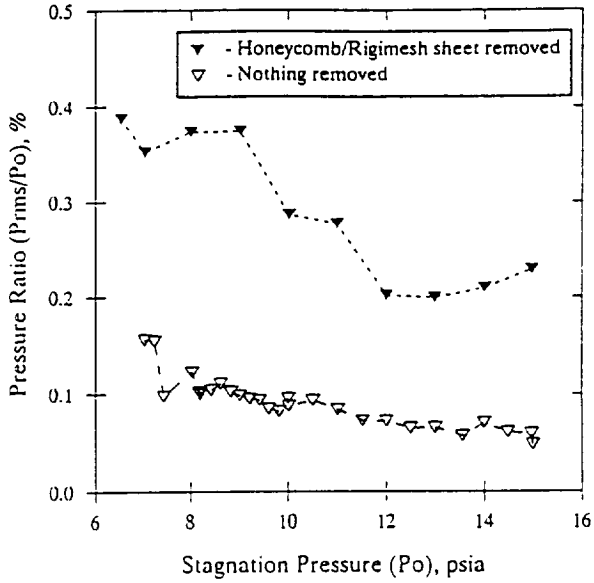


*Fig. 3 - Summary of Kulite pressure data from the PoC settling chamber.*

### Test Section

A hot-wire, mounted on the PoC test section floor, was used to detect transition occurring in a familiar non-bypass process with transition bursting. (See the hot-wire signals in Figure 4.) The uncalibrated hot-wire data, taken with two levels of core flow disturbances are compared in Figure 5. Clearly, the increase of core flow disturbances promoted transition onset, at the same location, at a lower Po of about 6 psia (0.41 bar) instead of 9 psia (0.61 bar) found with low-disturbance core flow on the same day. A result later substantiated with Preston tube measurements.[3] This result is actually a repeat of Laufer's work[1] at JPL, which highlighted the strong effect of free stream turbulence on transition, particularly at Mach numbers less than 2.5. This result is further proof that the settling chamber is a key element in the LFSWT design and will decide the extent of laminar flow at higher Re.

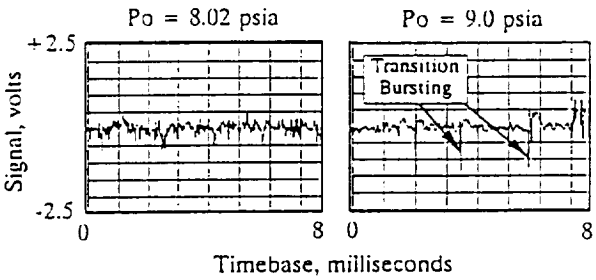


*Fig. 4 - Comparison of hot-wire signals from the PoC test section at Po values near transition onset.*

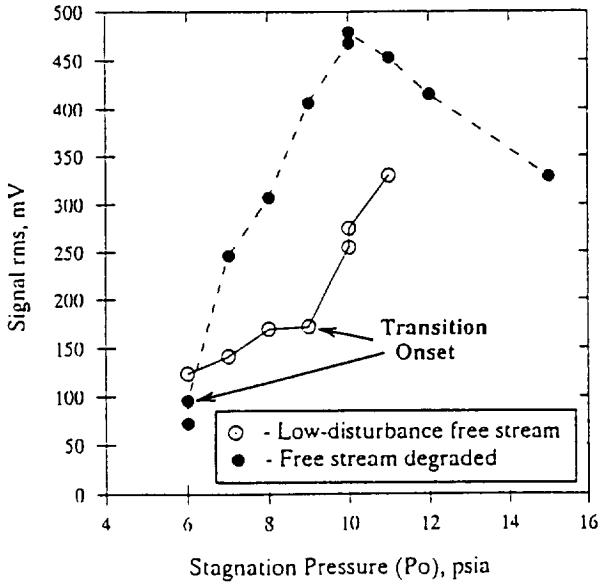


*Fig. 5 - Effect of different free stream disturbance levels on PoC test section hot-wire data at Mach 2.5.*

## LFSWT Design

The LFSWT drive system for Mach 2.5 operation requires up to 184 lbs/sec (83.4 kg/sec) of mass flow. Unfortunately, recent investigations of the FML compressor have revealed that a $P_E$ of 8 psia (0.34 bar) cannot be maintained at the high mass flows now required for Mach 2.5 operation. In fact, $P_E$ rises to 8.8 psia (0.6 bar) at high mass flows precluding PoC operation below a Po of 15 psia (1.02 bar). A decision has therefore been made to concentrate the initial LFSWT operating envelope on lower Mach numbers below Mach 2. We have chosen Mach 1.6 in order to support the F-16XL flight tests.

This change in Mach number means that both the secondary injectors and the supersonic diffuser will not be needed for the initial LFSWT configuration. Furthermore, the adjustment range for the LFSWT primary injectors has been increased for drive system tuning. The range of primary injector exit Mach number is 1.8 to 2.2. The LFSWT primary injector mass flow can be varied independent of the exit Mach number from 62-124 lbs/sec (28-56 kg/sec).

The effectiveness of the PoC settling chamber has been verified by the existence of laminar flow in the PoC test section. However, the existence of laminar flow in a small wind tunnel like PoC (with short flow lengths) does not guarantee long lengths of laminar flow in a larger wind tunnel like the LFSWT. Preliminary CFD analyses[3] predicted that transition would not occur along the PoC Mach 2.5 nozzle or test section. Unfortunately, this prediction was disproved by the PoC experiments. Nevertheless, this outcome, and the PoC data, both emphasize the dominance of core flow disturbances in the transition processes present in the PoC and, eventually, the LFSWT. Two transition measurements (hot-wire and Preston tube) agree that transition onset occurs further than 84% along the PoC test section floor over the Po range from 5.4 psia (0.37 bar) to Po = 8.5 psia (0.59 bar). So, the PoC quiet Re range is from 1.25 to 1.97 million per foot, with a stagnation temperature (To) of about $50^{\circ}$F (283 K), as shown in Figure 1.

## Conclusions

1) Laminar flow exists over 84% of the PoC test section at Re from 1.25 to 1.97 million per foot, validating our concept of achieving natural laminar flow by initial passive means.

2) Quiet flow studies in the PoC settling chamber indicate that the core flow is low-disturbance, with pressure disturbances of order 0.1%, but lower disturbances may be required to maintain laminar flow on the nozzle/test section walls at higher Re.

3) A linear stability analysis ($e^N$ method) is now available at NASA-Ames to assist our quiet wind tunnel development. Currently, we think that the failure of CFD to predict transition in the PoC is due to the unknown influences of core flow disturbances.

4) The settling chamber is very important in the design of quiet low-supersonic wind tunnels.

5) Design of the LFSWT is near completion for Mach 1.6 operation and we expect the LFSWT to be commissioned in 1993.

## References


1. Laufer, J.: **Aerodynamic Noise in Supersonic Wind Tunnels.** Journal of the Aerospace Sciences, vol. 28, no. 9, September 1961, pp. 685-692.

2. Pate, S.R.; and Schueler, C.J.: **Radiated Aerodynamic Noise Effects on Boundary-layer Transition in Supersonic and Hypersonic Wind Tunnels.** AIAA Journal, vol. 7, no. 3, March 1969, pp. 450-457.

3. Wolf, S.W.D.; Laub, J.A.; King, L.S.; and Reda, D.C.: **Development of the NASA-Ames Low-Disturbance Supersonic Wind Tunnel for Transition Research up to Mach 2.5.** AIAA Paper 92-3909. Presented at AIAA 17th Aerospace Ground Testing Conference, July 1992.

4. Wilkinson, S.P.; Anders, S.G.; Chen, F.-J.; and Beckwith, I.E.: **Supersonic and Hypersonic Quiet Tunnel Technology at NASA Langley.** AIAA Paper 92-3908. Presented at AIAA 17th Aerospace Ground Testing Conference, July 1992.

# APPENDIX D

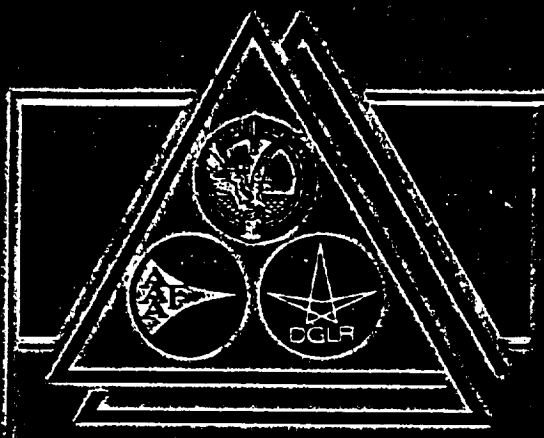


Paper 28

# DESIGN FEATURES OF A LOW-DISTURBANCE SUPERSONIC WIND TUNNEL FOR TRANSITION RESEARCH AT LOW SUPERSONIC MACH NUMBERS

Stephen W.D. Wolf, James A. Laub, Lyndel S. King and Dante C. Reda

Fluid Dynamics Research Branch
Fluid Mechanics Laboratory
NASA Ames Research Center
Moffett Field, CA 94035-1000, USA

Preprint of paper for the European Forum on
Wind Tunnels and Wind Tunnel Test Techniques

September 14-17, 1992
Southampton, England

# DESIGN FEATURES OF A LOW-DISTURBANCE SUPERSONIC WIND TUNNEL FOR TRANSITION RESEARCH AT LOW SUPERSONIC MACH NUMBERS

Stephen W.D. Wolf*, James A. Laub**, Lyndell S. King***, and Daniel C. Reda+
Fluid Mechanics Laboratory
Fluid Dynamics Research Branch
NASA Ames Research Center
Moffett Field, California 94035-1000, USA

## Abstract

A unique, low-disturbance supersonic wind tunnel is being developed at NASA-Ames to support supersonic laminar flow control research at cruise Mach numbers of the High Speed Civil Transport (HSCT). The distinctive design features of this new quiet tunnel are a low-disturbance settling chamber, laminar boundary layers along the nozzle/test section walls, and steady supersonic diffuser flow. This paper discusses these important aspects of our quiet tunnel design and the studies necessary to support this design. Experimental results from an 1/8th-scale pilot supersonic wind tunnel are presented and discussed in association with theoretical predictions. Natural laminar flow on the test section walls is demonstrated and both settling chamber and supersonic diffuser performance is examined. The full-scale wind tunnel should be commissioned by the end of 1993.

## Symbols

| | |
|---|---|
| Cp | Pressure coefficient $[(Ppt-P)/(\tau PMe^2/2)]$ |
| Me | Free stream Mach number |
| P | Local static pressure |
| Po | Tunnel stagnation pressure |
| PE | Exit (manifold) total pressure |
| Ppt | Preston tube pressure |
| Prms | Pressure measurement rms |
| Re | Unit Reynolds number per foot |
| To | Tunnel stagnation temperature |
| u | Local velocity in boundary layer |
| Ue | Free stream velocity |
| X | Streamwise position relative to nozzle throat station (positive downstream) |
| $\tau$ | Ratio of specific heats |

## Introduction

Low-disturbance or "quiet" wind tunnels are now an essential and indispensable part of meaningful boundary layer transition research at supersonic speeds. This realization is based on many years of experience with old "noisy" supersonic wind tunnels, and a growing respect for the pioneering research of Laufer[1,2] at the Jet Propulsion Laboratory (JPL) from the mid-1950s to the early-1960s, supported by the work of Pate and Schueler[3] in the late-1960s. In addition, this realization has received recent emphasis due to an appreciation of the risk associated with inadequate flight test measurements "validating" CFD transition predictions. Of course, the wind tunnel can provide controlled test environments and is much better suited to the job of validating CFD predictions. It is the combination of wind tunnel, CFD and flight test that provides the best hope of solving one of the last great mysteries of aerodynamics, namely transition to turbulence. Based on this premise, NASA-Ames has embarked on the development of a unique Laminar Flow Supersonic Wind Tunnel (LFSWT) in the Fluid Mechanics Laboratory (FML) at NASA-Ames to fill the void.

The concept behind the LFSWT design is based on the now decommissioned (but soon to be rebuilt) JPL 20-inch supersonic wind tunnel, which just happened to be the first documented quiet supersonic wind tunnel because of its high-quality origins.[4] From its outset, the LFSWT has been designed as a quiet research tunnel which is capable of continuous operation. The proposed test envelope of the LFSWT was chosen to cover a significant portion of the potential HSCT operating envelope, with a Re range of 1 to 3 million per foot and a Mach number (Me) range from 1.6 to 2.5. In addition, this LFSWT test envelope will cover the test conditions flown by NASA's F-16XL aircraft in support of Supersonic Laminar Flow Control (SLFC) studies, as shown in Figure 1. The maximum test section size was fixed by the desire to utilize an existing dry air source.

---

* Research Scientist, MCAT Institute. Senior Member AIAA. AMRAeS.

** Facility Operations Manager, Fluid Dynamics Research Branch.

*** Research Scientist, Fluid Dynamics Research Branch. Member AIAA.

\+ Senior Research Scientist, Fluid Dynamics Research Branch. Assoc. Fellow AIAA.

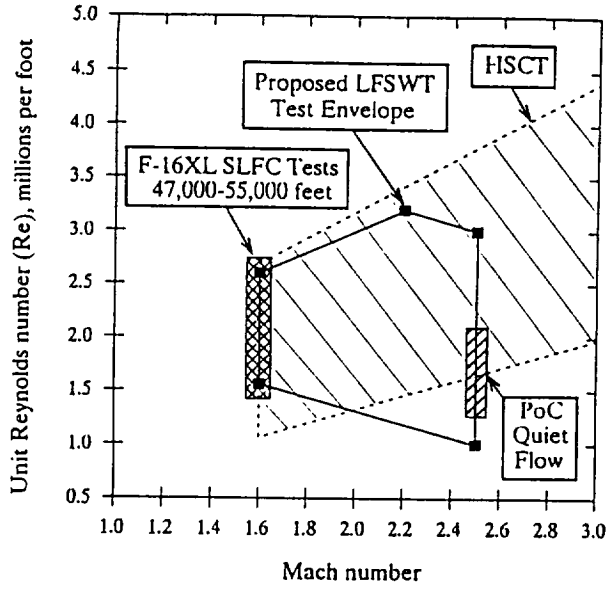


*Fig. 1 - Proposed LFSWT test envelope compared with the flight envelopes of the HSCT at cruise and the F-16XL SLFC flight tests.*

What actually defines a quiet supersonic wind tunnel? Pressure fluctuations of 0.05% in the test core is considered to be quiet enough. This low level of turbulence is achieved with a combination of a low-disturbance free stream, laminar flow along the nozzle/test section walls, steady diffuser flow and minimal mechanical vibration of nozzle and test section.

The LFSWT is currently being designed with an 8 inch (20.32 cm) high, 16 inch (40.64 cm) wide and 32 inch (81.28 cm) long test section, sized to operate at mass flows up to 21 lbs/sec (9.52 kg/sec). The use of existing support equipment (the FML indraft compressor and the NASA-Ames 3000 psi (207 bar) dry air supply) will reduce project costs and allow the LFSWT to be brought on-line more rapidly than would normally be the case for a new facility. Consequently, the LFSWT should be able to impact the critical technology development phase of the HSCT before 1997.

The decision to use the FML non-specialist indraft compressor to power the LFSWT created several technical concerns. To achieve the low end of the Re range, the LFSWT must operate with a Po which is less than the minimum $P_E$. This means that the LFSWT compression ratios will be uniquely less than unity ($P_o/P_E$ down to 0.625:1 with Re = 1 million per foot at Po = 5 psia - 0.34 bar). So, the utilization of the FML compressor precludes the use of a conventional drive system to achieve the desired Re range. Consequently, a novel drive system was developed using an 1/8th-scale model of the LFSWT, which we call the Proof-of-Concept (PoC) supersonic wind tunnel.

A detailed description of this drive system is beyond the scope of this paper and has already been covered by Wolf et al.[5,6] The drive system requires less than half of the normal run compression ratio to both start and run. The drive system works by utilizing the huge compressor mass flow capability (which greatly exceeds the mass flow necessary for the test section flow alone) to drive one or two stages of ambient injectors. It is these injectors which pull the flow through the test section at low Po. Two stages of injectors became necessary for Mach 2.5 operation to allow the primary injectors to operate at a higher exit Mach number. This in turn lowered the exit pressure of the test section flow and allowed the PoC to operate at compression ratios less than unity. The LFSWT drive system for Mach 2.5 operation will require up to 184 lbs/sec (83.4 kg/sec) mass flow at a maximum Po of 15 psia (1.02 bar), if the Po range from 5 to 15 psia (0.34 to 1.02 bar) is to be preserved with $P_E$ = 8 psia (0.54 bar).

It is expected that the LFSWT, when commissioned, will be the only quiet tunnel to operate at low-supersonic Mach numbers. Researchers at NASA Langley have chosen to devote over 10 years of quiet wind tunnel work at Mach 3.5 and above, and appear wary of the problems of building a low-supersonic quiet tunnel.[7] This is a surprising situation considering the research interest in transition at low-supersonic Mach numbers. The concerns at Langley stem from the need to maintain laminar boundary layers further downstream from the nozzle throat. This need arises because the Mach lines, along which acoustic disturbances radiate from turbulent boundary layers, are much more normal to the flow at low-supersonic speeds. Consequently, longer lengths of laminar flow are required to provide the same length of quiet test core at low-supersonic Mach numbers as found at higher Mach numbers (as shown in Figure 2).

We do not have similar concerns at NASA-Ames for three reasons. At low-supersonic Mach numbers, the length and curvature necessary for the supersonic nozzle are less, which deters the development of Tollmein-Schlichting (TS) waves and Görtler vortices (known transition promoting

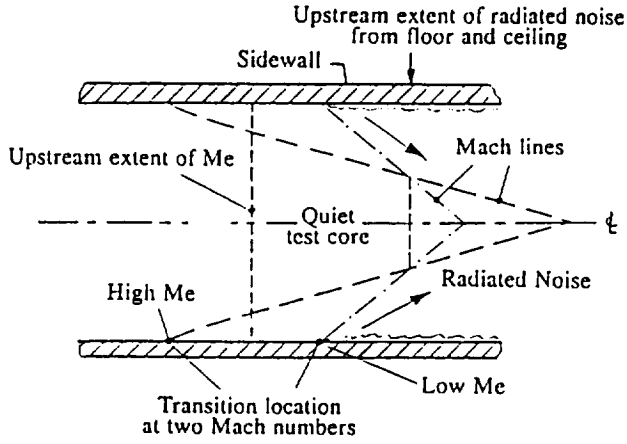


*Fig. 2 - Different lengths of laminar flow are required to maintain the same size quiet test core at two Mach numbers.*

disturbances). Furthermore, the unit Reynolds numbers (Re) necessary to match flight values are low, generally less than 3 million per foot (as shown in Figure 1). Operating the tunnel at low Re, helps promote natural laminar flow on all the tunnel walls, and also relaxes the requirement for a highly polished surface finish on the walls of the nozzle throat. Finally, it is reported[2] that the free stream disturbances have a dominant effect on the transition process at Mach numbers below 2.5. Hence, we can reasonably expect the importance of a quiet nozzle to be less than that of the settling chamber at low-supersonic Mach numbers. Fortunately, the settling chamber of a supersonic tunnel can be treated in a similar fashion to that of a large low-disturbance subsonic tunnel about which much is already known.[8] It is for these reasons, that we consider the design of a low-supersonic quiet wind tunnel to be less complex than that of any existing high Reynolds number high-supersonic/hypersonic quiet tunnel.

We have embarked on a combination of theoretical and experimental research efforts at NASA-Ames, to ensure that the LFSWT will provide the necessary quiet test core. While we are using the PoC for design studies, we are also developing and gaining experience with the latest instrumentation for transition research, in particular hot-films, focusing schlieren and liquid crystals. This experience will aid our development of quiet nozzles, improve flight test measurements, and also give FML the tools required for future transition research, when the LFSWT comes on-line.

This paper highlights important features of the ongoing LFSWT design and discusses the necessary studies to support this design. We intend that this paper should help others engaged in supersonic transition research by outlining the important aspects of developing a *State-of-the-Art* supersonic transition research facility.

## Tunnel Design Studies

The PoC has been used extensively to study the aerodynamic lines of the LFSWT settling chamber, nozzle/test section and supersonic diffuser. A schematic of the PoC layout is shown in Figure 3 to illustrate the novel dual-stage injector drive system. The two stages of injectors are orientated at right angles to one another, from practical considerations (see Figure 4). The PoC test section is 1 inch (2.54 cm) high, 2 inches (5.08 cm) wide, and 4 inches (10.16 cm) long.

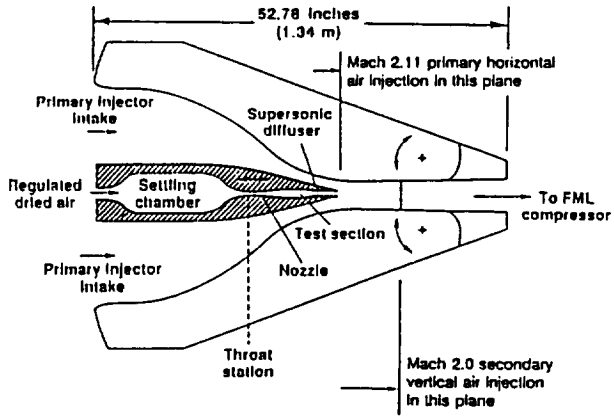


*Fig. 3 - A schematic layout of the PoC supersonic wind tunnel.*

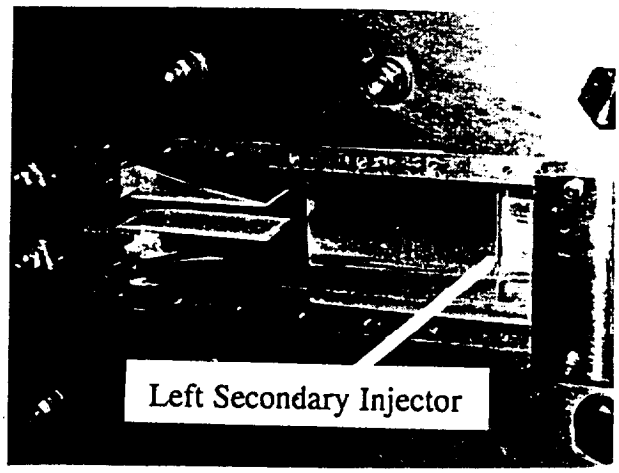


*Fig. 4 - The relative position of the primary and secondary stages of ambient injectors in the PoC, with the right-hand secondary injector and window removed.*

The test section is fed with regulated, dried air which has a dew point of about -50°F (227 K) from the existing NASA-Ames

3000 psi (207 bar) supply. Of course, the dried air is necessary to eliminate any condensation effects in the test section. The PoC dual-stage injectors draw in ambient air from the surrounding room. The exit Mach number of the primary injectors is 2.11, while the secondary injectors operate at Mach 2. The air mass flow ratio between injectors and test section rises to a massive 27:1 at the minimum Po of 5.4 psia (0.37 bar) during Mach 2.5 operation.

The only nozzle used in the work reported here is a two-dimensional, fixed-block, Mach 2.5 type, designed according to the methodology of Riise[9] used at JPL. The nozzle design is considered long, with the surface curvature minimized. The nozzle has a throat to exit length of 5.114 inches (13 cm), with a throat height of 0.38 inch (9.65 mm). The nozzle and test section are made from 6061-T6 aluminum. The flow surfaces along the nozzle are hand finished to about a 2L standard (roughness height 2 microinches - 0.05 micron). We consider the laminar flow requirements for the nozzle surface finish at low Re to be less stringent than those required in other quiet supersonic tunnels like the NASA-Langley Mach 3.5 Pilot Quiet Tunnel.[7]

A two-dimensional nozzle was chosen to minimize focusing of disturbances, due to shape imperfections, on the tunnel centerline. In addition, a two-dimensional nozzle allows important optical and physical access to the nozzle for transition studies and cleaning. A seal between the nozzle and the enclosing side plates is provided by close tolerance mating surfaces and vacuum grease.

The relatively large three-dimensional PoC contraction is designed using a fifth-order polynomial to minimize the possibility of flow separations. The contraction is 6 inches (15.24 cm) long on the floor and ceiling and 2.5 inches (6.35 cm) long on both sidewalls. The contraction ratio is 12:1, based on the test section cross-sectional area, and is a minimum of 15.6:1 based on the variable nozzle throat area over the Mach number range. The sidewall contractions are shorter to allow windows to be fitted upstream of the nozzle throat for optical access to the complete throat.

The PoC is fitted with a three-dimensional settling chamber equipped with an array of flow management devices intended for low-disturbance operation. These devices include a sintered wire mesh (Rigimesh) cone and flat sheet, a honeycomb flow straightener and 4 flow smoothing screens, combined with the previously described contraction. A schematic of the settling chamber is shown in Figure 5, highlighting its modular design, which allows component holder inter-changeability. The flow velocity in the settling chamber is 20 fps (6.1 m/sec) with Po = 15 psia (1.02 bar) and To = 50°F (283 K) for Mach 2.5 operation. At Mach 1.6, the flow velocity in the settling chamber will rise to about 40 fps (12.2 m/sec). Figure 6a shows the new PoC settling chamber in situ.

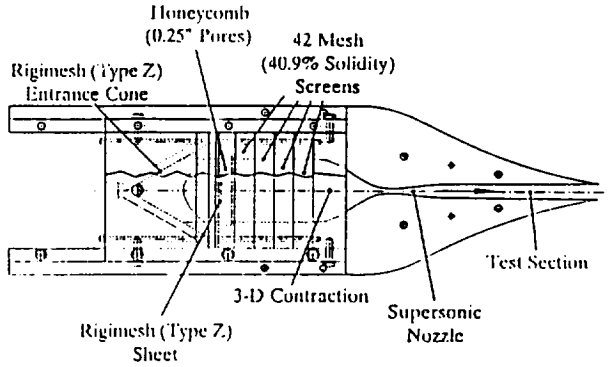


*Fig. 5 - Schematic of the new PoC settling chamber.*

The settling chamber design is based on knowledge of the literature and is largely conventional.[10] The only unusual feature is the use of sintered wire mesh (Rigimesh) based on the recommendations of Beckwith.[11] The sintered wire mesh provides acoustic isolation of the settling chamber from the upstream piping and valves necessary to regulate the dry air source. We also use this filter material in the PoC settling chamber to help spread the inlet pipe flow into the settling chamber. To this end, we utilize both a cone and flat sheet of Rigimesh type-Z material. This filter material is 0.009 inch (0.23 mm) thick and has a pore size of approximately 39 microinches (1 micron). The pressure load on the 60° cone is supported by a perforated sheet on the downstream side of the cone. This perforated sheet is sufficiently open to minimize flow blockage effects. The flat sheet is supported by a 1 inch (2.54 cm) thick honeycomb sheet with a 0.125 inch (3.17mm) cell size.

The honeycomb sheet is followed by 4 screens, as shown in Figure 5. Each screen is made from 42-mesh stainless steel cloth with a 59.1% open ratio. The screen separation is equivalent to 63 mesh lengths. This length is more than the 50 mesh lengths required for small structure turbulence decay according to

Groth and Johansson.[12] There is the equivalent of 31 mesh lengths between the last, most downstream screen and the entrance to the contraction. The most downstream screen holder is hand finished to the contraction to remove disturbance generating steps or gaps.

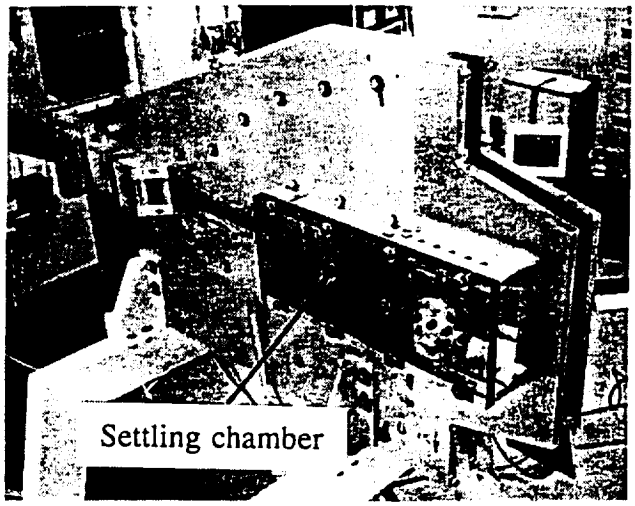


*Fig. 6a - The PoC settling chamber in situ.*

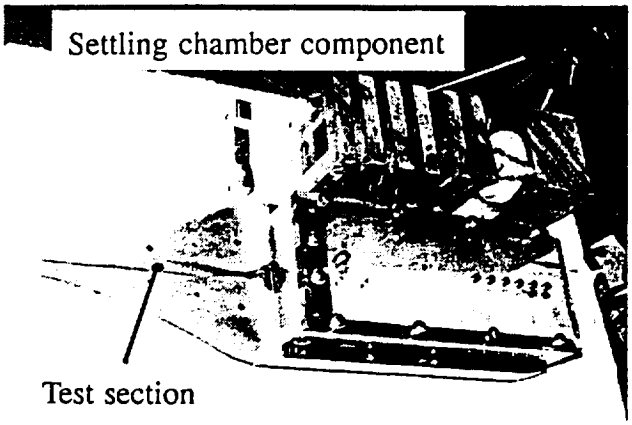


*Fig. 6b - A display of PoC settling chamber /nozzle/test section components.*

The three-dimensional contraction was made integral with the Mach 2.5 nozzle/test section/supersonic diffuser (see Figure 6b). This design removes all hardware joints on the nozzle floor and ceiling upstream of the test section. The test section has a slightly diverging floor and ceiling to allow for boundary layer growth. The supersonic diffuser is a parallel wall type developed experimentally[5,6], with a throat height of 0.76 inch (1.93 cm) and a length of 5.125 inches (13 cm).

## Tunnel Instrumentation

The instrumentation used in the PoC is directly transferable to the LFSWT. This instrumentation includes pressure taps for steady-state measurements, and hot-wires (single 4 and 5 micron Tungsten wire types), Kulite (XCS-093) pressure transducers, and TSI (Model 1237) platinum hot-film gages for dynamic measurements.

The static pressures are measured using a scanivalve system connected to a standard PC A/D converter card. The hot-wires are powered by FML's own constant-temperature bridge circuit with the output signal fed to a Tektronix 2642A Fourier Analyzer (TFA) system, as are all the dynamic measurements. The Kulites are powered by high frequency response signal conditioners (Dynamic 8000s with a 3dB dropoff at 500KHz). The hot-film gage is powered by a constant-current bridge devised by Demetriades at Montana State University.

The TFA system can sample an input signal at up to 512KHz with 16-bit resolution, and provides averaged 4096-point real-time FFTs, data capture and display. Data is then stored on a PC computer for data archiving, post processing and data presentation.

PoC dynamic measurements can be made in either the test section or in the settling chamber. In the test section, the hot-wire is buried in the supersonic diffuser molding to minimize blockage, as shown in Figure 7. The hot-wire probe protrudes 0.625 inch (15.9 mm) upstream into the test section, at an X location of 8.375 inches (21.27 cm), and sits about 0.069 inch (1.75 mm) above the test section floor. A Preston tube with a 0.029 inch (0.73 mm) outside diameter was fitted in place of the test section hot-wire for some tests. The hot-film gage was flush mounted in the left sidewall, on the test section centerline, at an X location of 6.69 inches (16.99 cm).

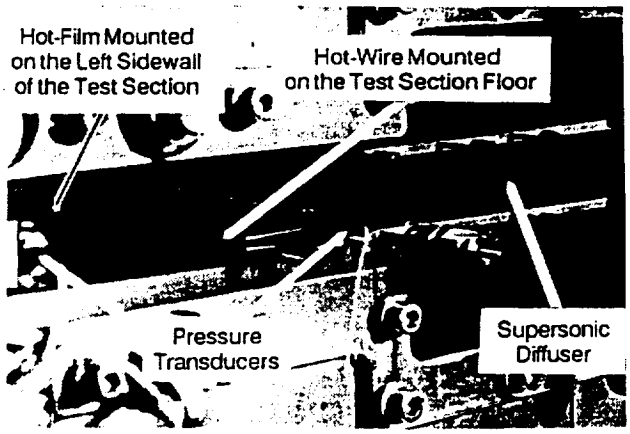


*Fig. 7 - Hot-wire and hot-film instrumentation mounted in the PoC test section.*

In the settling chamber, a special instrumentation holder block allows two probes to be mounted side-by-side and inserted in any holder location. Three interchangeable traversable probes are available: pitot pressure probe fitted with a Kulite; a temperature probe fitted with a type-T thermocouple; and a hot-wire probe fitted with a 4 micron Tungsten wire. These probes can be used for detailed mapping of the flow field at any location in the settling chamber. However, only one position is reported in the data discussed later.

The PoC polycarbonate Lexan-type windows have been used with a focusing schlieren system[5,13] to observe wave patterns in the supersonic diffuser and mixing region. Alternatively, one window can be replaced by an aluminum blank for use of shear-stress-sensitive liquid crystal coatings.

To ensure good flow quality in PoC, we use a Nyad model 140 hydrometer to continuously monitor the dew point of the test section air to check for sufficient dryness. We define sufficient dryness as a dew point of less than $-15^{0}$ F (247 K). A dew point greater than this generates an alarm to the tunnel operator.

## Numerical Studies

For the LFSWT, it is desirable that the boundary layers remain laminar within the nozzle and test section as far as possible. Malik[14] and others have shown that compressible stability theory with the $e^{N}$ method predicts boundary layer transition onset arising from Tollmein-Schlichting (TS) waves and Görtler vortices. For sufficiently small free stream turbulence levels in the tunnel, the value of N may approach 10, which is the value associated with high altitude flight in the quiescent atmosphere. Stability calculations within the present context may then serve two purposes: (1) as a predictive tool in designing the nozzle and test section; and (2) as a diagnostic tool in analyzing the experimental results.

The flow through a two-dimensional nozzle, test section, and supersonic diffuser is analyzed computationally with three different codes in order to predict both the mean flow and boundary layer stability and transition. A Navier-Stokes (NS) code, previously described by Wolf et al[5], is used to predict the mean flow quantities in the tunnel. For purposes of analyzing the stability characteristics of the wall boundary layers, the mean flow is assumed laminar in the nozzle and test section, but with turbulent boundary layers in the supersonic diffuser. A boundary layer code by Harris and Blanchard[15] is next employed to provide detailed boundary layer quantities and derivatives for use by the stability code of Malik[14], since the resolution requirements to accurately obtain first and second derivatives in the boundary layer are not easily met with a NS code. The Malik code uses linear spatial stability theory to analyze the stability of two-dimensional and axisymmetric, compressible wall-bounded flows. Wall curvature is accounted for, so the analysis considers both TS waves (1st, 2nd, etc. modes) and Görtler vortices. Transition onset is predicted with the $e^{N}$ method.

The PoC/LFSWT nozzle in the present study was intentionally made long so that instabilities arising from curvature effects would not cause transition. This decision was supported by the study of Wolf.[16] Calculations indicate that this approach was successful, in that the maximum N factor due to Görtler vortices thus far computed is less than 4. No significant TS instabilities at the PoC operating conditions have yet been found numerically.

## Experimental Program

The recent experimental program has focused on studying laminar flow in the PoC operating at Mach 2.5 and the effectiveness of the settling chamber. Similar work combined with drive system tuning is just starting at Mach 1.6. Preliminary flow measurements have been made in the settling chamber and the extent of natural laminar flow that exists along the PoC test section walls has been documented at Mach 2.5. Of course, the existence of laminar flow on the nozzle walls is a critical element of any quiet supersonic wind tunnel. Our intent with the LFSWT is to go beyond this requirement and obtain laminar flow throughout the test section. This situation will provide a large quiet test core, which allows model testing anywhere in the test section. This elimination of the normal quiet test rhombus[7] removes the need to position the model upstream of the nozzle exit, which greatly simplifies the method of model support.

Initially, we are concerned with obtaining natural laminar flow on the nozzle and test section walls using passive laminar flow control. These passive means are a low-disturbance free stream, a low curvature, long

nozzle and a smooth wall finish. The documentation of natural laminar flow, using the solid block Mach 2.5 nozzle, is the first stage of an ongoing verification of the LFSWT test envelope.

For the quiet flow studies, the PoC was fitted with a low-disturbance settling chamber/nozzle/test section, instrumentation for dynamic measurements, and a closed-loop control system for precisely setting and maintaining Po. Dynamic flow measurements in the test section and settling chamber were then made to document the flow quality in PoC over the Re range. To assist with verification of our instrumentation, the settling chamber was degraded and the associated effects on laminar flow in the PoC test section were documented and are discussed later.

## Quiet Flow Studies

### Settling Chamber

The PoC low-disturbance settling chamber (previously described) has been operated over a Po range from 5 to 15 psia (0.34 to 1.02 bar). This Po range for Mach 2.5 operation corresponds to a mass flow range of 0.097 lbs/sec (0.044 kg/sec) to 0.358 lbs/sec (0.162 kg/sec) for To = $50^{0}$F (283 K). The static pressure distributions across the components of the settling chamber are shown in Figure 8 for different Po. It can be seen that the maximum pressure drop of about 2.5 psia (0.17 bar) occurs across the flat sheet of sintered wire mesh (Rigimesh). The Rigimesh cone supports minimal pressure load, which simplifies the necessary support structure for a full-scale LFSWT cone, if this should become necessary.

Preliminary flow disturbance measurements were made in the plane of the settling chamber exit (at a single location on the tunnel centerline) using a Kulite total pressure probe and a 4 micron Tungsten hot-wire. The Kulite data are shown in Figure 9 over the Po range for two settling chamber configurations (with and without the honeycomb and Rigimesh sheet installed). The pressure disturbances (the

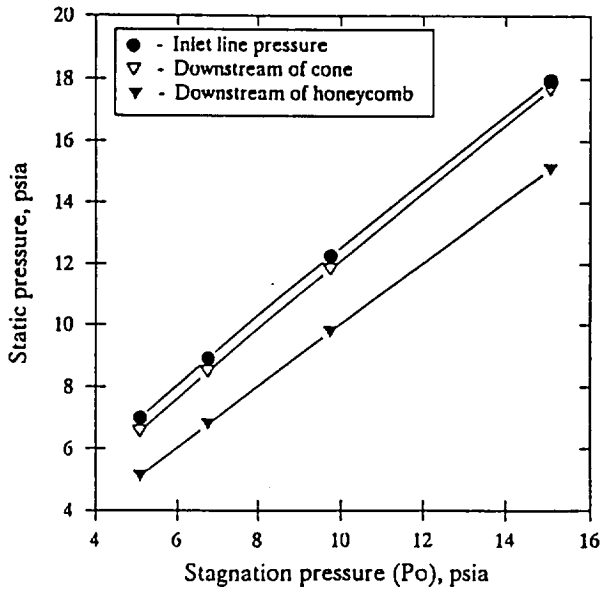


*Fig. 8 - Pressure distributions through the PoC settling chamber.*

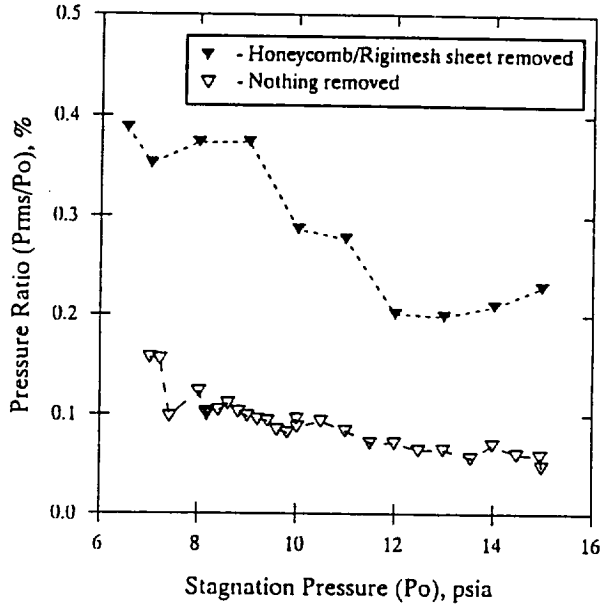


*Fig. 9 - Summary of Kulite pressure data from the PoC settling chamber.*

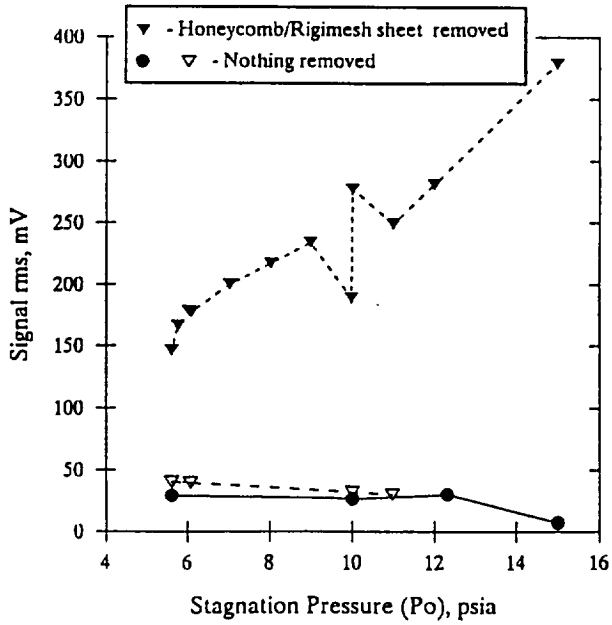


*Fig. 10 - Summary of the uncalibrated hot-wire data from the PoC settling chamber.*

ratio of the Prms to Po) show a significant rise of 0.2-0.3% with the honeycomb and Rigimesh sheet removed. The pressure disturbances drop with increasing Po and hence mass flow. With all the settling chamber components in place, the pressure fluctuations are of the order 0.1%. The sharp increase in pressure disturbances at low Po has been traced to tunnel leaks which caused unstarting of the test section flow.

The corresponding hot-wire data from the settling chamber are shown in Figure 10. Again, about a fourfold increase of signal rms is associated with the removal of the honeycomb and Rigimesh sheet. The signal levels, with all the settling chamber components in place, are reasonably low compared to the 0.7 mV wind-off noise level. However, in the absence of a hot-wire calibration of volts-vs-velocity, these data can only be discussed qualitatively.

Test Section

Our laminar flow studies in the PoC test section have involved the use of different types of instrumentation to confirm the state of the test section boundary layer. We find that the detection of boundary layer transition tends to be qualitative. Consequently, it was our goal to find at least 2 measurement techniques which were in reasonable agreed about the location of transition in the PoC.

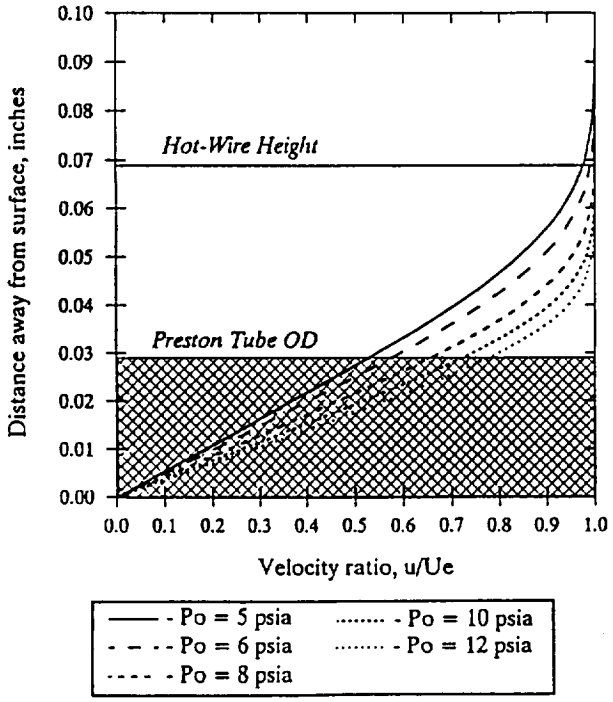


*Fig. 11 - Calculated laminar boundary layer profiles in the PoC test section (X = 8.375 inches - 21.27 cm).*

We found that the hot-wire measurements made above the PoC test section floor, in the outer portions of the boundary layer (see Figure 11), show a sharp rise in signal rms when Po is about 9 psia (0.61 bar). The actual hot-wire signals for Po = 8.02 psia (0.54 bar) and 9 psia (0.61 bar) are shown in Figure 12a. The differences between the signals is indicative of transition bursting. The signal spectrums are broadband with no discrete frequencies.

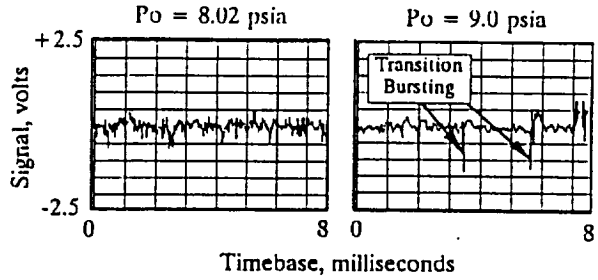


*Fig. 12a - Comparison of hot-wire signals from the PoC test section at Po values near transition onset.*

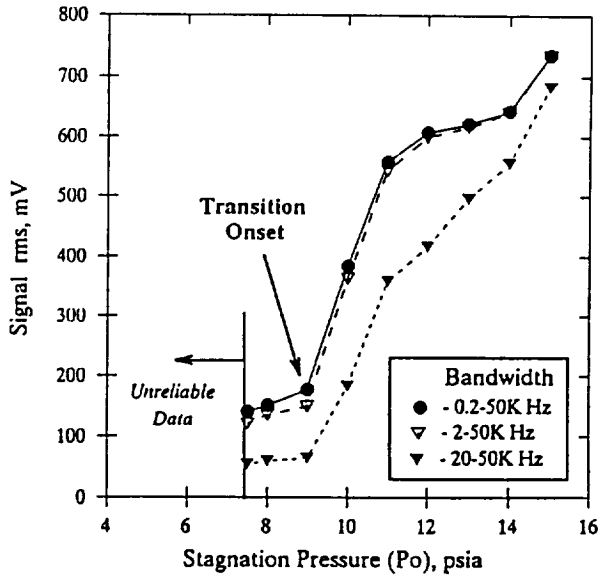


*Fig. 12b - Summary of hot-wire data from the PoC test section at Mach 2.5 (X = 8.375 inches - 21.27 cm).*

The associated rise in the hot-wire signal rms is independent of the signal bandwidth, as shown in Figure 12b. In fact, the hot-wire signals follow a pattern over the Po range which is associated with a familiar non-bypass transition process[17], where the transition bursting reaches a maximum frequency. Unfortunately, the hot-wire data at lower Po, in this test series, were unreliable due to tunnel leaks, but low signal rms was observed down to a Po of 5.4 psia (0.37 bar).

To check the reliability of the hot-wire data from the PoC test section, the honeycomb and Rigimesh sheet were removed from the settling chamber. The uncalibrated hot-wire data taken with and without the honeycomb and Rigimesh sheet installed, are shown in Figure 13. Clearly, the increase of free stream turbulence (discussed in the previous sub-section) had the effect of promoting transition onset, at the same location, at a lower Po of about 6 psia (0.41 bar) and hence a lower Re. Note, in this data set that a low signal rms was achieved down to a Po of 6 psia (0.41 bar) before tunnel leaks occurred.

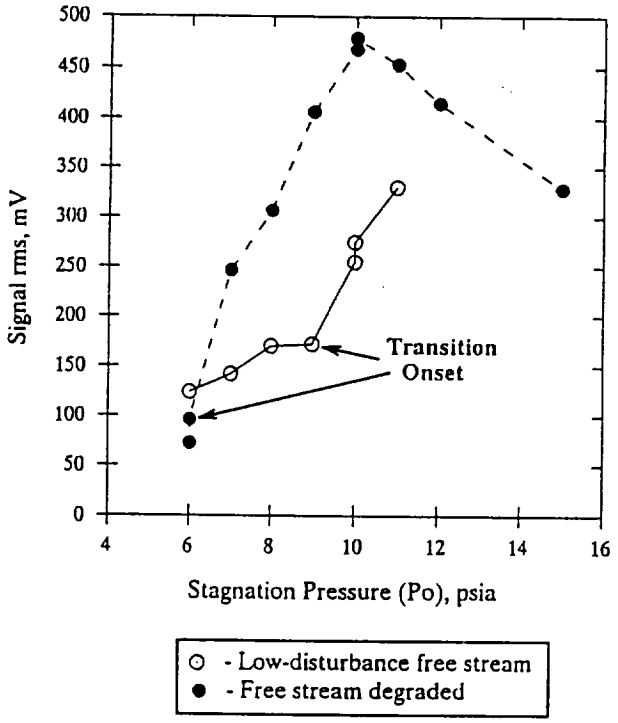


*Fig. 13 - Effect of different free stream disturbance levels on hot-wire data from the PoC test section at Mach 2.5.*

In another series of tests, the hot-wire was replaced by a Preston tube. This tube was sized to fit in the lower half of the floor boundary layer (See Figure 11). The data from the Preston tube are shown in Figure 14, over an extended Po range from 5.4 psia (0.37 bar) to 20 psia (1.36 bar). This Po range corresponds to an Re range from 1.25 to 4.64 million per foot. It is clear that there is a significant rise in the probe Cp at a Po of about 8.5 psia (0.58 bar). This rise is associated with transition onset where the boundary layer profile starts to change from a laminar type to a turbulent type.[18] The probe Cp reaches a plateau at about 16 psia (1.09 bar).

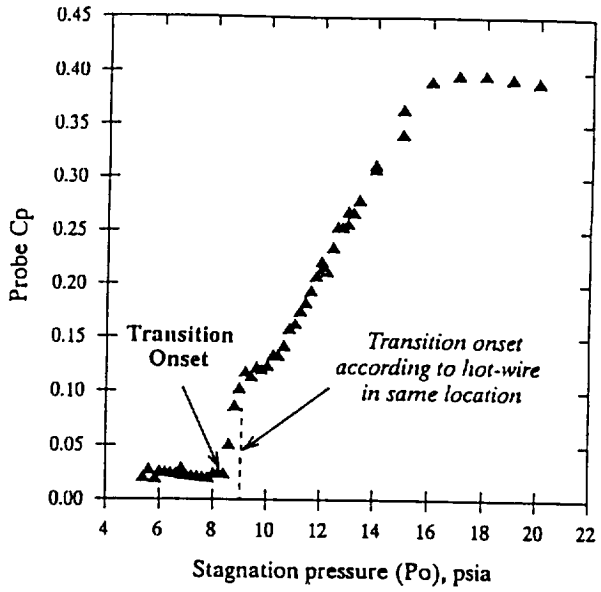


*Fig. 14 - Summary of Preston tube data from the PoC test section at Mach 2.5 (X = 8.375 inches - 21.27 cm).*

The sidewall boundary layers were studied with a flush-surface-mounted hot-film. The hot-film data are shown in Figure 15 over an extended Po range up to 20 psia (1.37 bar). The calibration of the hot-film is only qualitative[19] as indicated on Figure 15. Nevertheless, the hot-film data show that the boundary layer on the sidewall remained

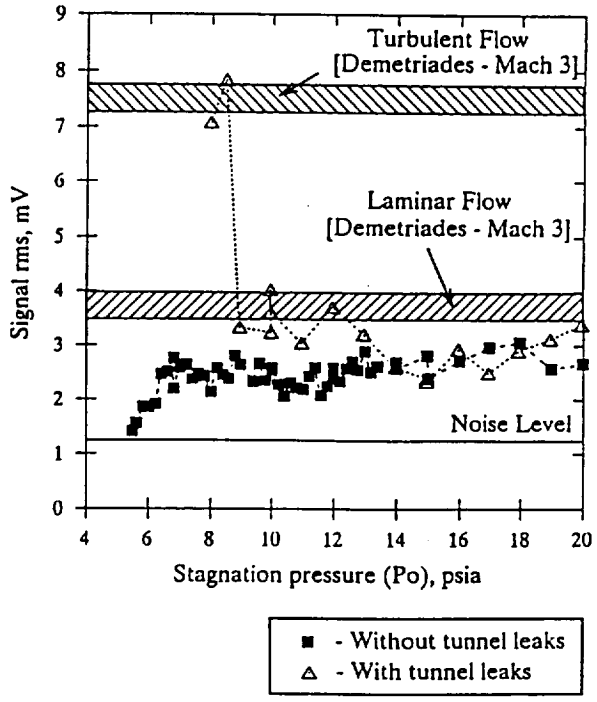


*Fig. 15 - Summary of hot-film data from the PoC test section sidewall at Mach 2.5 (X = 6.69 inches - 17 cm).*

laminar over the entire Re range, at an X location of 6.69 inches (17 cm), with no tunnel leaks. The hot-film signal rms is seen to jump to expected levels for turbulent flow only when tunnel leaks caused the test section flow to unstart. This flow break down caused transition bypass to occur on the sidewall, as shown in Figure 15, where hot-film data with and without tunnel leaks are compared. In addition, the same leaks cause transition bypass to occur on the test section floor and ceiling, as measured by the hot-wire probe in the test section.

During these laminar flow studies there was some concern about the drift in temperature of the inlet air and the PoC nozzle/test section structure. The air supply to the PoC is not heated and the inlet air temperature is always lower than ambient due to the expansion across a single air regulator. We monitored the inlet air temperature on a regular basis to check for repeatability of test conditions. The thermal mass of the PoC is large compared to the heat transfer associated with the nozzle/test section flow. We have observed the PoC structure reaching near temperature equilibrium within about the first 5 minutes of running. This temperature equilibrium is affected only slightly by changes of inlet air mass flow, despite noticeable changes in the inlet air temperature. To assess the long term effects of temperature drift, we operated the PoC for 2 1/2 hours continuously and monitored our hot-wire and hot-film instrumentation. No significant changes in the test section flow were observed during this test.

## LFSWT Design

The LFSWT drive system for Mach 2.5 operation requires up to 184 lbs/sec (83.4 kg/sec) of mass flow. Unfortunately, recent investigations of the FML compressor have revealed that a $P_E$ of 8 psia (0.34 bar) cannot be maintained at the high mass flows now required for Mach 2.5 operation. In fact, $P_E$ rises to 8.8 psia (0.6 bar) at high mass flows which would preclude LFSWT operation below a Po of 15 psia (1.02 bar). A decision has therefore been made to concentrate the initial LFSWT operating envelope on lower Mach numbers below Mach 2. We have chosen Mach 1.6 in order to support the F-16XL SLFC flight tests.

This change in Mach number means that both the secondary injectors and the supersonic diffuser will not be needed for the initial LFSWT configuration. Furthermore, the adjustment range for the LFSWT primary injectors has been increased for drive system tuning. The range of exit Mach numbers for the LFSWT primary injectors is 1.8 to 2.2. The mass flow of the LFSWT primary injectors can be varied independent of Mach number from 62-124 lbs/sec (28-56 kg/sec).

Of course, the PoC settling chamber effectiveness has been verified by the existence of laminar flow in the PoC test section. Two transition measurements (hot-wire and Preston tube) agree that transition occurs 84% along the test section floor at a Po of about 8.5 psia (0.58 bar) which corresponds to a Re of about 2 million per foot. Furthermore, when the settling chamber effectiveness is reduced by removing the honeycomb and Rigimesh sheet, transition occurs at a lower Po. This result is actually a repeat of Laufer's work[2] at JPL, which highlighted the strong effect of free stream turbulence on transition, particularly at Mach numbers less than 2.5. This result is further proof that the settling chamber is a key element in the LFSWT design and will largely control the extent of laminar flow as Re is raised.

Preliminary measurements in the PoC settling chamber show that the free stream flow entering the nozzle/contraction is low-disturbance. (Pressure disturbances less than 0.15% according to Wilkinson et al.[7]) Of course, the flow entering the LFSWT settling chamber will be different on account of the different array of valves and pressure reducers at 64 times larger mass flows. However, we are sure that the noise and turbulence entering the LFSWT settling chamber will be less than that of a blowdown wind tunnel.[20] Nonetheless, the LFSWT design will preserve the modularity of the PoC design to provide sufficient flexibility for future improvement.

The need to minimize the size of the inlet piping has led to the use of a pressure reducing module immediately upstream of the LFSWT settling chamber. This module is designed to take a 30 psia (2.04 bar) pressure drop and resembles a silencer design of concentric cylinders. Sintered wire mesh (Rigimesh) will be used to provide the pressure drop and will therefore act as the equivalent of the cone in the PoC design. The first part of the settling chamber will now contain 3 screens upstream of the honeycomb sheet, with increasing mesh size in the flow direction.

These extra screens are expected to provide a much more uniform flow into the honeycomb than expected from a sheet of sintered wire mesh (Rigimesh).[7]

An empty screen holder will be permanently attached to the contraction to provide the equivalent of 168 mesh lengths between the last screen and the entrance to the contraction. This empty screen holder will provide space for instrumentation to measure Po and turbulence parameters (pressure, velocity, and temperature) at the entrance to the contraction.

The LFSWT nozzle and contraction will be manufactured as one assembly. The nozzle/contraction geometries have been determined by the same methods as for the PoC. A 0.005 inch (0.127 mm) tolerance has been placed on the nozzle geometry. A 10 microinch (0.25 micron) surface finish has been specified for the nozzle walls based on CFD predictions of boundary layer thicknesses. In addition, we have specified a 0.001 inch (0.025 mm) tolerance on steps and gaps which puts great emphasis on expected wall temperatures.

The steadiness of the supersonic diffuser flow has been verified in the PoC tests, by the documentation of laminar flow in the test section. Furthermore, our dynamic instrumentation in the test section has allowed us to document the extent of steady flow at the inlet of the supersonic diffuser, as part of our laminar flow studies. The minimum Po at which Mach 2.5 could be maintained steadily was 5.4 psia (0.37 bar) without tunnel leaks. Below this Po, the average test section Mach number dropped and the hot-wire probe in the test section experienced significant velocity fluctuations. This onset of unstart has previously been observed (with the aid of our focusing schlieren system) as the entire supersonic diffuser flow becoming oscillatory and highly unstable. It is clear that once the inlet flow to the supersonic diffuser becomes oscillatory that laminar flow is lost.

At Mach 1.6, we envisage that the supersonic diffuser will not be required because the test section exit Mach number will be less than the primary injector exit Mach number. In addition, the run lengths downstream of the test section need to be shortened (relative to the Mach 2.5 case) to minimize the number of shock reflections from any model mounted in the test section. Too many shock reflections could cause the test section to unstart at this low Mach number.

The absence of transition on the PoC sidewall was expected, because of the short run lengths coupled with favourable pressure gradients and the absence of curvature. Consequently, we can surmise that the extent of quiet flow in the PoC is determined by the transition location on the floor and ceiling of the test section. Although, there are some concerns now about the effect of corner flows in the transition process, which need to be addressed.

In the LFSWT, transition may indeed occur first on the sidewalls (as occurs in the Mach 3.5 Langley Pilot Quiet Tunnel[7,20]) and this is one of the reasons for making the test section cross-section rectangular. By placing the sidewalls further from the tunnel centerline than the floor and ceiling, we can potentially maintain a quiet test core to higher Re. Also, the rectangular shape of the test section and supersonic diffuser means the primary injectors need only be mounted on the long floor and ceiling of the test section/supersonic diffuser, leaving the test section sidewalls clear of ducting for optical and physical access to the nozzle and test section.

The LFSWT design allows for variable tunnel length from the primary injector exit upstream. The support structure includes two rails which carry the movable tunnel components. Furthermore, the settling chamber, contraction, nozzle and test section are mechanically isolated from the rest of the tunnel components. Consequently, the vibration from the inlet piping and the injectors can not be considered a factor in the transition processes which will be investigated in the nozzle/test section.

Obviously, the tunnel leaks in the PoC (referred to earlier) have severely hampered research at low Po. The problem is peculiar to the small-scale of the PoC and has been traced to internal leak paths around the PoC windows. This is a legacy of using the PoC for much longer than originally planned. A solution to the problem has now been found by potting the windows in a silicone-based sealer instead of vacuum grease.

The existence of laminar flow in a small wind tunnel like PoC (with short flow lengths) does not guarantee long lengths of laminar flow in a larger wind tunnel like the LFSWT.

Preliminary CFD analyses predicted that transition would not occur along the PoC Mach 2.5 nozzle or test section. Unfortunately, this prediction was disproved by the PoC experiments. Nevertheless, this outcome, and the PoC data, both emphasize the dominance of core flow disturbances in the transition processes present in the PoC and, eventually, the LFSWT. Presently, we know that laminar flow exists along 84% of the PoC test section floor at Mach 2.5 from Po = 5.4 psia (0.37 bar) to Po = 8.5 psia (0.59 bar). So the PoC quiet Re range is from 1.25 to 1.97 million per foot (To $\approx$ 50°F - 283 K) as shown in Figure 1.

## Future Plans

The switch to Mach 1.6 has changed the LFSWT design as previously discussed. Validation of the LFSWT test envelope will continue by running PoC at Mach 1.6 with a single stage of injectors in the near future. We hope to study and document quiet flow and LFSWT drive system parameters for Mach 1.6 before the end of October 1992. We are confident that there is sufficient flexibility in the LFSWT design to accommodate any important findings from these tests. At the same time, further flow measurements will be made in the settling chamber with different configurations.

The LFSWT design should be complete by the end of August 1992 and fabrication will start immediately. We are planning to commission the LFSWT by the end of 1993. Work on the first model for the LFSWT is already underway and will consist of a full scale F-16XL leading edge for studies of crossflow instabilities and attachment-line contamination.

Tests of the dry air supply system are underway to determine the need for a heater. The expected low LFSWT wall temperatures have caused concerns (due to step and gap tolerances and the use of liquid crystals) which may make a heater essential. However, the exact size and type of heater has yet to be determined for realistic mass flows and run times. It is probable that this decision can only be made with any certainty when the LFSWT is built. However, provisions for a heater are included in the LFSWT design.

Instrumentation development will continue using commercially available hot-film arrays, which span the entire length of one wall of the contraction/nozzle/test section. This measurement technique should allow documentation of where transition occurs at a given Re. In addition, work with the focusing schlieren and liquid crystals will continue to document PoC transition. The streamwise location of the test section hot-wire and Preston tube probes will be varied to provide a more detailed study of the PoC flow. In addition, the effects of corner flows will be examined by mounting our dynamic instrumentation at different spanwise locations across the test section.

Quiet wind tunnel development work will continue with CFD analyses directed at active control of supersonic transition using nozzle wall heating and cooling together with nozzle contour and length changes. This effort will support the eventual expansion of the LFSWT quiet test envelope to cover the proposed test envelope shown in Figure 1.

## Conclusions

1) Laminar flow has been documented along at least 84% of the PoC test section at Re from 1.25 to 1.97 million per foot, validating our concept of achieving natural laminar flow by initial passive means.

2) Quiet flow studies in the PoC settling chamber indicate that the core flow is low-disturbance, with pressure disturbances of order 0.1%, but lower disturbances may be required to maintain laminar flow on the nozzle/test section walls at higher Re.

3) A linear stability analysis ($e^N$ method) is now available at NASA-Ames to assist our quiet wind tunnel development. Currently, we think that the failure of CFD to predict transition in the PoC is due to the unknown influences of core flow disturbances.

4) The settling chamber performance is very important in the design of quiet low-supersonic wind tunnels.

5) Design of the LFSWT is near completion for Mach 1.6 operation and we expect the LFSWT to be commissioned in 1993.

## References

1. Laufer, J.: **Factors Affecting Transition Reynolds Numbers on Models in Supersonic Wind Tunnels.** Journal of Aeronautical Sciences, vol. 21, no. 7, July 1954, pp. 497-498.

2. Laufer, J.: **Aerodynamic Noise in Supersonic Wind Tunnels.** Journal of the Aerospace Sciences, vol. 28, no. 9, September 1961, pp. 685-692.

3. Pate, S.R.; and Schueler, C.J.: **Radiated Aerodynamic Noise Effects on Boundary-layer Transition in Supersonic and Hypersonic Wind Tunnels.** AIAA Journal, vol. 7, no. 3, March 1969, pp. 450-457.

4. Kendall, J.M.: **Supersonic Boundary Layer Transition Studies.** JPL Space Programs Summary 37-62, April 1970, pp. 43-47.

5. Wolf, S.W.D.; Laub, J.A.; and King, L.S.: **An Efficient Supersonic Wind Tunnel Drive System for Mach 2.5 Flows.** AIAA Paper 91-3260. In: Proceedings of AIAA 9th Applied Aerodynamics Conference, vol. 1, September 1991, pp. 461-471.

6. Wolf, S.W.D.; Laub, J.A.; King, L.S.; and Reda, D.C.: **Development of the NASA-Ames Low-Disturbance Super-sonic Wind Tunnel for Transition Research up to Mach 2.5.** AIAA Paper 92-3909. Presented at AIAA 17th Aerospace Ground Testing Conference, July 1992.

7. Wilkinson, S.P.; Anders, S.G.; Chen, F.-J.; and Beckwith, I.E.: **Supersonic and Hypersonic Quiet Tunnel Technology at NASA Langley.** AIAA Paper 92-3908. Presented at AIAA 17th Aerospace Ground Testing Conference, July 1992.

8. Mueller, T.J.; Scharpf, D.F.; Batill, S.M.; Strebinger, R.B.; Sullivan, C.J.; and Subramanian, S.: **The Design of a Subsonic Low-Noise, Low-Turbulence Wind Tunnel for Acoustic Measurements.** AIAA Paper 92-3883. Presented at AIAA 17th Aerospace Ground Testing Conference, July 1992.

9. Riise, H.N.: **Flexible-Plate Nozzle Design for Two-Dimensional Supersonic Wind Tunnels.** JPL Report no. 20-74, June 1954.

10. Mehta, R.D.; and Bradshaw, P.: **Design Rules for Low Speed Wind Tunnels.** *Aeronautical Journal*, November 1979, pp. 443-449.

11. Beckwith, I.E.: **Comments on Settling Chamber Design for Quiet, Blowdown Wind Tunnels.** NASA TM-81948, March 1981.

12. Groth, J.; and Johansson, A.V.: **Turbulence Reduction by Screens.** Journal of Fluid Mechanics, vol. 197, 1988, pp. 139-155.

13. Weinstein, L.M.: **An Improved Large Field Focusing Schlieren System.** AIAA Paper 91-0567, January 1991.

14. Malik, M.R.: **$e^{Malik}$: A New Spatial Stability Analysis Program for Transition Prediction Using the $e^N$ Method.** High Technology Corporation, Report No. HTC-8902, March 1989.

15. Harris, J.E.; and Blanchard, D.K.: **Computer Program for Solving Laminar, Transitional, or Turbulent Compressible Boundary-Layer Equations for Two-Dimensional and Axisymmetric Flow.** NASA TM-83207, 1982.

16. Wolf, S.W.D.: **Supersonic Wind Tunnel Nozzles - A Selected, Annotated Bibliography to Aid in the Development of Quiet Wind Tunnel Technology.** NASA CR-4294, July 1990.

17. Owen, F.K.; Horstman, C.C.; Stainback, P.C.; and Wagner, R.D.: **Comparison of Wind Tunnel Transition and Freestream Disturbance Measurements.** AIAA Journal, vol. 13, no. 3, March 1975, pp. 266-269.

18. Hopkins, E.J.; and Keener, E.R.: **Study of Surface Pitots for Measuring Turbulent Skin Friction at Supersonic Mach Numbers - Adiabatic Walls.** NASA TN-D-3478, July 1966.

19. Demetriades, A.: **Boundary Layer Transition in a Supersonic Nozzle Throat in the Presence of Cooling and Surface Roughness.** Montana State University /Supersonic Wind-Tunnel Laboratory TR-82-01, August 1981.

20. Beckwith, I.E.; Chen, F.-J.; and Creel, T.R.: **Design Requirements for the NASA Langley Supersonic Low-Disturbance Wind Tunnel.** AIAA Paper 86-0763-CP. AIAA 14th Aerodynamic Testing Conference, March 1986.

# APPENDIX E

# Adaptive Wall Technology for Minimization of Wind Tunnel Boundary Interferences - Where Are We Now?

Stephen W. D. Wolf

MCAT Institute
Moffett Field
California, USA

Preprint of paper for the Symposium
on
**Aerodynamics and Aeroacoustics**

Tucson, Arizona
February 28 - March 2, 1993

# ADAPTIVE WALL TECHNOLOGY FOR MINIMISATION OF WIND TUNNEL BOUNDARY INTERFERENCES - WHERE ARE WE NOW?

Stephen W. D. Wolf
MCAT Institute
Moffett Field, California, USA

Abstract

The status of adaptive wall technology to improve wind tunnel simulations for 2- and 3-D testing is reviewed. This technology relies on the test section flow boundaries being adjustable, using a tunnel/computer system to control the boundary shapes without knowledge of the model under test. This paper briefly overviews the benefits and shortcomings of adaptive wall testing techniques. A historical perspective highlights the disjointed development of these testing techniques from 1938 to present. Currently operational transonic Adaptive Wall Test Sections (AWTSs) are detailed, showing a preference for the simplest AWTS design with two solid flexible walls. Research highlights show that quick wall adjustment procedures are available and AWTSs, with impervious or ventilated walls, can be used through the transonic range up to Mach 1.2. The requirements for production testing in AWTSs are discussed, and conclusions drawn as to the current status of adaptive wall technology. In 2-D testing, adaptive wall technology is mature enough for general use, even in cryogenic wind tunnels. In 3-D testing, this technology is not been pursued aggressively, because of the inertia against change in testing techniques, and preconceptions about the difficulties of using AWTSs.

Symbols

| | | |
|---|---|---|
| c | - | Chord |
| Cd | - | Drag coefficient |
| Cn | - | Normal force coefficient |
| Cp | - | Pressure coefficient |
| d | - | Body diameter |
| h | - | Test section height |
| $M_\infty$ | - | Free stream Mach number |
| P | - | Local static pressure |
| Po | - | Stagnation pressure |
| $U_\infty$ | - | Free stream velocity |
| X | - | Streamwise location |
| Y | - | Local wall deflections from straight |
| $\alpha$ | - | Angle of attack |
| $\Delta u$ | - | Induced streamwise velocity |
| $\Delta w$ | - | Induced upwash velocity |
| $\Delta Y$ | - | Local wall streamlining adjustment |

## 1. Introduction

Progress in the science of aeronautics is measured by the improvements in the efficiency of flight vehicles. It is now generally accepted that these improvements are best achieved by using ground testing, CFD and flight testing technologies together. In effect, we must use a balanced combination of all available technologies to understand the remaining mysteries of aeronautics. In ground testing, this means we strive for better and better simulations of the "real" flow in our wind tunnel experiments. Consequently, wind tunnel improvements are, and will remain, the subject of considerable research effort in different parts of the world.

Ideally, for complete simulation of "real" flow conditions about a scale model within the confines of a wind tunnel, the values of test Reynolds number, Mach number, free stream turbulence level and the flow field shape must all be properly matched to full scale. Unfortunately, it is normal practice to test at the correct Mach number with the other three parameters seldom matched. Consequently, wind tunnel data still suffers from significant wall interference effects, particularly at transonic speeds. Traditionally, the wind tunnel community uses several well-known techniques to minimise wall interferences. Models are kept small compared with the test section size (sacrificing the test Reynolds number range). Ventilated test sections are used to relieve transonic blockage and prevent choking (but introduce other more complex boundary interferences). Post-test Wall Interference and Assessment Corrections (WIAC), of varying sophistication, are applied to the model data in an effort to remove wall interferences. Usually, all three techniques are used together in transonic testing. Alas, these techniques still fail to produce the high levels of data accuracy possible with modern testing techniques. In addition, these old techniques have led to expensive compromises in terms of test section size and drive power, which are not tolerable in today's economy.

A "modern" testing technique necessary to minimise wall interferences has existed, in a conceptual form, for about 55 years. This technique is a very intuitive solution to the problem, and involves minimising wall interferences at the very source of these disturbances. The technique adapts the test section boundaries to streamline shapes, so the test section walls become nearly invisible to the model under test. We know this concept as the **Principle of Wall Streamlining**, which was first used in 1938 as a means of relieving transonic blockage at NPL, England.[1] The concept effectively splits the real infinite flow field into two parts: the real flow field in the test section which contains all the viscous flow interactions with the model; and an imaginary flow field surrounding the test section and extending to infinity, as shown in Figure 1. The boundary between the two flow fields is a streamtube (ignoring the boundary layer growth on the test section walls).

The paper considers the benefits and shortcomings of adaptive wall testing techniques as a precursor to discussing the current status of the technology. A brief review of the development of adaptive walls shows the contribution of Professor Sears, whose work we are commemorating at this symposium.

Operational transonic AWTSs are detailed (which are currently used for both conventional and turbomachinery research) to demonstrate the current wave of enthusiasm. From these AWTSs, 2- and 3-D adaptive wall research is reviewed to illustrate the *State of the Art*. Finally, we consider the operational aspects of AWTSs, since the practicalities of adaptive walls play a critical factor in the more widespread use of this technology. In conclusion, an assessment of the accumulated adaptive wall experience is presented and possible directions for future developments are indicated.

## 2. Adaptive Wall Benefits

Although the potential rewards for using adaptive wall testing techniques have been reported many times, a brief overview is appropriate. Adaptive walls offer several important advantages other than the major benefit of minimising wall interferences. With wall interferences minimised, we are free to increase the size of the model for a given test section. We can double the test Reynolds number and have a larger model to work with. Alternatively, we can shrink the test section and reduce the tunnel size and operating costs. Interestingly, the task of magnetically suspending models (to remove support interferences) becomes simpler in an AWTS because the supporting coils can be positioned closer to the model.

With solid adaptive walls (called flexible walls), the test section boundaries are smooth and impervious in contrast to the complex boundaries of a ventilated test section. This smoothness

minimises disturbances to the tunnel free stream significantly improving flow quality. Of course, the considerable noise generated by flow through slots or perforations is eliminated. (A benefit that is gaining more and more significance in transition to turbulence experiments at transonic speeds.) Furthermore, this improved flow quality reduces the tunnel drive power required for a given test condition, with the model and test section size fixed. Flexible walls eliminate the plenum volume found in conventional transonic wind tunnel reducing settling times and minimises flow resonance, which is particularly important for blowdown tunnels.

With flexible walls, the boundary control is achieved by direct wall movement. This strong control of the test boundaries provides good data repeatability compared with the indirect and passive control of the boundaries in a conventional ventilated test section.

Adaptive walls can provide the aerodynamicist with real-time "corrected" data, even in the transonic regime, which presents another significant advantage to the wind tunnel user. Since, the final results are know real-time, test programmes can be much more focused and test matrices can be minimised. Consequently, the use of adaptive walls can significantly reduce the number of data points and tunnel entries necessary to achieve test objectives.

It should be noted that the simulation of free-air conditions is one of 6 flow field simulations[2] that adaptive wall technology can provide. These simulations are: free air; cascade; open jet; closed tunnel; ground effect; and steady pitching. It is possible to use multiple simulations with the same model and AWTS. This feature of AWTSs can and has been shown to be a useful advantage for CFD validation work and tunnel versatility.

## 3. Adaptive Wall Shortcomings

The simple, intuitive concept of adaptive walls is complicated by the need to continually adjust the test section boundaries for each test condition. This complication causes the AWTS hardware to be more complex than that of a conventional test section. However, this complexity is nothing new to a wind tunnel designer and should be considered as equivalent to the complexity of a flexible supersonic nozzle. As shown later, it would now seem that the AWTS complexity can be limited to only two adaptive walls, further reducing this shortcoming. In addition, it must be remembered that increasing the complexity of the test section hardware reduces the complexity of the correction codes. In effect the use of an AWTS reduces the computational overhead necessary to implement WIAC codes.

A sophisticated control system is required for an AWTS because wall streamlining is necessarily iterative (See Figure 2). The control system must be even more sophisticated if no-expert users are involved. However this shortcoming is not new and the AWTS control system is equivalent to a feedback control system for positioning other wind tunnel components like a sting support. Of course, sophisticated control systems are now very common with the advent of PC computers.

The number of data points per hour of tunnel run-time will be reduced with adaptive walls, because the wall adaptation will never be instantaneous. Computer control of the adaptation has greatly reduced this "wasted" tunnel time, but the associated time is still significant. However, the real-time AWTS data are the final data (as shown later) and therefore one must assess the importance of quality versus quantity.

Any AWTS must be designed with a good understanding of the expected testing requirements. The AWTS design can limit the test envelope as easily as other aspects of a wind tunnel system, such as drive power, diffuser design etc. Fortunately, there are guidelines published to help design an AWTS for a given test envelope.

## 4. Historical Overview of Adaptive Wall Research

The adaptive wall testing techniques we know today are a rediscovery of the first solution to severe transonic wall interferences (i.e. choking). The National Physical Laboratory (NPL), UK, built the first adaptive wall test section in 1938, under the direction of Dr. H. J. Gough,[1] about 8 years before the first ventilated test section appeared. The pioneering research at NPL proved that streamlining the flexible walls of an AWTS was the first viable technique for achieving high speed (transonic) flows in a wind tunnel. In fact, NPL had transonic testing capability 8 years before NACA. NPL researchers opted for minimum mechanical complexity in their AWTS and used only two flexible walls.

The absence of computers made wall streamlining a labour intensive process which was surprisingly fast, of the order 20 minutes. Sir G. I. Taylor developed the first wall adjustment procedure,[3] which has since been validated in a modern AWTS.[4] NPL researchers went on to successfully use flexible walled AWTSs for general testing up until the early 1950s. They generated an extraordinary amount of 2- and 3-D transonic data[5] during this 14-year period, which is probably more than half of all the AWTS data produced to date. The NPL 20 x 8 inch (50.8 x 20.3cm) High Speed Tunnel even became the first adaptive wall wind tunnel to operate at low supersonic Mach numbers. Some early adaptive wall work was also carried out in Germany during the 1940s. Despite the building of the largest ever AWTS, with a 3m (118 inch) square cross-section, this effort came to nought.

The arrival of ventilated test sections at NACA Langley in 1946, provided a "simpler" approach to high speed testing. The adjustments to the test section boundaries are passive with ventilated walls, while the adaptive wall adjustments are active. The apparent simplicity of ventilated test sections led to the obsolescence of NPL's AWTSs and adaptive wall technology became forgotten in time.

After about 20 years (See Figure 3), interest in AWTSs was rekindled. In April 1971, an AGARD Fluid Dynamics Panel Specialist's meeting in Göttingen, Germany highlighted serious shortcomings in wind tunnel testing techniques at transonic speeds.[6] This serious concern led several researchers, in Europe and the USA, to independently rediscovered the concept of adaptive wall testing techniques. One of the **Fathers of Modern Adaptive Walls**, who presented and publish his ideas in 1973, was of course Professor Sears.[7] The goal of these researchers was better free air simulations in transonic wind tunnels. The adaptive wall approach offered them an elegant way to simplify the wall interference problem. Adaptive wall adjustment procedures need only consider the flow at the test section boundaries (in the farfield), the complex flow field round the model need never be considered. Therefore, the adaptive wall concept allows us to simplify the "correction codes" at the expense of increasing the complexity of the test section hardware.

This renewed interest produced 5 adaptive wall research groups around the world. During the mid-1970s, these groups directed their initial research efforts towards low speed 2-D testing, because this provided a relatively quick way to re-invent the adaptive wall concept. Two methods of applying the adaptive wall principles were investigated. One was a modification of the conventional ventilated test section using variable porosity. The other was a complete re-invention of the NPL approach. In this early phase, notably work at Southampton University (England) demonstrated the AWTS versatility to create 6 flow field simulations and produced the first predictive wall adjustment procedure of Judd et al.[8] In addition, the intuitive design principles for 2-D flexible walled AWTSs were quantified and optimized.

In the mid to late 1970s, the successful low-speed research effort paved the way for transonic 2-D research, which introduced fast automatic wall adjustments (taking only seconds in some cases) with notable work at Southampton University, ONERA/CERT (France) and Technical University of Berlin (Germany). Rapid progress was made in the development of subsonic and transonic 2-D adaptive wall testing techniques, helped along by the growing

availability of computers. During the 1980s, this progress led to successful 2-D tests at high lift and high blockage conditions, and the use of AWTSs in cryogenic wind tunnels (i.e. in the NASA Langley 0.3-m Transonic Cryogenic Tunnel and the ONERA/CERT T2 tunnel). All these successes were achieved in flexible walled AWTSs. Parallel research using ventilated walled AWTSs (led by Professor Sears) was as vigorous at Calspan (Buffalo, NY) and AEDC, but alas this approach encountered some fundamental limitations. Boundary measurements proved difficult, and intrusive Calspan static pipes had to be used. Researchers also found it was impossible to achieve sufficient control of the ventilated adaptive walls, if relatively large model disturbances were present, and wall adjustment procedures were difficult to implement.[9]

Initial research using AWTSs for 3-D testing began in the late 1970s, and concentrated on exotic and extremely complex AWTS designs like the rod-wall tunnel at AFFDL at Dayton, Ohio (USA),[10] the rubber-tube DAM AWTS at DFVLR Göttingen (Germany)[11] and the octagonal AWTS at TU-Berlin.[12] These designs proved that 3-D AWTSs using intuitive wall adjustments could minimise boundary interferences, but confirmed that these complex AWTS designs are impractical for general use. Fortunately, the research with the rod-wall tunnel did show that 2-D adaptive walls could be successfully used in 3-D testing. This important finding resulted in numerous 3-D subsonic and low transonic tests in the 1980s. Research at the Von Karman Institute (Belgium) and DFVLR Göttingen produced the first predictive wall adjustment procedure for 2-D AWTSs used in 3-D testing. This procedure was developed by Wedemeyer and Lamarche.[13] Meanwhile, studies of the residual interferences at Southampton University, established the usefulness of 2-D AWTSs in 3-D testing up to Mach 0.97. Other notable work at TU-Berlin, DFVLR Göttingen and Northwestern Polytechnical University - NPU (China)[14] involved preliminary 3-D tests at Mach 1.2, in which oblique shock wave reflections were successfully attenuated by local flexible wall bending. Again, all these advances were achieved in flexible walled AWTSs. Parallel research with ventilated walled AWTSs for 3-D tests occurred at NASA Ames and AEDC in the 1980s. This work was eventually abandoned with the failure to develop fast wall adjustment procedures, and to achieve adequate boundary control when significant model disturbances are present. However, since 1986, researchers at TsAGI (Russia) have been performing production testing in the large, 2.75m (9 foot) square, ventilated walled AWTS of their transonic T-128 tunnel. This automated AWTS has a simplified wall adjustment procedure that relies extensively on the use of WIAC codes to remove wall interferences from the data (See sub-section 5.12).[15]

Unfortunately, adaptive wall research has been significantly slowed in recent years by low priority funding and the demise of active research groups in the United States and TU-Berlin. The development of 3-D transonic adaptive wall testing techniques in the 1990s currently rests with 4 organizations: DLR Göttingen, ONERA, NPU, and Southampton University.

Research has continued into advanced 2-D testing techniques with the goal of extending the useful speed range up to low supersonic Mach numbers and improving cascade simulations. Initial supersonic 2-D testing at NPL was followed some 40 years later by preliminary research at Mach 1.2 performed at ONERA during the mid-1980. More recently there have been significant strides at Southampton University[16] again at Mach 1.2. Cascade simulations, pioneered at Southampton University in 1974 using a single blade at low speeds, are currently only performed in Genoa University (Italy) at transonic speeds.

We find that AWTSs are now available for commercial use at NASA Langley (2-D only), ONERA/CERT (2- and 3-D), and TsAGI (3-D only). There are plans to build new transonic cascade AWTSs at Genoa University and DLR Göttingen, and new transonic flexible walled AWTSs in China (for the CARDC 0.6m high speed tunnel) and Germany (for the DLR TWG 1m transonic wind tunnel and the DLR transonic cryogenic Ludwieg tube). Furthermore, the French cryogenic T'3 transonic tunnel, with a flexible walled AWTS, is now being recommissioned at the Von Karman Institute in Belgium.

## 5. Transonic AWTSs Currently Operational
(In alphabetical order by organization)

### 5.1 Aerodynamic Institute, RWTH Aachen, Germany

The test section of the Transonic- and Supersonic Tunnel (TST) at RWTH Aachen was equipped with flexible walls in 1985/6. The AWTS is 40 cm (15.75 inches) square and 1.414 m (4.64 feet) long. The top and bottom walls are flexible and mounted between two parallel sidewalls. The flexible walls are made from 1.3 mm (0.051 inch) thick spring steel. Each wall is supported by 24 motorized jacks (See Figure 4).

The TST is an intermittent tunnel capable of operation at Mach numbers between 0.2 and 4, with run times between 3 to 10 seconds. The AWTS has only been used for 2-D testing up to about Mach 0.8.[17] Usually 3 or 4 tunnel runs are required for each data point at transonic Mach numbers. Boundary measurements are static pressures measured along the flexible walls. Wall adaptation calculations and automatic wall adjustments are made between tunnel runs.

Empty test section calibrations reveal Mach number discrepancies less than 2%, where the model is usually mounted, at Mach 0.82. Lower Mach numbers produce lower discrepancies. Mach number is controlled, up to low transonic Mach numbers, by a downstream sonic throat. The average accuracy of the wall contours, measured by potentiometers at each wall jack, is ±0.1 mm (±0.004 inch).

### 5.2 DLR - Institute of Experimental Fluid Mechanics, Göttingen, Germany

During 1987/8, researchers at DLR modified the 2-D supersonic nozzle of the DLR High Speed Wind Tunnel (HKG) into an AWTS. The top and bottom nozzle walls are made of highly flexible 4 mm (0.157 inch) thick steel plates. The shape of each wall is set by 17 pairs of equally spaced hydraulic jacks (See Figure 5).

The AWTS consists of an initial contraction followed by a 2.2 m (7.22 foot) straight section. This straight portion, in which the model is mounted, is nominally 0.67 m (2.2 feet) high and 0.725 m (2.38 feet) wide. Each wall of the test section is equipped with 3 rows of pressure taps for boundary measurements. The wall adjustment procedure of Wedemeyer/Lamarche[13] is used to minimise interferences along the tunnel centerline.

This AWTS is used for evaluation of 2-D wall adaptation in 3-D testing. Researchers have tested sting mounted 3-D models, both lifting and non-lifting, up to about Mach 0.8.[18]

### 5.3 Genoa University, Italy

The Department of Energy Engineering at Genoa University operates 2 adaptive wall cascade tunnels. These tunnels are the only current examples of the use of AWTSs in non free-air flow simulations. Both tunnels have a cross-section of 0.2 m (7.87 inches) high and 5 cm (1.97 inches) wide. One is the Low Deflection Blade Cascade Tunnel (LDBCT), which became operational in 1982. The other is the High Deflection Blade Cascade Tunnel (HDBCT) which became operational in about 1985.

The LDBCT can test up to 12 blades, at Mach numbers up to 2.0, with flow deflections up to about 35°. The AWTS has two flexible walls and two solid transparent sidewalls. The flexible walls are 1.58 m (5.18 feet) long and each is shaped by 36 manual jacks (See Figure 6). Wall streamlining is performed upstream and downstream of the cascade.

The HDBCT has a similar configuration except the AWTS is 1.6 m (5.25 feet) long and wall adaptation is performed only downstream of the cascade. The top flexible wall is

supported by 13 manual jacks and the bottom flexible wall by 26 manual jacks (See Figure 7). The AWTS can accommodate flow deflections up to 140°. Up to 13 blades can be fitted in the cascade, with test Mach numbers up to 1.18 reported.[19]

Both AWTS need only approximate wall adaptation procedures due to the large number of blades used in the cascade. The smooth flexible walls have provided remarkably good flow quality for cascade research. The LDBCT is also used for probe calibration.[19]

5.4 NASA Ames Research Center, California

The Thermo-Physics Facilities Branch at NASA Ames has an AWTS for use in their intermittent High Reynolds Number Channel-2 (HRC-2) facility. The AWTS was constructed in 1981. The AWTS is fitted with two flexible walls and two parallel solid sidewalls. The AWTS has a rectangular cross-section which is 0.61 m (24 inches) high and 0.41 m (16 inches) wide. The AWTS is 2.79 m (9.15 feet) long. The Ames AWTS has 7 manually adjusted jacks supporting each flexible wall (See Figure 8). An automated version of the AWTS was built and then dismantled without ever being used.

The flexible walls are made of 17-4 PH stainless steel plates and are 2.53 m (8.32 feet) long. The flexible walls are 15.9 mm (0.625 inch) at the ends tapering to 3.17 mm (0.125 inch) in the middle for increased flexibility. The downstream ends of the flexible walls each house a pivot joint which attaches to a variable sonic throat for Mach number control. Sidewall Boundary Layer Control (BLC) is available by installing porous plates in the sidewall, upstream of the model location. Mach number variations along the test section, due to BLC suction, were removed by suitable wall adaptation based on simple influence coefficients.[20]

More recently, the Ames AWTS has been used for 2-D and 3-D CFD code validation. No wall adjustment procedure is used. The flexible walls are simply set to predetermined shapes depending on the investigation underway, and move apart to prevent choking. Studies of LDA wake measurements behind 2-D aerofoils have also been carried out. CFD validation 3-D tests with a sidewall-mounted half-model have been performed by Olsen with fixed diverging walls.[21]

5.5 NASA Langley Research Center, Virginia

The NASA Langley 0.3-m Transonic Cryogenic Tunnel (TCT) was fitted with an AWTS during 1985. The AWTS has two flexible walls mounted between two solid parallel sidewalls. The flexible walls are made of 304 stainless steel, 3.17 mm (0.125 inch) thick at the ends, and thinning down to 1.57 mm (0.062 inch) thick in the middle for increased flexibility.

The cross-section of the AWTS is 0.33 m (13 inches) square and the AWTS is 1.417 m (55.8 inches) long. The flexible wall shapes are controlled by 18 motorized jacks per wall. The downstream ends of the flexible walls are attached, by sliding joints, to a 2-D variable diffuser (formed by flexible wall extensions) between the AWTS and the rigid tunnel circuit. The shape of the variable diffuser is controlled by 6 motorized jacks. The wall jacks are designed with insufficient stepper motor power to permanently damage the flexible walls.

The AWTS functions over the complete operating envelope of the continuous running TCT.[22] The test gas is nitrogen. The AWTS has been operated continuously over an 8 hour work shift at temperatures below 120 K. In addition, the AWTS is contained in a pressure vessel for operation up to stagnation pressures of 90 psia (6 bars). The jack motors and position sensors are located outside the pressure shell in a near-ambient environment (See Figure 9). Sidewall boundary layer control is available by fitting porous plates in the sidewalls, upstream of the model location. Boundary layer suction has been successfully used in 2-D testing with normal wall adaptation. We take 2-D wake measurements using a traversing pitot/static probe

mounted in one of 3 positions downstream of the aerofoil location.

We have used the wall adjustment procedure of Judd et al[23] for 2-D testing. The 2-D test envelope includes normal force coefficients up to 1.54 (and through stall) and Mach numbers up to 0.82, with a model blockage of 12%. The use of a large model combined with cryogenic test conditions has allowed testing at a record breaking Reynolds number of 72.4 million. Boundary measurements are static pressures measured along the centerline of the flexible walls at the jack locations. Wall streamlining takes on average less than 2 minutes and is paced by slow wall movements. A generalized and documented non-expert system[24] is used for AWTS operation within known 2-D test envelopes. We have demonstrated the taking of up to 50 data points (each with wall streamlining) during a 6 hour period.

Researchers have carried out tests at Mach numbers up to 1.3, using sidewall mounted 3-D wings. For 3-D testing at Mach numbers below 0.8, we have used the wall adjustment procedure of Rebstock[25] to minimise wall interferences along a pre-set streamwise target line anywhere in the test section. Boundary measurements are static pressures from 3 rows of pressure taps on each flexible wall and a row of taps on the centerline of the sidewall opposite the model. Downstream flexible wall curvature is automatically minimised by rotation of the tunnel centerline. For low supersonic tests, the adapted wall shapes are based on wave theory and form a 2-D supersonic nozzle ahead of the model.

The flexible walls are set to a nominal accuracy of ±0.127 mm (±0.005 inch). No aerodynamic effect of AWTS shrinkage, due to cryogenic operation, has been reported. Mach number is controlled by a feedback control system (based on a PC computer) to better than 0.002 during wall streamlining.

### 5.6 Northwestern Polytechnical University (NPU), Xian, China

Researchers fitted an AWTS to the NPU WT52 supersonic wind tunnel in May/June 1990. The test section was originally 30 cm (11.8 inches) square and is now 21.4 cm (8.42 inches) high, 30 cm (11.8 inches) wide and 1.08 m (42.52 inches) long. The floor and ceiling are impervious flexible walls, each positioned by 16 manually operated jacks (See Figure 10). Three rows of static pressure taps are provided along each flexible wall. The tunnel can operate at Mach numbers up to 1.3 using suitable nozzle blocks.

The flexible walls are made of 1 mm (0.039 inch) thick bronze alloy. In the model region, the wall jack spacing is 6cm (2.36 inches). Each flexible wall is connected to the diffuser by a porous plate to balance the pressure across the flexible walls.

Wall adaptation around a 2-D aerofoil was successfully achieved in WT52 at Mach 0.8, using a correction method based on Transonic Small Perturbation (TSP) theory. The model blockage was 8% and the test section height 30 cm (11.8 inches). In 3-D testing, much work has been done to verify the use of two flexible walls in low supersonic testing. Cone-cylinder models have been tested with blockage of 1% and 2%. Successful engineering and analytical adjustments were made to the flexible walls to alleviate bow shock reflections.[14] Further 3-D testing with a wing-body model has been completed up to Mach 0.87 at zero angle of attack, with the test section height reduced. This change has allowed the blockage in these tests to rise to 5.2%. Preliminary results show a significant reduction of wall interference with wall streamlining. This work continues as part of a joint research programme with DLR Göttingen.

### 5.7 ONERA/CERT, Toulouse, France

The AWTS fitted in the intermittent ONERA/CERT T2 transonic cryogenic tunnel has been operational since 1978. This AWTS became the first cryogenic AWTS in 1981, when the T2 tunnel was modified to operate cryogenically for 1 to 2 minutes at a time. This French

AWTS is 0.37 m (14.57 inches) high, 0.39 m (15.35 inches) wide and 1.32 m (51.97 inches) long. The AWTS has two flexible walls and two solid parallel sidewalls (See Figure 11). The flexible walls are made of 1.5 mm (0.059 inch) thick Invar steel plates. The shape of each flexible wall is controlled by 16 hydraulic jacks attached to wall ribs. These ribs are electron beam welded to the outside of the flexible walls. The hydraulic jacks move the flexible walls very rapidly at about 6 mm (0.24 inch) per second. The wall jacks have enough power to damage the flexible walls in bending. During a cryogenic run, the flexible walls rapidly reach the low test temperatures, while the jack mechanisms remain at near ambient temperatures. Sidewall BLC is available for 2-D testing by placing porous plates around the aerofoil/sidewall junctions. BLC suction is routinely used with wall adaptation. In 2-D tests, a pitot/static rake, mounted on a sting support downstream of the wing, is used for wake measurements.

A wall adjustment procedure developed by Chevallier et al is used for 2-D testing. This procedure is tunnel dependent and has no documented test envelope for non-expert use. Computer controlled wall streamlining in about 10 seconds is possible. However, 2 short tunnel runs are normally required per data point for 2-D tests at about Mach 0.8. Boundary measurements are static pressures measured equidistant along the centerline of the flexible walls.

For 3-D testing, the Wedemeyer/Lamarche wall adjustment procedure is used. Both lifting and non-lifting models have been tested up to Mach 0.97.[26] Researchers have carried out several production-type studies for Airbus Industries, including riblet studies on 3-D models (See Figure 11). Boundary measurements are static pressures measured along 3 rows on each flexible wall and a single row on one sidewall.

The shape of the flexible walls can be measured to 0.05 mm (0.002 inch). The wall curvature is checked before any wall movement is initiated. Mach number is control by a downstream sonic throat, which acts as a fairing between the AWTS and the fixed diffuser. In general, the Mach number is not held constant during each wall adaptation process. The pressure fluctuations measured in the test section are a low 0.18%.[27]

5.8 ONERA, Chalais-Meudon, France

The ONERA S3Ch transonic wind tunnel was fitted with an AWTS in 1992 and 3-D testing is about to commence. The tunnel can operate over a Mach number range from 0.3 to 1.3. The AWTS is 80 cm (31.49 inches) square and 2.2 m (86.61 inches) long. The floor and ceiling of the test section are impervious flexible walls mounted between solid parallel sidewalls. The adaptation of the floor and ceiling is controlled by 15 eqi-spaced wall jacks, 12.8 cm (5 inches) apart (See Figure 12). Each wall jack is driven by a computer controlled stepper motor. The flexible walls are made from duralumin alloy and are 3mm (0.12 inch) thick.

The unique design features of this flexible walled AWTS are as follows: the wall jacks have mechanical stops to prevent damage to the flexible walls; the wall jacks are eqi-spaced; and only one movable no-contact laser position sensor is used to measure the shape of each flexible wall. The wall can be moved ±50 mm (±1.97 inch) from straight, with a position accuracy of ±0.1 mm (±0.004 inch).

After considerable effort, it was decided that the boundary measurements for 3-D testing will consist of 4 streamwise rows of 50 static pressures along each flexible wall.[28] The wall adjustment procedure has been developed by Le Sant with a variable target line for test versatility. The AWTS boundary measurements will allow wall interferences to be evaluated everywhere in the test section after wall streamlining. With full computer control of the AWTS, wall streamlining is expected in about 1 minute per test condition.

5.9 Rensselaer Polytechnic Institute, New York, USA

Since the mid-1980s, the Rensselaer Polytechnic Institute has operated two AWTSs for rotorcraft research, in particular the study of 2-D aerofoils with passive boundary layer control. The RPI 3 x 8 transonic wind tunnel is fitted with a rectangular AWTS, 20.3 cm (8 inches) high, 7.6 cm (3 inches) wide, and 0.6 m (23.62 inches) long. The top wall is flexible and supported by 6 jacks. The other three walls are solid. The 2-D aerofoil is mounted in the bottom wall with a boundary layer removal slot ahead of the leading edge. A relatively large aerofoil with a 10.16 cm (4 inch) chord has been tested in this AWTS at Mach numbers up to 0.86 (See Figure 13).[29] Testing of such large models would be impossible at these Mach numbers without an AWTS. Interestingly, oscillatory flow field simulations have also been carried out in the RPI 3 x 8 AWTS with the top wall shape fixed.[30]

The RPI 3 x 15 transonic tunnel has a similar AWTS arrangement except the test section height is increased to 38 cm (15 inches). Also the top wall is not flexible and different wall shapes are set in the AWTS by using interchangeable wooden wall inserts. Tests of 14% thick aerofoils at Mach numbers up to 0.9 are reported.[29]

Researchers use a simple wall adjustment procedure in these AWTSs. One-dimensional wall influence coefficients are used to remove the blockage effects associated with testing a large aerofoil in these small test sections. Boundary measurements are static pressures measured along the test section walls.

5.10 Southampton University, Hampshire, England

The Transonic Self-Streamlining Tunnel (TSWT) at Southampton University is one of the first fully automated AWTSs. Built in 1976/7, TSWT has a 15 cm (6 inch) square test section which is 1.12 m (3.67 feet) long. The floor and ceiling are flexible and made from woven man-made fibre (Terylene). The flexible walls are 5 mm (0.2 inch) thick at the ends tapering to 2.5 mm (0.1 inch) thick in the middle for increased flexibility. Each flexible wall is supported by 19 motorized jacks (See Figure 14). A sliding joint attaches the downstream ends of the flexible walls to a 2-D variable diffuser (which is two plates, each controlled by a single motorized jack). The wall jacks are designed with insufficient stepper motor power to damage the flexible walls. The two sidewalls are solid and parallel.

The wall adjustment procedure of Judd et al[8] for 2-D testing was developed in TSWT, and is used routinely for all 2-D tests, up to speeds where the flow at the flexible walls is just sonic. Wall streamlining is generally achieved in less than 2 minutes. If the walls become sonic, a Transonic Small Perturbation (TSP) code is included in the Judd procedure and 2-D testing has been successfully carried out up to Mach 0.96.[31] For low supersonic 2-D testing at up to Mach 1.2, a wall adjustment procedure based on wave theory is used to generate a simple 2-D supersonic nozzle in the AWTS, upstream of the model.[16] Since 1978, researchers have used TSWT to build up a substantial database on 2-D testing in an AWTS, with blockage ratios up to 12% and test section height to model chord ratios down to unity.[2]

In addition, TSWT has been used for 3-D tests with sidewall and sting mounted models with blockage ratios up to 4%. A wall adjustment procedure developed by Goodyer et al is used for 3-D test up to about Mach 0.9.[16,31] Boundary measurements are static pressures measured along 5 rows on each flexible wall and a single row on one sidewall.

The wall shapes are measured by potentiometers at each wall jack to an accuracy of ±0.127 mm (±0.005 inch). Free stream Mach number is controlled by automatic throttling of the inducing air pressure. Mach number variation up to .002 is typical during a test at Mach 0.8. Calibration of TSWT with an empty test section reveals a standard deviation in Mach number variation of about 0.003 at Mach 0.8.

5.11 Technical University of Berlin, Germany

During 1980, an octagonal AWTS was built at the Technical University of Berlin (TUB) to study the use of adaptive walls in 3-D testing. This AWTS is currently available for undergraduate teaching. This unusual test section is 15 cm (5.9 inches) high, 18 cm (7.09 inches) wide and 83 cm (32.68 inches) long.[12] The test section is formed by 8 flexible walls supported by a total of 78 jacks powered by individual DC motors (See Figure 15). The flexible walls are made of thin steel plates. The corners are sealed by spring steel lamellas so the test section boundary is impermeable and continuous.

This 3-D AWTS uses a wall adjustment procedure developed by Rebstock et al. Wall adaptation is possible in 2 iterations at Mach numbers up to 0.95. Model blockage ratios up to 1.3% have been successfully tested, both with lifting and non-lifting sting mounted models. Boundary measurements are static pressures measured along the centerline of each flexible wall. Low supersonic tests of non-lifting bodies indicate that bow shock reflections from the flexible walls can be deflected away from the model.[32]

### 5.12 TsAGI (Central Aero-Hydrodynamic Institute), Zhukovsky, Russia

Since 1986, TsAGI has been operating the largest AWTS anywhere for industrial testing. The massive Russian T-128 tunnel has a test section size of 2.75 m (9 foot) square and 8 m (26.25 feet) long, and is enclosed within a building (See Figure 16a). The T-128 has 5 interchangeable test sections and can operate at Mach numbers up to 1.7, over a dynamic pressure range up to 10.15 psi (0.71 bar). The first test section is an AWTS with all 4 walls perforated (See Figure 16b). The turbulence level in the test section is quoted as 0.5%. Each wall of the AWTS is made up of 32 segments. The porosity of each of the 128 segments can be varied between 0 and 18%. Each segment is made up of 2 porous plates (one on top of the other). These 2 plates are moved relative to one another by computer control, to achieve a desired porosity over the segment (See Figure 17).

A simplified wall adjustment procedure has been developed by Neiland for 3-D testing at transonic speeds, which requires knowledge and representation of the model under test.[15] Moreover, wall streamlining is only used for the few test conditions where WIAC is deemed inaccurate, mostly around Mach 1. Boundary measurements are static pressures measured along rows on the centerline of each wall. These pressures are assumed accurate for low wall porosities necessary for testing near sonic speeds. These simple boundary measurements made T-128 the first major transonic tunnel to be fully instrumented for WIAC use. The maximum reported blockage ratio for 3-D testing is about 3%, as shown on Figure 16b. This high blockage ratio is beyond the capabilities of other reported variable porosity AWTS. The T-128 tunnel is a world-class industrial wind tunnel, which has received recent notoriety because the Boeing Company is one of the major users.

## 6. An Overview of AWTS Designs

In 2-D testing, only two walls need to be adaptable and a simple AWTS is sufficient. Meanwhile in 3-D testing, the logical desire to control the AWTS boundaries in 3-D has led to a variety of AWTS designs. Moreover, some approximation in the shape of the test section boundaries is inevitable. The magnitude of this approximation has been the subject of much research. The most favoured number of adaptive walls for a 3-D AWTS is now two, which provides an acceptable design compromise. From practical considerations, this compromise is between size/correctability of residual wall interferences (after wall streamlining), hardware complexity, model accessibility, and the existence of rapid wall adjustment procedures.

There are strong theoretical[13] and experimental[31] indications that the simpler the AWTS design the better the testing technique (see sub-section 7.2). A simple design reduces both the complexity of calculating the residual wall interferences and the complexity of the tunnel

hardware, and gives better model access as a bonus. A major factor in the design of new AWTSs will undoubtedly be the trade-off between the complexity of the boundary adjustments and the quality/cost of the residual wall interference corrections. The Russian T-128 tunnel represents the case where WIAC is used instead of adaptive walls for all but a limited number of test conditions.

Published data clearly shows that flexible walled AWTSs provide testing capabilities superior to that of similar sized variable porosity AWTS designs. We can summarize the effectiveness of flexible walls thus:

a) Flexible walls can be rapidly streamlined.
b) Flexible walls provide more powerful and direct adaptation control of the test section boundaries, necessary for large models and high lift conditions.
c) Flexible walls provide simple test section boundaries for adaptation measurements, residual wall interference assessments and setting of test conditions.
d) Flexible walls improve flow quality providing reduced tunnel interferences and reduced tunnel disturbances which lower operating costs.
e) No plenum is required around the test section reducing tunnel volume.

Interestingly, of the 16 transonic AWTSs now operational worldwide, only two AWTSs do not have flexible walls (see Table 1). In the low speed regime, there are 7 AWTSs currently operational which are all fitted with flexible walls. So the current total of AWTSs is 23, of which, 21 have flexible walls and 16 have only two flexible walls.

The optimum 2-D AWTS has two flexible walls supported by jacks closely grouped in the vicinity of the model. A good example of this optimum design is the AWTS fitted in the NASA Langley 0.3-m TCT, shown on Figure 18. The flexible walls (made of thin metal) are anchored at the upstream ends and the downstream ends are attached by a sliding joint to a variable 2-D diffuser (Refer to sub-section 5.5). The AWTS requires a square cross-section for optimum 2-D testing (i.e. maximizing Reynolds number capability). For 3-D testing, a rectangular cross-section, which is wider than it is tall, seems better for minimising wall induced gradients with 2-D wall adaptation.[13] However, we find that only 3 of the AWTSs used for 3-D testing have this desirable cross-section. To offset this situation, researchers have found that swept target lines for zero interference can compensate for less than optimum AWTS cross-sections.[16]

## 7. Review of AWTS Research

Research into adaptive wall testing techniques, with both variable porosity and flexible wall AWTS designs, has concentrated on the following goals:

1) To define fast adaptive wall testing techniques for different test regimes.
2) To identify acceptable measurement tolerances.
3) To find the optimum AWTS design for different applications.
4) To find if any fundamental limitations to the adaptive wall concept exist.

However, we now know that a variable porosity AWTS is much less effective than a flexible walled AWTS. Therefore, only flexible wall research will be considered in this review.

Since 1938, researchers have made significant reductions to the time associated with wall streamlining. A major factor in this progress has been the development of rapid wall adjustment procedures for flexible walled AWTSs. (The term *rapid* refers to minimisation of the number of iterations necessary in any wall adaptation procedure.) Early empirical type methods (requiring 8 iterations) have given way to analytical methods (requiring 1 or 2 iterations) as computer support has improved. These analytical methods now use both linear and non-linear theory, and require no prior knowledge of the model. Nevertheless, simple

empirical methods are still appropriate where the use of large models (relative to the test section size) is not important, as found in some of the AWTSs (particularly the cascade AWTSs) described in section 5.

For 2-D free air simulations, the linear wall adjustment procedure of Judd et al[23] (Southampton University) is now well established for reasons of speed, accuracy, simplicity (Non-experts can easily use the method on any PC computer), and adaptability for general use with any flexible walled AWTS. A non-linear version is also available for use in 2-D testing where the flow at the walls is sonic.[31] For free air simulations in 3-D testing, researchers use the linear methods of Wedemeyer/Lamarche[13] (DLR), Rebstock[25] (NASA), Goodyer et al[16] (Southampton), and Le Sant[28] (ONERA). However, all these 3-D methods are still under development. Supersonic 2- and 3-D testing is possible using the method of characteristics (wave theory) to predict the wall shapes necessary to generate supersonic flow.[14,16,32]

Another time-saving feature of modern AWTSs is automatic wall streamlining. Researchers have shown that computer controlled movement of the adaptive walls and automatic acquisition of wall data dramatically reduce the time attributed to wall streamlining, from weeks to seconds! In addition, researchers have found that fast wall streamlining requires a good practical definition of when the walls are streamlined. We call this definition the *streamlining criterion* (the point at which we stop wall adaptation). The criterion is directly related to the accuracy of the tunnel/wall measurements (discussed later). For 2-D free air simulations, the best approach appears to be a quantitative approach which is to set, as the streamlining criterion, an acceptable maxima for the residual wall interferences.[2] This approach is used at the Southampton University, NASA Langley and the University of Naples (Italy). At present there are only qualitative streamlining criterions in 3-D testing, whereby the walls are streamlined when the model data is unaffected by subsequent iterations of the wall adjustment procedure. On-line residual wall interference codes are available but require development for 3-D testing techniques in AWTSs.[31,33,34]

Researchers have probed the limits of 2-D adaptive wall testing techniques. These limits are related to aerodynamic, theoretical basis and mechanical aspects of the wind tunnel tests. The use of sidewall BLC is only a factor in altering the wall curvature requirements. In 2-D testing, the operating envelope of an AWTS is bounded by the limitations of the test section geometry, the wall adjustment procedure and the instrumentation. These are the same factors that need to be defined in the design phase of a new AWTS. Researchers have provided many design guidelines to eliminate wall hardware problems, so far encountered, from future AWTS designs. With good design, only theoretical assumptions should restrict the operating envelope for 2-D testing.

In 3-D testing, the situation is far less clear, as no AWTS operating envelopes are well defined. Research has been spread thinly over many AWTS designs and numerous model configurations. The result is that the favoured AWTS design for 3-D testing has become the simplest design (as described earlier), because hardware complexity does not produce significant improvements.

Researchers have examined the effects of measurement accuracy on AWTS operation, particularly for flexible wall designs.[2] With flexible walls, we can only measure the position of each wall at a finite number of points. The measurement accuracy at each of these points is of the order ±0.127 mm (±0.005 inch) in current AWTSs. The relative position of these measurement points, along each wall, can be optimized for 2-D flexible walled AWTS designs (as shown on Figure 18). Operationally, flexible walled AWTSs have proved tolerant to wall jacks being disconnected due to hardware failures.[22] Interestingly, because the wall position accuracy requirements are proportional to (1/h), the measurement accuracy requirements reduce significantly for a large AWTS. This situation is already proven in large supersonic nozzle systems operational to-day, and should encourage use of large AWTSs amongst potential

operators.

We have found the flexible wall adaptation procedures to be tolerant to uncertainties in the wall pressures. This important feature is due to the smearing effect of the wall boundary layers. However, at high Reynolds numbers (when the wall boundary layers are thin) or with near sonic flow at the adaptive walls, this tolerance to measurement uncertainties reduces. The uncertainties in the wall pressures can be caused by wall imperfections or fluctuations in the tunnel test conditions. Again, large AWTS should provide more tolerance to these uncertainties. However, we do know that if the model perturbations at the adaptive walls are small (as found in 3-D testing), the accuracy of the wall pressures needs to be better than when the model perturbations are large (as found in 2-D testing).

Furthermore, the allowance necessary for the boundary layer growth on the test section flexible walls is dependent on the accuracy of the wall pressures. In theory, each test condition should require a different boundary layer allowance (i.e. a change in test section cross-sectional area). In practice, researchers have shown that a series of say 4 *Aerodynamically Straight* wall contours are sufficient to provide uniform Mach number distributions, through an empty AWTS, for Mach numbers up to 0.9.[2,22] In addition, we do not need to make an allowance for the wall boundary layer thinning due to the presence of the model itself, until the flow on the flexible walls is sonic. Most AWTS operators monitor this boundary layer thinning real-time. Researchers have demonstrated that the adaptive wall testing techniques are tolerant to simple boundary layer allowances. In the NASA Langley 0.3-m TCT, for example, approximate *Aerodynamically Straight* contours are used which are simply linear divergence contours. This situation is a result of unacceptable wall waviness in the experimentally determined wall contours, with an empty test section. The quality of TCT data is unaffected by the use of these approximate wall boundary layer allowances.

The application of adaptive walls to different testing regimes is ongoing. Some interesting examples are: High lift 3-D testing of V/STOL aircraft at low speeds in an AWTS at the University of Arizona,[35] under the supervision of Professor Sears; Swept wing studies and minimum test section height studies with height to cord ratio of less than 0.5:1 in a low speed 2-D AWTSs at the University of Southampton (See Figure 19); Laminar flow studies using very large chord models (order 1 m - 39.37 inches) in low-speed flexible walled AWTSs at NPU and FFA, Sweden; Automotive testing at Sverdrup, Tennessee, and Southampton University using large blockage models (order 10%).[36] Of the 6 AWTS flow field simulations (investigated by Goodyer[37]), adaptive wall research has tended to concentrate on free-air and cascade simulations, because these are of most interest. Nevertheless, we now find closed tunnel simulations are proving to be very useful for CFD code validation.[21]

## 7.1 2-D Testing Experience in AWTSs

Validation data shows that real-time 2-D data from AWTSs is essentially free of top and bottom wall interferences.[38,39] We have found no problems with testing an aerofoil through stall (no wall shape induced model hysteresis present). Routine testing is possible up to drag rise Mach numbers (Mach 0.8-0.85). Data repeatability from day to day is excellent (order 0.001 in Cn and 0.0005 in Cd) but, in common with all wind tunnel measurements, calibration procedures affect long term repeatability.

We have observed that the wake of a 2-D model in an AWTS shows minimal spanwise variation. We can speculate that the use of large models (with blockage up to 12%) intrinsically minimises secondary flows at the aerofoil-sidewall junction, particularly when sidewall boundary layers are thin in high Reynolds number testing. This observation may explain why sidewall BLC does not significant effect wing performance in a relatively small AWTS. There are strong indications that the flow in an AWTS can be an excellent simulation of a 2-D flow field. If we ever need to use sidewall BLC in an AWTS, then researchers have found that no

special testing procedures are necessary. The wall adjustment procedure simply sensing the boundary layer mass removal as a model change.

Researchers have found many limitations to the various 2-D adaptive wall testing techniques, none of which are fundamental. These limitations are associated with wall movement (hardware), model size (theoretical assumptions) and Mach number (theory sophistication). Researchers have made 2-D tests close to Mach 1.0, and up to Mach 1.2, as shown in Figure 20.[16] In supersonic tests, researchers used local wall curvature (aided by wall boundary layer smearing) to remove oblique shock reflections on to the model. This work disproves long standing preconceptions that flexible walled AWTSs cannot be used through the speed of sound. However, the usefulness of 2-D testing in the supersonic regime is probably only academic, providing experience leading to production-type supersonic 3-D testing.

7.2 3-D Testing Experience in AWTSs

Limited 3-D validation tests support the claim that wall interferences are minimised in AWTSs.[38,39] However, the wall interferences present before any wall streamlining tend to be already small. Consequently, the effectiveness of AWTSs to minimise severe wall interferences in 3-D testing has not been studied.

This situation is due to the low blockage of the 3-D models so far tested in AWTSs. We can increase the model disturbances in the test section by using larger models or testing only at high speeds. Unfortunately, the roughly square cross-section of current AWTSs restricts the size of non-axisymmetric lifting models. Researchers have found that they must use low aspect ratio models to increase the model blockage above the normally accepted value of 0.5 percent. (This is because the model span must be limited to about 70 percent of the test section width to minimise interactions between the tip vortices and the tunnel sidewalls.) Consequently, there is a need for a new generation of 3-D AWTSs with rectangular cross-sections, which are wider than they are tall. These new AWTSs will help find the maximum 3-D model blockage we can successfully test in an AWTS (5.2% is the maximum reported).

Numerous 3-D AWTS designs have been studied (as discussed earlier). In fact, researchers have spent considerable time and effort to develop a wide range of complex 3-D AWTS designs, when it now appears the simpler 2-D design is adequate. (In hindsight, this effort appears unnecessary but the contribution to overall knowledge is nevertheless important.) An example of the promise of simple AWTSs in 3-D testing is shown on Figure 21. Data from residual interference codes (based on the work of Ashill and Weeks) are presented as contour plots of blockage and upwash wall interferences on a simple cropped delta wing, mounted on a sidewall of the 2-D AWTS in the Southampton TSWT. Notice how the blockage interference patterns, with straight walls, are normal to the flow and 2-D in nature. We can see 2-D wall streamlining, with a straight target line, eliminates the blockage interference. Similarly, the upwash interference pattern with the walls straight exhibits some two-dimensionality, and again 2-D wall streamlining significantly reduces the upwash. If necessary, these remaining gradients could be further reduced by use of swept target lines in the wall adjustment procedure.

We have not found any fundamental limits to Mach number when using AWTSs in 3-D testing. Preliminary tests at Mach 1.2 show that bending AWTSs' flexible walls in 2-D or 3-D can eliminate oblique shock reflections on to the model (See Figure 22). The smearing of the shock/wall interaction does much to ease the curvature requirements on the flexible walls, as found in 2-D testing. The example shown in Figure 22 has been repeated in two other AWTSs. Nevertheless, in supersonic testing, the quality of the model data after wall streamlining needs to be better defined and robust wall adjustment procedures are required.

The wall adjustment procedures for 3-D testing have taken advantage of the fast and large capacity mini-computers available for real-time 3-D flow computations. Fast wall

adjustment procedures are available up to about Mach 0.97. Adaptive wall and WIAC research continues to identify when wall streamlining can be stopped and corrections applied with confidence. The various wall adjustment procedures for 3-D testing attempt to minimise wall interferences along pre-determined target lines (as discussed earlier). For example, the Rebstock method[25] minimises interferences along a pre-set streamwise target line anywhere in the test section. The Goodyer method has shown that swept target lines are very effective at reducing wall induced gradients.[16] In addition, the Rebstock method minimises wall curvature by introducing a uniform angle of attack error throughout the test section. Currently, we do not know where best to place the target line to eliminate the wall induced gradients for different model configurations. We also do not know where the concept of a uniform angle of attack error will break down.

The type of wall pressure measurements necessary to adequately assess the residual wall interferences is also an unknown. The exploitation of real-time residual interference assessment and WIAC codes is now critical to progress in 3-D adaptive wall testing techniques. This has come about because we now realize that 3-D wall interferences cannot be eliminated with even the most complex AWTS system.[28,33]

Hardware limitations currently restrict AWTS test envelopes (in particular model lift) for reported 3-D tests in small AWTSs. These hardware limitations have arisen because the AWTS design criteria was inadequate, or the AWTSs were originally designed for only 2-D testing. Unfortunately, these limitations have hampered 3-D adaptive wall research. It would appear that this situation is caused by low priority funding.

Despite these problem, some routine AWTS use in 3-D testing has been demonstrated in the ONERA T-2 and TsAGI T-128. This situation indicates that even first-generation adaptive wall testing techniques can be used for production 3-D testing if the demand is present.

## 8. Production Requirements

The production requirements for an adaptive wall testing technique is the same as for any modern testing technique. Firstly, the technique must be easy to use. Consequently, we need to make the complexities of the AWTS invisible to the tunnel operators (similar to operating large flexible supersonic nozzles). Secondly, the technique must not require excessive tunnel time for wall streamlining. So we require the AWTS wall movements to be quick. Thirdly, the technique must have a known test envelope for successful use. Therefore, we must ensure the testing technique is well researched, so that we know the limitations and restrictions to be avoided during normal operations. Fourthly, the technique must be financially and politically acceptable.

How can the adaptive wall testing technique meet the production requirements shown above? First, lets consider the complexity of an adaptive wall testing technique. We must design the associated test section hardware so the wall shapes can be continually changed. We also need an interaction between the AWTS and a computer system to set the wall to streamline shapes. If we make the AWTS of simple design then access to the model is unaffected. Furthermore, if we make the wall adjustments automatic via a user-friendly computer system, the operator need only issue *Go/Stop* commands (See Figure 23). Consequently, the complexity of the testing technique is invisible to the operator. The tunnel operator's contact with the AWTS becomes similar to setting angle of attack or changing tunnel test conditions.

Second, lets consider the time factor. Adjusting walls in the test section takes time. How much time depends on the AWTS hardware (jack type) and the wall adjustment procedure. We can design the wall jacks to be very responsive. The wall adjustment procedure can find the streamline shapes in one or two iterations. The result is that wall streamlining can be quick. Researchers at ONERA have already demonstrated wall streamlining in 10 seconds for 2-D

testing. Computer advances will make this possible for 3-D testing in the future. Another time factor is the elimination of post-test corrections and lengthy test programmes, because real-time AWTS data are the final data. We show the importance of this fact on Figure 24. In this example, we compare real-time transonic 2-D lift data from a deep slotted walled test section with equivalent real-time data from a shallow flexible walled AWTS, at the same test conditions with transition fixed. The differences in maximum Cn and the lift-curve-slope are alarming. With the final data known real-time, AWTS operators can and should save overall tunnel run time.

Third, lets consider the test envelopes for AWTSs. Researchers have defined the test envelope for various 2-D adaptive wall testing techniques (described earlier). So we can direct non-expert users away from these known limitations. Alas, in 3-D testing, we are still learning what the limitations are, but the experience base is growing.

Fourth, let us consider the cost and political factors. The simplest AWTS design can be incorporated in existing wind tunnels by the replacement of only two walls. Also, the plenum, which surrounds ventilated transonic test sections, can provide adequate volume, within the pressure vessel, for the jack mechanisms. These factors will reduce the overall hardware costs. Furthermore, the advent of inexpensive, but powerful, PC computer systems means that an AWTS control system can cost considerably less now. In addition, an AWTS control system can be integrated with other tunnel systems, which must not operate at the same time as wall streamlining, such as the sting positioning system. Other favourable cost factors are the reduction of tunnel operating costs possible by using a smaller AWTS (as much as 75% smaller than the original), and by removing test section ventilation through use of flexible walls.

Politically, minimisation of risk is of major concern when considering the use of a new testing technique. It is always easier to copy what has gone before, but if we do not take risks, progress invariably suffers. Surprisingly, even providing simple boundary measurements for WIAC, with little or no risk involved, has met with resistance from tunnel managers. Naturally, adaptive walls introduce a level of risk which is all too often assessed on out-dated misconceptions, such as:

1) Adaptive walls are too complex for industrial use.
2) Adaptive walls are only effective in small scale facilities.
3) Model flow field calculations are required.
4) A rubber tube with a large number of jacks is required for 3-D testing.
5) Sonic flow at the AWTS flexible walls is a fundamental limit to test Mach number.

In reality, if the adaptive walls remain structurally sound, only the quality of the real-time data is put at risk by using adaptive walls. The tunnel test envelope can only be restricted by mechanical problems. Of course, there is the natural tendency to ignore improvement unless there is a significant reason for making that improvement. Clearly, the problem of wall interferences is perceived by many as more of a nuisance than a serious problem that must be overcome. This is certainly the current situation in the United States.

Interestingly of the three wind tunnels with AWTSs which come closest to being production-type tunnels, non-experts can only use one. The Langley 0.3-m TCT has the only *User Friendly* AWTS control system that allows non-expert 2-D testing within defined test envelopes. However, the TsAGI T-128 is currently the only major transonic wind tunnel where effort is being made to improve experimental testing techniques, and non-expert use is probably close at hand.

The extensive Langley experience with adaptive walls has identified several special requirements for production use of AWTS. An accurate technique for setting the flexible walls to a straight datum is required. The wall position transducers should have high priority

calibration status on a par with pressure instrumentation. The stability of the test Mach number should be checked during wall pressure scans. Finally, robust control software should be used which is unable to perpetuate data errors from test to test. These requirements may seem trivial but are crucial and often overlooked.

## 9. The Future of AWTSs?

The vast and successful 2-D AWTS testing experience will continue to be a catalyst for the development of 3-D adaptive wall testing techniques. There is now a need to build more AWTSs with two flexible walls specially for 3-D testing, to probe design principles and testing technique limitations. Currently, 6 research groups around the world are actively pursuing the development of 3-D adaptive wall testing techniques. This effort needs to focus on current research problems in 3-D testing (such as low supersonic testing) to bridge the gap between academic and industrial interests. Furthermore, this research needs to emphasis the importance of adaptive walls in transition research and CFD code validation to gain popular support for the many advantages of AWTSs. We must consolidate limited resources on developing flexible wall testing techniques and WIAC, which together offer the best chance for success.

The current status of adaptive wall technology is ongoing and positive. There are 4 new AWTSs being designed and built at this time. If production testing is the ultimate goal, then we have finished developing 2-D adaptive wall testing techniques for free-air simulations.[39] The last gathering of adaptive wall researchers at ICAW '91 in June 1991 set a precedent for discussing adaptive wall and WIAC interests together.[40] The comments from this meeting repeated those from previous such meetings, notably:

a) Flexible walls are usable over the transonic range up to Mach 1.3.
b) AWTSs can significantly reduce wall induced gradients in 3-D testing.
c) The choice of where to place the target line for interference elimination in 3-D testing is critical to success.
d) WIAC is effective at benign test conditions where CFD is almost as effective as the wind tunnel.

An International Working Group was established, in June 1991, to promote progress in WIAC and adaptive wall testing techniques, utilizing the readership of the **Adaptive Wall Newsletter**. The group will help coordinate research effort on mutual problems of wall interferences. Currently, the most pressing concern amongst group members is how best to tackle low supersonic 3-D testing. In this era of shrinking research budgets, this group will serve progress very well. The next group meeting is expected in December 1993, when plans will be laid for a programme to validate 3-D testing techniques.

Much has been achieved since the start of the modern era of adaptive walls in 1971. However, we find that AWTSs are incorporated in only one of the major transonic wind tunnels built worldwide in the last 20 years. However, several of these wind tunnels do include provisions in the test section design for the eventual use of adaptive wall technology, during the life of the wind tunnel. (The European Transonic Windtunnel - ETW is a prime example of this practice because of a 1988 management disagreement as to which AWTS design to use.) Some projects, like the refurbishment of the NASA 12-foot wind tunnel, are managed in such a manner as to precluded any inclusion of modern testing techniques regardless of the benefits. The inclusion of WIAC and/or adaptive walls in new wind tunnel projects requires an advocate. To quote Orville Wright, "*I had thought that truth must eventually prevail, but I have found silent truth cannot withstand error aided by continual propaganda.*" Without advocates, preconceptions, based on limited practical experience or an over-exposure to the use of ventilated test sections, will continue to delay the proper utilization of adaptive wall technology.

We can summarize the current status as the development of a "new" technology to a point

where this technology could be made very useful to the aerodynamicist (both theoretician and experimentalist) given the right priority. I am certain that if adaptive wall research had been given the same priority as the development of complex transonic "correction codes", we would have production 3-D adaptive wall testing techniques available for general use right now.

Lack of progress and loss of aerospace prowess in the United States may cause more risk-taking in ground testing in the future. The recent statement by the NASA Administrator, Daniel Goldin, that NASA aeronautical facilities should be improved and "... *we've got to be prepared to spend what it takes.*" is good news indeed.[41] NASA aeronautical research is still highly respected around the world and leads by example. During the last 5 years we have seen a major scaling down of NASA's research into experimental testing techniques, which has sent a message to the world that our wind tunnels are just fine as they are. This new NASA initiative, caused by US aerospace companies seeking out better ground testing facilities outside the United States, could have a profound influence on wind tunnel design worldwide, by encouraging more risk-taking and progress. I certainly hope so.

Now that the expectations of CFD have become more realistic, the relationship between wind tunnel and computer has become much more mature and stronger. The adaptive wall concept embodies a near-perfect combination (marriage even) of experimental and theoretical aerodynamics (wind tunnel and computer) to improve our understanding of aerodynamics in the future. Our wind tunnels are not perfect and adaptive wall technology is available to help us aspire to higher levels of data accuracy.[42]

## 10. Conclusions

1. Adaptive wall testing techniques, particularly those which utilize flexible walls, offer major advantages over conventional techniques in transonic testing.

2. We can significantly improve transonic data quality by using adaptive wall technology available for use now.

3. Computer advances have removed any impractical aspects of adaptive wall technology.

4. Non-expert use of AWTSs for routine 2-D testing has been demonstrated, even in cryogenic wind tunnels.

5. We can now design new AWTSs with no hardware restrictions to the 2-D and 3-D operating envelopes.

6. In 2-D testing, adaptive wall testing techniques are well proven and are already in use for production-type transonic testing in cryogenic wind tunnels.

7. Adaptive wall technology can significant reduce wall-induced gradients in 3-D testing with just two adaptive walls.

8. The next major step for adaptive wall technology is the development of testing techniques for general 3-D transonic testing, particularly at low supersonic speeds.

9. For general acceptance of adaptive wall testing techniques in 3-D testing, advocates are required to overcome the inertia against change in testing techniques, and preconceptions about the practicalities of AWTSs.

10. The current status of adaptive wall technology is ongoing and positive.

## References


1. Bailey, A.; and Wood, S.A.: **Further Development of a High-Speed Wind Tunnel of Rectangular Cross-Section.** British ARC R&M 1853, September 1938, 16 pp.

2. Wolf, S.W.D.: **The Design and Operational Development of Self-Streamlining Two-Dimensional Flexible Walled Test Sections.** Ph.D. Thesis. NASA CR-172328, March 1984, 281 pp. N84-22534#.

3. Hilton, W.F.: **High-Speed Aerodynamics.** Longmans, Green and Co., 1951, pp. 425-429.

4. Lewis, M.C.: **An Evaluation in a Modern Wind Tunnel of the Transonic Adaptive Wall Adjustment Strategy Developed by NPL in the 1940's.** NASA CR-181623, February 1988, 110 pp.

5. Holder, D.W.: **The High-Speed Laboratory of the Aerodynamics Division, N.P.L., Parts I, II and III.** British ARC R&M 2560, December 1946, 190 pp.

6. **Facilities and Techniques for Aerodynamic Testing at Transonic Speeds and High Reynolds Number.** AGARD CP-83, April 1971.

7. Sears, W.R.: **Self Correcting Wind Tunnels.** 16th Lanchester Memorial Lecture, May 1973. In: *Aeronautical Journal*, vol. 78, Feb/Mar 1974, pp. 80-89. A74-27592#.

8. Judd, M.; Goodyer, M.J.; and Wolf, S.W.D.: **Application of the Computer for On-site Definition and Control of Wind Tunnel Shape for Minimum Boundary Interference.** Presented at AGARD Specialist Meeting on "Numerical Methods and Windtunnel Testing, VKI, June 1976. In: AGARD CP-210, October 1976, Paper 6, 14 pp. N77-11975#.

9. Sears, W.R.; Vidal, R.J.; Erickson, J.C.; and Ritter, A.: **Interference-Free Wind Tunnel Flows by Adaptive-Wall Technology.** *Journal of Aircraft*, vol. 14, no. 11, November 1977, pp 1042-1050.

10. Harney, D.J.: **Three-Dimensional Testing in a Flexible-Wall Wind Tunnel.** AIAA Paper 84-0623. Presented at the AIAA 13th Aerodynamic Testing Conference, San Diego, March 1984. In: Technical Papers, pp 276-283. A84-24203#.

11. Heddergott, A.; Kuczka, D.; and Wedemeyer, E.: **The Adaptive Rubber Tube Test Section of the DFVLR Göttingen.** Paper presented at the 11th International Congress on Instrumentation in Aerospace Simulation Facilities, August 1985. In: ICIASF '85 RECORD, IEEE publication 85CH2210-3, pp. 154-156. A86-38244.

12. Ganzer, U.; Igeta, Y.; and Ziemann, J.: **Design and Operation of TU-Berlin Wind Tunnel With Adaptable Walls.** ICAS Paper 84-2.1.1. In: Proceedings of the 14th Congress of the International Council of the Aeronautical Sciences, vol. 1, September 1984., pp. 52-65. A84-44926.

13. Wedemeyer, E.; and Lamarche, L.: **The Use of 2-D Adaptive Wall Test Sections for 3-D Flows.** AIAA Paper 88-2041. Presented at the AIAA 15th Aerodynamic Testing Conference, May 1988, 10 pp. A88-37943#.

14. He, J.J.; Zuo, P.C.; Li, H.X.; and Xu, M.: **The Research of Reducing 3-D Low Supersonic Shock Wave Reflection in a 2-D Transonic Flexible Walls Adaptive Wind Tunnel.** AIAA Paper 92-3924. Presented at the 17th AIAA Aerospace Ground Testing Conference, July 1992, 7 pp. A92-56755.

15. Neiland, V.M.: **Adaptive Wall Wind Tunnels with Adjustable Permeability Experience of Exploitation and Possibilities.** Paper A3. In: Proceedings of International Conference on Adaptive Wall Wind Tunnel Research and Wall Interference Correction, NPU, Xian, China, June 1991, pp. A3-1 to A3-6. A91-52779.

16. Lewis, M.C.; Taylor, N.J.; and Goodyer, M.J.: **Adaptive Wall Technology for Three-Dimensional Models at High Subsonic Speeds and Aerofoil Testing Through the Speed of Sound.** In: Proceedings of the European Forum on Wind Tunnels and Wind Tunnel Testing Techniques, Southampton, England, September 1992, pp. 42.1-42.12.

17. Romberg, H.-J.: **Two-Dimensional Wall Adaptation in the Transonic Windtunnel of AIA.** *Experiments in Fluids*, vol. 9, no. 3, May 1990, pp. 177-180. A90-38497.

18. Holst, H.; and Raman, K.S.: **2-D Adaptation for 3-D Testing.** DFVLR-IB 29112-88 A 03, June 1988, 114 pp.

19. Pittaluga, F.; and Benvenuto, G.: **A Variable Geometry Transonic Facility for Aerodynamic Probe Calibration.** In: Proceedings of 8th Symposium on Measuring Techniques for Transonic and Supersonic Flow in Cascades and Turbomachines, Genoa, Italy, October 1985, pp. 1-1/23.

20. McDevitt, J.B.; and Okuno, A.F.: **Static and Dynamic Pressure Measurements on a NACA 0012 Airfoil in the Ames High Reynolds Number Facility.** NASA TP-2485, January 1985, 78 pp. N85-27823#.

21. Olsen, M.E.; and Seegmiller, H.L.: **Low Aspect Ratio Wing Code Validation Experiment.** AIAA Paper 92-0402. Presented at the 30th AIAA Aerospace Sciences Meeting, Reno, Nevada, January 1992, 13 pp.

22. Wolf, S.W.D.: **Application of a Flexible Walled Testing Technique Section to the NASA Langley 0.3-m Transonic Cryogenic Tunnel.** ICAS Paper 88-3.8.2. In: Proceedings of the 16th Congress of the International Council of the Aeronautical Sciences, August-September 1988, vol. 2, pp. 1181-1191. A89-13620#.

23. Wolf, S.W.D.; and Goodyer, M.J.: **Predictive Wall Adjustment Strategy for Two-Dimensional Flexible Walled Adaptive Wind Tunnel. A Detailed Description of the First One-Step Method.** NASA CR-181635, January 1988, 29 pp. N88-19409#.

24. Wolf, S.W.D.: **Wall Adjustment Strategy Software for Use With the NASA Langley 0.3-Meter Transonic Cryogenic Tunnel Adaptive Wall Test Section.** NASA CR-181694, August 1988, 195 pp. N89-13400#.

25. Rebstock, R.; and Lee, E.E.: **Capabilities of Wind Tunnels with Two Adaptive Walls to Minimize Boundary Interference in 3-D Model Testing.** In: Proceedings of the NASA Langley Transonic Symposium, NASA CP-3020, vol. 1, part 2, April 1988, pp 891-910. N89-20942.

26. Archambaud, J.-P.; and Mignosi, A.: **Two-Dimensional and Three-Dimensional Adaptation at the T2 Transonic Wind Tunnel of ONERA/CERT.** AIAA Paper 88-2038. Presented at the AIAA 15th Aerodynamic Testing Conference, May 1988, 10 pp. A88-37940#.

27. Archambaud, J.P.; Michonneau, J.F.; and Prudhomme, S.: **Use of Flexible Walls to Minimise Interferences at T2 Tunnel.** Presented at the European Forum on Wind Tunnels and Wind Tunnel Testing Techniques, Southampton, England, September 1992, Paper 15, 13 pp.

28. Le Sant, Y.; and Bouvier, F.: **A New Adaptive Test Section at ONERA Chalais-Meudon.** In:

Proceedings of the European Forum on Wind Tunnels and Wind Tunnel Testing Techniques, Southampton, England, September 1992, pp. 41.1-41.14.

29. Nagamatsu, H.T.; and Trilling, T.W.: **Passive Transonic Drag Reduction of Supercritical and Helicopter Rotor Airfoils.** In: Proceedings of the 2nd AHS International Conference on Rotorcraft Basic Research, February 1988, 13 pp. A88-51785.

30. Mitty, T.J.; Nagamatsu, H.T; and Nyberg, G.A.: **Oscillatory Flow Field Simulation in Blow-Down Wind Tunnel and the Passive Shock Wave/Boundary Layer Control Concept.** AIAA Paper 89-0214. Presented at the AIAA 27th Aerospace Sciences Meeting, January 1989, 15 pp.

31. Lewis, M.C.: **Aerofoil Testing in a Self-Streamlining Flexible Walled Wind Tunnel.** Ph. D. Thesis. NASA CR-4128, May 1988, 270 pp. N88-22865

32. Rill, S.L.; and Ganzer, U.: **Adaptation of Flexible Wind Tunnel Walls for Supersonic Flows.** AIAA Paper 88-2039. Presented at the AIAA 15th Aerodynamic Testing Conference, May 1988, 6 pp. A88-37941#.

33. Mokry, M.: **Residual Interference and Wind Tunnel Wall Adaption.** In: Proceedings of the NASA Langley CAST-10-2/DOA 2 Airfoil Studies Workshop Results, NASA CP-3052, September 1988, pp. 175-193. N90-17655#.

34. Holst, H.: **Determination of 3-D Wall Interference in a 2-D Adaptive Test Section Using Measured Wall Pressures.** In: Proceedings of the 13th International Congress on Instrumentation in Aerospace Simulation Facilities, September 1989, 11 pp.

35. Sears, W.R.: **Adaptable Wind Tunnel for Testing V/STOL Configurations at High Lift.** *Journal of Aircraft*, vol. 20, no. 11, November 1983, pp. 968-974.

36. Whitfield, J.D.; Jacobs, J.L.; Dietz, W.E.; and Pate, S.R.: **Demonstration of the Adaptive Wall Concept Applied to an Automotive Wind Tunnel.** AIAA Paper 82-0584. Presented at the AIAA 12th Aerodynamic Testing Conference, March 1982, 10 pp.

37. Goodyer, M.J.: **The Self Streamlining Wind Tunnel.** NASA TM-X-72699, August 1975, 45 pp. N75-28080#.

38. Tuttle, M.H.; and Mineck, R.E.: **Adaptive Wall Wind Tunnels - A Selected, Annotated Bibliography.** NASA TM-87639, August 1986, 53 pp. N86-29871#.

39. Hornung, H.G. (Editor): **Adaptive Wind Tunnel Walls: Technology and Applications.**AGARD AR-269, April 1990.

40. He, J.J. (Editor): **ICAW 1991: International Conference on Adaptive Wall Wind Tunnel Research and Wall Interference Correction.** Proceedings, Xian, China, June 1991, 290 pp. A91-52776. (For individual papers see A91-52777 to A91-52805.)

41. **Goldin Defines Policy to Reinvigorate Aeronautics Research, Infrastructure.** *Aviation Week and Space Technology*, December 14/21 1992, pp.71.

42. Steinle, F.; and Stanewsky, E.: **Wind Tunnel Flow Quality and Data Accuracy Requirements.** AGARD AR-184, 1982.

# Currently Used Adaptive Wall Test Sections

| Organization | Tunnel | X-Section (h x w) m | Length, m | Approx. Max. Mach No. | Approx. Max. $R_c$ (millions) | Walls | Adaptation Control | Remarks |
|---|---|---|---|---|---|---|---|---|
| Aachen, Aero. Institute [2] | TST | 0.4 Square | 1.414 | 4.0 | 2.8 | 2 Flexible 2 Solid | 24 Jacks/Wall | Issue 10 |
| DLR [3] | DAM | 0.8 Circular | 2.40 | 1.2 | ... | Rubber Tube | 64 Jacks Total | Issue 5 |
| DLR [3] | HKG | 0.67 x 0.725 Rectangular | 4.0 | >1.2 | ... | 2 Flexible 2 Solid | 17 Jacks/Wall | Issues 7,14 |
| Genova University [2] | Low Defl. Cascade | 0.2 x 0.05 Rectangular | 1.58 | 2.0 | 1 | 2 Flexible 2 Soild | 36 Jacks/Wall | Issue 7 |
| Genova University [2] | High Defl. Cascade | 0.2 x 0.05 Rectangular | 1.6 | >1.18 | 1 | 2 Flexible 2 Solid | 13 Jacks-Ceiling 26 Jacks-Floor | Issue 7 |
| NASA Ames [2&3] | HRC-2 AWTS1 | 0.61 x 0.41 Rectangular | 2.79 | >0.8 | 30 | 2 Flexible 2 Solid | 7 Jacks/Wall | |
| NASA Langley [2&3] | 0.3-m TCT | 0.33 Square | 1.417 | >1.3 | 120 | 2 Flexible 2 Solid | 18 Jacks/Wall | Issues 1-5,7, 8,13 |
| N P Univ. [2&3] Xian, China | WT52 | 0.21 x 0.3 Rectangular | 1.08 | 1.2 | ... | 2 Flexible 2 Solid | 16 Jacks/Wall | Issue 14 |
| N P Univ. [2&3] Xian, China | Low Speed | 0.256 x 0.238 Rectangular | 1.3 | 0.12 | 0.50 | 2 Flexible 2 Solid | 19 Jacks/Wall | Issues 2,5,9, 14, 15 |
| N P Univ. [2] Xian, China | LTWT | 1.0 x 0.4 Rectangular | 6 | 0.23 | 4 | 2 Flexible 2 Solid | 15+ Jacks/Wall | |
| ONERA/CERT [2&3] | T2 | 0.37 x 0.39 Rectangular | 1.32 | >1.0 | 30 | 2 Flexible 2 Solid | 16 Jacks/Wall | Issue 2 |
| ONERA [3] | S3Ch | 0.8 Square | 2.2 | 1.3 | ... | 2 Flexible 2 Solid | 15 Jacks/Wall | |
| RPI [2] Troy, NY | 3 x 8 | 0.20 x 0.07 Rectangular | 0.6 | 0.86 | ... | 1 Flexible 3 Solid | 6 Jacks | |
| RPI [2] Troy, NY | 3 x 15 | 0.39 x 0.07 Rectangular | 0.6 | 0.8 | ... | 4 Solid | Multiple Top Wall Inserts | |
| Southampton University [2&3] | SSWT | 0.152 x 0.305 Rectangular | 0.914 | 0.1 | 0.38 | 2 Flexible 2 Solid | 17 Jacks/Wall | Variable T.S. Height |
| Southampton University [2] | AWT | 0.305 x 0.305 Square | 0.914 | 0.1 | ... | 3 Flexible 1 Solid | ? Jacks/Wall | |
| Southampton University [2&3] | TSWT | 0.15 Square | 1.12 | >1.0 | 2.5 | 2 Flexible 2 Solid | 19 Jacks/Wall | Issue 1 |
| Sverdrup Technology [3] | AWAT | 0.305 x 0.61 Rectangular | 2.438 | 0.2 | -- | 3 Multi-Flexible Slats 1 Solid | 102 Jacks-Ceiling 15 Jacks/Sidewall | Issue 4 |
| Tech. University Berlin [3] | III | 0.15 x 0.18 Octagonal | 0.83 | >1.0 | -- | 8 Flexible | 78 Jacks Total | Issue 6 |
| TsAGI [3] U.S.S.R. | T-128 | 2.75 Square | 8.0 | 1.7 | 9 | 4 Porous | 32 Control Panels per Wall | Issues 11,13 |
| Umberto Nobile [2] | FWWT | 0.2 Square | 1.0 | 0.6 | 3.5 | 2 Flexible 2 Solid | 18 Jacks/Wall | |
| VKI [2] Belgium | T'3 | 0.10 x 0.12 Rectangular | ? | 0.2 | ... | 2 Flexible 2 Solid | ? Jacks/Wall | |
| Waterloo [2] Univ., Canada | LSWT | 0.91 x 0.61 Rectangular | 6.55 | 0.1 | ... | 2 Flexible 2 Solid | 48 Jacks/Wall | |

[2] - 2D Testing Capability
[3] - 3D Testing Capability
[2&3] -2D and 3D Testing Capability

February 1993
SWDW

**Note:** The Remarks column refers to issues of the *Adaptive Wall Newsletter* which contain related articles.

Table 1

# Principle of Wall Streamlining

## General 3-D Case

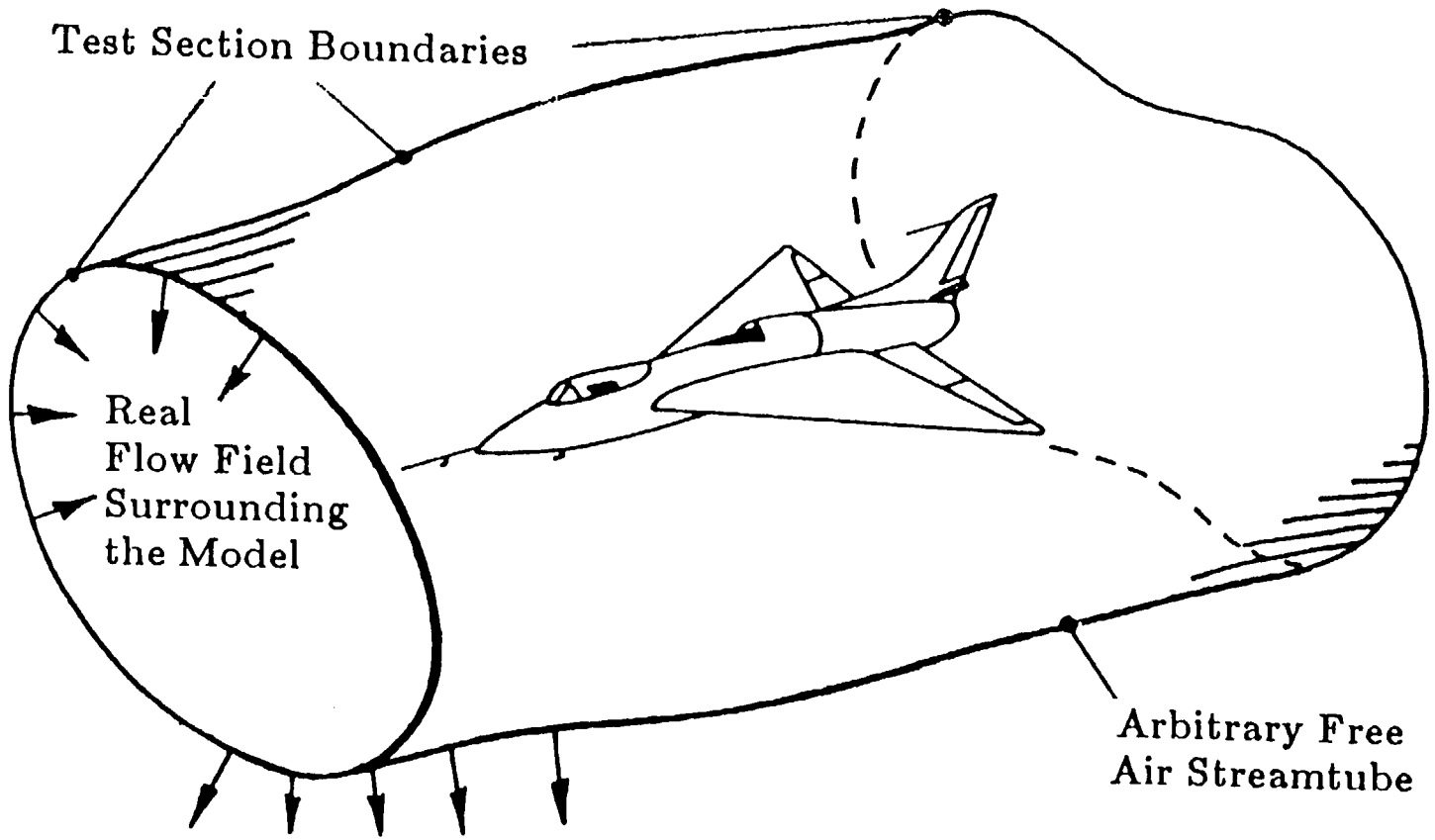


Fig. 1

# WALL STREAMLINING PROCEDURE

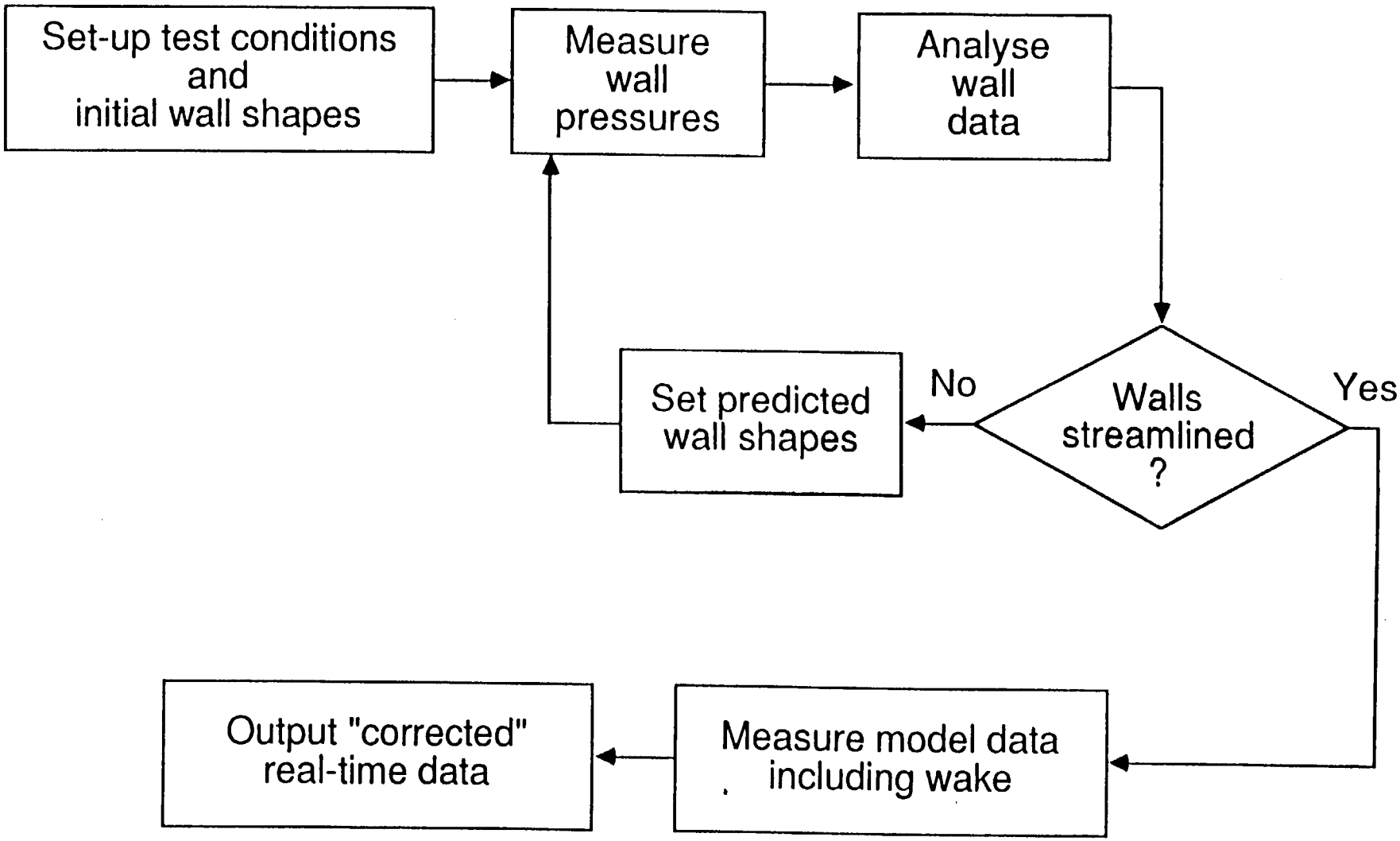


Fig. 2

# Historical Background to the Current Status of Adaptive Wall Technology

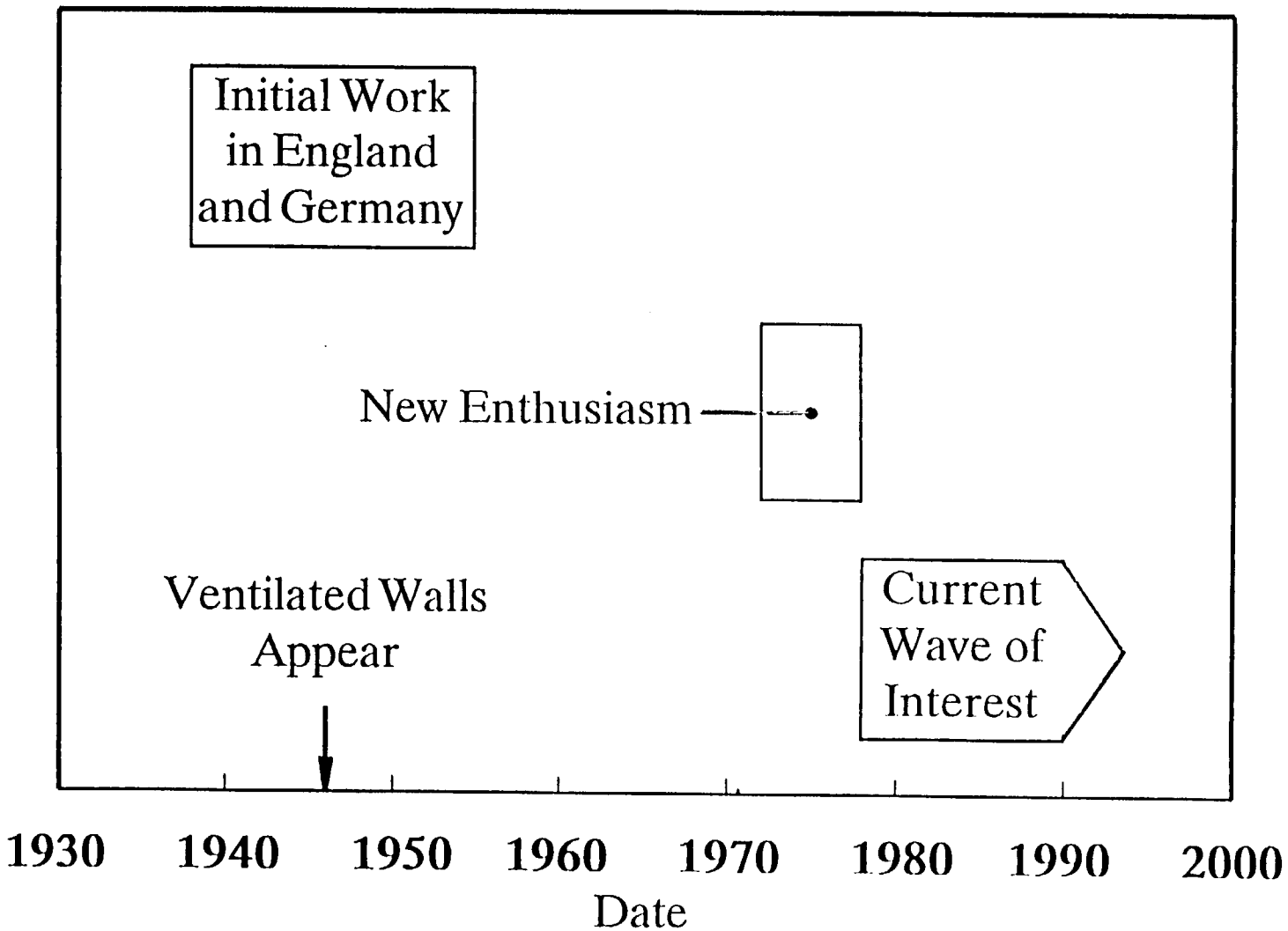


Fig. 3

Transonic- and Supersonic-Tunnel (TST)
RWTH Aachen, Germany

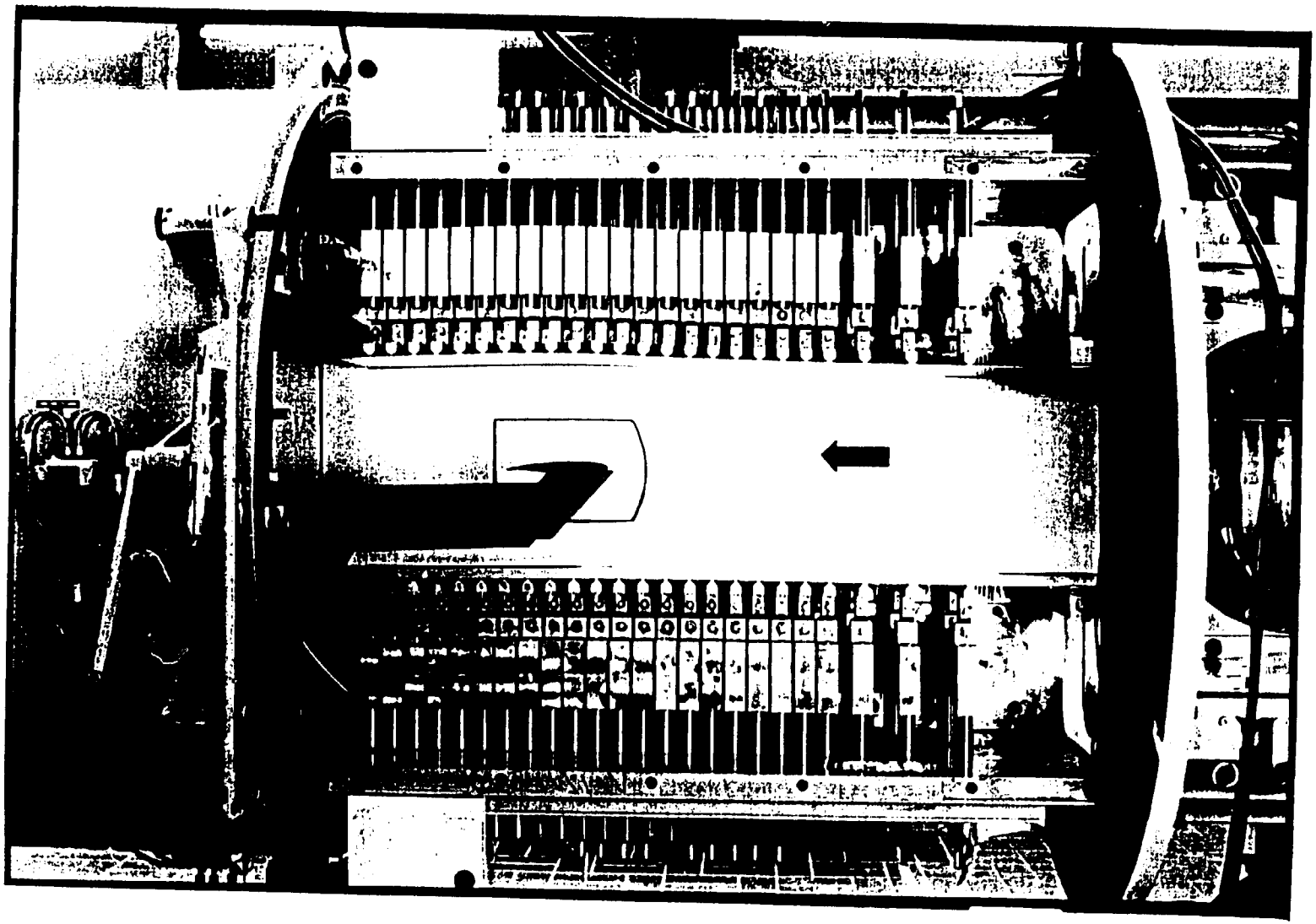

Fig. 4

# DLR High Speed Wind Tunnel (HKG)
# AWTS/Supersonic Nozzle
# Göttingen, Germany

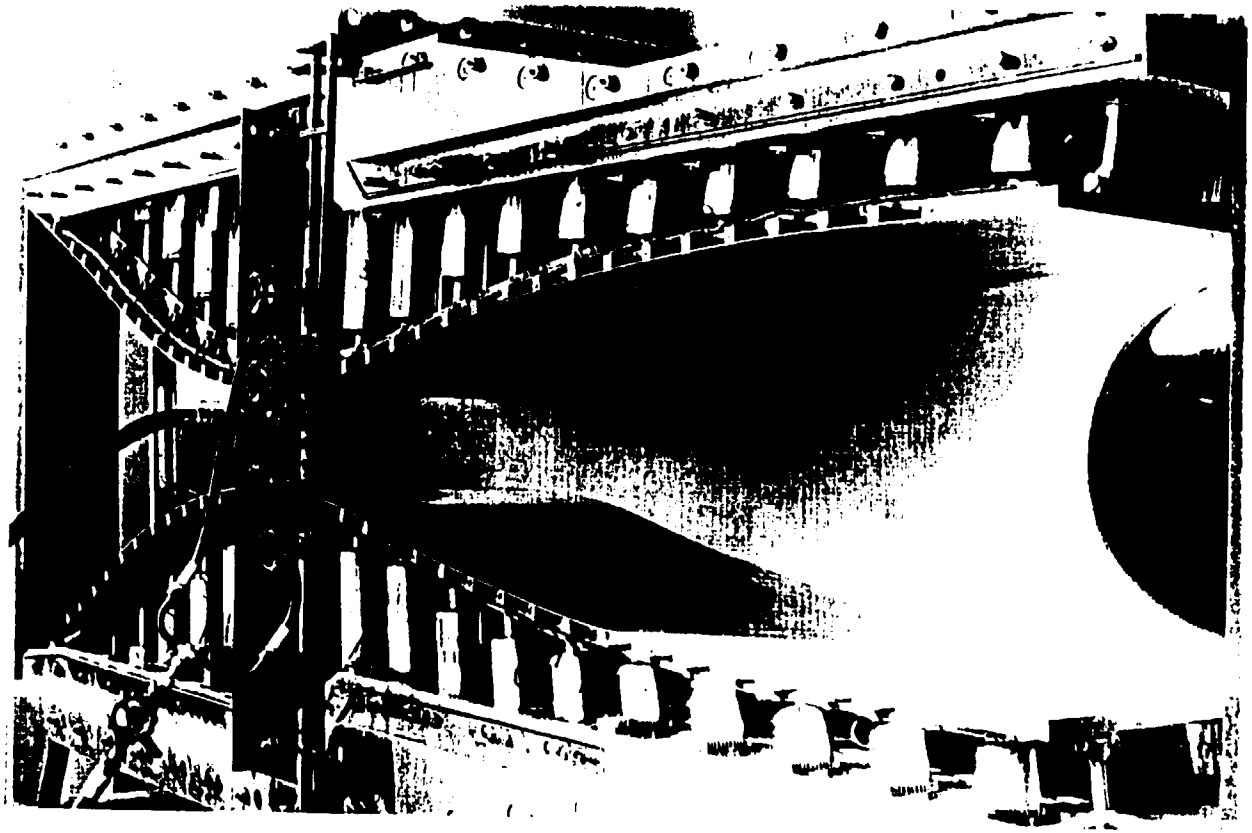

Fig. 5

The Low Deflection Blade Cascade Tunnel
at Genoa University, Italy

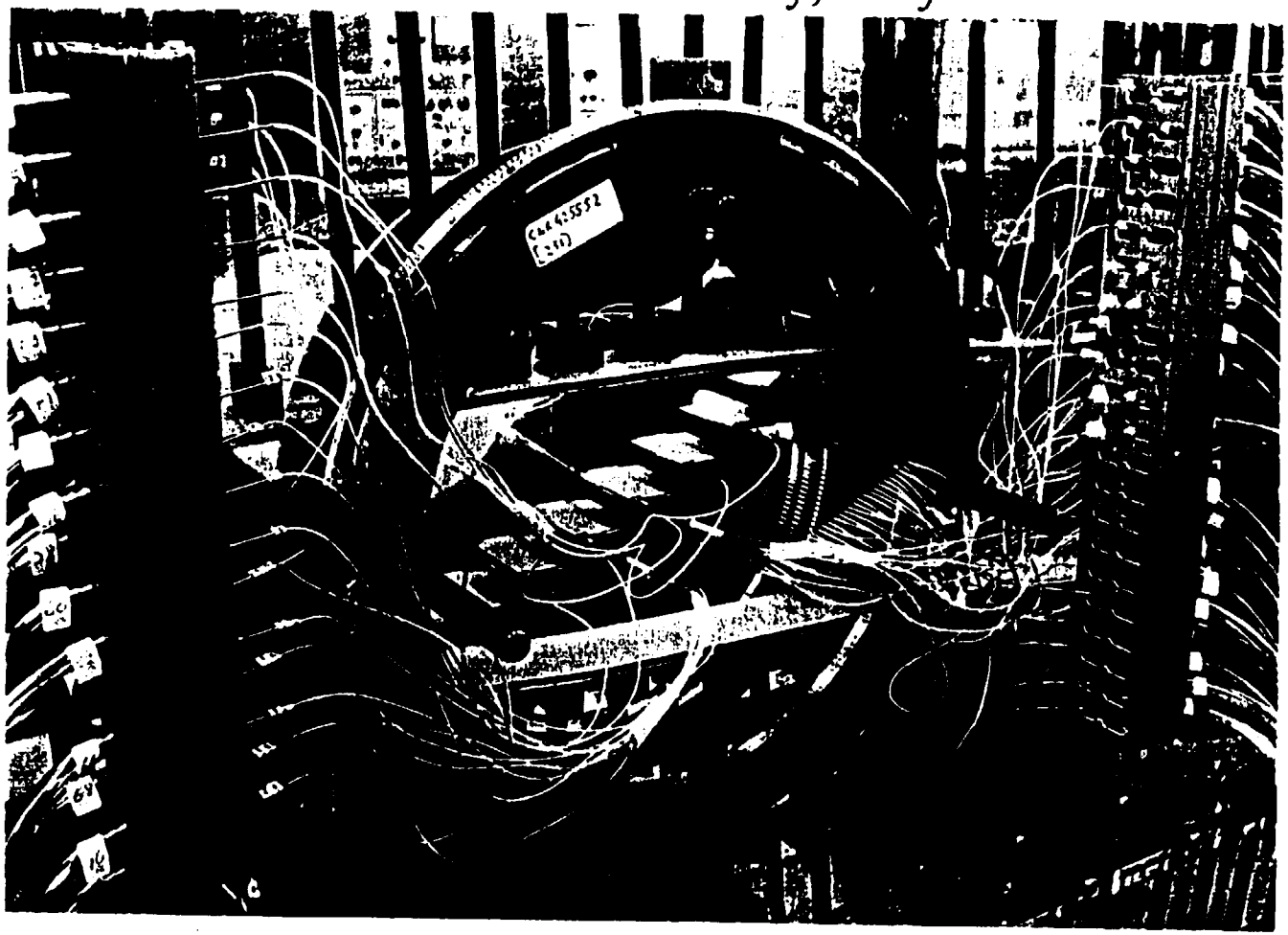

Fig. 6

# The High Deflection Blade Cascade Tunnel at Genoa University, Italy

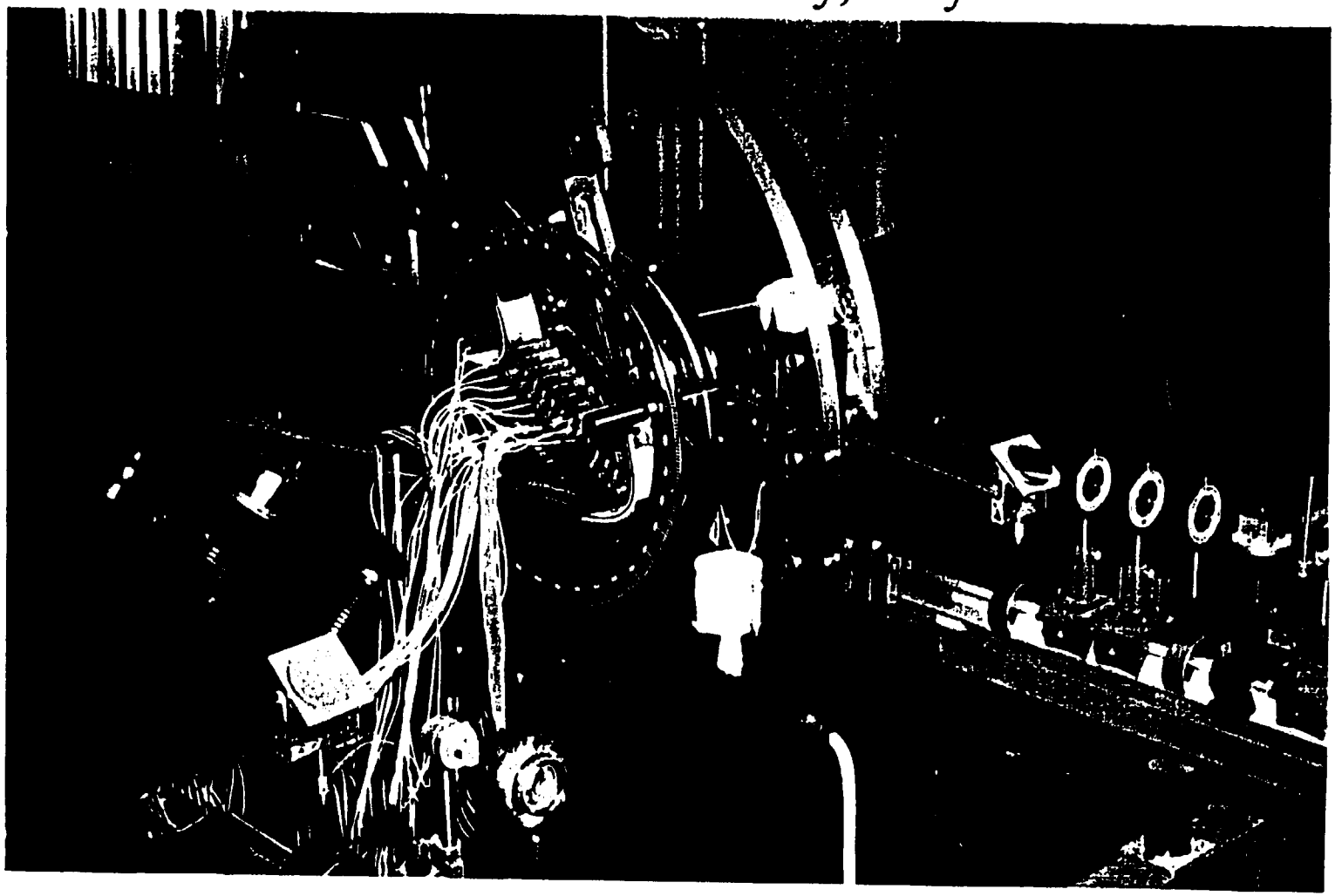

Fig. 7

# NASA Ames High Reynolds Channel - 2 AWTS

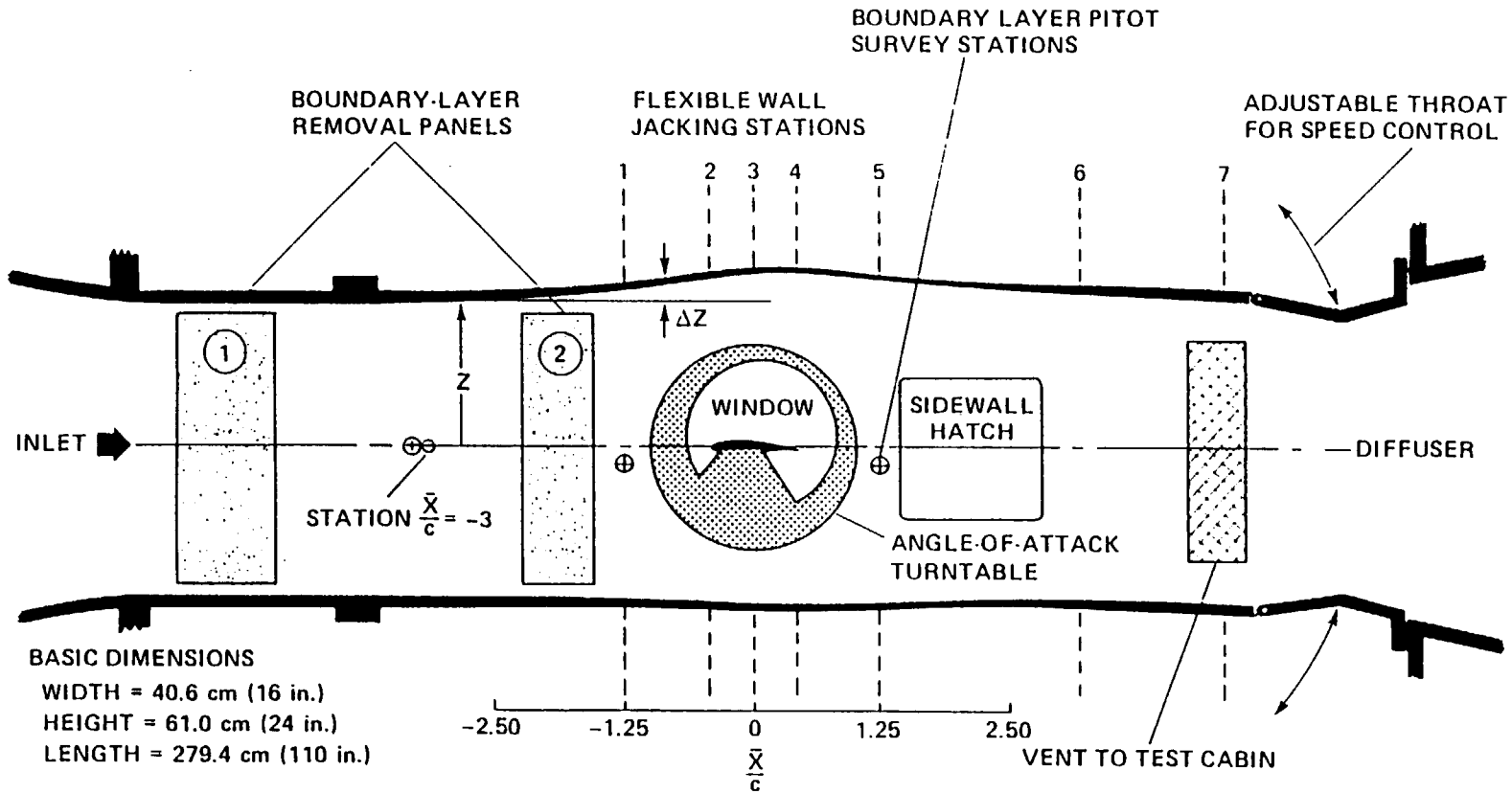


Fig. 8

# NASA Langley 0.3-m Transonic Cryogenic Tunnel

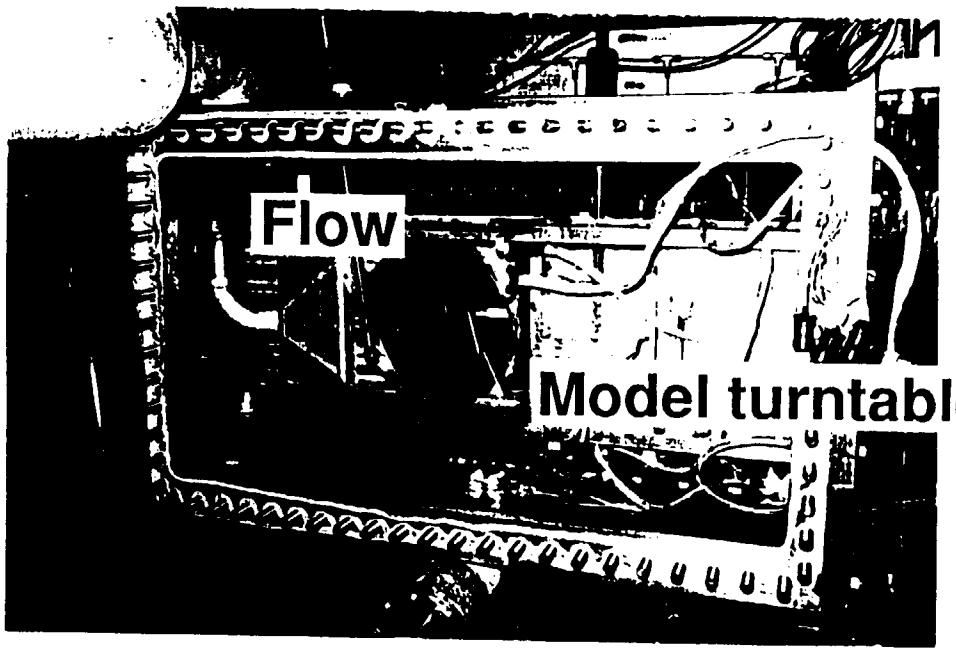


AWTS with Pressure Shell Sidewall Removed

Ice Buildup on AWTS Pressure Shell after a Long Cryogenic Run

Fig. 9

# Northwestern Polytechnical University
# High Speed WT52 AWTS in Xian, China

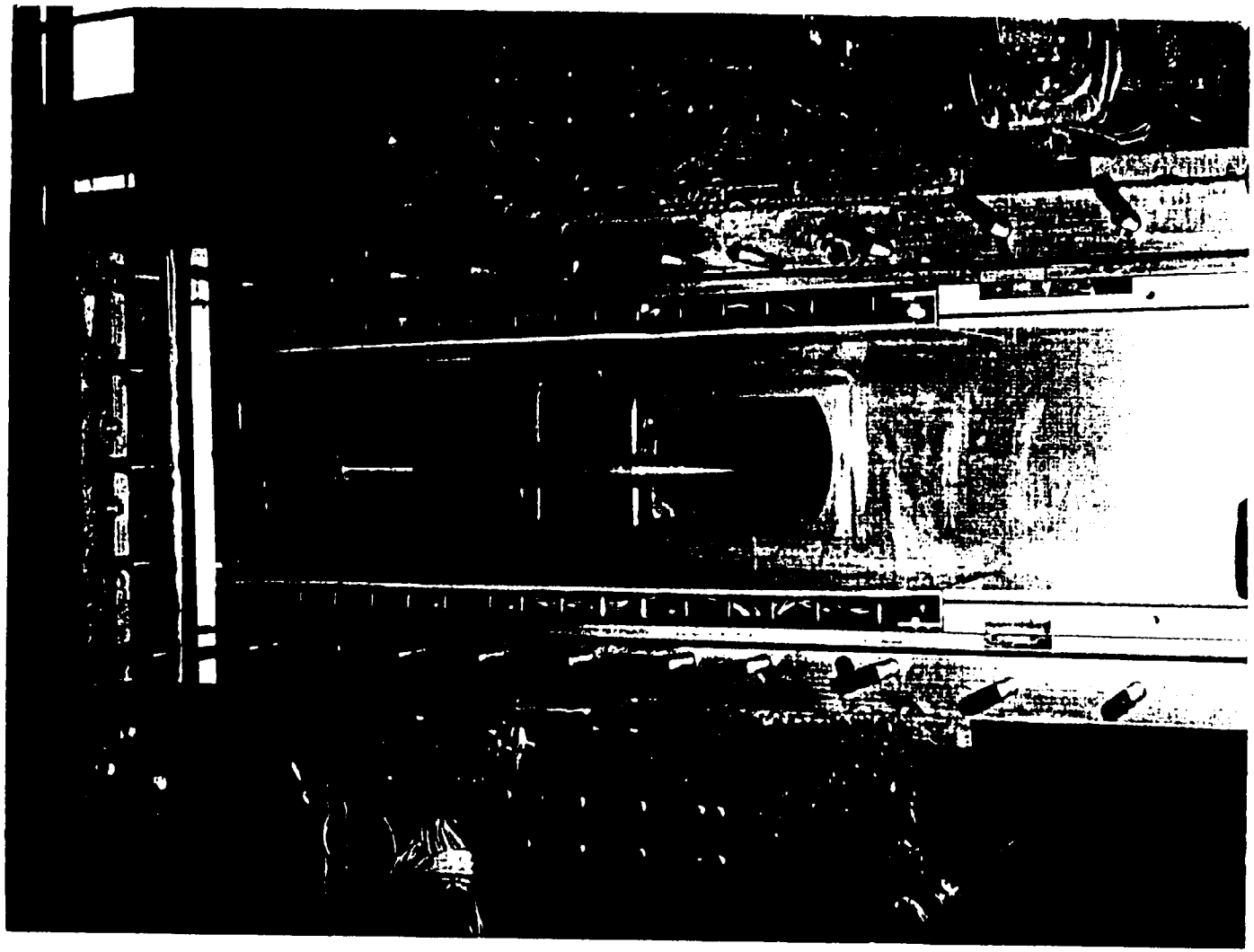

Fig. 10

ONERA/CERT T2 Transonic Cryogenic AWST
Toulouse, France

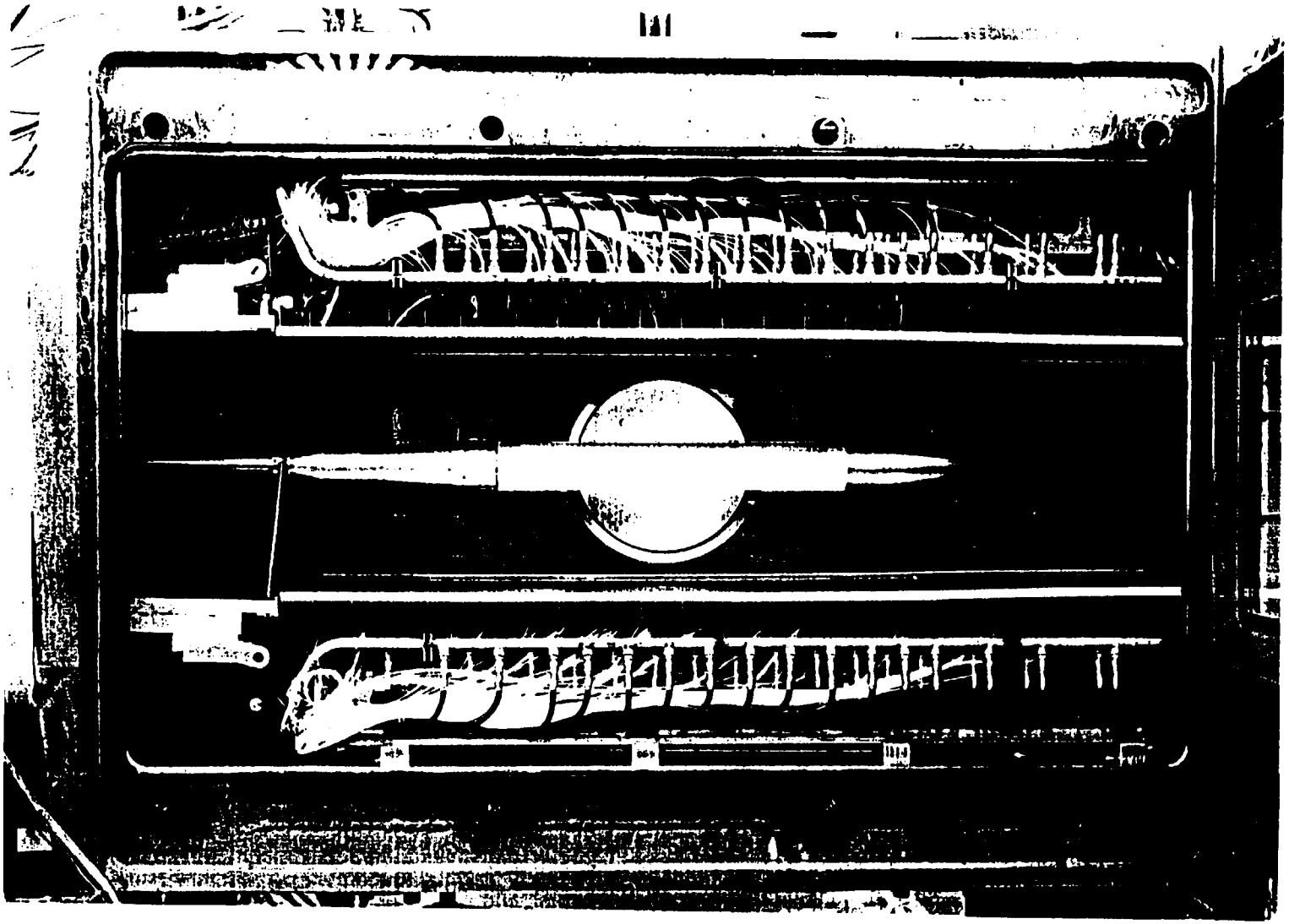

Fig. 11

ONERA S3Ch Transonic Wind Tunnel AWTS
Chalais-Meudon, France

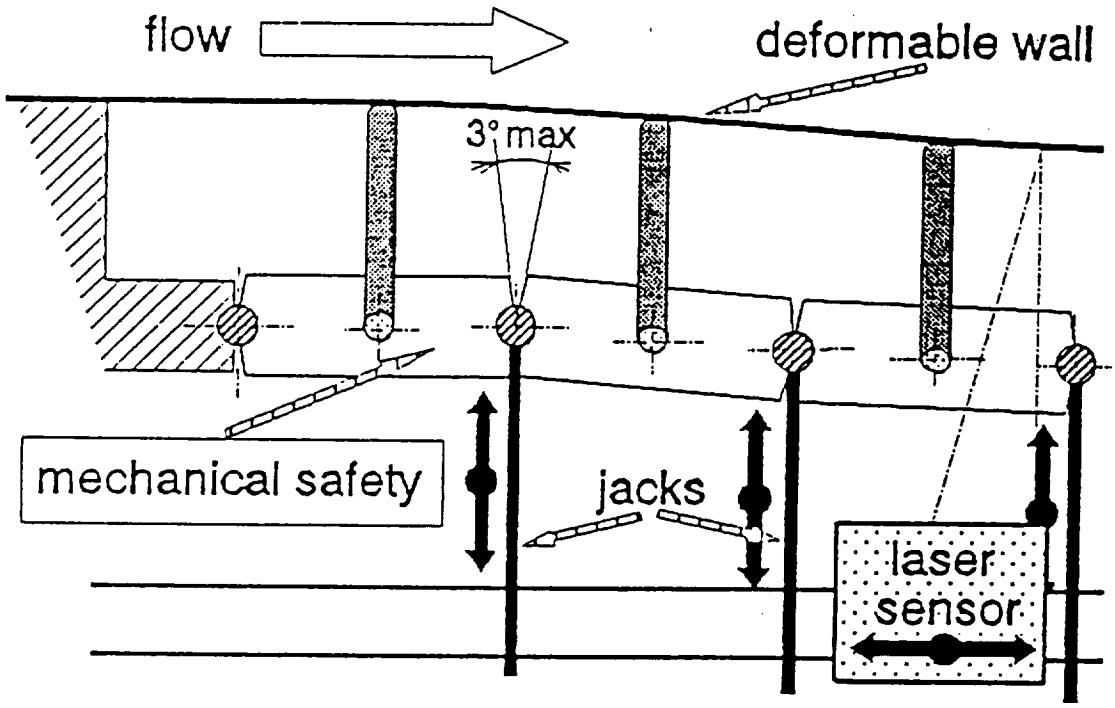


Fig. 12

Rensselaer Polytechnical Institute 3 x 8 Transonic
Wind Tunnel
Troy, New York

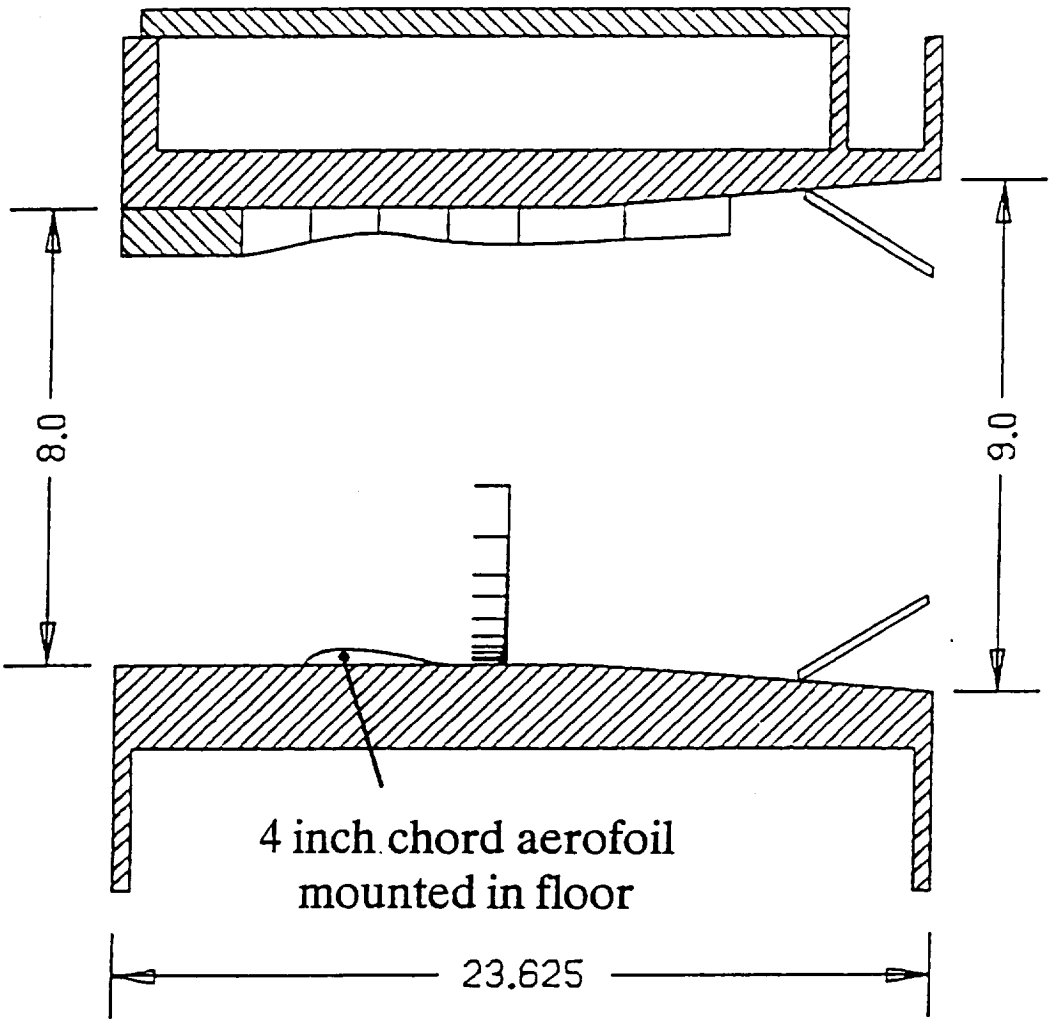


Fig. 13

# Transonic Self-Streamlining Wind Tunnel
# Southampton University, England

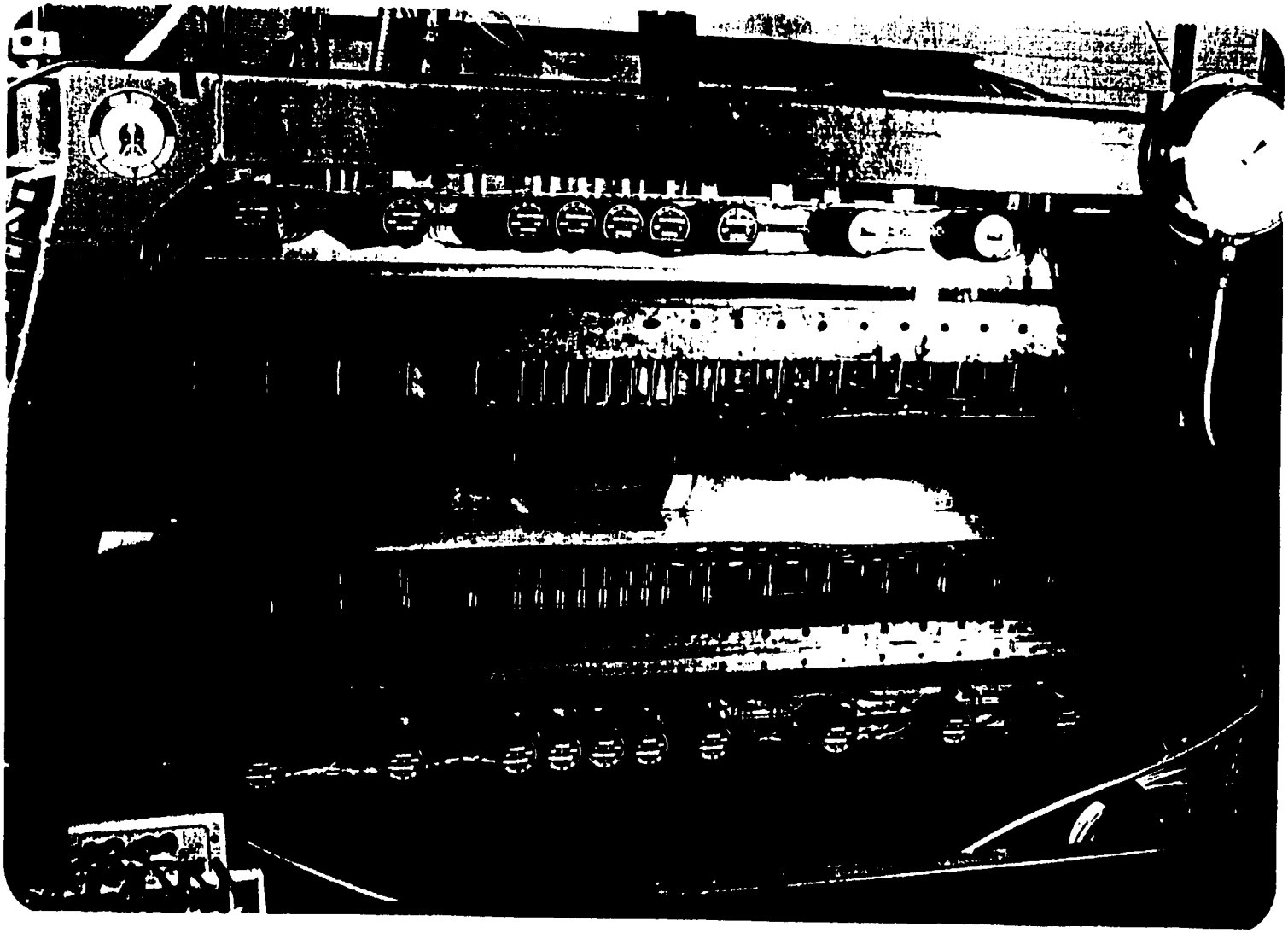

Fig. 14

Octagonal Flexible Walled AWTS III
Technical University of Berlin (TUB), Germany

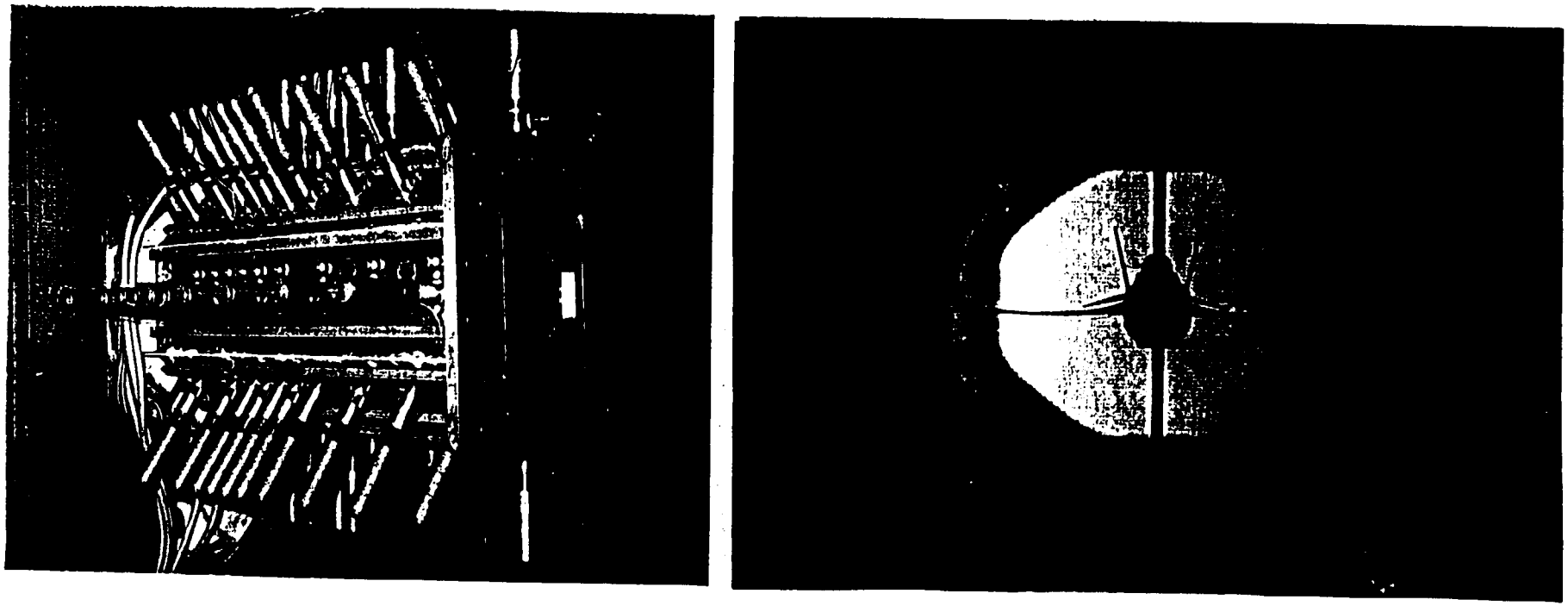

Fig. 15

TsAGI T-128 Transonic Wind Tunnel, Zhukovsky, Russia

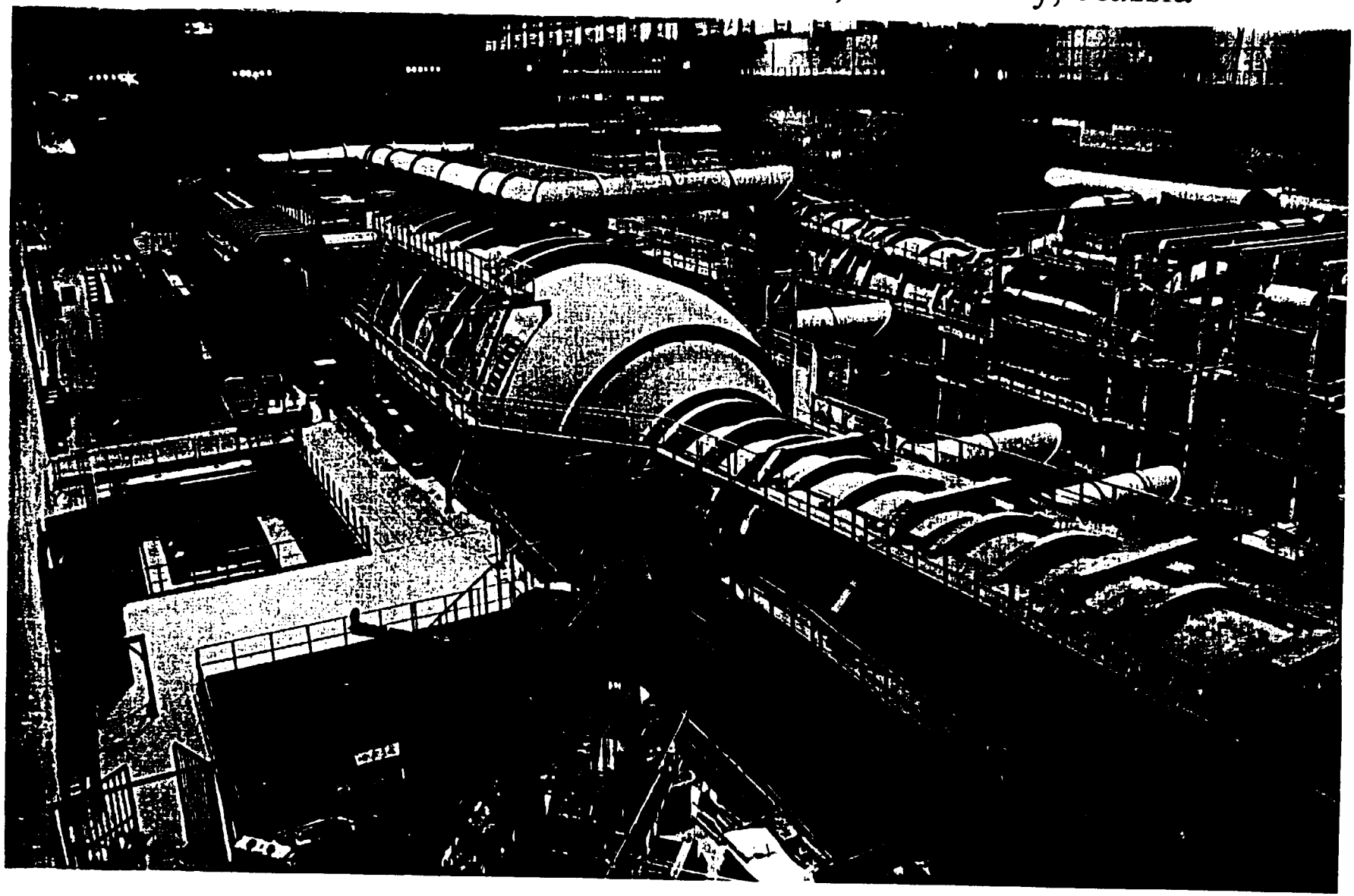

Fig. 16a

TsAGI T-128 Variable Porosity AWTS with a 3% Buron Model
Zhukovsky, Russia

Fig. 16b

# TsAGI T-128 AWTS Variable Porosity Segments Showing Sliding Plate Assembly, Zhukovsky, Russia

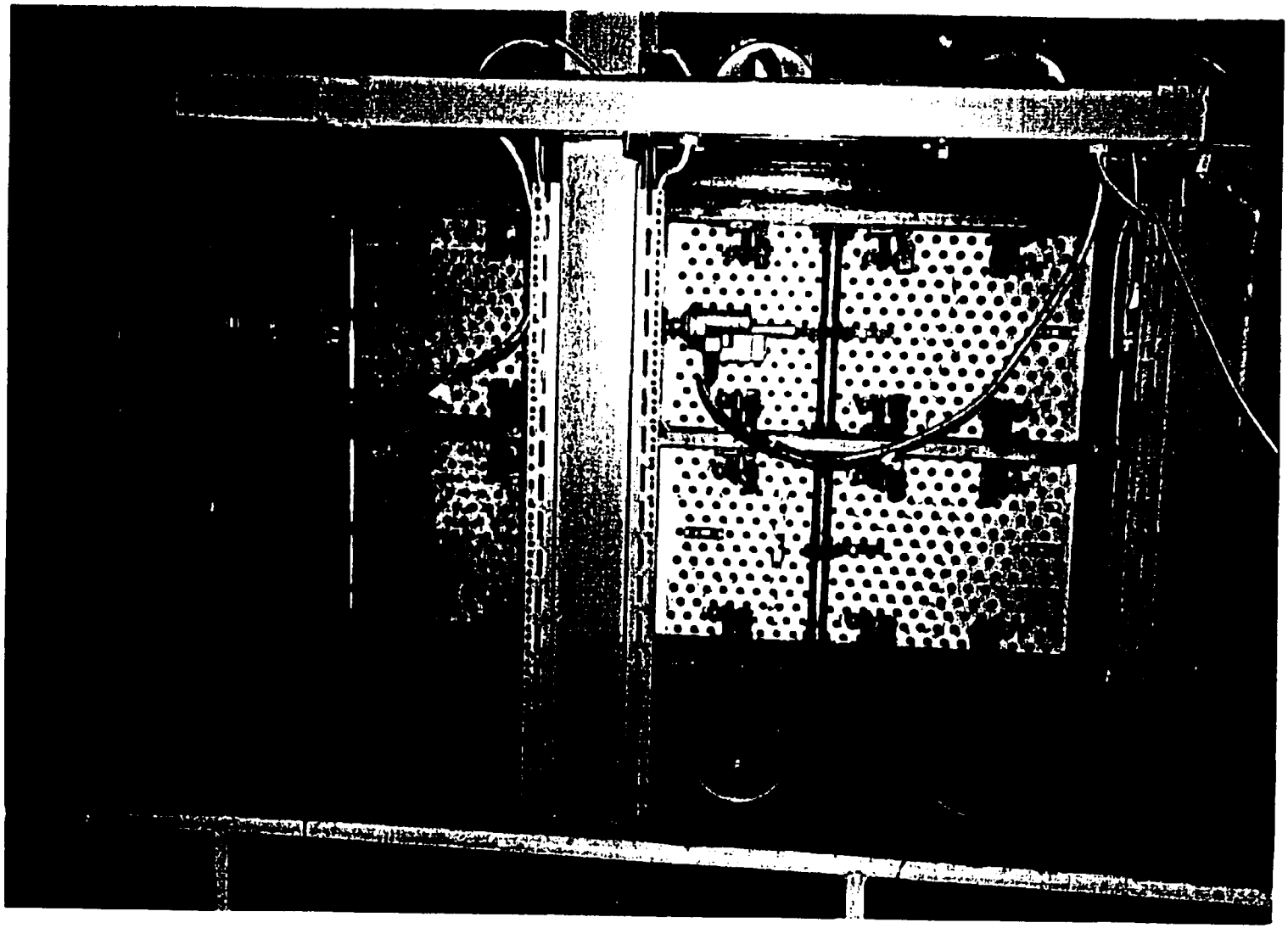

Fig. 17

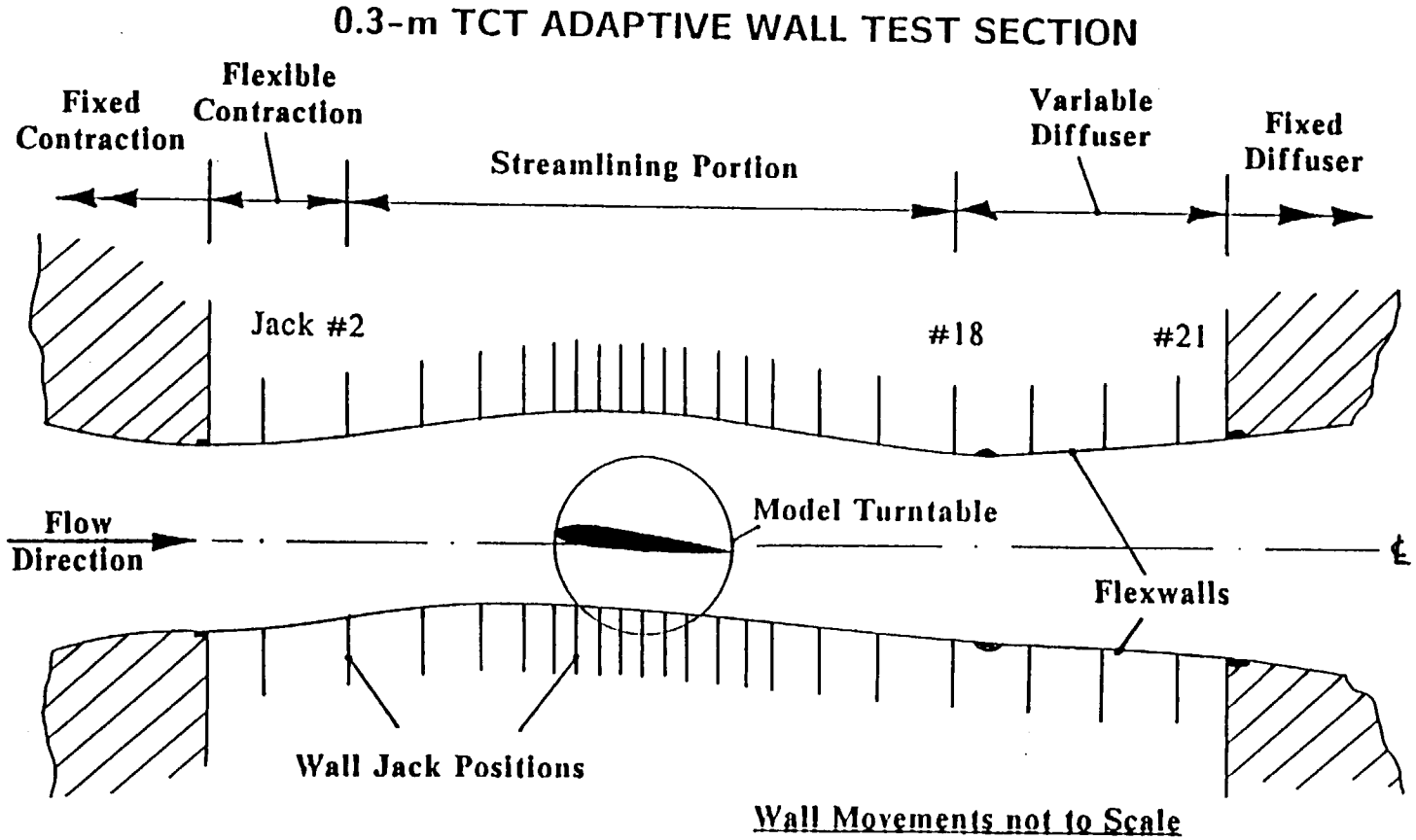
0.3-m TCT ADAPTIVE WALL TEST SECTION
Fixed Contraction
Flexible Contraction
Streamlining Portion
Variable Diffuser
Fixed Diffuser
Jack #2
#18
#21
Flow Direction
Model Turntable
Flexwalls
Wall Jack Positions
Wall Movements not to Scale

Fig. 18

Low Speed Self-Streamlining Wind Tunnel (SSWT)
Southampton University, England

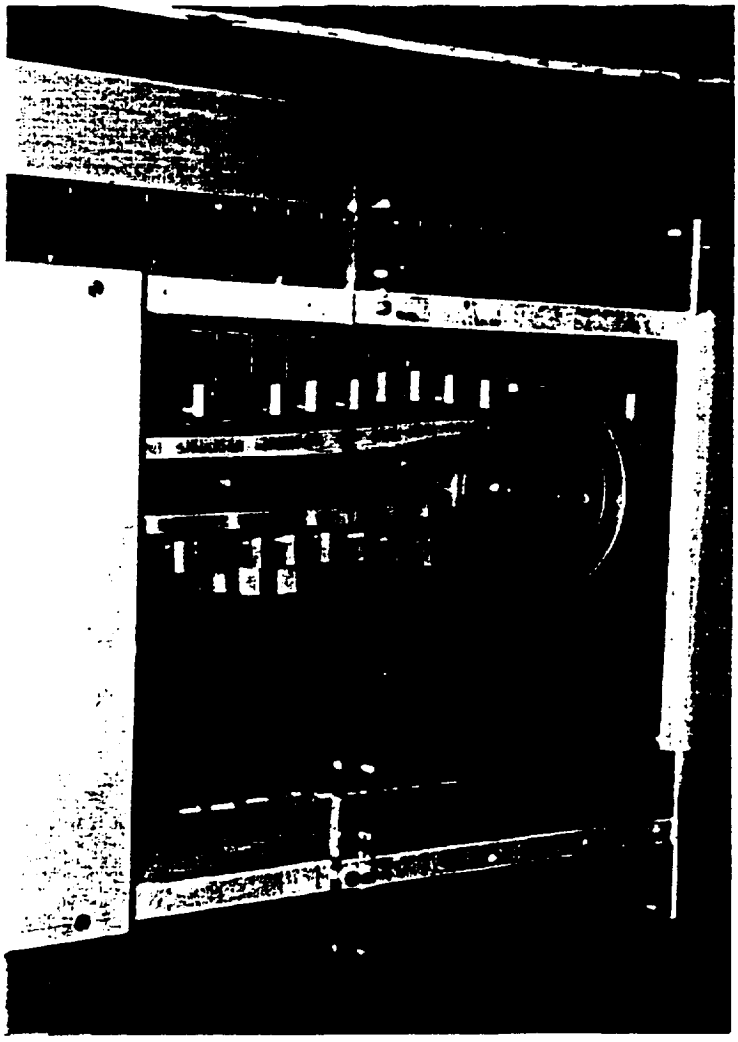

Fig. 19

**Low Supersonic 2-D Testing in a Flexible Walled AWTS**

University of Southampton TSWT data

NACA 0012-64 Aerofoil (Mach 1.2; $\alpha \approx 1.0°$)

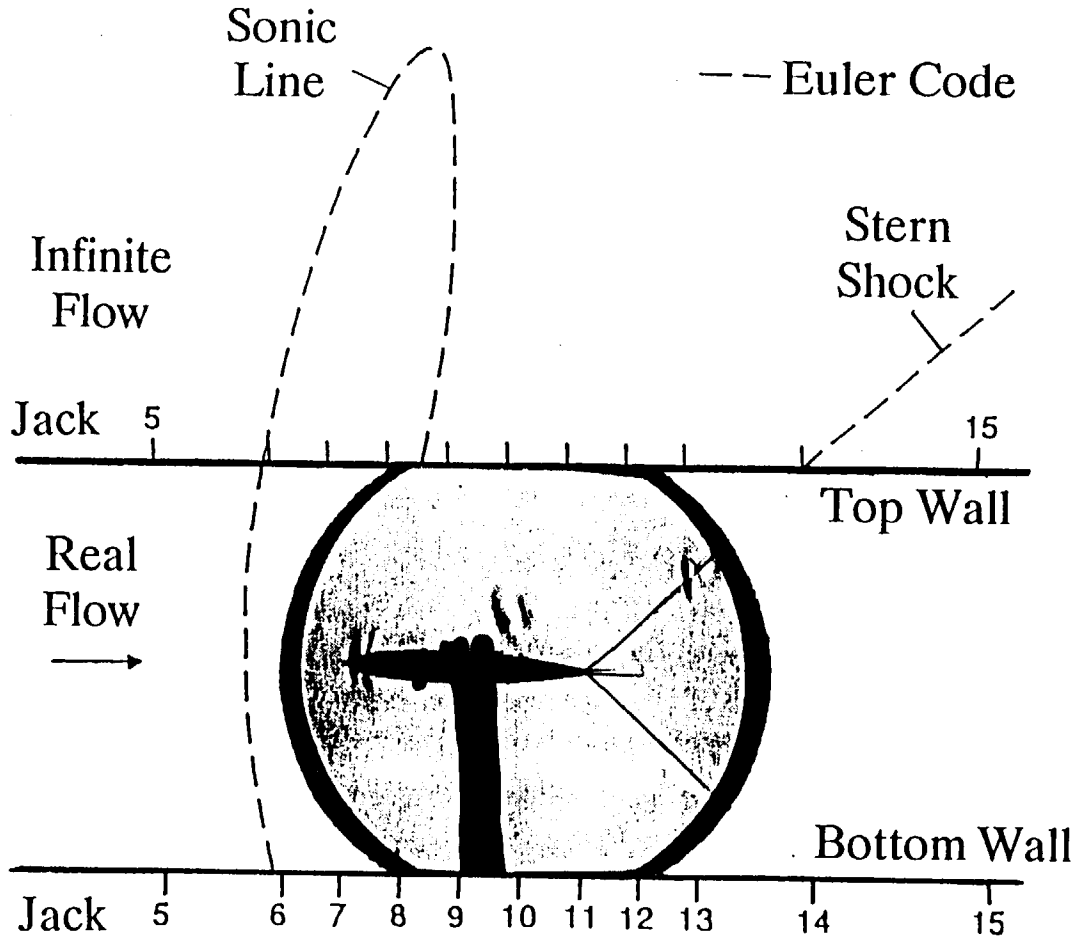


Montage of Experimental and Theoretical Aerofoil Flow Fields

With the Walls Streamlined.

Fig. 20

# Boundary Interference Minimization with 2-D Wall Adaptation in 3-D Tests

University of Southampton AWTS Data - Mach 0.7; Alpha = 8 deg.

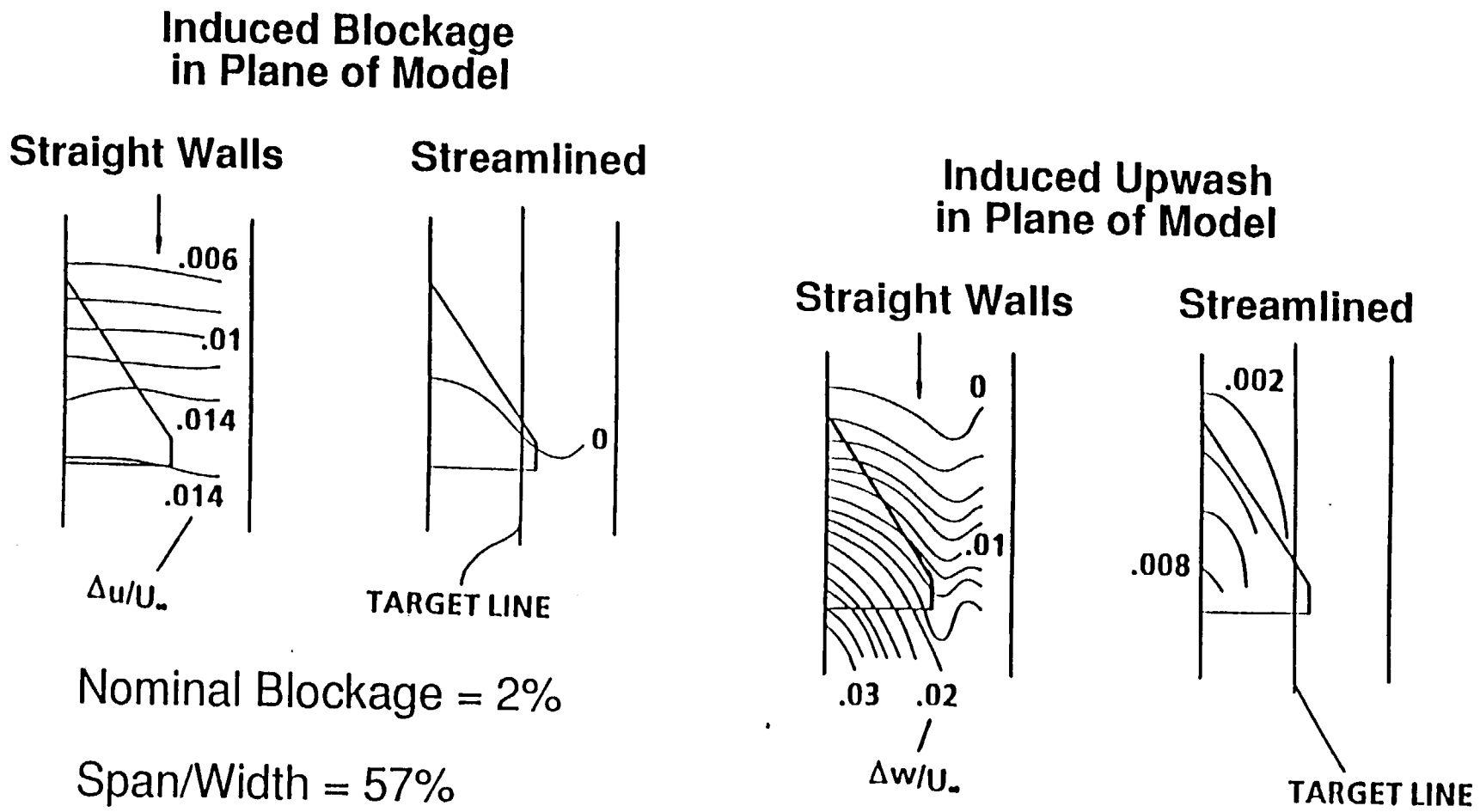


Nominal Blockage = 2%

Span/Width = 57%

Fig. 21

# Supersonic Tests in a Three-Dimensional AWTS

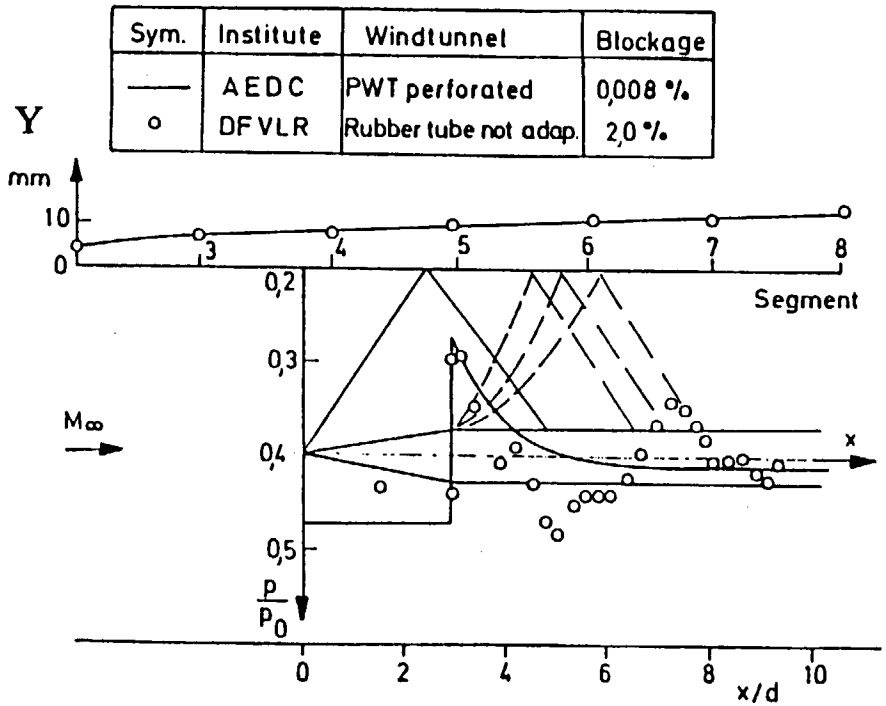


$C_p$ distribution before adaptation

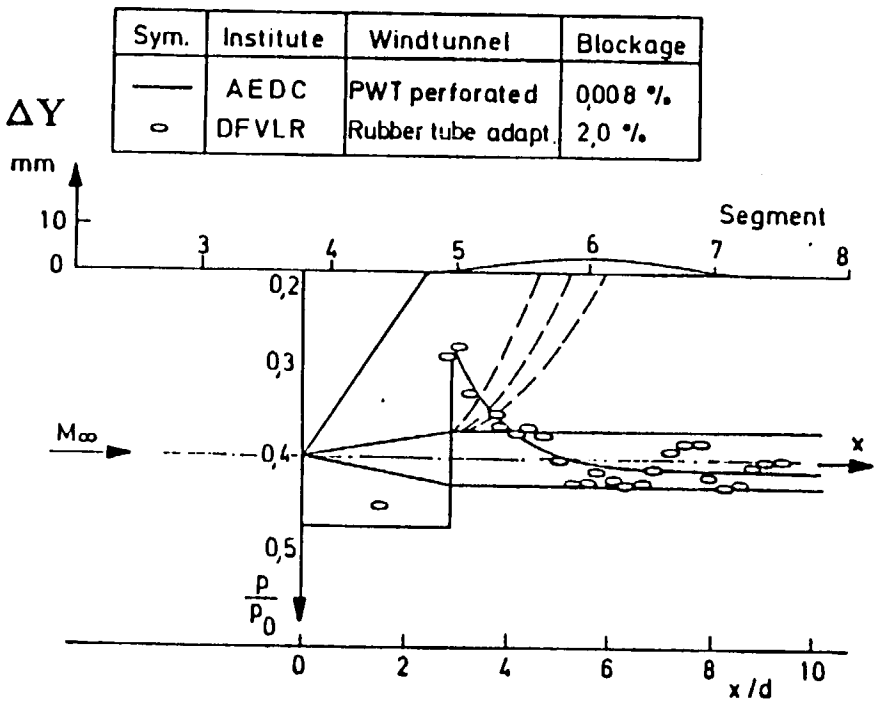


$C_p$ distribution after adaptation
Wall displacement, $\Delta Y$ = 3.5 mm at 6th segment

Fig. 22

# General AWTS Control System for Non-Expert Use

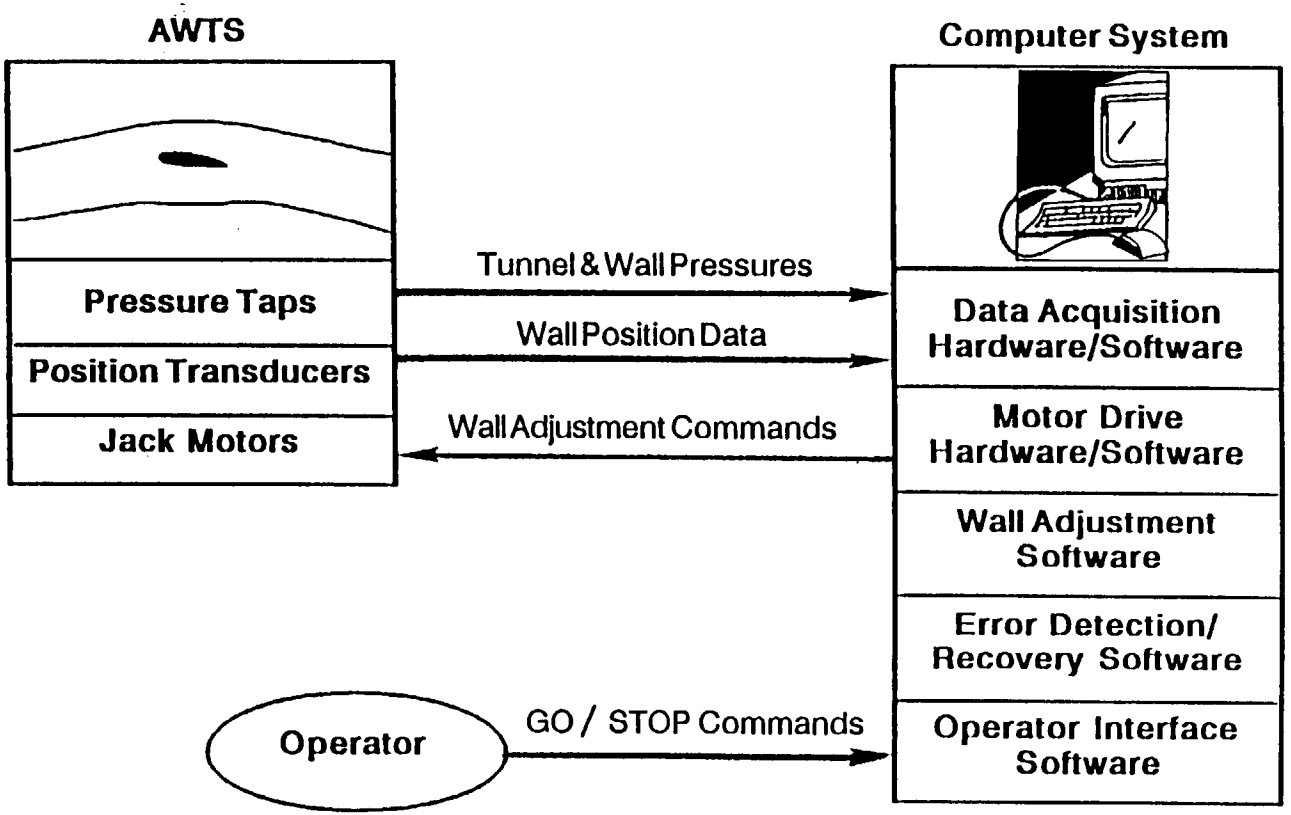


Fig. 23

# The Importance of Corrected Real-Time 2-D Data

NASA Langley 0.3-m TCT Aerofoil Data - Mach 0.765; Transition Fixed

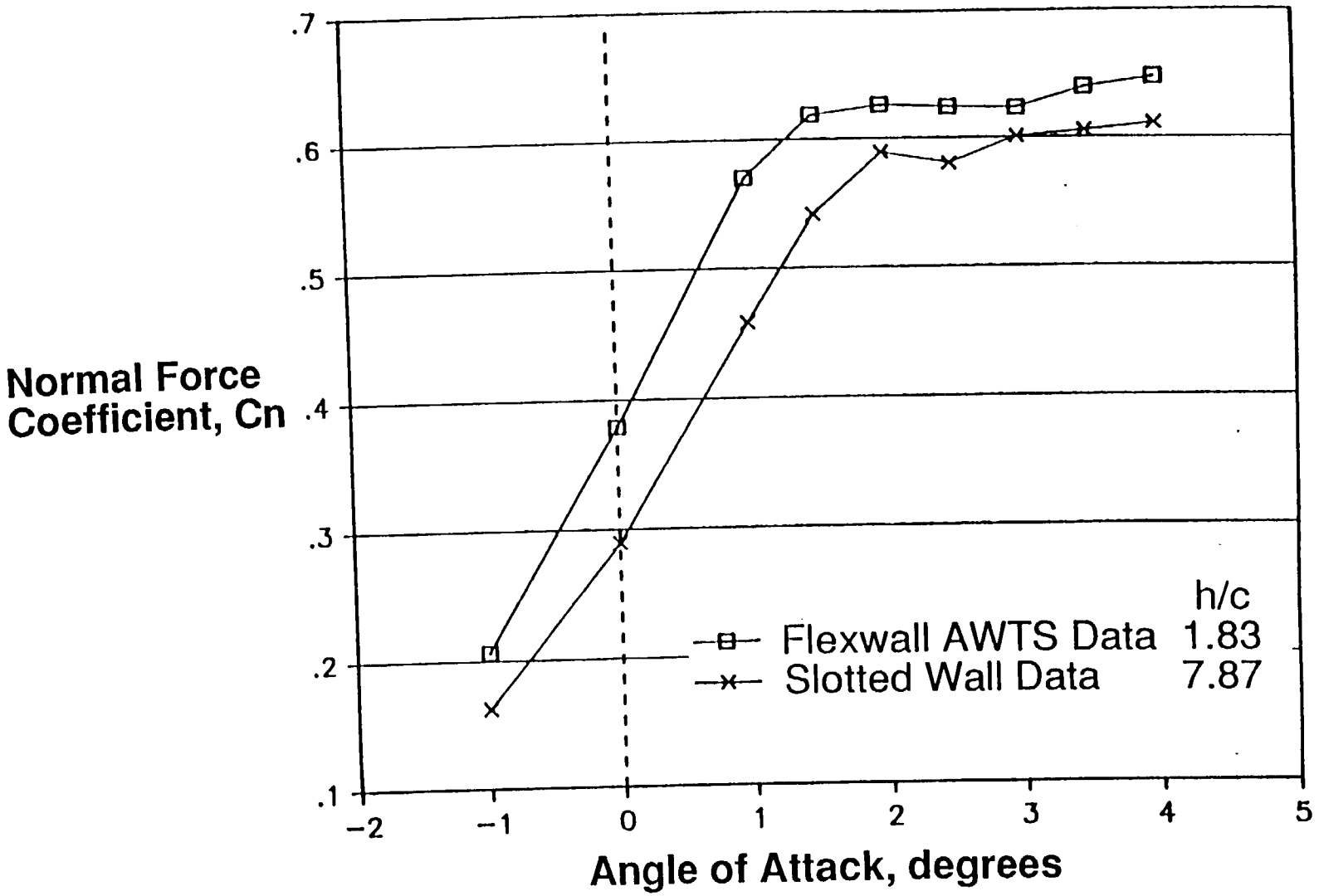


Fig. 24